

**Stock Assessment of Tilefish
off the Southeastern United States
SEDAR 89 Operational Assessment**



Southeast Fisheries Science Center
National Marine Fisheries Service

Report issued: July, 2024
Last revision: October 24, 2024

Document History

July, 2024 Original release

October 24, 2024 Revision

- Added additional projection scenarios for $P^*=30\%$ and $P^*=20\%$.
- Revised labels to projection tables to differentiate scenarios.

Contents

1 Introduction 9

1.1 Executive Summary 9

1.2 Workshop Time and Place 10

1.3 Terms of Reference 10

1.4 List of Participants 11

1.5 Document List 13

1.6 Statements Addressing Each Term of Reference 14

2 Data Review and Update 17

2.1 Data Review 17

2.2 Data Update 18

 2.2.1 Life History 18

 2.2.2 Landings 19

2.3 Discards 19

2.4 Indices of abundance 19

2.5 Length Composition 19

2.6 Age Composition 20

3 Stock Assessment Methods 20

3.1 Overview 20

3.2 Data Sources 20

3.3 Model Configuration and Equations 21

 3.3.1 Stock dynamics 21

 3.3.2 Initialization 21

 3.3.3 Natural mortality rate 21

 3.3.4 Growth 21

 3.3.5 Spawning stock 22

 3.3.6 Recruitment 22

 3.3.7 Landings 23

 3.3.8 Discards 23

 3.3.9 Fishing Mortality 23

3.3.10	Selectivities	23
3.3.11	Indices of abundance	24
3.3.12	Catchability	24
3.3.13	Fitting criterion	24
3.3.14	Parameters Estimated	25
3.3.15	Biological reference points	25
3.3.16	Configuration of base run	25
3.4	Sensitivity Analysis	26
3.5	Retrospective Analysis	26
3.6	Per Recruit and Equilibrium Analysis	26
3.7	Benchmarks and Reference Points	26
3.8	Comparison to Previous Assessments	27
3.9	Monte Carlo/Bootstrap Ensemble (MCBE) Analysis	28
3.9.1	Bootstrapping of Observed Data	29
3.9.2	Monte Carlo Sampling	29
3.10	Projection Analysis	30
3.10.1	Initialization of Projections	30
3.10.2	Uncertainty of Projections	31
3.10.3	Projection Scenarios	31
4	Stock Assessment Results	32
4.1	Measures of Overall Model Fit	32
4.2	Parameter Estimates	32
4.3	Total Abundance, Spawning Biomass, and Recruitment	32
4.4	Selectivity	32
4.5	Landings, Fishing Mortality, Quotas, and Biomass	33
4.6	Spawner-Recruitment Parameters	33
4.7	Per Recruit and Equilibrium Analyses	33
4.8	Benchmarks / Reference Points	34
4.9	Status of the Stock and Fishery	34
4.10	Comparison to Previous Assessments	35
4.11	Sensitivity Analyses	35
4.12	Retrospective Analyses	36
4.13	Projections	36

5	Discussion	36
5.1	Comments on Assessment Results	36
5.2	Comments on Projections	37
6	Research Recommendations	37
7	References	38
8	Tables	41
9	Figures	64
	Appendices	106
A	Abbreviations and symbols	106
B	B ADMB Parameter Estimates	107
C	C Additional diagnostic plots	109
C.1	Parameter bounding plots	109
C.2	Composition fit plots	111
C.3	Pooled Composition fits	115
C.4	Likelihood Profiles	119
C.5	Fixed MCBE parameters	132
D	D ADMB code	137

List of Tables

1 Observed time series of landings. 41

2 Observed time series of CVs used in Monte Carlo/Bootstrap Ensemble (MCBE) for landings. 42

3 Sample sizes of length and age compositions (numbers of fish). 43

4 Sample sizes of length and age compositions (numbers of fish). 44

5 Observed time series of indices of abundance. 45

6 Life history at age. 46

7 Estimated total abundance at age (1000 fish) 47

8 Estimated total abundance at age (mt) 48

9 Estimated total abundance at age (1000 lb) 49

10 Estimated time series of status indicators, fishing mortality, biomass, and recruitment. 50

11 Selectivities by survey or fleet 51

12 Estimated time series of fully selected fishing mortality rates by fleet. 52

13 Estimated instantaneous fishing mortality rate. 53

14 Estimated total landings at age in numbers (1000 fish) 54

15 Estimated total landings at age in gutted weight (1000 lb) 55

16 Estimated time series of landings in numbers (1000 fish) by fleet. 56

17 Estimated time series of landings in weight (1000 lb) by fleet. 57

18 Estimated status indicators and benchmarks 58

19 Projection results for $P^* = 0.50$ 59

20 Projection results for $F = F_{MSY}$ 60

21 Projection results for $P^* = 0.325$ 61

22 Projection results for $P^* = 0.30$ 62

23 Projection results for $P^* = 0.20$ 63

24 Abbreviations and Symbols 106

List of Figures

1 Data Availability 64

2 Length, female maturity, and reproductive output at age. 65

3 Observed and estimated annual age and length compositions by fleet 66

4 Observed and estimated landings: commercial handline 70

5 Observed and estimated landings: commercial longline 71

6 Observed and estimated landings: recreational 72

7 Observed and estimated index of abundance: commercial longline 73

8 Observed and estimated index of abundance: MARMAP longline survey 74

9 Estimated annual abundance (numbers) at age 75

10 Estimated annual biomass (weight) at age 76

11 Estimated recruitment time series 77

12 Estimated total and spawning stock biomass time series 78

13 Selectivity by fleet: MARMAP longline index 79

14 Selectivity by fleet: commercial landings 80

15 Selectivity by fleet: recreational landings 81

16 Average selectivity from the terminal assessment year 82

17 Estimated fully selected fishing mortality rates by fleet 83

18 Estimated landings in numbers by fleet 84

19 Estimated landings in weight by fleet 85

20 Spawner recruit curve 86

21 Probability densities of spawner-recruit quantities 87

22 Yield per recruit and spawning potential ratio at F 88

23 Equilibrium removals and spawning stock at F 89

24 Probability densities of MSY-related benchmarks from MCBE analysis 90

25 Estimated time series of SSB and F relative to benchmarks 91

26 Estimated time series of SSB 92

27 Probability densities of terminal status estimates from MCBE analysis 93

28 Phase plot of terminal status estimates from MCBE analysis 94

29 Estimated age structure from a series of individual years during the assessment, relative to the equilibrium expected at F_{MSY} 95

30 Sensitivity to natural mortality (S1-S4) 96

31 Sensitivity to steepness (S5-S6) 97

32 Sensitivity to F_{init} (S7-S8) 98

33 Sensitivity to fixed t_0 value (S9-S10) 99

34 Retrospective plots 100

35 Projections with fishing mortality rate at fixed F that provides $P^* = 0.50$ 101

36 Projections with fishing mortality rate fixed at $F = F_{MSY}$ 102

37 Projections with fishing mortality rate at fixed F that provides $P^* = 0.325$ 103

38 Projections with fishing mortality rate at fixed F that provides $P^* = 0.30$ 104

39 Projections with fishing mortality rate at fixed F that provides $P^* = 0.20$ 105

40 Diagnostic plot of parameter estimates to check for bounding issues, where the red lines indicate the upper and lower parameter bounds, orange is the initial model parameter starting value and blue is the final model estimate. 109

41 Continued: Diagnostic plot of parameter estimates to check for bounding issues, where the red lines indicate the upper and lower parameter bounds, orange is the initial model parameter starting value and blue is the final model estimate. 110

42 Diagnostic plots for the commercial handline age composition. 111

43 Diagnostic plots for the commercial longline age composition. 112

44 Diagnostic plots for the MARMAP survey age composition. 113

45 Diagnostic plots for the general recreation length composition. 114

46 Observed and estimated age composition: Commercial longline 115

47 Observed and estimated age composition: Commercial handline 116

48 Observed and estimated age composition: MARMAP bottom longline survey 117

49 Observed and estimated length composition: General recreational 118

50 Likelihood Profile for Age 50 descending limb of commercial handline domed selectivity 119

51 Likelihood Profile for Age 50 descending limb of commercial longline domed selectivity 120

52 Likelihood Profile for slope descending limb of commercial handline domed selectivity 121

53 Likelihood Profile for slope descending limb of commercial longline domed selectivity 122

54 Likelihood Profile for Beverton-Holt steepness 123

55 Likelihood Profile for initial fishing mortality rate F_{init} 124

56 Likelihood Profile for Beverton-Holt R_0 125

57 Likelihood Profile for the recruitment deviate in 2015, 126

58 Likelihood Profile for the recruitment deviate in 2016, 127

59 Likelihood Profile for the recruitment deviate in 2017, 128

60 Likelihood Profile for the recruitment deviate in 2018, 129

61 Likelihood Profile for the recruitment deviate in 2019, 130

62 Likelihood Profile for the recruitment deviate in 2020, 131

63 Density of fixed MCBE parameters 133

64 Density of age specific MCBE ogives 134

65 Density of MCBE reproductive ogives 135

66 Density of fixed MCBE parameters 136

1 Introduction

1.1 Executive Summary

This operational assessment evaluated the status of Tilefish (*Lopholatilus chamaeleonticeps*; a.k.a. Golden Tilefish, Great Northern Tilefish) off the Southeastern United States (i.e. the US South Atlantic stock). The primary objectives of this assessment were to build on previous assessments [SEDAR 04, SEDAR 25, and the SEDAR 66 (hereafter SEDAR 66)] to provide recent estimates of benchmarks and conduct updated stock projections.

Data compilation and assessment methods were guided by methods used in previous Tilefish assessments and other recent SEDAR assessments and output from the topical working group for this assessment. The benchmark assessment for Tilefish was completed in 2004 with an assessment period 1961-2002 (SEDAR 04 2004). SEDAR 25 was a standard assessment completed in 2011 with an assessment period spanning 1962-2010 (SEDAR 25 2011). An updated assessment of South Atlantic Tilefish was completed in 2016 with an assessment period of 1962-2014 (SEDAR 25 2016). Management of Tilefish in the South Atlantic is currently based on an operational assessment conducted in 2021 with an assessment time period of 1972-2018. This assessment was conducted by the Southeast Fisheries Science Center in cooperation with regional data providers, for the time period 1972-2022.

Available data on this stock included indices of abundance, landings, and samples of annual length compositions and age compositions from fishery-dependent and fishery-independent sources. Two indices of abundance were developed during the SEDAR process and fit by the model: one fishery dependent index based on the commercial longline fleet logbooks and one fishery independent index based on the Marine Resources Monitoring, Assessment, and Prediction program 'long' bottom longline survey (MARMAP longline). These indices of abundance were not updated since the previous operational assessment as no new data were available or deemed usable due to management restrictions potentially influencing fishing behavior and catch rates. Landings data were available from all significant recreational and commercial sources.

The model used in all previous assessments of this stock—and updated here—was the Beaufort Assessment Model (BAM), an integrated statistical catch-age formulation (Williams and Shertzer 2015). A base run of BAM was configured and a mixed Monte Carlo/Bootstrap Ensemble (MCBE) analysis was conducted to provide estimates of key management quantities, such as stock and fishery status.

Estimated time series of stock status (SSB/MSST) showed a rapid decline during the 1980s and a slower decline during the 1990s, to a minimum value in 1996. From 1996 to 2010 stock status improved, but has been in decline again since 2011. This decline has slowed since 2020 to near SSB_{MSY} in 2022.

Current stock status was estimated in the base run to be $SSB_{2022}/MSST = 1.261$, indicating that the stock is not overfished. Through its history, SSB did not drop below MSST. Results from the MCBE suggested that the estimate of SSB relative to SSB_{MSY} and the status relative to MSST is highly uncertain (Figures 27 and 28). A small majority (54%) of MCBE runs agreed with the stock status result from the base assessment model. The base model, median and majority of the MCBE suggests that the stock is not overfished, but is below SSB_{MSY} .

The estimated time series of F/F_{MSY} from the assessment model suggests that although F has exceeded F_{MSY} sporadically for individual years during the assessment period, it has not been consistently above the limit since the period of overfishing during 1990-1995. However, fishing mortality has been increasing considerably since 2010 and is estimated to be above F_{MSY} in the terminal year of the model. There is considerable uncertainty in F/F_{MSY} as demonstrated by the MCBE, especially toward the end of the assessment period. Current fishery status in the terminal year, with current F represented by the geometric mean from 2020 – 2022 ($F_{current} = F_{2020-2022} = 0.216$), was estimated by the base run to be $F_{2020-2022}/F_{MSY} = 1$. Thus, at the end of the assessment Tilefish was fully exploited. However, results from the MCBE show that there is a lot of uncertainty in the fishing status of the species. Only 35% of MCBE runs agreed with the fishing status result from the base model, and the median value of $F_{2020-2022}/F_{MSY}$ from the MCBE runs (1.16).

Compared to SEDAR 66, stock status has declined slightly and the stock is fully exploited in the base model but overfishing in the median of the MCBE. The estimated trends from this operational assessment are similar to those from the SEDAR 04, SEDAR 25, and SEDAR 66. However, this assessment did show some differences from previous assessments, which was not surprising, given modifications made to both the data and model (described throughout the report).

1.2 Workshop Time and Place

The SEDAR 89 South Atlantic Tilefish topical working group took place over a series of webinars held from November, 2023 to March, 2024.

1.3 Terms of Reference

1. Submit all data used in the SEDAR 66 South Atlantic Tilefish SEDAR process. Add all new and recent available data sufficient for use in the stock assessment through 2023. Data providers may decide to include additional preliminary or partial data that could be used in the stock assessment models or projection analyses (check with analysts if unsure about what could or could not be used).
2. Update the approved SEDAR 66 Atlantic Tilefish models with all provided and relevant data. Incorporate the latest and most appropriate BAM model methodologies, including relevant advances in fisheries science, biology, population dynamics, and stock assessment science.
3. Apply appropriate model diagnostics and make expert determinations for data and model changes as necessary to improve the accuracy and precision of population estimates.
4. Detail all the input data and model changes made between the SEDAR 66 South Atlantic Tilefish Operational assessment model and the proposed SEDAR 89 Operational assessment model. Write a final report describing all necessary details of the stock assessment model, data, and important issues. Include required management reference points and other important population dynamic information relevant for managers. Include a list of unresolved issues and research recommendations for future consideration.
5. Convene a topical working group including SSC representatives, industry representatives, and outside experts to meet via webinar or in-person. This group of specialists will evaluate the following subjects and document specific changes in input data or deviations from the SEDAR 66 South Atlantic Tilefish.
 - Review and explore the potential utility and incorporation of new life history information, including:
 - Data collected from expanded SCDNR SBLI survey, new cooperative SADLS survey, and SCDNR CRP pilot study (abundance, life history, etc). Examine spatial differences.
 - Evidence for hermaphroditism in the South Atlantic (specifically the interpretation and applicability of analyses conducted in Gulf of Mexico by Lombardi-Carlson (2012)).
 - Evidence for age or size dependence of spawning frequency and spawning season duration.
 - Genetic evidence of connectivity between northern and southern stocks (McDowell, VIMS).
 - Evidence for potential northward range shift.
6. Develop a stock assessment update report to address these ToRS and fully document the input data, methods, and results of the stock assessment update.

1.4 List of Participants

Appointee	Function	Affiliation
ANALYTICAL TEAM		
Matt Vincent, Lead Analyst	NMFS/SEFSC	
Walter Bubley	SAFMC SSC/SCNDR	
Jeff Moore	NCDMF	
Marcel Reichert	SAFMC/SSC	
Mike Rinaldi	ACCSP	
Kevin Spanik	SCDNR	
Michael Thompson	NCDNR	
Brent Winner	FLFWC	
Kyle Shertzer	NMFS/SEFSC	
Erik Williams	NMFS/SEFSC	
Data Providers and Observers		
Kelly Adler	NMFS/SEFSC	
Vincent Bonura	SGAP	
Christopher Bradshaw	FLFWC	
Bridget Cermak	FLFWC	
Manuel Coffill-Rivera		
Amy Dukes	SCDNR	
Lindon Fairweather		
Mike Freeman	Industry Rep	
Elizabeth Gooding	SCDNR	
Hannah Hart	MAFMC	
Eric Hiltz	SCDNR	
José Montañez	MAFMC	
Brandon Muffley	MAFMC	
Paul Nitschke	NEFSC	
Douglas Potts	NMFS/SEFSC	
Walt Rogers	NMFS/SEFSC	
Bev Sauls	FLFWC	
Rebecca Scott	FLFWC	
Tracey Smart	SCDNR	
Michelle Willis	SCDNR	
Council Representative		
Tim Griner	SAFMC	
Laurilee Thompson	SAFMC	
Staff		
Meisha Key	SEDAR	
Kathleen Howington	SEDAR	
Julie Neer	SEDAR	
Chip Collier	SAFMC Staff	
Judd Curtis	SAFMC Staff	
Mike Schmidtke	SAFMC Staff	
Dominique Lazarre	SERO	

1.5 Document List

Document number	Title	Authors	Date Submitted
Documents Prepared for SEDAR 89			
SEDAR89-WP-01	Headboat Data for Tilefish in the Southeast US Atlantic	Matthew E. Green, Robin T. Cheshire, and Kenneth Brennan	12 March 2024
SEDAR89-WP-02	General Recreational Survey Data for Tilefish in the South Atlantic	Samantha M. Binion-Rock	16 April 2024
SEDAR89-WP-03	Characterization of Reproductive Parameters for Tilefish (<i>Lopholatilus chamaeleonticeps</i>) in Atlantic Waters from North Carolina to Florida	Walter J. Bubley, Kevin J. Kolmos, and Matthew Vincent	19 April 2024
SEDAR89-WP-04	South Atlantic Tilefish (<i>Lopholatilus chamaeleonticeps</i>) length compositions from the recreational fishery	Samantha M. Binion-Rock	22 April 2024
SEDAR89-WP-05	Estimated Commercial Discards of South Atlantic Golden Tilefish (<i>Lopholatilus chamaeleonticeps</i>) Using Limited Observer Data	Kevin Thompson, Sarina Atkinson, Gary Decossas	19 April 2024
SEDAR89-WP-06	South Atlantic Golden Tilefish (<i>Lopholatilus chamaeleonticeps</i>) Commercial Landings Length and Age Compositions	Michaela Pawluk	22 April 2024
Final Stock Assessment Report			
SEDAR89-SAR1	SEDAR 89 Stock Assessment Report (<i>current document</i>)	Prepared by the SEDAR 89 panel	26 July 2024

1.6 Statements Addressing Each Term of Reference

Note: Original ToRs are in normal font. Statements addressing ToRs are in italics and preceded by a dash (–).

- 1) Submit all data used in the SEDAR 66 South Atlantic Tilefish SEDAR process. Add all new and recent available data sufficient for use in the stock assessment through 2023. Data providers may decide to include additional preliminary or partial data that could be used in the stock assessment models or projection analyses (check with analysts if unsure about what could or could not be used).
 - *All data used in SEDAR 66 were collated and used in SEDAR 89. The assessment includes data through the end of 2022. Additional life history data were collected including ages, lengths, and weights. Conversion factors from length to whole weight, length to gutted weight and growth curves were updated with additional life history data. Additional data related to the reproductive biology of the species have become available since the previous assessment and have been incorporated into the assessment model. Recreational landings were calculated as the sum of MRIP and headboat (SRHS) estimates to better account for all sources of mortality. Estimates of longline discards were incorporated into the longline landings fit by the assessment model.*
- 2) Update the approved SEDAR 66 Atlantic Tilefish models with all provided and relevant data. Incorporate the latest and most appropriate BAM model methodologies, including relevant advances in fisheries science, biology, population dynamics, and stock assessment science.
 - *SEDAR 89 updated the SEDAR 66 Atlantic Tilefish assessment model and incorporated data through the end of 2022 and included updated conversion factors and life history information. The current stock assessment incorporated numerous changes that were advances in fisheries science, the biology, and population dynamics of Atlantic tilefish. Recreational landings were modeled in numbers of fish to reduce some uncertainty in these estimates as the sample sizes for estimating weight were very small. Natural mortality relationships were updated using the most recent age data and the [Hamel and Cope \(2022\)](#) maximum age to natural mortality conversion. Natural mortality at age was modeled following [Lorenzen \(2022\)](#) as the inverse of length at age scaled to the constant M value. Natural mortality at age was coded into BAM so that the oldest age and youngest age over which to scale to the constant M could be changed to incorporate uncertainty in these values. The steepness parameter was estimated in this stock assessment after likelihood profiles and numerous testings suggested the parameter could be estimated. Biomass was reported in 1000 lb instead of metric tons to be more interpretable. Spawning stock biomass was calculated using age specific fecundity and is reported in units of trillions of eggs (see details below Terms of Reference 5 a. iii). In SEDAR 66, the last 7 years of the model did not estimate recruitment deviates. In SEDAR 89, likelihood profiling suggested that recruitment deviates could be extended so that only the last three terminal years were assumed to be driven solely by the stock recruitment function. A selectivity block in the commercial fisheries was implemented in 2009 for SEDAR 66, but this increase in number of parameters did not result in a sufficiently large change in the likelihood to warrant the increase in model complexity. Instead, a shift to smaller fish caught by the commercial fishery was observed to begin in 2020 and very few fish in the plus group were caught. To account for this drastic shift in the age composition, a dome-shaped time-block selectivity beginning in 2020 for the commercial fisheries was implemented in the model and resulted in an improvement in the likelihood. To account for the difficulty in ageing this species, an ageing error matrix was calculated from comparison of three readers from a reference set. The ageing error matrix was incorporated into the stock assessment model and resulted in a better likelihood and fit to the data.*
- 3) Apply appropriate model diagnostics and make expert determinations for data and model changes as necessary to improve the accuracy and precision of population estimates.
 - *Changes to the SEDAR 66 BAM assessment model were made through the investigation of various diagnostics including likelihood profiles, likelihood value comparisons, runs tests, visual examination of residuals and one-step ahead residual of composition data. All model decisions resulted in better fits to the data in terms of the likelihood and accounted for a parsimonious model so as not to be overly complex. Model diagnostics are presented in the figures and the appendix.*

- 4) Detail all the input data and model changes made between the SEDAR 66 South Atlantic Tilefish Operational assessment model and the proposed SEDAR 89 Operational assessment model. Write a final report describing all necessary details of the stock assessment model, data, and important issues. Include required management reference points and other important population dynamic information relevant for managers. Include a list of unresolved issues and research recommendations for future consideration.
 - *Changes to the model are described above in Terms of Reference 2 and are presented in further detail in the report. This report includes the necessary details of the stock assessment model, data, issues encountered and unresolved, research recommendations, management reference points, and population dynamics information relevant for managers.*
- 5) Convene a topical working group including SSC representatives, industry representatives, and outside experts to meet via webinar or in-person. This group of specialists will evaluate the following subjects and document specific changes in input data or deviations from the SEDAR 66 South Atlantic Tilefish.
 - (a) Review and explore the potential utility and incorporation of new life history information, including:
 - i. Data collected from expanded SCDNR SBLL survey, new cooperative SADLS survey, and SCDNR CRP pilot study (abundance, life history, etc). Examine spatial differences.
 - *SADLS: The South Atlantic Deepwater Longline Survey (SADLS) targets multiple deepwater species, with a focus on tilefishes and deepwater groupers. Catches of golden tilefish individuals by survey year were as follows: 2020: 166; 2021: 898; 2022: 434; 2023: 631. An SSC working group was convened in 2023 to assess the utility of the SADLS index in stock assessments. This working group determined that “at least 5 years of survey data should be available before an index of relative abundance should be considered for use in a stock assessment.” For age compilations during the current assessment, the working group advised to “use age/biological information as available and appropriate.” The compiled life history data for the current assessment contains 1179 samples collected from the SADLS. Age, weight, length and histology data collected by this survey were incorporated into the updated life history conversion equations. SCDNR SBLL survey/CRP pilot study: The expanded short bottom longline survey (SBLL) samples high relief bottom types, and catches relatively few golden tilefish. Compiled life history data for the current assessment had only 140 sampled individuals from the SBLL survey. The age, length, and weight samples from all available sources were incorporated into the updated growth models and length-weight models.*
 - ii. Evidence for hermaphroditism in the South Atlantic (specifically the interpretation and applicability of analyses conducted in Gulf of Mexico by Lombardi-Carlson (2012)).
 - *Analyses conducted by members of the SCDNR concluded that golden tilefish do not meet the criteria to be considered hermaphroditic in the South Atlantic. Findings from these analyses are reported in SEDAR89-WP-03 (Bubley et al. 2024).*
 - iii. Evidence for age or size dependence of spawning frequency and spawning season duration.
 - *As reported in SEDAR89-WP-03 (Bubley et al. 2024), spawning season duration was linearly related to total length and spawning fraction was logistically related to total length. Age specific fecundity estimates resulting from these models were incorporated into the stock assessment and used to calculate spawning stock.*
 - iv. Genetic evidence of connectivity between northern and southern stocks (McDowell, VIMS).
 - *The scientific literature was searched for any studies that investigated the stock structure of golden tilefish in the Atlantic Ocean and Gulf of Mexico. A single study was identified (Katz et al. 1983). This study included samples from a number of sites in the Mid-Atlantic Bight, Gulf of Mexico, and a single site off the coast of South Carolina. The study presented evidence that the morphological data for the South Carolina samples were contradictory with the electrophoretic analysis and the two showed conflicting results. Morphometric characteristics compared between the SC samples and the Mid-Atlantic Bight indicated no significant difference. However, there was a highly significant*

difference between the Mid-Atlantic Bight and southern samples (Gulf of Mexico and SC) in the genotype distributions from liver electrophoresis. The authors state that the interpretation of the data may be hampered by the small sample sizes for the southern populations and the great distances between sampling sites. Jan McDowell was contacted to determine if she had conducted any studies on this species of tilefish. She confirmed that she had not conducted any genetic analysis for golden tilefish, but had conducted and published research for blueline tilefish. A study is currently being conducted by David Portnoy and Shannon O'Leary on golden tilefish genetics in the Gulf of Mexico and Atlantic Ocean. However, this research is not yet completed and has not been peer reviewed. Therefore, there is no information currently available to determine the genetic evidence of connectivity between the northern and southern stocks.

- v. Evidence for potential northward range shift.
 - Tilefish were first discovered in 1879 just south of Nantucket, MA. Since then, the distribution of tilefish has been described as extending from Nova Scotia to Suriname (Doolet 1978). The South Atlantic population falls squarely within the middle of the latitudinal range of this species. Tilefish have been described as relatively sedentary as a result of a mark-recapture study that recaptured all fish within 2 km of the tagging site up to 1.6 years after release (Grimes et al. 1983). The northern extent of the South Atlantic population of tilefish has been delineated at Cape Hatteras, NC. The upper middle continental slope near Hatteras has been hypothesized as a potential barrier between the northern and southern stock of tilefish (Steimle et al. 1999). This area of the continental shelf has either continuous or episodic hypoxia in the benthic boundary layer, which would prove problematic for the burrowing tilefish (Sulak and Ross 1996). Additionally, the area was noted to be devoid of active benthopelagic foragers and species present were of smaller size than elsewhere on the shelf. The lack of movement in the adult phase of the species and the inhospitable habitat near Cape Hatteras make a northward shift of adults in the population unlikely. The other potential route of a northward range shift would be the dispersal of eggs and larvae and their eventual settlement in favorable habitats in northern regions. This would likely overlap with the current northern stock of tilefish. A plethora of information would be needed to prove such a phenomenon was occurring. First, evidence delineating the historical and current differences in stock structure and characteristics of the northern and southern stocks would need to be clearly defined through a multi-faceted approach (genetics, meristics, etc.). Second, a clear methodology to accurately classify individuals as either from the northern or southern stock would need to be developed. Third, a time series of the proportion of northern and southern stock individuals that occur north of Cape Hatteras would need to show an increase in the proportion of individuals from the southern stock. Currently, there is limited data available to delineate and classify the stock structure in the Atlantic Ocean (Katz et al. 1983), and no time series exists documenting northward movement of southern individuals. Anecdotal evidence from commercial fishermen during the Topical Working Group suggested that tilefish continue to be caught in the same areas that have historically been observed in both the northern and southern extent of the population. Therefore, there is no evidence suggesting a northward range shift.
- 6) Develop a stock assessment update report to address these ToRS and fully document the input data, methods, and results of the stock assessment update.
 - Please see this report.

2 Data Review and Update

The benchmark assessment for Tilefish (*Lopholatilus chamaeleonticeps*) off the Southeastern United States (i.e. the US South Atlantic stock), SEDAR 04, was completed in 2004 with an assessment period 1961-2002 (SEDAR 04 2004). SEDAR 25 was a standard assessment completed in 2011 with an assessment period spanning 1962-2010 (SEDAR 25 2011). An update assessment of South Atlantic Tilefish was completed in 2016 with an assessment period of 1962-2014 (SEDAR 25 2016). Current management of Tilefish of the Southeastern United States is based on SEDAR 66 with an assessment period of 1972-2018 (SEDAR 66 2021).

In the current SEDAR 89 assessment, data through 2022 were considered. For most data sources, the data were simply updated with the additional years of data (2018-2022) using the same methods as in the prior assessments. However, for some sources, it was necessary to update data prior to 2019 as well. The input data for this assessment are described below, with emphasis on the data that required modification beyond just the addition of years. A summary timeline of data sources fit to in this assessment is plotted in Figure 1.

2.1 Data Review

In this operational assessment, the Beaufort assessment model (BAM) was fit to many of the same data sources as in SEDAR 04 and the SEDAR 25, SEDAR 66 (hereafter SEDAR 66).

- Landings: commercial handline, commercial longline, and general recreational
- Indices of abundance: commercial longline and Marine Resources Monitoring, Assessment, and Prediction program 'long' bottom longline survey (MARMAP longline)
- Length compositions of landings: general recreational
- Age compositions of landings: commercial handline, commercial longline, and MARMAP longline survey.

Contrasts to data used in the SEDAR 66 assessment include:

- Recreational landings were calculated as the sum of landings estimated from the Marine Recreational Information Program (MRIP) and Southeast Region Headboat Survey (SRHS). Landings were fit in number of fish caught. This was to remove the necessity of converting landings to pounds whole weight and then converting to pounds gutted weight as in SEDAR 66. For calculations of total landings, number of fish were converted directly to pound gutted weight using new conversion factors.
- Estimates of commercial longline discard were incorporated into the landings estimates for this fleet.
- Data on age estimates by multiple readers of a reference set of tilefish otoliths were used to create an ageing error matrix, which was used in the assessment model to characterize the uncertainty in this data source.
- Natural mortality was updated using recent maximum age data and the Hamel and Cope (2022) maximum age equation. Natural mortality at age (M_a) was calculated by scaling the inverse length to the constant M for a specified range of ages (Lorenzen 2022).
- All conversion factors were updated by fitting appropriate models to all currently available data from fishery-dependent and -independent sources. These conversion factors include length-length conversions, von Bertalanffy growth, length to whole weight, and length to gutted weight.
- Length compositions used in the assessment and the age compositions that were weighted by the lengths were slightly different than previous assessments as a result of changes to the conversion factors.
- Maturity at age was fit as maturity at length and mean length at age from the von Bertalanffy growth curve was used to determine maturity at age. Fecundity at age was determined using a plateau model and batch fecundity model (Buble et al. 2024), which were multiplied together and with the maturity at age to provide total reproductive output in trillions of eggs. Spawning stock biomass (SSB) was calculated based on this total reproductive output at age. SEDAR 66 had calculated SSB as gonad weight.

2.2 Data Update

2.2.1 Life History

Numerous changes to conversion equations of life history inputs were made compared to SEDAR 04 and SEDAR 66. It was discovered that in previous assessments, data providers had incorrectly assumed that the conversions of TL listed in SEDAR 4 were for natural TL. However, all samples from MARMAP are measured in maximum TL and therefore the conversion from SL and FL would be to maximum TL. Therefore, the order of conversion and preference for length type changed as a result of this understanding. To ensure that all life-history conversions factors were in the appropriate units and were up to date using new available information, regressions were performed using all currently available data.

Age was used to predict maximum total length using a von Bertalanffy growth curve fit to all available information for tilefish. Two growth curves were fit, one to both sexes that provided a population growth curve and the other to only females. The female growth curve was used in the calculations of spawning stock biomass, whereas the population growth curve was used to calculate total biomass and landings. Estimation of the t_0 parameter resulted in biologically unreasonable estimates that were less than -1. Therefore, the t_0 parameter was fixed at -0.5, but sensitivity to this parameter was incorporated into the Monte Carlo/Bootstrap Ensemble (MCBE) analysis by fitting numerous models to the data using values within the range of -1 to 0 (Figure 64). The mean length at age for the population was determined by the equation

$$\text{Population } L_a = 830.18 * (1 - e^{0.20482*(age+0.5)}), \quad (1)$$

while the mean length of females as determined by the equation:

$$\text{Female } L_a = 731.53 * (1 - e^{0.25073*(age+0.5)}). \quad (2)$$

Conversion factors for length to whole weight and gutted weight were obtained by fitting non-linear models to available fishery-independent and -dependent data. Whole weight (WW) was converted from maximum total length (TL) using the equation $WW = 3.966e - 06 * TL^{3.159}$ and gutted weight (GW) from maximum total length (TL) by the equation $GW = 3.113e - 06 * TL^{3.190}$.

Maturity at age and fecundity at age were estimated using recently available data (Bublely et al. 2024). These new life history relationships were used in combination with the female growth curve to calculate SSB. Additionally, the peak time of spawning in the assessment was changed to May 15th (i.e., 0.37 fraction of the year or the 135th day Bublely et al. 2024). Uncertainty in maturity at age, reproductive output at age, and peak spawning time were incorporated into the MCBE analysis by drawing parameter estimates from the covariance matrix of the respective models and recalculating the quantities of interest. Primary life-history information for the base model is summarized in Table 6.

Maximum age (t_{max}) remained age $t_{max} = 40$ for the base model. However, uncertainty in this value was incorporated in the MCBE analysis by applying values between the range of 37 and 45. Thirty-seven was chosen as the lower bound because it was the last age for which all previous ages had at least one age sample and forty-five was the oldest observed age in the dataset. Constant natural mortality (M) used for scaling age-varying natural mortality (M_a) was calculated using the equation from Hamel and Cope (2022, $M = 5.40/A_{max}$) such that $M = 0.135$. M_a was calculated by an inverse length scaled so that mortality from ages 6 to the maximum age was consistent with the constant natural mortality rate across these ages (Lorenzen 2022). Sensitivity to the youngest age used for the Lorenzen M_a was explored in the sensitivity analysis and the MCBE.

2.2.2 Landings

Landings estimates were combined into three fleets: commercial handline, commercial longline, and general recreational (Table 1). Commercial landings of Tilefish were compiled from 1950 through 2022 in gutted weight (GW). Only landings from 1972 to 2022 were included in this assessment as landings prior to 1972 were minimal. Sources for landings in the U.S. South Atlantic (Florida through North Carolina) included the Florida Trip Ticket program (FTT), South Carolina Department of Natural Resources (SCDNR), North Carolina Division of Marine Fisheries (NCDMF), and the Atlantic Coastal Cooperative Statistics Program (ACCSP). Commercial handline landings included gear types such as hook and line, bandit reels, and similar hook gear. Landings from gear types other than handline and longline were negligible and were not included in the assessment. Commercial landings include data from the North Carolina-Virginia border to the Florida Keys in Monroe County, Florida along US Highway 1. Landings in Monroe County were apportioned by data providers to exclude landings north of the Florida Keys, which are considered part of the Gulf of Mexico. Estimates of commercial discards from the longline fleet were obtained (Thompson et al. 2024) using new methodology. Since the estimates were minimal and no size composition were available for these discards, the landings and discards were summed by year to be fit by the model.

For this assessment, estimates of recreational landings from the private and charter modes were based on current Marine Recreational Information Program (MRIP) methodology. Estimates account for changes in the Fishing Effort Survey, the redesigned Access Point Angler Intercept Survey, and the For Hire Survey. A large value of recreational landings in 1981 (227,080 fish) was associated with one trip which reported 12 Tilefish (Nuttall and Matter 2020). The Southeast Region Headboat Survey (SRHS) also provided landings estimates for tilefish. Landings for the general recreational fleet were the sum of the MRIP and SRHS landings estimates. Years where landings were estimated as 0 were replaced with the next lowest value in the time series because years with no landings were not expected. This is similar to the methodology of SEDAR 66 (SEDAR 66 2021). Landings were provided in number of fish and whole weight. The number of landed fish for the recreational fleet were used in the assessment model as these estimates had slightly lower uncertainty compared to landed weight.

2.3 Discards

Commercial longline discards were estimated by new methodology (Thompson et al. 2024). Discards for this fleet were minimum and information regarding the size of discarded fish was not available. Therefore, discards were added to landings assuming complete mortality and fit as total landings for the commercial longline fleet. Discards estimates were not available for the commercial handline fleet or the SRHS and therefore were assumed to be zero. Discards estimates from MRIP were minimal and were not included in the stock assessment.

2.4 Indices of abundance

The indices of abundance used in SEDAR 66 included the fishery-independent MARMAP longline index and the fishery dependent longline logbook index (Table 5). These indices of abundance remained unchanged since the previous assessment as no new information were available or deemed usable in a standardized index.

2.5 Length Composition

Length compositions were developed from the commercial handline, commercial longline, and recreational sampling data. Sample sizes by year and fleet are reported in Table 3 (trips) and Table 4 (fish). Following the methodology of SEDAR 66, the contribution of each length was weighted by the landings associated by state, gear, and year.

2.6 Age Composition

Age data were available from the commercial handline, commercial longline, and MARMAP longline sampling programs. For commercial data, ages greater than 20 yr were pooled to age-20 creating a plus group. For the MARMAP age compositions, there were few ages > 16 yr, so ages ≥ 16 yr were pooled as a plus group. Sample sizes by year and fleet are reported in [Table 3](#) (trips) and [Table 4](#) (number of fish).

An ageing error matrix was estimated from data from ageing of a reference set of otoliths by three readers. This ageing error matrix was applied to the age compositions in the BAM assessment model to represent uncertainty in the ageing process.

3 Stock Assessment Methods

This assessment updates the primary model applied during the SEDAR 04 and the SEDAR 66 for Tilefish (*Lopholatilus chamaeleonticeps*) off the Southeastern United States (hereafter South Atlantic Tilefish). The methods are reviewed below, and any changes since the SEDAR 66 are emphasized.

3.1 Overview

This operational assessment updated the primary model applied in SEDAR 66, which was developed using the Beaufort Assessment Model (BAM) software ([Williams and Shertzer 2015](#)). BAM applies a statistical catch-age formulation, coded in AD Model Builder ([Fournier et al. 2012](#)). BAM is referred to as an integrated model because it uses multiple data sources relevant to population and fishery dynamics (e.g. removals, length and age compositions, and indices of abundance) in a single framework. In essence, the catch-age model simulates a population forward in time while including fishing processes ([Quinn and Deriso 1999](#); [Shertzer et al. 2008](#)). Quantities to be estimated are systematically varied until characteristics of the simulated population match available data on the real population. The model is similar in structure to Stock Synthesis ([Methot and Wetzel 2013](#)) and other stock assessment models used in the United States ([Dichmont et al. 2016](#); [Li et al. 2021](#)). Versions of BAM have been used in previous SEDAR assessments of reef fishes in the U.S. South Atlantic, such as Black Sea Bass, Blueline Tilefish, Gag, Greater Amberjack, Red Grouper, Red Porgy, Red Snapper, Snowy Grouper, Tilefish, and Vermilion Snapper, as well as in the previous SEDAR assessment of Tilefish ([SEDAR 66 2021](#)).

3.2 Data Sources

The catch-age model included data from the commercial longline logbook program, the fishery independent MARMAP longline survey, and three fleets that caught South Atlantic Tilefish: commercial handline, commercial longline, and the recreational fishery. The model was fit to annual landings and discards in gutted weight for commercial fleets and numbers for the recreational fleet ([Table 1](#)). Data providers also supplied coefficients of variation (CVs) associated with landings ([Table 2](#)), which were used to generate bootstrap data sets during the MCBE analysis. The model was also fit to annual length composition of recreational landings and annual age compositions from commercial handline and commercial longline landings and from the MARMAP longline survey. Samples sizes associated with composition data are provided in numbers of trips ([Table 3](#)) and numbers of fish ([Table 4](#)). The model was also fit to the fishery dependent commercial longline logbook standardized CPUE and the fishery independent MARMAP longline survey index of abundance ([Table 5](#)). Data used in the model are described in §2 of this report and in previous reports of South Atlantic Tilefish.

3.3 Model Configuration and Equations

Model structure and equations of the BAM are detailed in [Williams and Shertzer \(2015\)](#). The assessment time period for this assessment was 1972-2022. A general description of the assessment model follows.

3.3.1 Stock dynamics

In the assessment model, new biomass was acquired through growth and recruitment, while abundance of existing cohorts experienced mortality from fishing and natural sources. The population was assumed closed to immigration and emigration. The model included age classes 1–20⁺, where the oldest age class 20⁺ allowed for the accumulation of fish (i.e., plus group).

3.3.2 Initialization

Initial (1972) abundance at age was estimated in the model as follows. The equilibrium age structure was computed for ages 1–20⁺ based on natural and fishing mortality (F_{init}), where F_{init} was set equal to a value that resulted in the 1972 biomass level equaling 90% of the unfished level. This was done in SEDAR 25 and the SEDAR 66 based on the assumption by the SEDAR 25 workshop panel that the stock was lightly exploited prior to the 1960's. In SEDAR 89, landings data showed minimal exploitation prior to 1972, and the same method was followed. Lognormal deviations around that equilibrium age structure were found not to deviate from zero during model development and thus were fixed at zero. Sensitivity of the assessment model to the assumed value of F_{init} were tested by randomly sampling a value of F between 0 and 0.2 as suggested by a change in 2 likelihood values by the profile of this parameter ([Figure 55](#)).

3.3.3 Natural mortality rate

The natural mortality rate (M) was assumed constant over time, but decreasing with age. Constant M was calculated by the [Hamel and Cope \(2022\)](#) relationship with a maximum age of 40, which yielded a value of $M = 0.135$. The form of M as a function of age was based on [Lorenzen \(2022\)](#) and are inversely related to length at age. The age-dependent estimates of M_a were rescaled to provide the same fraction of fish surviving from age-6 through the oldest observed age (40 yr) as would occur with constant $M = 0.135$. The starting age class for this calculation was chosen as the age of full selectivity to the fishery because most estimates of M in the database compiled by [Then et al. \(2014\)](#) are based on fully selected individuals of the population. For the MCBE analysis, the oldest observed age used to calculate the constant M and rescale M_a was randomly drawn between 37 and 45. Additionally, the minimum age used to scale M_a was randomly drawn age between 5 and 8 as possible ages of full selectivity.

3.3.4 Growth

Mean length at age in the population [l_a ; total length (TL) in millimeters, (mm)] was modeled with the von Bertalanffy function of age (a)

$$l_a = L_{\infty}(1 - \exp[-K(a - t_0 + \tau)]) \quad (3)$$

where $L_{\infty} = 830.2$, $K = 0.2048$, and $t_0 = -0.5$, are parameters estimated external to the assessment model during the SEDAR 89 process and $\tau = 0.5$, representing a fraction of the year. Here, l_a is being computed at midyear. In

the model fitting to the age and length data the t_0 was estimated to be a biologically unreasonable value much less than -1, thus, the parameter was fixed at -0.5 for the base model.

A similar von Bertalanffy equation was derived for female tilefish where $L_\infty = 731.5$, $K = 0.2507$, and $t_0 = -0.5$

All parameters in Equation (3) of the population and female growth curves were treated as fixed input to the assessment model. However, uncertainty in the t_0 parameter was incorporated into the stock assessment model through the MCBE procedure by randomly drawing a value between -1 and 0, then refitting both von Bertalanffy growth curves to the age and length data and using these new estimates in the stock assessment model. For fitting length composition data, the distribution of size at age was assumed normal with coefficient of variation estimated by the assessment model ($CV_l = 0.1397$). A constant CV, rather than constant standard deviation, was suggested by the size at age data.

Whole weight at age [WW_a ; WW in kilograms (kg)] was modeled as a power function of l_a maximum total length (TL in mm)

$$WW_a = \theta_1 l_a^{\theta_2} \quad (4)$$

where $\theta_1 = 3.966e-06$ and $\theta_2 = 3.159$ are parameters estimated external to the assessment model during the current operational assessment and treated as fixed input to the assessment model (Table 6 and Figure 2). Where necessary (e.g. converting recreational landings to GW), total length at age (l_a) was converted to gutted weight (GW_a) with the power function

$$GW_a = \alpha l_a^\beta \quad (5)$$

where $\alpha = 3.113e-06$ and $\beta = 3.19$ Uncertainty in the length to weight functions were incorporated into the MCBE analysis by drawing values using the covariance matrix of the parameters from the model fit.

3.3.5 Spawning stock

Spawning stock was modeled using total egg production measured at the time of peak spawning. For Tilefish, peak spawning was considered to occur in the middle of May (May 15th; *spawn_time_frac* = 0.37). Total egg production at age was calculated as the product of maturity at age, batch fecundity at age, and spawning frequency at age (Bublely et al. 2024). Total reproductive output at age (Table 6 and Figure 2) was multiplied by the female abundance at age and summed across ages to calculate the spawning stock biomass.

3.3.6 Recruitment

Expected annual recruitment (\bar{R}_y) of age-1 fish (i.e. recruits) was predicted from spawning stock in year y (S_y) using the Beverton–Holt spawner-recruit model

$$\bar{R}_{y+1} = \frac{0.8R_0hS_y}{0.2R_0\phi_0(1-h) + S_y(h-0.2)} \quad (6)$$

where R_0 is virgin recruitment, h is steepness, and ϕ_0 is the unfished spawners per recruit (Williams and Shertzer 2015). In SEDAR 89 R_0 and h were estimated as likelihood profiling suggested these parameters were estimable for

this model. For years where data were considered useful for providing information on year-class strength, annual recruitment deviations (r_y) were estimated, assuming a lognormal distribution with standard deviation (σ_R)

$$N_{1,y} = \bar{R}_y \exp(r_y) \quad (7)$$

In early runs of the model, σ_R had a tendency to be estimated at the lower bound and thus was fixed at a value of 0.6 from a meta-analysis based on [Beddington and Cooke \(1983\)](#) and [Mertz and Myers \(1996\)](#)

Annual variation in recruitment was assumed to occur with lognormal deviations for years 1982 – 2019 only. The start of recruitment residuals in 1982 was based on examination of a series of different starting years and the start of the age composition data that have information on year class strength. The first year of age composition data was 1992 from the commercial longline landings. In those early age compositions, the number of fish diminishes beyond age-10 ([Figure 3](#)) which is the approximate age at full selection ([Figure 14](#)). Thus, 1982 seemed to be about the earliest year that the composition data could reliably provide information on year class strength (i.e. estimate a recruitment residual) and is consistent with SEDAR 66. The ending year of estimated recruitment residuals (2019) was determined by conducting likelihood profiles of the recruitment in the terminal year for 2015-2020. The terminal year of 2019 was chosen because the likelihood profile of the following year suggested there was a wide range of values that had a change in total likelihood value of less than 2 ([Figures 57 to 62](#)).

3.3.7 Landings

The model included time series of landings from three fleets: commercial longlines (1972–2022), commercial handlines (1972 – 2022), and general recreational (1981 – 2022). Landings were modeled with the Baranov catch equation ([Baranov 1918](#)) and were fit in units of weight (1000 lb GW) for the commercial fishery and numbers for the recreational fleet.

3.3.8 Discards

As noted above, observed discards were only available for the longline fleet and were incorporated into the landings for this fleet assuming a 100% discard mortality due to the depth of capture and lack of other data.

3.3.9 Fishing Mortality

For each time series of landings, the assessment model estimated a separate full fishing mortality rate (F). Age-specific rates were then computed as the product of full F and selectivity at age. Apical F was computed as the maximum of F at age summed across fleets.

3.3.10 Selectivities

As in SEDAR 66, selectivity at age was estimated using a two-parameter, flat-topped, logistic model for years prior to 2020. However, in 2020 there was a marked increase in the proportion of fish less than age 5 and a decrease in the fish older than age 15. Therefore, a time block and domed selectivity were incorporated into the model to account for this change in the age composition. Likelihood profiling of the parameters controlling the dome shaped selectivity suggested that the model was able to estimate these parameters, though some tended to be close to the lower bound. The cause of this selectivity change is currently unknown, but is hypothesized to be in response to the decrease in quota in recent years. During the SEDAR 66 workshop multiple fishermen (appointed observers)

confirmed that decreases in the fishing season affected behavior of the commercial fleet in ways that might cause a change in selectivity. Age and size composition data were critical for estimating selectivity functions.

As in the SEDAR 66, separate selectivity functions were estimated for commercial handline, commercial longline, and general recreational fleets, as well as for the MARMAP longline index. In contrast to the SEDAR 66, the time blocks occurred for different time periods. The break for the two time blocks for both commercial fisheries in SEDAR 66 occurred in 2009. For SEDAR 89 selectivity functions for both the commercial handline and commercial longline fleets were estimated for two time blocks (1972-2019, 2020-2022), where the later assumed a domed selectivity. The time block in 2009 was removed from the current assessment because it did not result in a significant improvement in the model fit to warrant the additional parameters.

No selectivity parameters are fixed in SEDAR 89, but a normal prior distribution was applied to the slope parameter for the general recreational fleet selectivity which was not well estimated. Values for this normal prior were based on SEDAR 66.

3.3.11 Indices of abundance

The model was fit to two indices of relative abundance: commercial longline (1993-2006) and MARMAP longline survey (discontinuous years from 1996 to 2016; [Table 5](#)). Predicted indices were conditional on selectivity of the corresponding fleet or survey and were computed from abundance (MARMAP) or biomass (commercial) at the midpoint of the year.

In this assessment, commercial CPUE units within the model code were converted from GW to WW to better match the population units of WW. This conversion does not affect model results, as the predicted index is ultimately scaled by the catchability parameter.

3.3.12 Catchability

In the BAM, catchability scales indices of relative abundance to the estimated vulnerable population at large. As in prior assessments, catchability coefficients of both indices were assumed constant through time.

3.3.13 Fitting criterion

The fitting criterion was a penalized negative log-likelihood approach in which observed landings were fit closely, and observed composition data and abundance indices were fit to the degree that they were compatible. Landings and index data were fit using lognormal likelihoods. Length and age composition data were fit using the Dirichlet-multinomial distribution, with sample size represented by the annual number of trips ([Table 5](#)), adjusted by an estimated variance inflation factor (i.e. one additional parameter for each fleet's composition data).

The assessment model fit composition data using the Dirichlet-multinomial distribution ([Francis 2017](#); [Thorson et al. 2017](#)). This distribution is self-weighting through estimation of an additional variance inflation parameter for each composition component, making iterative re-weighting unnecessary. Another advantage is that it can better account for overdispersion, or, larger variance in the data than would be expected by the multinomial. Overdispersion can result from intra-haul correlation, which results when fish caught in the same set are more alike in length or age than fish caught in a different set ([Pennington and Volstad 1994](#)). The effectiveness of the Dirichlet-multinomial distribution for composition data has been demonstrated through simulation studies and applications ([Fisch et al. 2021](#); [2022](#)). The Dirichlet-multinomial has been implemented in Stock Synthesis ([Methot and Wetzel 2013](#); [Thorson et al. 2017](#)) and in the BAM, and since SEDAR41 has become the standard likelihood for fitting composition data in assessments of South Atlantic reef fishes.

The model includes the capability for each component of the likelihood to be weighted by user-supplied values. When applied to landings and indices, these weights modify the effect of the input CVs. In this application to Tilefish, CVs of landings (in arithmetic space) were assumed equal to 0.05 to achieve a close fit to these data while allowing some imprecision. In practice, the small CVs are a matter of computational convenience, as they help achieve a close fit to the landings, while avoiding having to solve the Baranov equation iteratively (which is complex when there are multiple fisheries). Similar to SEDAR 66, data weights were all equal in the base model.

In addition, the compound objective function included several prior distributions, applied to the Dirichlet-multinomial variance inflation factor parameters associated with each set of composition data and the slope parameter for the selectivity function of the general recreational fleet. Priors were applied to maintain parameter estimates near reasonable values, and to prevent the optimization routine from drifting into parameter space with negligible gradient in the likelihood which can result in a non-positive definite Hessian matrix (an indication of incomplete or incorrect parameter solutions).

3.3.14 Parameters Estimated

The model estimated a total of 210 parameters including average fishing mortality rates (3 parameters) and annual fishing mortality rates (144 parameters) for each fleet, selectivity parameters (16 parameters), Dirichlet-multinomial variance inflation factors (4 parameters), a catchability coefficient associated with each index (2 parameters), coefficient of variation of length at age (CV_L ; 1 parameter), virgin recruitment (R_0 ; 1 parameter), Beverton–Holt stock recruitment steepness (h ; 1 parameter), and annual recruitment deviations (38 parameters).

3.3.15 Biological reference points

Biological reference points (benchmarks) were calculated based on maximum sustainable yield (MSY) estimates in gutted pounds from the Beverton–Holt spawner-recruit model with bias correction (expected values in arithmetic space). Computed benchmarks included MSY, fishing mortality rate at MSY (F_{MSY}), and spawning stock at MSY (SSB_{MSY}) by the method of [Shepherd \(1982\)](#). In this assessment spawning stock measures total egg production. These benchmarks are conditional on the estimated selectivity functions and the relative contributions of each fleet’s fishing mortality. The selectivity pattern used here was the effort-weighted selectivities at age, with effort from each fishery estimated as the full F averaged over the last three years of the assessment (2020-2022).

Reference points are sensitive to changes in selectivity and ratios of F among the removal fleets. These reference points are based on the domed shaped selectivity which assumes that the oldest ages are not vulnerable to fishing. If the fishing behavior were to change such that the selectivity were to return to a logistic selectivity then the reference points based on the domed selectivity could result in overfishing of the species. Care must be taken in such scenarios so as not to reduce the population below sustainable levels.

3.3.16 Configuration of base run

The base run was configured as described above. However, the base run configuration was not considered to represent all uncertainty. Sensitivity analyses, retrospective analyses, and ensemble modeling was conducted to better characterize the uncertainty in base run point estimates.

3.4 Sensitivity Analysis

Sensitivity of results to some key model inputs and assumptions was examined through sensitivity analyses. Sensitivity runs were chosen to address specific questions that arose during the SEDAR 89 assessment process. They were intended to demonstrate directionality of results with changes in inputs or simply to explore model behavior. These model runs vary from the base run as follows.

- S1-S2: Low/high values of maximum age used to calculate constant natural mortality ($M = 0.120, 0.146$) and Lorenzen natural mortality at age (Maximum M age = 45, 37)
- S3-S4: Low/high values of minimum age used to calculate Lorenzen natural mortality at age (Minimum M age = 5, 8)
- S5-S6: Low/high values of steepness ($h = 0.323, 0.975$)
- S7-S8: Low/high values of initial F ($F_{init} = 0, 0.2$).
- S9-S10: Low/high values of fixed t_0 growth parameter ($t_0 = -1, 0$)

3.5 Retrospective Analysis

Retrospective analyses were run by reducing the terminal year of the model from 2022 to 2015-2021, thereby trimming all time series accordingly, and rerunning the assessment model. This analysis facilitates investigation of patterns in model results, particularly terminal status estimates, that may occur when recent data are excluded.

Retrospective analyses should be interpreted with caution because several data sources are not continuous between 2015 and 2022 (Figure 1). These include the MARMAP longline index and age compositions, commercial handline age compositions, and recreational length compositions. Additionally, the time block selectivity occurs in the last 3 years and has limited data as years are removed to estimate the domed selectivity parameters. The final year of recruitment deviations in each retrospective run was set to the terminal year minus 3 years to mirror the base run model configuration.

3.6 Per Recruit and Equilibrium Analysis

Yield per recruit and spawning potential ratio were computed as functions of F , as were equilibrium landings and spawning biomass. Equilibrium landings were also computed as functions of biomass B , which itself is a function of F . As in computation of MSY-related benchmarks (described in §3.7), per recruit and equilibrium analyses applied the most recent selectivity patterns averaged across fleets, weighted by each fleet's F from the last three years (2020-2022) of the assessment.

3.7 Benchmarks and Reference Points

In this assessment of Tilefish, the quantities F_{MSY} , SSB_{MSY} , B_{MSY} , and MSY were estimated by the method of Shepherd (1982). In that method, the point of maximum yield is calculated from the spawner-recruit curve and parameters describing growth, natural mortality, maturity, and selectivity. The value of F_{MSY} is the F that maximizes equilibrium landings.

On average, expected recruitment is higher than that estimated directly from the spawner-recruit curve, because of lognormal deviation in recruitment. Thus, in this assessment, the method of benchmark estimation accounted for lognormal deviation by including a bias correction in equilibrium recruitment. The bias correction (ς) was computed

from the variance (σ_R^2) of recruitment deviation in log space: $\varsigma = \exp(\sigma_R^2/2)$. Then, equilibrium recruitment (R_{eq}) associated with any F is,

$$R_{eq} = \frac{R_0 [\varsigma 0.8h\Phi_F - 0.2(1-h)]}{(h-0.2)\Phi_F} \quad (8)$$

where R_0 is median-unbiased virgin recruitment, h is steepness, and Φ_F is spawning potential ratio given growth, maturity, and total mortality at age. In BAM, the calculation of total mortality includes natural and fishing mortality rates. The R_{eq} and mortality schedule imply an equilibrium age structure and an average sustainable yield (ASY). The estimate of F_{MSY} is the F giving the highest ASY, and the estimate of MSY is that ASY. The estimate of SSB_{MSY} follows from the corresponding equilibrium age structure

Estimates of MSY and related benchmarks are conditional on the selectivity pattern. The selectivity pattern used here was an average of terminal-year selectivities from each fleet, where each fleet-specific selectivity was weighted in proportion to its corresponding estimate of F averaged over the last three years (2020-2022) of the assessment. If the selectivities or relative fishing mortalities among fleets were to change, so would the estimates of MSY and related benchmarks.

The maximum fishing mortality threshold (MFMT) is defined as F_{MSY} , and the minimum stock size threshold (MSST) is defined by the SAFMC as 75% SSB_{MSY} (Restrepo et al. 1998). Overfishing is defined as $F > MFMT$ and overfished as $SSB < MSST$. Current stock size is represented as SSB in the last assessment year (2022), and current fishing mortality ($F_{current}$) is represented by the geometric mean of F from the last three years of the assessment (2020-2022). Thus, $F_{current} = F_{2020-2022}$.

3.8 Comparison to Previous Assessments

This SEDAR 89 operational assessment builds upon the SEDAR 66 with an additional 4 years of data, substantial improvements to the structure of the BAM, updates to most life history parameters, and minor changes to the configuration of the model. No new data sources were included. See §2 for changes to data included in SEDAR 89 compared with the SEDAR 66.

Changes to the life history information used in the model included:

1. constant natural mortality calculated by Hamel and Cope (2022),
2. M_a calculated proportional to inverse length following Lorenzen (2022),
3. population and female growth curves were updated using available length and age data,
4. maximum total length to whole weight and gutted weight were estimated using additional data,
5. maturity-at-age was estimated from a logistic model fit to length and converted to age using the mean length at age from the von Bertalanffy growth curve,
6. reproductive output was calculated as the number of eggs produced at age,
7. peak spawning time was derived from the plateau model of fecundity (Bubley et al. 2024),
8. uncertainty in all parameters fixed within the stock assessment were incorporated into the MCBE analysis by drawing parameters from the estimated covariance matrix or refitting the model across the range of reasonable fixed parameters (i.e., t_0).

Changes to model configuration include:

1. natural mortality at age calculated internally within the model to allow for changes in maximum and minimum age for Lorenzen M_a ,
2. biomass calculated in 1000 lb instead of metric tons,
3. recreational landings were modeled in numbers of fish and incorporated MRIP and SRHS data,
4. selectivity of commercial longline and handline included two time blocks with the break occurring after 2019 instead of after 2009,
5. selectivity of commercial longline and handline in the terminal time block was modeled as a domed shape,
6. an ageing error matrix was incorporated into the stock assessment model,
7. Beverton-Holt steepness was estimated within the model, while previously it was fixed,
8. the last year of recruitment deviates was set to 2019 based on likelihood profiling of the terminal year recruitment parameter,
9. commercial longline landings incorporated discard estimates, and
10. spawning stock biomass was calculated in trillions of eggs.

3.9 Monte Carlo/Bootstrap Ensemble (MCBE) Analysis

For the base run of the catch-age model (BAM), uncertainty in results and precision of estimates was computed through an ensemble modeling approach (Scott et al. 2016; Jardim et al. 2021) using a mixed Monte Carlo and bootstrap framework (Efron and Tibshirani 1993; Manly 1997). Monte Carlo and bootstrap methods are often used to characterize uncertainty in ecological studies, and the mixed approach has been applied successfully in stock assessment (Restrepo et al. 1992; Legault et al. 2001; SEDAR4 2004; SEDAR19 2009; SEDAR24 2010; SEDAR 66 2021). The approach is among those recommended for use in SEDAR assessments (SEDAR Procedural Guidance 2010).

The approach translates uncertainty in model input into uncertainty in model output, by fitting the model many times with different values of “observed” data and key input parameters. A chief advantage of the approach is that the results describe a range of possible outcomes, so that uncertainty is characterized more thoroughly than it could be by any single fit or small set of sensitivity runs. A minor disadvantage of the approach is that computation times can be long, though current parallel computing techniques largely mitigate those demands (i.e. computing results many times as fast as a single processor).

In this assessment, the BAM was re-fit in $n = 4000$ trials that differed from the original inputs by bootstrapping on data sources, and by Monte Carlo sampling of several key input parameters. Of the 4000 trials, 3018 were ultimately retained in the uncertainty analysis. The remaining runs were discarded because of lack of model convergence (hessian was not invertible) or unrealistic values of R_0 , steepness, or the slopes of the domed shaped selectivity curves estimated at the upper bound. Similar filtering procedure was also done in SEDAR 66, though the criterion used were different.

The MCBE should be interpreted as providing an approximation to the uncertainty associated with each output. The results are approximate for two related reasons. First, not all combinations of Monte Carlo parameter inputs are equally likely, as biological parameters might be correlated. Second, all runs are given equal weight in the results, yet some might provide better fits to data than others. Additionally, given the large CV of the recreational landings some Monte Carlo datasets are more likely than others.

3.9.1 Bootstrapping of Observed Data

To include uncertainty in time series of observed landings, and indices of abundance, multiplicative lognormal errors were applied through a parametric bootstrap. To implement this approach in the MCBE trials, random variables ($x_{s,y}$) were drawn for each year y of time series s from a normal distribution with mean 0 and variance $\sigma_{s,y}^2$ [that is, $x_{s,y} \sim N(0, \sigma_{s,y}^2)$]. Annual observations were then perturbed from their original values ($\hat{O}_{s,y}$),

$$O_{s,y} = \hat{O}_{s,y}[\exp(x_{s,y} - \sigma_{s,y}^2/2)] \quad (9)$$

The term $\sigma_{s,y}^2/2$ is a bias correction that centers the multiplicative error on the value of 1.0. Standard deviations in log space were computed from CVs in arithmetic space, $\sigma_{s,y} = \sqrt{\log(1.0 + CV_{s,y}^2)}$. The CVs used to generate bootstrap data sets of landings were supplied by the data providers (Table 2). Note that these values are different and generally higher than the CVs used to estimate landings when fitting the assessment model (i.e. 0.05 for all years and fleets). The CVs used to generate bootstrap data sets of indices of abundance were the same as those used when fitting the assessment model (Table 5).

Uncertainty in age and length compositions were included by drawing new distributions for each year of each data source, following a multinomial sampling process. Ages (or lengths) of individual fish (Table 4) were drawn at random with replacement using the cell probabilities of the original data. For each year of each data source, the number of fish sampled was the same as in the original data (Table 5).

3.9.2 Monte Carlo Sampling

In each successive fit of the model, several parameters were fixed (i.e., not estimated) at values drawn at random from distributions described below.

3.9.2.1 Maximum age for natural mortality calculation The maximum age of tilefish was randomly drawn from a uniform distribution between 37 and 45. The maximum age was used in conjunction with a bootstrap sampling of the [Then et al. \(2014\)](#) natural mortality dataset fit using the [Hamel and Cope \(2022\)](#) model to estimate constant natural mortality. The maximum age was also used to determine the oldest age over which the mortality should scale to the constant natural mortality rate.

3.9.2.2 Minimum age for natural mortality calculation The minimum age for determining the M_a re-weighting using the [Lorenzen \(2022\)](#) formulation was randomly drawn as an integer between ages 5 and 8. These values were input into the assessment model to calculate the natural mortality at age in conjunction with the growth parameters.

3.9.2.3 von Bertalanffy t_0 The t_0 parameter was a fixed value that was randomly sampled between -1 and 0. A von Bertalanffy growth model was fit to the age and length data with this fixed parameter. A growth curve for the population and for females only was determine for each fixed value of t_0 . The resulting growth curves were then input as fixed values into the stock assessment model.

3.9.2.4 Standard deviation of recruitment deviations (σ_R) In the base model, the standard deviation of recruitment deviations (σ_R) was fixed at 0.6. For each MCBE trial, a new value of σ_R was drawn from a truncated normal distribution defined by $\mu = 0.6$ and $\sigma = 0.15$ truncated to 0.3 to 1.0.

3.9.2.5 Length to weight relationship parameters Parameters for the length-weight relationship for gutted and whole weights were drawn from the covariance matrix of the respective model fits using a multivariate distribution. Parameter for these relationships were fixed within the assessment model.

3.9.2.6 Reproductive output ogive The reproductive output ogive was calculated through numerous models and uncertainty from each of the models was incorporated into the fixed ogive in the stock assessment model. Parameters for the logistic maturity at length were drawn from a multivariate distribution centered at the parameter estimates with the estimated covariance matrix. Mean length at age from the respective growth curve was used to determine proportion mature at age. Batch fecundity at age was calculated by randomly drawing parameters for the exponential relationship from the covariance matrix and run specific mean length at age. Number of batches at age were determined by the drawing parameters for the plateau model from the covariance matrix. These parameters were inserted into the function and integrated across the year to provide the number of batches per year for each model specific length at age (Bubley et al. 2024). Reproductive output was determined as the product of age specific maturity, batch fecundity, and number of batches (Figure 65)).

3.9.2.7 Time of peak spawning The parameter drawn from the plateau model for calculating the reproductive output ogive above were used to derive the peak spawning time as described in Bubley et al. (2024). This date of peak spawning was fixed within the assessment model and had very little uncertainty in the values used in the MCBE.

3.9.2.8 Initial Fishing mortality rate (F_{init}) Values of initial fishing mortality were randomly drawn from a uniform distribution between 0 and 0.2 based on similar likelihood values in a profile of the parameter (Figure 55)).

3.10 Projection Analysis

Projections were run to determine the overfishing limit (OFL) as requested in the ToRs. The structure of the projection model was the same as that of the assessment model, and parameter estimates were those from the assessment. Any time-varying quantities, such as selectivity, were fixed to the most recent values of the assessment period. A single selectivity curve was applied to calculate landings computed by averaging selectivities across fleets using geometric mean F s from the last three years of the assessment period, similar to computation of MSY benchmarks (§3.7).

Expected values of SSB (time of peak spawning), F , recruits, and landings were represented by deterministic projections using parameter estimates from the base run. These projections were built on the estimated spawner-recruit relationship with bias correction, and were thus consistent with estimated benchmarks in the sense that long-term fishing at F_{MSY} would yield MSY from a stock size at SSB_{MSY} . Uncertainty in future time series was quantified through stochastic projections that extended the ensemble model fits of the stock assessment model.

3.10.1 Initialization of Projections

Although the terminal year of the assessment is 2022, the assessment model computes abundance at age (N_a) at the start of 2023. For projections, those estimates were used to initialize N_a . However, the assessment has no information to inform the strength of 2023 recruitment, and thus it computes 2023 recruits (N_1) as the expected value, that is, without deviation from the spawner-recruit curve, and corrected to be unbiased in arithmetic space. In the stochastic projections, log-normal stochasticity was applied to these abundances after adjusting them to be unbiased in log space, with variability based on the estimate of σ_R . Thus, the initial abundance in year one of projections (2023) included this variability in N_1 . Additionally, variability was added to the abundance of ages 2

through 4 to account for the lack or recruitment deviates in the last 3 years of the assessment. The deterministic projections were not adjusted in this manner, because deterministic recruitment follows Beverton-Holt expectation.

Fishing rates that define the projections were assumed to start in 2023. Because the assessment period ended in 2022, the projections required an interim period (2023–2024). Fishing mortality during this interim period was set at the estimate of F_{current} from the assessment model.

3.10.2 Uncertainty of Projections

To characterize uncertainty in future stock dynamics stochasticity was included in replicate projections, each an extension of a single assessment fit from the ensemble. Thus, projections carried forward uncertainties in natural mortality, life history relationships, as well as in estimated quantities such as spawner-recruit parameters (R_0 , h , and σ_R), selectivity curves, and in initial (start of 2023) abundance at age.

Initial and subsequent recruitment values were generated with stochasticity using a Monte Carlo procedure, in which the estimated Beverton-Holt model of each MCB fit within the ensemble is used to compute expected annual recruitment values (\bar{R}_y). Variability is added to the mean values by choosing multiplicative deviations at random from a log-normal distribution,

$$R_y = \bar{R}_y \exp(\epsilon_y). \quad (10)$$

Here ϵ_y is drawn from a normal distribution with mean 0 and standard deviation σ_R , where σ_R is the standard deviation from the relevant ensemble model run.

The procedure generated 20,000 replicate projections of models within the ensemble drawn at random (with replacement) from the MCBE. In cases where the same model run was drawn, projections would still differ as a result of stochasticity in projected recruitment streams. Central tendencies were represented by the deterministic projections of the base run, as well as by medians of the stochastic projections. Precision of projections was represented graphically by the 5th and 95th percentiles of the replicate projections.

3.10.3 Projection Scenarios

Projections were run to determine the overfishing limit (OFL) as requested in the ToRs. In the projections, management started in 2023, the earliest year likely to implement management changes. Projections were carried forward to 2027. Scenarios 1 and 2 were considered to determine the OFL and scenarios 3 was considered to determine the ABC. A P^* of 32.5 is presented based on the projections from SEDAR 66, though a range of different values were run but were not presented for brevity. In all scenarios $F = F_{\text{current}}$ from 2023 to 2024:

- Scenario 1: $F = F_{P^*_{50\%}}$ from 2023 to 2027
- Scenario 2: $F = F_{\text{MSY}}$ from 2023 to 2027
- Scenario 3: $F = F_{P^*_{32.5\%}}$ from 2023 to 2027

4 Stock Assessment Results

4.1 Measures of Overall Model Fit

The Beaufort assessment model (BAM) generally fit well to the available data. Predicted age compositions from each fishery were reasonably close to observed data in most years (Figure 3). Fits to length compositions for the recreational fleet were not quite as good, but the data were also very variable, probably due to small sample sizes (often < 50 fish per year; Figure 3 and Tables 3 and 4). The model was configured to fit observed commercial and recreational landings closely (Figures 4 to 6). The fit to the commercial longline index captured the general trend well but not all annual fluctuations (Figure 7). The fit to the MARMAP longline survey index (Figure 8) did not capture the general trend very well due in part to the large CVs associated with the index (Table 5).

4.2 Parameter Estimates

Estimates of all parameters from the catch-age model are shown in §B. No parameters were hitting bounds (Figures 40 and 41). Estimates of management quantities and some key parameters, such as those of the spawner-recruit model, are reported in sections below.

4.3 Total Abundance, Spawning Biomass, and Recruitment

Total abundance shows a decline in the early 1980s (Figure 9 and Table 7) concurrent with large increase in landings, especially in the commercial longline fleet (Figures 18 and 19 and Tables 16 and 17). Abundance declined until the late 1990s and then rapidly increased around 2000. Since then, abundance has fluctuated between approximately 1.5-2 million fish peaking in the mid 2000s, but then declining until 2019 and slightly increase at the end of the assessment attributed to the recruitment determined by the stock recruitment without deviates. Older ages classes were truncated beginning in the 1980s; abundance in older ages declined through the mid 1990s and then expanded after the 2010s (Figure 9 and Table 7). Spawning stock biomass (SSB) declined in the early 1980s and continued to decline to a low point in 1995 and 2000. Since 2000, SSB increased until 2009 but has decreased gradually since then (Figure 12 and Table 10). Recruitment has fluctuated during the period when deviations were estimated (1982-2019) ranging from 194,685 to 914,761 fish with peaks in 1988, 1991, and 1999, but with little evidence of a long term trend (Figure 11 upper panel ; Table 10). Similarly, recruitment deviations showed fluctuations over this same period with no evidence of a long-term trend (Figure 11 lower panel).

4.4 Selectivity

Selectivity of the MARMAP longline survey is shown in Figure 13, selectivities of landings from commercial and recreational fleets are shown in Figures 14 and 15. In the most recent years, full selection occurred near age-4 in the recreational fleet, age-6 in the commercial handline fleet, age-9 in the MARMAP longline survey, and age-7 in the commercial longline fleet. Logistic selectivity functions were used for all fleets prior to 2020, but domed selectivities were used for the commercial handline and longline fleets in the latter time block.

Average selectivities of landings were computed from F -weighted selectivities in the most recent period of regulations (Figure 16). These average selectivities were used to compute point estimates of benchmarks. All selectivities from the most recent period, including average selectivities, are tabulated in Table 11. In the average selectivity, full selection occurred near age-7, like the commercial longline fleet which is responsible for > 80% of the total F in most years (Figure 17).

4.5 Landings, Fishing Mortality, Quotas, and Biomass

From 1972 to 1980, total landings were low (< 200 klb; [Figures 18 and 19](#) and [Tables 16 and 17](#)) and estimated fishing mortality rate (F) was very low (≤ 0.02 ; [Figure 17](#) and [Table 12](#)), with stock biomass still near virgin (B_0). Since this early period of low exploitation, landings and F have occurred in about five main periods of exploitation, each lasting 5-10 years. The first period from 1981 to 1986 represents a set of years with the highest landings in the South Atlantic Tilefish stock, all of which were near or above 1000 klb, with peak landings in 1982 over 2600 klb. During this period F increased to range between 0.1 to nearly 0.4. Estimated biomass during this first period dropped dramatically, from 92 to about 45% of B_0 . The second period begins in 1987 with landings dropping sharply down below 300 klb, but quickly increasing again to a range of 600 to 900 klb for most years through 1995. Due to the decline in biomass during the first period, this second period exhibits lower landings but higher F than the first period, with most values of F 0.2 to above 0.4. During the second period, biomass continued to decline to 32% of B_0 . In the third period, from 1996 to 2002, landings decreased sharply again, remaining between 300-400 klb in most years through 2002. Total F also declined but remained within a range similar to the first period (0.1-0.3). Biomass in 1995 was the lowest in the history of the stock, but increased slightly over the period. In 2003 landings dropped to 235 klb, the lowest level in the history of the stock since 1980. This fourth period from 2003 to 2011 was characterized by a gradual increase back up to the mid-300 klb range, as F remained low (0.1-0.18). This fourth period marks a period of recovery from 32 to 47% of B_0 . In 2006 the commercial quota was substantially reduced from 1,001 klb to 295 klb, and resulted in a reduced fishing season from 365 to 295 days in 2006 (see §I. Table 2.6.2). The quota remained at this level through 2010, and was reduced slightly in 2011 (282 klb) resulting in the commercial fishery being open for only 67 days. In 2012, the commercial quota increased to 541 klb following results of SEDAR 25, and remained at this level through 2017. An increase in landings followed as the commercial fleets repeatedly reached the quota, and total landings remained in the 490-670 klb range again through 2017, until dropping back below 340 klb in 2018 when the quota was again reduced to 313 klb. Values of F generally increased during this period (0.16-0.22) while biomass was again in decline.

4.6 Spawner-Recruitment Parameters

The estimated Beverton–Holt spawner-recruit curve is shown in [Figure 20](#), along with the effect of density dependence on recruitment, depicted graphically by recruits per spawner as a function of spawners (spawning biomass). Values of recruitment-related parameters were as follows: steepness $h = 0.6$, unfished age-1 recruitment $R_0 = 509,900$, unfished spawning biomass (1000 lb) per recruit $\phi_0 = 2.759$, and standard deviation of recruitment residuals in log space $\hat{\sigma}_R = 0.6$ (fixed; which resulted in bias correction of $\zeta = 1.2$). Uncertainty in these quantities was estimated from the MCBE ([Figure 21](#)).

4.7 Per Recruit and Equilibrium Analyses

Yield per recruit and spawning potential ratio were computed as functions of F ([Figure 22](#)). As in computation of MSY-related benchmarks, per recruit analyses applied the most recent selectivity patterns averaged across fisheries, weighted by F from the last three years (2020 – 2022). The F that provides 40% SPR is $F_{40\%} = 0.213$, and 30% is $F_{30\%} = 0.306$.

As in per recruit analyses, equilibrium landings and spawning biomass were computed as functions of F ([Figure 23](#)). By definition, the F that maximizes equilibrium landings is F_{MSY} , and the corresponding landings and spawning biomass are MSY and SSB_{MSY} .

4.8 Benchmarks / Reference Points

As described in §3.7, biological reference points (benchmarks) were derived analytically assuming equilibrium dynamics, corresponding to the expected spawner-recruit curve (Figure 20). These benchmarks are conditional on the estimated selectivity functions and the relative contributions of each fleet's fishing mortality. Furthermore the selectivity pattern used here was the effort-weighted selectivities at age, with effort from each fishery estimated as the full F averaged over the last three years of the assessment (2020-2022).

Reference points estimated were F_{MSY} , MSY , B_{MSY} and SSB_{MSY} . Estimates of benchmarks are summarized in Table 18. Standard errors of benchmarks were approximated as those from the MCBE (§3.9).

Maximum likelihood estimates (base run) of benchmarks, as well as median values from MCBE, are summarized in Table 18. Point estimates of MSY -related quantities were $F_{MSY} = 0.216$ (y^{-1}), $MSY = 545$ (1000 lb GW), $B_{MSY} = 6191$ (1000 lb), $MSST = 0.385$ (trillion eggs), and $SSB_{MSY} = 0.514$ (trillion eggs). The estimate of SSB_{MSY} is about 37% of the unfished spawning biomass. Median estimates were $F_{MSY} = 0.183$ (y^{-1}), $MSY = 564$ (1000 lb GW), $B_{MSY} = 7264$ (100 lb), $MSST = 0.488$ (trillion eggs), and $SSB_{MSY} = 0.651$ (trillion eggs). Distributions of these benchmarks from the MCBE are shown in Figure 24.

4.9 Status of the Stock and Fishery

Estimated time series of stock status ($SSB/MSST$) showed a rapid decline during the 1980s and a slower decline during the 1990s, to a minimum value in 1995. From 1995 through 2011 stock status improved, but has been in decline again since 2012 (Figure 25 and Table 10).

Current stock status was estimated in the base run to be $SSB_{2022}/MSST = 1.261$ (Table 18), indicating that the stock is not overfished. Throughout its history, the stock has not dropped below $MSST$ but was below the SSB_{MSY} in the late 1990s. However, this result should be viewed with caution because the $msst$ is based on the domed shaped selectivity at the end of the assessment, whereas the fishing during this time period exhibited a logistic selectivity curve. Results from the MCBE suggested that the estimate of SSB relative to SSB_{MSY} and the status relative to $MSST$ is highly uncertain (Figures 27 and 28). The slight majority of MCBE runs (54%) agreed with the stock status result from the base model and the median of the MCBE analysis ($SSB_{2022}/MSST = SSBMSST_{medVal}$). However, the majority of models in the MCBE analysis (74.4%), the base model, and the median of the MCBE models show that the SSB is below SSB_{MSY} . Therefore, the stock is technically not overfished but is likely below the spawning stock size that will yield MSY .

Age structure estimated by the base run during 2022 shows numbers of fish at all age classes declined over the assessment period but especially older age classes. Numbers of Tilefish ages-15 and older reached their lowest point in 2000. During the recovery of the stock in the late 2010s, numbers of older fish increased substantially back above the predicted numbers at F_{MSY} equilibrium by 2016. At the end of the assessment, the plus group was higher than in 2016, but ages 7-19 years older have declined (Figure 29).

F/F_{MSY} has been continually increasing since 2008 and exceeds F_{MSY} in the terminal year (Figure 25 and Table 10). Additionally, there is considerable uncertainty in F/F_{MSY} as demonstrated by the MCBE, especially toward the end of the assessment period (Figure 25). Current fishery status in the terminal year, with current F represented by the geometric mean from 2020 to 2022 ($F_{current} = F_{2020-2022} = 0.216$), was estimated by the base run to be $F_{2020-2022}/F_{MSY} = 1$ (Table 18). However, the median from the MCBE was estimated as $F_{2020-2022}/F_{MSY} = 1.16$ and the analysis shows that there is a lot of uncertainty in the status of the fishery (Figures 27 and 28). Only 35% of MCBE runs agreed with the fishing status result from the base model, while the majority of models agree with the fishing status of the median of the MCBE. Note that F_{MSY} is based on average F s from last three years of the assessment and thus it is not the technically correct denominator for all years going back in time. Thus, caution should be applied when interpreting F status back in time. Additionally, F_{MSY} is based on the assumption that the domed shape selectivity means that older fish are not vulnerable to fishing mortality, which is likely only a transient artifact of management restrictions on harvest and not a limitation of the gear to catch these older fish.

4.10 Comparison to Previous Assessments

The benchmark assessment for Tilefish, SEDAR 04, was completed in 2004 with an assessment period 1961-2002 (SEDAR 04 2004). SEDAR 25 was a standard assessment completed in 2011 with an assessment period spanning 1962-2010 (SEDAR 25 2011). Several important changes were made during SEDAR 25 (e.g. M , h , SSB units) that make it somewhat difficult to compare SEDAR 04 with later assessments. An update assessment was completed in 2016 with an assessment period of 1962-2014 (SEDAR 25 2016). Current management of South Atlantic Tilefish is based on SEDAR 66 with an assessment period of 1972-2018 (SEDAR 66 2021).

As of 2002, the stock was not overfished ($SSB_{2002}/MSST = 1.27$), but overfishing was occurring ($F_{2002}/F_{MSY} = 1.53$; SEDAR 04 2004). Terminal status estimates in SEDAR 25 found that the Tilefish stock was not overfished ($SSB_{2010}/MSST = 2.42$), and it was also not undergoing overfishing ($F_{2008-2010}/F_{MSY} = 0.36$; SEDAR 25 2011). Terminal status estimates in the SEDAR 25 showed the stock was not overfished ($SSB_{2014}/MSST = 1.13$), but overfishing was occurring ($F_{2008-2010}/F_{MSY} = 1.22$; SEDAR 25 2016). SEDAR 66 found that the status of the stock was not overfishing ($SSB_{2018}/MSST = 1.235$) and was not undergoing overfishing ($F_{2016-2018}/F_{MSY} = 0.95$; SEDAR 66 2021). However, SEDAR 66 showed there was considerable uncertainty in the fishing status and the stock in 2018 was below SSB_{MSY} .

Values from the current SEDAR 89 assessment contrast with the stock status designation from SEDAR 04 ($SSB_{2002}/MSST = 1.31$) but concur with the not overfished status from SEDAR 25 ($SSB_{2011}/MSST = 1.93$), the SEDAR 66 ($SSB_{2018}/MSST = 1.49$; Table 10).

The general pattern in time series of $SSB/MSST$ in SEDAR 89 was similar to the SEDAR 66. However, the stock did not start at as high of a value and the minimum value reached in the mid-1990s did not go below 1. The general pattern in the time series of F/F_{MSY} in SEDAR 89 was also similar to the SEDAR 66, but was shifted downward so that it appears lower in all years. This is particularly true of the period from approximately 1990-2005. The trend and magnitude of F/F_{MSY} in SEDAR 66 were quite similar to SEDAR 89, but there is much less uncertainty at the end of the time series in the current assessment.

Input values of constant M have been lower for the previous four Tilefish assessments (terminal years: 2002, 2010, 2014, 2018, 2022; M : 0.07, 0.1083, 0.1083, 0.1038, 0.135), where M in SEDAR 04 was the lowest value and was not used to scale age-varying M . Steepness was fixed in previous assessments at a value near that estimated in the current assessment (h : 0.72, 0.84, 0.84, 0.84, 0.6). The estimate of F_{MSY} in SEDAR 04 was considerably lower than in later assessments (F_{MSY} : 0.043, 0.185, 0.236, 0.3, 0.216). The estimate of MSY was also much lower in SEDAR 04 than in later assessments (MSY , klb: 335, 638, 560, 518, 545). In SEDAR 04 SSB was measured in units of female biomass ($MSST$, mt: 659) and thus was not comparable to later assessments which were in units of gonad weight ($MSST$, mt W_{gonad} : 19.0, 16.4, 14) and is not comparable to the current assessment in units of trillions of eggs ($MSST = 0.385$).

4.11 Sensitivity Analyses

Sensitivity runs, described in §3.3, may be useful for evaluating implications of assumptions in the base model, and for interpreting MCBE results in terms of expected effects from input parameters. Time series of F/F_{MSY} and $SSB/MSST$ are plotted to demonstrate sensitivity to natural mortality (Figure 30), the steepness of the stock-recruit relationship (Figure 31), the value of initial F (F_{init} ; Figure 32), and the fixed growth t_0 parameter and resulting growth curve and natural mortality (Figure 33).

The qualitative results on terminal stock and fishing status were the same for eight of the sensitivity runs (S1-S4: sensitivity to M , S6: high h , S7: low F_{init} , and S9-S10: both sensitivities to t_0 Figures 30 to 33).

However, the other two sensitivity runs disagreed, and suggested that the stock was overfished ($SSB_{2022} < MSST$) and undergoing overfishing ($F_{2020-2022} > F_{MSY}$). These exceptions were runs S5 (low h) and S8 (high F_{init}). Sensitivity analyses were in general agreement with those of the MCBE that there is considerable uncertainty in the stock and fishing status of South Atlantic Tilefish.

4.12 Retrospective Analyses

Retrospective analyses did not suggest any patterns of substantial over- or underestimation in terminal-year estimates of F/F_{MSY} , SSB/MSST , or B (Figure 34). Recruitment plots show an increase through the entire time series as a result of estimating steepness at the upper bound once the terminal year is removed. The domed selectivity at the end of the time series also changed as a result of the loss of one of the three years of age compositions that informed these parameters. This suggests that there may be considerable uncertainty in the steepness parameter and estimation is data dependent, which is generally true of statical catch at age models. It appears that steepness is informed primarily by the age composition of the commercial longline in 2022 and the removal of this data source results in an unreasonable estimated value of 0.99 for all models in the retrospective analysis. Despite this, calculated Mohn's rho were within reasonable values for all parameters.

4.13 Projections

Projection results for Tilefish are shown in Figures 35 to 37 and Tables 19 to 21. Among all scenarios considered, the probability that SSB_{MSY} exceeds MSST [$P(> \text{MSST})$] is at least 0.50 in all years of all projections. Thus, under no management prescription considered in the current projections is the South Atlantic Tilefish stock predicted to be overfished.

5 Discussion

5.1 Comments on Assessment Results

Estimated benchmarks played a central role in this assessment. Values of MSST and F_{MSY} were used to gauge the status of the stock and fishery. Computation of benchmarks was conditional on selectivity in the terminal year of the stock assessment. A significant change in the age composition of the commercial fisheries occurred in 2020. The cause of this drastic shift to younger ages and the absence of older fish is unclear. It is currently hypothesized that there has been a recent change in fishing behavior in response to the restriction implemented in 2017. However, if the change observed in the age composition is due to a change in the population dynamics of tilefish then the model will likely be misspecified and could be in a much worse status. If selectivity patterns change in the future, for example an increase in the catch of older fish resulting in a return to a logistic selectivity, estimates of benchmarks would likely change as well and could result in overfishing of the species.

The base run of the BAM indicated that the stock is not overfished ($\text{SSB}_{2022}/\text{MSST} = 1.261$), and that overfishing is not occurring, but is fully exploited ($F_{2020-2022}/F_{\text{MSY}} = 1$). However, the median of the MCBE analysis indicates that the stock is barely not overfished ($\text{SSB}_{2022}/\text{MSST} = 1.04$), is currently undergoing overfishing ($F_{2020-2022}/F_{\text{MSY}} = 1.16$) and is below SSB_{MSY} ($\text{SSB}/\text{SSB}_{\text{MSY}2022} = 0.78$). MCBE analyses show that there is a lot of uncertainty in these status results (Figure 28).

The median of the MCBE analysis did not provide the same status as the base BAM model. Additionally, the base BAM model was not generally in the center of the distribution of stock status or benchmarks. The initial fishing mortality (F_{init}) was the only parameter fixed during the MCBE analysis where the value of the base model was not close to the median of the distribution and was not near the center. Therefore, this parameter likely causes the apparent difference between the MCBE median and the base model.

The current assessment lacked an index of abundance for years after 2016 (i.e., the last 6 years of the assessment). The likelihood profiles of model parameters indicated that the age composition was influential in the estimation of the stock recruitment parameters (R_0 and h , i.e., key parameters that set the scale of the population). Future assessments will likely benefit from the addition of SADLS data to provide a fishery-independent index of abundance. Future assessments should pay close attention to the age composition in the commercial fisheries for a potential return to logistic selectivity and potentially implement another time block in the selectivity.

5.2 Comments on Projections

As usual, projections should be interpreted in light of the model assumptions and key aspects of the data. Some major considerations are the following:

- In general, projections of fish stocks are highly uncertain, particularly in the long term (e.g., beyond 5–10 years).
- Although projections included many major sources of uncertainty, they did not include structural (model) uncertainty. That is, projection results are conditional on one set of functional forms used to describe population dynamics, selectivity, recruitment, etc.
- Fisheries were assumed to continue fishing at their estimated current proportions of total effort, using the estimated current selectivity patterns. Benchmarks (e.g. MSY) are conditional on the estimated selectivity functions and the relative contributions of each fleet’s fishing mortality. New management regulations that reallocate harvest in a way that alters proportions of F by fleet or selectivity patterns would likely affect projection results.
- The projections assumed that the estimated spawner-recruit relationship applies in the future and that past residuals represent future uncertainty in recruitment. If future recruitment is characterized by runs of large or small year classes, possibly due to environmental or ecological conditions, stock trajectories may be affected.
- Projections apply the Baranov catch equation to relate F and landings using a one-year time step, as in the assessment. The catch equation implicitly assumes that mortality occurs throughout the year. This assumption is violated when seasonal closures are in effect, introducing additional and unquantified uncertainty into the projection results.

6 Research Recommendations

1. From the previous assessment (SEDAR 66)
 - (a) Re-examine the quantity and quality of biological samples collected by "Other" commercial gears. If adequate, consider methods for inclusion.
 - (b) Monitor the quantity of commercial and recreational discards and consider methods for inclusion if deemed necessary.
 - (c) More closely examine historical length composition data used in the assessment and consider alternate methods for incorporating this information in the model.
 - (d) Collect data to investigate the stock structure of tilefish in the Atlantic ocean through a multifaceted approach (e.g., genetics, meristics, diet, otolith chemistry, life history characteristics, etc.)
 - (e) Increase age sampling to improve composition data
2. From the current assessment (SEDAR 89)
 - (a) following the guidance of the SADLS review, incorporate the fishery-independent standardized index of abundance and associated age composition
 - (b) Investigate potential mechanisms for the domed selectivity that started in 2020
 - (c) Collect and process more histological samples to reduce the uncertainty in the batch fecundity estimates to provide better estimates of SSB.

7 References

- Baranov, F. I. 1918. On the question of the biological basis of fisheries. *Nauchnye Issledovaniya Ikhtiologicheskii Instituta Izvestiya* **1**:81–128.
- Beddington, J. R., and J. G. Cooke, 1983. The potential yield of fish stocks. *FAO Fish. Tech. Pap.* 242, 47 p.
- Bubley, W. J., K. J. Kolmos, and M. T. Vincent, 2024. Characterization of Reproductive Parameters for Tilefish (*Lopholatilus chamaeleonticeps*) in Atlantic Waters from North Carolina to Florida. Technical report, SEDAR89-WP-03, North Charleston, SC.
- Dichmont, C. M., R. A. Deng, A. E. Punt, J. Brodziak, Y. Chang, J. Cope, J. N. Ianelli, C. M. Legault, R. D. Methot Jr., C. E. Porch, M. H. Prager, and K. W. Shertzer. 2016. A review of stock assessment packages in the United States. *Fisheries Research* **183**:447–450.
- Doolet, J. K., 1978. Systematics and biology of the tilefishes (Perciformes: Brachistegidae and Malacanthidae), with descriptions of two new species. Technical report, NOAA Tech. Rep. NMFS Circ. 411.
- Efron, B., and R. Tibshirani. 1993. *An Introduction to the Bootstrap*. Chapman and Hall, London.
- Fisch, N., R. Ahrens, K. Shertzer, and E. Camp. 2022. An empirical comparison of alternative likelihood formulations for composition data, with application to cobia and Pacific hake. *Canadian Journal of Fisheries and Aquatic Sciences* **79**:1745–1764.
- Fisch, N., E. Camp, K. Shertzer, and R. Ahrens. 2021. Assessing likelihoods for fitting composition data within stock assessments, with emphasis on different degrees of process and observation error. *Fisheries Research* **243**:106069.
- Fournier, D. A., H. J. Skaug, J. Ancheta, J. Ianelli, A. Magnusson, M. N. Maunder, A. Nielsen, and J. Sibert. 2012. AD Model Builder: using automatic differentiation for statistical inference of highly parameterized complex nonlinear models. *Optimization Methods and Software* **27**:233–249.
- Francis, R. 2017. Revisiting data weighting in fisheries stock assessment models. *Fisheries Research* **192**:5–15.
- Grimes, C. B., S. Turner, and K. Able. 1983. A technique for tagging deep-water fish. *Fishery Bulletin* **81**:663–666.
- Hamel, O. S., and J. M. Cope. 2022. Development and considerations for application of a longevity-based prior for the natural mortality rate. *Fisheries Research* **256**:106477.
- Jardim, E., M. Azevedo, J. Brodziak, E. N. Brooks, K. F. Johnson, N. Klibansky, C. P. Millar, C. Minto, I. Mosqueira, R. D. M. Nash, P. Vasilakopoulos, and B. K. Wells. 2021. Operationalizing ensemble models for scientific advice to fisheries management. *ICES Journal of Marine Science* URL <https://doi.org/10.1093/icesjms/fsab010>.
- Katz, S. J., C. B. Grimes, and K. W. Able. 1983. Delineation of tilefish, *Lopholatilus chamaeleonticeps*, stocks along the United States east coast and in the Gulf of Mexico. *Fisheries Bulletin* **81**:41–50.
- Legault, C. M., J. E. Powers, and V. R. Restrepo. 2001. Mixed Monte Carlo/bootstrap approach to assessing king and Spanish mackerel in the Atlantic and Gulf of Mexico: Its evolution and impact. *American Fisheries Society Symposium* **24**:1–8.
- Li, B., K. W. Shertzer, P. D. Lynch, J. N. Ianelli, C. M. Legault, E. H. Williams, R. D. Methot Jr., E. N. Brooks, J. J. Deroba, A. M. Berger, S. R. Sagarese, J. K. T. Brodziak, I. G. Taylor, M. A. Karp, C. R. Wetzel, and M. Supernaw. 2021. A comparison of four primary age-structured stock assessment models used in the United States. *Fishery Bulletin* **119**:149–167.
- Lorenzen, K. 2022. Size- and age-dependent natural mortality in fish populations: Biology, models, implications, and a generalized length-inverse mortality paradigm. *Fisheries Research* **106454**.

- Manly, B. F. J. 1997. *Randomization, Bootstrap and Monte Carlo Methods in Biolog*, 2nd edition. Chapman and Hall, London.
- Mertz, G., and R. Myers. 1996. Influence of fecundity on recruitment variability of marine fish. *Canadian Journal of Fisheries and Aquatic Sciences* **53**:1618–1625.
- Methot, R. D., and C. R. Wetzel. 2013. Stock synthesis: a biological and statistical framework for fish stock assessment and fishery management. *Fisheries Research* **142**:86–99.
- Nuttall, M. A., and V. M. Matter. 2020. Recreational Survey Data for Tilefish in the South Atlantic. SEDAR66-WP01. SEDAR, North Charleston, SC. pages 1–25.
- Pennington, M., and J. H. Volstad. 1994. Assessing the effect of intra-haul correlation and variable density on estimates of population characteristics from marine surveys. *Biometrics* **50**:725–732.
- Quinn, T. J., and R. B. Deriso. 1999. *Quantitative Fish Dynamics*. Oxford University Press, New York, New York.
- Restrepo, V. R., J. M. Hoenig, J. E. Powers, J. W. Baird, and S. C. Turner. 1992. A simple simulation approach to risk and cost analysis, with applications to swordfish and cod fisheries. *Fishery Bulletin* **90**:736–748.
- Restrepo, V. R., G. G. Thompson, P. M. Mace, L. L. Gabriel, L. L. Wow, A. D. MacCall, R. D. Methot, J. E. Powers, B. L. Taylor, P. R. Wade, and J. F. Witzig, 1998. Technical guidance on the use of precautionary approaches to implementing Natinoal Standard 1 of the Magnuson-Stevens Fishery Conservation and Management Act. NOAA Technical Memorandum-F/SPO-31.
- Scott, F., E. Jardim, C. Millar, and S. Cervino. 2016. An applied framework for incorporating multiple sources of uncertainty in fisheries stock assessments. *PLOS ONE* **11**:1–21.
- SEDAR 04, 2004. SEDAR4 Stock Assessment Report 1 SECTION III.B Assessment of Tilefish, *Lopholatilus chamaeleonticeps*, in the South Atlantic Fishery Management Council Management Area. SEDAR, North Charleston, SC.
- SEDAR 25, 2011. SEDAR 25: South Atlantic Tilefish. SEDAR, North Charleston, SC.
- SEDAR 25, 2016. SEDAR 25: Stock Assessment of Golden Tilefish off the Southeastern United States, 2016 SEDAR Update Assessment. SEDAR, North Charleston, SC.
- SEDAR 66, 2021. SEDAR 60 SSouth Atlantic Tilefish Stock Assessment Report. SEDAR, North Charleston SC.
- SEDAR Procedural Guidance, 2010. SEDAR Procedural Workshop IV: Characterizing and Presenting Assessment Uncertainty.
- SEDAR19, 2009. SEDAR 19: South Atlantic Red Grouper. SEDAR, North Charleston, SC.
- SEDAR24, 2010. SEDAR 24: South Atlantic Red Snapper. SEDAR, North Charleston, SC.
- SEDAR4, 2004. SEDAR 4: Stock assessment of the deepwater snapper-grouper complex in the South Atlantic. SEDAR, North Charleston, SC.
- Shepherd, J. G. 1982. A versatile new stock-recruitment relationship for fisheries, and the construction of sustainable yield curves. *Journal du Conseil pour l'Exploration de la Mer* **40**:67–75.
- Shertzer, K. W., M. H. Prager, D. S. Vaughan, and E. H. Williams, 2008. Fishery models. Pages 1582–1593 *in* S. E. Jorgensen and F. Fath, editors. *Population Dynamics*. Vol. [2] of *Encyclopedia of Ecology*, 5 vols. Elsevier, Oxford.
- Steimle, F. W., C. A. Zetlin, P. L. Berrien, D. L. Johnson, and S. Chang, 1999. Essential fish habitat source document. Tilefish, *Lopholatilus chamaeleonticeps*, life history and habitat characteristics. Government document.

- Sulak, K. J., and S. W. Ross. 1996. Lilliputian bottom fish fauna of the Hatteras upper middle continental slope. *Journal of Fish Biology* **49**:91–113.
- Then, A. Y., J. M. Hoenig, N. G. Hall, and D. A. Hewitt. 2014. Evaluating the predictive performance of empirical estimators of natural mortality rate using information on over 200 fish species. *ICES Journal of Marine Science* **72**:82–92.
- Thompson, K., S. Atkinson, and G. Decossas, 2024. Estimated Commercial Discards of South Atlantic Golden Tilefish (*Lopholatilus chamaeleonticeps*) Using Limited Observer Data. Technical report, SEDAR89-WP-05.
- Thorson, J. T., K. F. Johnson, R. D. Methot, and I. G. Taylor. 2017. Model-based estimates of effective sample size in stock assessment models using the Dirichlet-multinomial distribution. *Fisheries Research* **192**:84–93.
- Williams, E. H., and K. W. Shertzer, 2015. Technical documentation of the Beaufort Assessment Model (BAM). NOAA Technical Memorandum-NMFS-SEFSC-671.

8 Tables

Table 1. Observed time series of landings (L) for commercial handline (cH), commercial longline (cL), and recreational (rA). Commerical landings are in units of 1000 lb gutted weight, while recreational landings are in thousands of fish.

Year	L.cH	L.cL	L.rA
1972	0.40	4.74	.
1973	2.17	25.82	.
1974	5.25	62.59	.
1975	8.98	106.29	.
1976	9.41	107.21	.
1977	8.82	40.63	.
1978	23.07	55.85	.
1979	16.61	85.14	.
1980	49.69	148.01	.
1981	117.47	665.27	227.08
1982	242.81	2421.11	0.01
1983	99.42	1392.88	0.39
1984	69.48	925.96	7.73
1985	64.64	855.30	40.28
1986	60.22	941.26	0.06
1987	20.52	248.92	2.06
1988	33.13	431.67	0.48
1989	51.64	686.18	0.01
1990	51.98	699.76	0.45
1991	53.41	706.62	0.14
1992	48.98	787.80	2.65
1993	12.75	960.01	0.01
1994	99.53	706.33	2.01
1995	79.33	594.19	0.01
1996	38.42	318.36	1.34
1997	42.47	337.94	11.31
1998	35.31	334.21	0.35
1999	28.45	477.80	1.17
2000	40.47	664.66	3.28
2001	118.73	274.57	4.00
2002	120.96	230.79	2.00
2003	70.68	162.68	7.89
2004	37.40	231.50	13.68
2005	35.35	221.38	35.67
2006	36.47	357.24	7.54
2007	37.73	233.59	1.66
2008	19.63	263.22	0.04
2009	12.61	283.49	25.40
2010	23.21	307.21	6.22
2011	9.44	317.89	10.62
2012	49.15	420.26	5.66
2013	39.71	456.35	4.85
2014	120.69	524.25	4.42
2015	124.43	362.80	8.45
2016	99.25	390.30	15.53
2017	102.59	436.90	4.04
2018	60.77	382.48	9.59
2019	75.62	423.81	43.02
2020	84.46	379.84	6.25
2021	88.22	415.40	7.94
2022	66.03	412.74	10.48

Table 2. Observed time series of CVs used in the Monte Carlo/Bootstrap Ensemble (MCBE) associated with landings (L) for commercial handline (cH), commercial longline (cL), and recreational (mrip and headboat srhs). These CVs were used to generate bootstrap data sets in the ensemble model analysis only. When fitting the assessment model, CVs of 0.05 were used for estimating landings.

Year	L.cH	L.cL	L.mrip	L.srhs
1972	0.05	0.05	.	.
1973	0.05	0.05	.	.
1974	0.05	0.05	.	.
1975	0.05	0.05	.	.
1976	0.05	0.05	.	.
1977	0.05	0.05	.	.
1978	0.05	0.05	.	.
1979	0.05	0.05	.	.
1980	0.05	0.05	.	.
1981	0.05	0.05	1.00	0.25
1982	0.05	0.05	.	0.49
1983	0.05	0.05	1.00	.
1984	0.05	0.05	1.00	.
1985	0.05	0.05	0.99	.
1986	0.05	0.05	1.00	.
1987	0.05	0.05	0.98	0.55
1988	0.05	0.05	1.00	.
1989	0.05	0.05	.	0.63
1990	0.05	0.05	1.00	0.58
1991	0.05	0.05	1.00	.
1992	0.05	0.05	0.69	0.44
1993	0.05	0.05	.	.
1994	0.05	0.05	0.94	0.54
1995	0.05	0.05	.	.
1996	0.05	0.05	0.98	.
1997	0.05	0.05	0.70	0.54
1998	0.05	0.05	1.00	.
1999	0.05	0.05	0.94	0.75
2000	0.05	0.05	0.67	.
2001	0.05	0.05	0.47	.
2002	0.05	0.05	0.70	.
2003	0.05	0.05	0.55	.
2004	0.05	0.05	0.72	.
2005	0.05	0.05	0.57	.
2006	0.05	0.05	0.56	.
2007	0.05	0.05	0.69	.
2008	0.05	0.05	1.00	.
2009	0.05	0.05	0.83	.
2010	0.05	0.05	0.59	.
2011	0.05	0.05	0.73	.
2012	0.05	0.05	0.50	.
2013	0.05	0.05	0.53	0.13
2014	0.05	0.05	0.56	0.05
2015	0.05	0.05	0.51	0.07
2016	0.05	0.05	0.40	0.22
2017	0.05	0.05	0.57	0.06
2018	0.05	0.05	0.65	0.06
2019	0.05	0.05	0.77	0.05
2020	0.05	0.05	0.71	0.05
2021	0.05	0.05	0.60	0.05
2022	0.05	0.05	0.36	0.05

Table 3. Sample sizes (number of trips) of length compositions (*lcomp*) or age compositions (*acomp*) by survey or fleet. Data sources are recreational (*rA*), commercial handline (*cH*), commercial longline (*cL*), and the MARMAP longline survey (*sM*).

Year	<i>lcomp.rA</i>	<i>acomp.cH</i>	<i>acomp.cL</i>	<i>acomp.sM</i>
1972
1973
1974
1975
1976
1977
1978
1979
1980
1981
1982
1983
1984
1985
1986
1987
1988
1989
1990
1991
1992	.	.	10	.
1993	.	.	16	.
1994
1995	.	.	24	.
1996	.	.	11	.
1997	.	5	8	11
1998	.	5	10	.
1999	.	5	16	19
2000	.	11	17	.
2001	10	5	11	8
2002	7	21	.	.
2003	7	.	9	.
2004	.	10	12	.
2005	11	10	17	.
2006	.	6	39	.
2007	.	12	46	5
2008	.	.	25	.
2009	.	.	26	21
2010	.	.	30	24
2011	.	.	22	17
2012	.	21	47	.
2013	8	18	26	.
2014	.	35	17	.
2015	19	25	21	.
2016	14	39	33	9
2017	.	21	43	.
2018	18	6	41	.
2019	.	12	19	.
2020	.	14	26	.
2021	.	27	26	.
2022	16	19	33	.

Table 4. Sample sizes (number of fish) of length compositions (*lcomp*) or age compositions (*acom*) by survey or fleet. Data sources are recreational (*rA*), commercial handline (*cH*), commercial longline (*cL*), and the MARMAP longline survey (*sM*).

Year	<i>lcomp.rA</i>	<i>acom.cH</i>	<i>acom.cL</i>	<i>acom.sM</i>
1972
1973
1974
1975
1976
1977
1978
1979
1980
1981
1982
1983
1984
1985
1986
1987
1988
1989
1990
1991
1992	.	.	124	.
1993	.	.	203	.
1994
1995	.	.	351	.
1996	.	.	216	.
1997	.	103	195	120
1998	.	39	165	.
1999	.	36	197	156
2000	.	241	302	.
2001	23	46	236	48
2002	38	199	.	.
2003	64	.	160	.
2004	.	255	265	.
2005	132	255	368	.
2006	.	196	793	.
2007	.	272	1115	33
2008	.	.	641	.
2009	.	.	749	206
2010	.	.	854	128
2011	.	.	528	130
2012	.	454	1247	.
2013	27	263	525	.
2014	.	462	399	.
2015	39	177	446	.
2016	29	197	662	25
2017	.	115	612	.
2018	29	13	694	.
2019	.	60	438	.
2020	.	159	604	.
2021	.	247	634	.
2022	28	154	623	.

Table 5. Observed indices of abundance and CVs from commercial longline (cL) and the MARMAP longline survey (sM).

Year	cL	sM	cv.cL	cv.sM
1972
1973
1974
1975
1976
1977
1978
1979
1980
1981
1982
1983
1984
1985
1986
1987
1988
1989
1990
1991
1992
1993	0.888	.	0.053	.
1994	0.850	.	0.069	.
1995	0.829	.	0.072	.
1996	0.571	0.62	0.062	0.57
1997	0.810	1.69	0.060	0.39
1998	0.963	1.11	0.076	0.57
1999	1.011	1.94	0.079	0.32
2000	1.159	0.76	0.078	0.38
2001	0.847	1.54	0.065	0.36
2002	0.880	.	0.117	.
2003	0.711	.	0.089	.
2004	0.904	.	0.085	.
2005	1.720	.	0.104	.
2006	1.858	.	0.093	.
2007	.	0.29	.	0.40
2008
2009	.	2.06	.	0.23
2010	.	0.61	.	0.24
2011	.	1.04	.	0.36
2012
2013
2014
2015	.	0.12	.	0.56
2016	.	0.20	.	0.52
2017
2018
2019
2020
2021
2022

Table 6. Life-history characteristics at age. Variables include total length (TL) in millimeters (mm) and inches (in), the coefficient of variation (CV) of TL, whole weight (WW) in kilograms (kg) and pounds (lb), gutted weight (GW) in pounds (lb), proportion female [P(fem.)] and proportion of females mature [P(fem. mat.)], Egg production (EP; product of the proportion of females mature and total fecundity), and natural mortality. All values were fixed model input, but most had different values in the MCBE analysis.

Age	TL (mm)	TL (in)	TL CV	WW (kg)	WW (lb)	GW (lb)	P(fem.)	P(fem. mat.)	EP (million eggs)	M
1	279	11.0	0.14	0.21	0.47	0.43	0.50	0.10	0.00	0.39
2	381	15.0	0.14	0.56	1.25	1.18	0.50	0.55	0.00	0.28
3	464	18.3	0.14	1.05	2.32	2.21	0.50	0.89	0.07	0.23
4	532	20.9	0.14	1.62	3.57	3.41	0.50	0.97	0.26	0.20
5	587	23.1	0.14	2.21	4.88	4.67	0.50	0.99	0.48	0.18
6	632	24.9	0.14	2.80	6.16	5.91	0.50	1.00	0.68	0.17
7	669	26.3	0.14	3.34	7.36	7.07	0.50	1.00	0.86	0.16
8	699	27.5	0.14	3.83	8.45	8.13	0.50	1.00	1.03	0.15
9	723	28.5	0.14	4.27	9.42	9.07	0.50	1.00	1.17	0.15
10	743	29.3	0.14	4.65	10.26	9.88	0.50	1.00	1.30	0.14
11	759	29.9	0.14	4.98	10.98	10.58	0.50	1.00	1.38	0.14
12	772	30.4	0.14	5.26	11.59	11.18	0.50	1.00	1.48	0.14
13	783	30.8	0.14	5.49	12.11	11.68	0.50	1.00	1.53	0.14
14	792	31.2	0.14	5.69	12.54	12.11	0.50	1.00	1.58	0.14
15	799	31.5	0.14	5.85	12.90	12.46	0.50	1.00	1.64	0.13
16	805	31.7	0.14	5.99	13.20	12.75	0.50	1.00	1.67	0.13
17	809	31.9	0.14	6.10	13.44	12.99	0.50	1.00	1.69	0.13
18	813	32.0	0.14	6.19	13.65	13.19	0.50	1.00	1.71	0.13
19	816	32.1	0.14	6.27	13.81	13.35	0.50	1.00	1.72	0.13
20	819	32.2	0.14	6.33	13.95	13.48	0.50	1.00	1.73	0.13

Table 10. Estimated time series of status indicators. Fishing mortality rate is apical F (F_{apical}). Total biomass (B , 1000 lb) is at the start of the year, while spawning stock biomass (SSB , trillion eggs) is at peak spawning. The MSST is defined by $MSST = 75\%SSB_{MSY}$. SPR is static spawning potential ratio and R_y is expected annual recruitment in million fish.

Year	F_{apical}	F/F_{MSY}	B	$B/B_{unfished}$	SSB	SSB/SSB_{MSY}	$SSB/MSST$	SPR	R_y
1972	0.001	0.002	15794	0.935	1.609	3.132	4.176	0.996	0.624
1973	0.003	0.013	15889	0.941	1.623	3.161	4.215	0.981	0.624
1974	0.007	0.031	15952	0.945	1.629	3.172	4.229	0.955	0.625
1975	0.011	0.053	15969	0.946	1.629	3.171	4.228	0.926	0.625
1976	0.012	0.054	15936	0.944	1.624	3.163	4.217	0.925	0.625
1977	0.005	0.023	15904	0.942	1.624	3.162	4.216	0.966	0.625
1978	0.008	0.036	15943	0.944	1.627	3.168	4.224	0.947	0.625
1979	0.010	0.047	15949	0.945	1.627	3.167	4.223	0.933	0.625
1980	0.020	0.090	15931	0.943	1.620	3.154	4.205	0.878	0.625
1981	0.233	1.076	15817	0.937	1.492	2.906	3.874	0.278	0.624
1982	0.394	1.822	13230	0.783	1.182	2.302	3.069	0.334	0.510
1983	0.293	1.356	10702	0.634	0.954	1.857	2.476	0.384	0.502
1984	0.237	1.098	9542	0.565	0.852	1.659	2.211	0.415	0.471
1985	0.278	1.289	8871	0.525	0.781	1.521	2.028	0.352	0.393
1986	0.292	1.352	8026	0.475	0.708	1.379	1.839	0.386	0.347
1987	0.081	0.375	7399	0.438	0.684	1.332	1.776	0.648	0.440
1988	0.130	0.600	7640	0.452	0.696	1.355	1.807	0.550	0.632
1989	0.209	0.968	7602	0.450	0.673	1.310	1.747	0.449	0.322
1990	0.230	1.065	7212	0.427	0.636	1.238	1.651	0.429	0.270
1991	0.257	1.189	6945	0.411	0.604	1.176	1.569	0.409	0.678
1992	0.325	1.507	6661	0.394	0.560	1.090	1.453	0.363	0.397
1993	0.435	2.016	6341	0.376	0.503	0.980	1.307	0.324	0.502
1994	0.399	1.849	5957	0.353	0.463	0.902	1.202	0.328	0.513
1995	0.374	1.734	5652	0.335	0.446	0.868	1.157	0.341	0.219
1996	0.200	0.927	5403	0.320	0.458	0.892	1.189	0.454	0.195
1997	0.200	0.926	5429	0.322	0.484	0.943	1.257	0.436	0.271
1998	0.163	0.755	5484	0.325	0.489	0.953	1.271	0.499	0.655
1999	0.213	0.985	5843	0.346	0.477	0.929	1.239	0.444	0.915
2000	0.313	1.448	6012	0.356	0.450	0.876	1.168	0.369	0.384
2001	0.187	0.864	5966	0.353	0.455	0.885	1.180	0.454	0.440
2002	0.169	0.784	6334	0.375	0.506	0.986	1.314	0.477	0.645
2003	0.113	0.521	6721	0.398	0.558	1.086	1.448	0.558	0.481
2004	0.118	0.548	7155	0.424	0.606	1.181	1.574	0.543	0.470
2005	0.120	0.556	7503	0.444	0.647	1.260	1.680	0.504	0.566
2006	0.128	0.592	7618	0.451	0.672	1.309	1.745	0.539	0.383
2007	0.079	0.367	7681	0.455	0.699	1.362	1.816	0.651	0.367
2008	0.076	0.351	7856	0.465	0.734	1.430	1.907	0.666	0.397
2009	0.102	0.474	8000	0.474	0.750	1.460	1.946	0.554	0.453
2010	0.089	0.411	7907	0.468	0.745	1.451	1.935	0.619	0.410
2011	0.091	0.423	7870	0.466	0.742	1.445	1.927	0.605	0.358
2012	0.121	0.562	7824	0.463	0.732	1.425	1.900	0.552	0.470
2013	0.134	0.618	7658	0.454	0.710	1.382	1.843	0.534	0.414
2014	0.181	0.836	7454	0.441	0.678	1.321	1.761	0.466	0.354
2015	0.149	0.690	7084	0.420	0.648	1.261	1.682	0.496	0.342
2016	0.166	0.770	6861	0.406	0.627	1.220	1.627	0.463	0.372
2017	0.177	0.818	6628	0.392	0.599	1.166	1.554	0.470	0.453
2018	0.160	0.740	6424	0.380	0.574	1.119	1.491	0.483	0.365
2019	0.233	1.081	6300	0.373	0.546	1.063	1.417	0.357	0.386
2020	0.194	0.898	5945	0.352	0.516	1.004	1.339	0.428	0.482
2021	0.225	1.040	5911	0.350	0.501	0.976	1.301	0.383	0.473
2022	0.231	1.071	5849	0.346	0.486	0.945	1.261	0.373	0.468

Table 11. Selectivity at age for landings from commercial handline (cH), commercial longline (cL), and recreational (rA) fleets, selectivity for the MARMAP longline (sM) survey, selectivity of landings averaged across fisheries (L.avg), and selectivity of total removals (Total = L.avg). For time-varying selectivities, values shown are from the first year of each constant selectivity time period.

Age	TL (mm)	TL (in)	cH- 1972	cH- 2020	cL- 1972	cL- 2020	rA	sM	L.avg	Total
1	279	10.99	0.00	0.00	0.00	0.00	0.00	0.00	0.00	0.00
2	381	15.00	0.00	0.00	0.00	0.00	0.01	0.00	0.00	0.00
3	464	18.28	0.01	0.01	0.00	0.01	0.59	0.00	0.04	0.04
4	532	20.95	0.06	0.13	0.01	0.09	1.00	0.01	0.15	0.15
5	587	23.12	0.22	0.79	0.05	0.47	1.00	0.08	0.54	0.54
6	632	24.89	0.58	0.99	0.22	0.91	1.00	0.40	0.92	0.92
7	669	26.34	0.87	1.00	0.61	1.00	1.00	0.83	1.00	1.00
8	699	27.51	0.97	0.99	0.89	0.98	1.00	0.97	0.98	0.98
9	723	28.47	0.99	0.97	0.98	0.91	1.00	1.00	0.92	0.92
10	743	29.25	1.00	0.92	1.00	0.81	1.00	1.00	0.84	0.84
11	759	29.89	1.00	0.83	1.00	0.68	1.00	1.00	0.72	0.72
12	772	30.40	1.00	0.67	1.00	0.53	1.00	1.00	0.57	0.57
13	783	30.83	1.00	0.47	1.00	0.37	1.00	1.00	0.42	0.42
14	792	31.17	1.00	0.28	1.00	0.24	1.00	1.00	0.29	0.29
15	799	31.45	1.00	0.15	1.00	0.15	1.00	1.00	0.19	0.19
16	805	31.68	1.00	0.07	1.00	0.09	1.00	1.00	0.13	0.13
17	809	31.87	1.00	0.03	1.00	0.05	1.00	1.00	0.10	0.10
18	813	32.02	1.00	0.01	1.00	0.03	1.00	1.00	0.08	0.08
19	816	32.14	1.00	0.01	1.00	0.02	1.00	1.00	0.07	0.07
20	819	32.24	1.00	0.00	1.00	0.01	1.00	1.00	0.06	0.06

Table 12. Estimated time series of fully selected fishing mortality rates for commercial handline (F_{cH}), commercial longline (F_{cL}), and recreational (F_{rA}). Also shown is apical F (F_{apical}), the maximum F at age summed across fleets.

Year	F_{cH}	F_{cL}	F_{rA}	F_{apical}
1972	0.000	0.000	0.000	0.001
1973	0.000	0.003	0.000	0.003
1974	0.000	0.006	0.000	0.007
1975	0.001	0.011	0.000	0.011
1976	0.001	0.011	0.000	0.012
1977	0.001	0.004	0.000	0.005
1978	0.002	0.006	0.000	0.008
1979	0.002	0.009	0.000	0.010
1980	0.005	0.015	0.000	0.020
1981	0.012	0.075	0.145	0.233
1982	0.033	0.361	0.000	0.394
1983	0.017	0.275	0.000	0.293
1984	0.014	0.217	0.007	0.237
1985	0.014	0.226	0.038	0.278
1986	0.015	0.277	0.000	0.292
1987	0.005	0.074	0.002	0.081
1988	0.008	0.121	0.001	0.130
1989	0.013	0.197	0.000	0.209
1990	0.014	0.216	0.001	0.230
1991	0.016	0.241	0.000	0.257
1992	0.016	0.306	0.003	0.325
1993	0.005	0.431	0.000	0.435
1994	0.040	0.356	0.003	0.399
1995	0.036	0.339	0.000	0.374
1996	0.016	0.182	0.002	0.200
1997	0.016	0.169	0.015	0.200
1998	0.013	0.150	0.001	0.163
1999	0.010	0.201	0.002	0.213
2000	0.015	0.293	0.005	0.313
2001	0.049	0.133	0.005	0.187
2002	0.050	0.117	0.002	0.169
2003	0.025	0.078	0.009	0.113
2004	0.011	0.093	0.014	0.118
2005	0.010	0.074	0.036	0.120
2006	0.009	0.111	0.008	0.128
2007	0.009	0.068	0.002	0.079
2008	0.004	0.071	0.000	0.076
2009	0.003	0.073	0.026	0.102
2010	0.005	0.077	0.007	0.089
2011	0.002	0.078	0.011	0.091
2012	0.011	0.104	0.006	0.121
2013	0.009	0.119	0.006	0.134
2014	0.029	0.146	0.005	0.181
2015	0.032	0.107	0.010	0.149
2016	0.027	0.121	0.019	0.166
2017	0.029	0.143	0.005	0.177
2018	0.018	0.130	0.013	0.160
2019	0.023	0.152	0.058	0.233
2020	0.030	0.155	0.009	0.194
2021	0.033	0.180	0.011	0.225
2022	0.026	0.190	0.015	0.231

Table 16. Estimated time series of landings in numbers (1000 fish) for commercial handline (cH), commercial longline (cL), and recreational (rA)

Year	L.cH	L.cL	L.rA
1972	0.04	0.45	0.00
1973	0.22	2.45	0.00
1974	0.53	5.94	0.00
1975	0.91	10.08	0.00
1976	0.95	10.16	0.00
1977	0.89	3.85	0.00
1978	2.33	5.29	0.00
1979	1.68	8.07	0.00
1980	5.02	14.03	0.00
1981	11.91	63.16	226.99
1982	25.10	232.14	0.01
1983	10.73	137.15	0.39
1984	7.82	94.10	7.73
1985	7.52	89.72	40.28
1986	7.18	101.58	0.06
1987	2.46	27.26	2.05
1988	3.93	47.08	0.48
1989	6.08	74.43	0.01
1990	6.10	75.62	0.45
1991	6.32	76.29	0.14
1992	5.96	86.03	2.65
1993	1.60	107.46	0.01
1994	12.68	81.02	2.01
1995	10.38	69.44	0.01
1996	5.14	37.57	1.34
1997	5.61	39.83	11.29
1998	4.57	39.10	0.35
1999	3.58	55.17	1.17
2000	4.95	76.03	3.28
2001	14.51	30.72	4.00
2002	15.33	25.66	2.00
2003	9.33	18.58	7.89
2004	4.92	27.19	13.67
2005	4.50	25.92	35.63
2006	4.52	40.91	7.55
2007	4.61	26.25	1.66
2008	2.36	29.20	0.04
2009	1.49	31.02	25.44
2010	2.70	33.19	6.23
2011	1.08	33.86	10.63
2012	5.52	44.05	5.66
2013	4.46	47.33	4.85
2014	13.63	54.46	4.42
2015	14.15	37.88	8.46
2016	11.35	40.88	15.53
2017	11.85	46.02	4.04
2018	7.06	40.66	9.59
2019	8.79	45.19	43.01
2020	11.91	52.06	6.25
2021	12.63	57.59	7.94
2022	9.51	57.87	10.48

Table 17. Estimated time series of landings in gutted weight (1000 lb) for commercial handline (cH), commercial longline (cL), and recreational (rA)

Year	L.cH	L.cL	L.rA
1972	0.40	4.74	0.00
1973	2.17	25.82	0.00
1974	5.25	62.59	0.00
1975	8.98	106.29	0.00
1976	9.41	107.21	0.00
1977	8.82	40.63	0.00
1978	23.06	55.85	0.00
1979	16.61	85.14	0.00
1980	49.69	148.00	0.00
1981	117.46	665.19	1725.12
1982	242.80	2419.98	0.09
1983	99.42	1392.43	2.57
1984	69.48	925.70	48.87
1985	64.64	855.00	250.83
1986	60.22	940.87	0.37
1987	20.52	248.90	12.73
1988	33.13	431.63	3.10
1989	51.64	686.01	0.06
1990	51.98	699.66	2.70
1991	53.41	706.68	0.82
1992	48.98	787.86	16.21
1993	12.75	954.26	0.06
1994	99.46	701.39	10.77
1995	79.38	597.05	0.05
1996	38.40	317.05	7.01
1997	42.40	332.74	63.53
1998	35.28	330.62	2.15
1999	28.44	474.00	7.43
2000	40.48	667.47	18.52
2001	119.07	276.50	19.66
2002	121.27	232.16	10.22
2003	70.72	162.96	43.07
2004	37.39	230.85	75.73
2005	35.35	220.95	203.84
2006	36.48	358.82	44.64
2007	37.76	234.73	9.94
2008	19.64	264.36	0.24
2009	12.61	284.91	164.83
2010	23.22	308.74	41.23
2011	9.44	318.91	70.30
2012	49.16	421.31	37.41
2013	39.72	457.09	32.25
2014	120.76	525.47	28.68
2015	124.48	363.20	53.81
2016	99.25	390.31	99.22
2017	102.57	436.58	25.90
2018	60.77	382.31	61.00
2019	75.61	423.57	265.07
2020	84.44	379.47	38.19
2021	88.21	415.07	48.53
2022	66.02	412.62	62.12

Table 18. Estimated status indicators, benchmarks, and related quantities from the base run of the BAM, conditional on estimated current selectivities averaged across fleets. Also presented are median values and measures of precision (standard errors, SE) from the Monte Carlo/Bootstrap ensemble analysis. Rate estimates (F) are in units of y^{-1} ; status indicators are dimensionless; biomass estimates are in units of thousands of pounds, as indicated; and recruits are in millions of age-1 fish. Spawning stock biomass (SSB) is measured as fecundity of mature females (trillion eggs). L_{current} are the average landings from 2020–2022.

Quantity	Units	Estimate	Median	SE
F_{MSY}	y^{-1}	0.22	0.18	0.06
$75\%F_{\text{MSY}}$	y^{-1}	0.16	0.14	0.04
B_{MSY}	1000 lb whole	6191.07	7263.71	2446.69
SSB_{MSY}	Trillions of Eggs	0.514	0.651	1.738
MSST	Trillions of Eggs	0.385	0.488	1.304
MSY	1000 lb gutted	545.08	564.30	70.90
$L_{75\%\text{MSY}}$	1000 lb gutted	524.22	540.50	68.97
L_{current}	1000 lb gutted	531.56	530.24	19.54
R_{MSY}	millions fish	0.05	0.05	0.01
$F_{2020-2022}/F_{\text{MSY}}$	—	1.00	1.16	0.52
$\text{SSB}_{2022}/\text{MSST}$	—	1.26	1.04	0.42
$\text{SSB}_{2022}/\text{SSB}_{\text{MSY}}$	—	0.95	0.78	0.32

Table 19. Projection results with fishing mortality rate fixed at F that provides $P^* = 0.50$ starting in 2025. R = number of age-1 recruits (million), F = fishing mortality rate (per year), S = spawning stock (trillion eggs), L = landings expressed in numbers (n , in 1000s) or gutted weight (w , in 1000 lb), $pr.ssb$ = percent of stochastic projection replicates with $SSB \leq SSB_{MSY}$, $pr.msst$ = percent of stochastic projection replicates with $SSB \leq MSST$. The extension b indicates expected values (deterministic) from the base run; the extension med indicates median values from the stochastic projections.

Year	R.b	R.med	F.b	F.med	S.b	S.med	L.b(n)	L.med(n)	L.b(w)	L.med(w)	pr.ssb	pr.msst
2023	0.462	0.384	0.216	0.215	0.480	0.477	70	69	482	481	74.6	46.4
2024	0.460	0.367	0.216	0.215	0.484	0.477	72	69	483	473	73.6	46.2
2025	0.462	0.366	0.216	0.183	0.489	0.485	75	63	495	427	72.6	45.5
2026	0.464	0.368	0.216	0.183	0.494	0.494	77	65	508	439	72.2	42.9
2027	0.465	0.372	0.216	0.183	0.497	0.501	78	66	517	451	71.7	41.2

Table 20. Projection results with fishing mortality rate fixed at $F = F_{MSY}$ starting in 2025. R = number of age-1 recruits (million), F = fishing mortality rate (per year), S = spawning stock (trillion eggs), L = landings expressed in numbers (n , in 1000s) or gutted weight (w , in 1000 lb), $pr.ssb$ = percent of stochastic projection replicates with $SSB \leq SSB_{MSY}$, $pr.msst$ = percent of stochastic projection replicates with $SSB \leq MSST$. The extension b indicates expected values (deterministic) from the base run; the extension med indicates median values from the stochastic projections.

Year	R.b	R.med	F.b	F.med	S.b	S.med	L.b(n)	L.med(n)	L.b(w)	L.med(w)	pr.ssb	pr.msst
2023	0.462	0.384	0.216	0.215	0.480	0.477	70	69	482	481	74.6	46.4
2024	0.460	0.367	0.216	0.215	0.484	0.477	72	69	483	473	73.6	46.2
2025	0.462	0.366	0.216	0.183	0.489	0.484	75	63	496	428	72.6	45.5
2026	0.464	0.368	0.216	0.183	0.494	0.494	77	65	508	439	72.2	42.9
2027	0.465	0.372	0.216	0.183	0.497	0.501	78	66	517	451	71.7	41.2

Table 21. Projection results with fishing mortality rate fixed at F that provides $P^* = 0.325$ starting in 2025. R = number of age-1 recruits (million), F = fishing mortality rate (per year), S = spawning stock (trillion eggs), L = landings expressed in numbers (n , in 1000s) or gutted weight (w , in 1000 lb), $pr.ssb$ = percent of stochastic projection replicates with $SSB \leq SSB_{MSY}$, $pr.msst$ = percent of stochastic projection replicates with $SSB \leq MSST$. The extension b indicates expected values (deterministic) from the base run; the extension med indicates median values from the stochastic projections.

Year	R.b	R.med	F.b	F.med	S.b	S.med	L.b(n)	L.med(n)	L.b(w)	L.med(w)	pr.ssb	pr.msst
2023	0.462	0.384	0.216	0.215	0.480	0.477	70	69	482	481	74.6	46.4
2024	0.460	0.367	0.216	0.215	0.484	0.477	72	69	483	473	73.6	46.2
2025	0.462	0.366	0.180	0.152	0.493	0.487	63	53	418	360	71.9	44.9
2026	0.465	0.369	0.180	0.152	0.507	0.506	66	56	439	378	69.8	41.0
2027	0.470	0.376	0.180	0.152	0.518	0.519	68	58	456	395	67.5	38.1

Table 22. Projection results with fishing mortality rate fixed at F that provides $P^* = 0.30$ starting in 2025. R = number of age-1 recruits (million), F = fishing mortality rate (per year), S = spawning stock (trillion eggs), L = landings expressed in numbers (n , in 1000s) or gutted weight (w , in 1000 lb), $pr.ssb$ = percent of stochastic projection replicates with $SSB \leq SSB_{MSY}$, $pr.msst$ = percent of stochastic projection replicates with $SSB \leq MSST$. The extension b indicates expected values (deterministic) from the base run; the extension med indicates median values from the stochastic projections.

Year	R.b	R.med	F.b	F.med	S.b	S.med	L.b(n)	L.med(n)	L.b(w)	L.med(w)	pr.ssb	pr.msst
2023	0.462	0.384	0.216	0.215	0.480	0.477	70	69	482	481	74.6	46.4
2024	0.460	0.367	0.216	0.215	0.484	0.477	72	69	483	473	73.6	46.2
2025	0.462	0.366	0.175	0.148	0.494	0.488	61	52	407	351	71.7	44.8
2026	0.465	0.370	0.175	0.148	0.509	0.507	64	54	429	369	69.4	40.8
2027	0.470	0.376	0.175	0.148	0.521	0.522	67	57	447	386	66.9	37.7

Table 23. Projection results with fishing mortality rate fixed at F that provides $P^* = 0.20$ starting in 2025. R = number of age-1 recruits (million), F = fishing mortality rate (per year), S = spawning stock (trillion eggs), L = landings expressed in numbers (n , in 1000s) or gutted weight (w , in 1000 lb), $pr.ssb$ = percent of stochastic projection replicates with $SSB \leq SSB_{MSY}$, $pr.msst$ = percent of stochastic projection replicates with $SSB \leq MSST$. The extension b indicates expected values (deterministic) from the base run; the extension med indicates median values from the stochastic projections.

Year	R.b	R.med	F.b	F.med	S.b	S.med	L.b(n)	L.med(n)	L.b(w)	L.med(w)	pr.ssb	pr.msst
2023	0.462	0.384	0.216	0.215	0.480	0.477	70	69	482	481	74.6	46.4
2024	0.460	0.367	0.216	0.215	0.484	0.477	72	69	483	473	73.6	46.2
2025	0.462	0.366	0.153	0.130	0.496	0.490	54	46	360	310	71.3	44.4
2026	0.466	0.370	0.153	0.130	0.516	0.515	58	49	385	331	68.0	39.6
2027	0.473	0.379	0.153	0.130	0.534	0.534	60	51	406	350	64.5	35.7

9 Figures

Figure 1. Timeline of data available to fit to in this assessment by source, data type, and year. Data sources include the commercial handline (cH), commercial longline (cL), and general recreational (rec all; rA) fleets, and the MARMAP longline survey (survey MARMAP; sM).

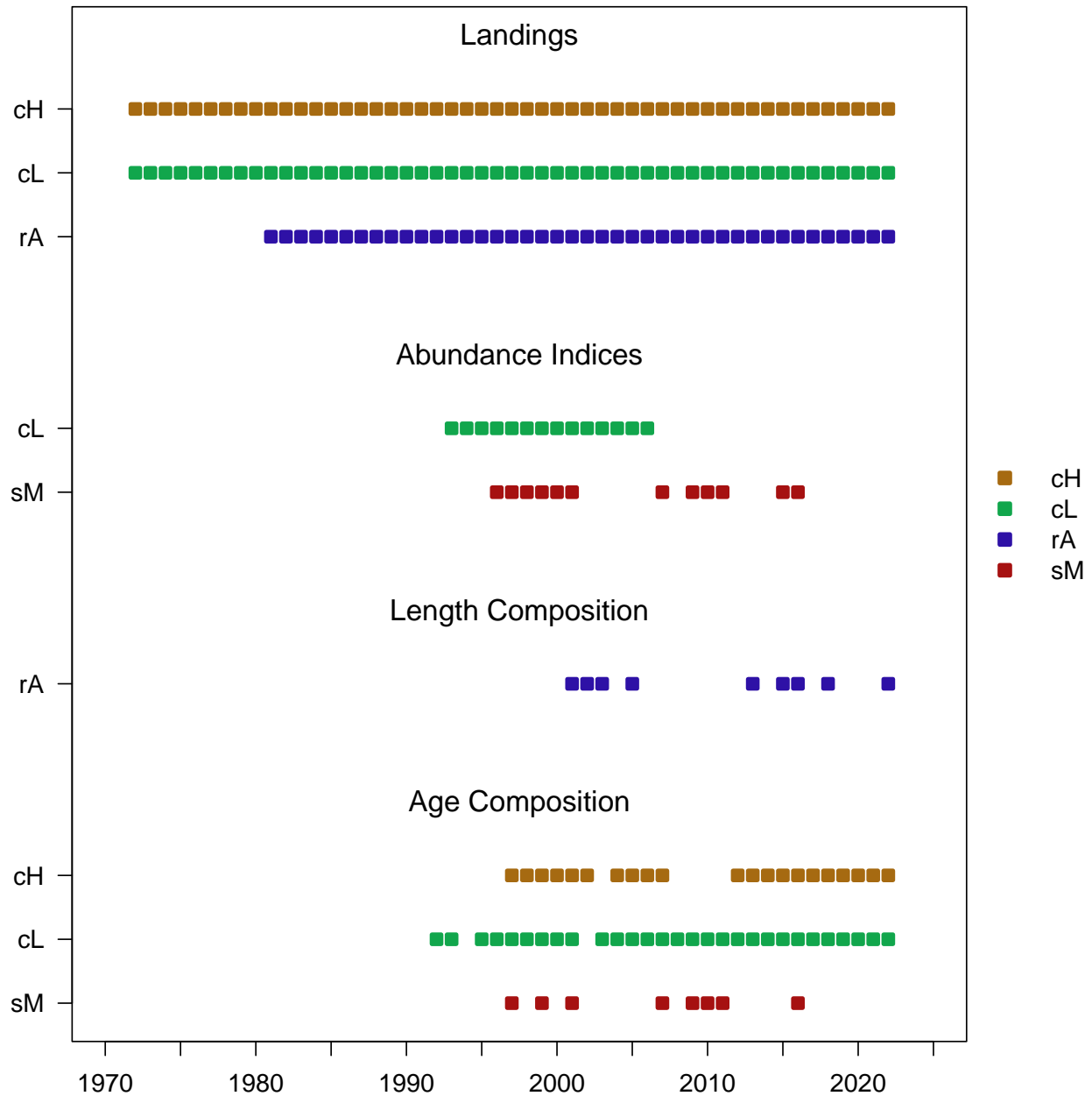


Figure 2. Length, female maturity, and reproductive output at age. Top panel: Mean length at age (mm) and estimated 90% confidence interval of the population. Middle panel: Female maturity by age. Bottom panel: Reproductive output (millions eggs) by age.

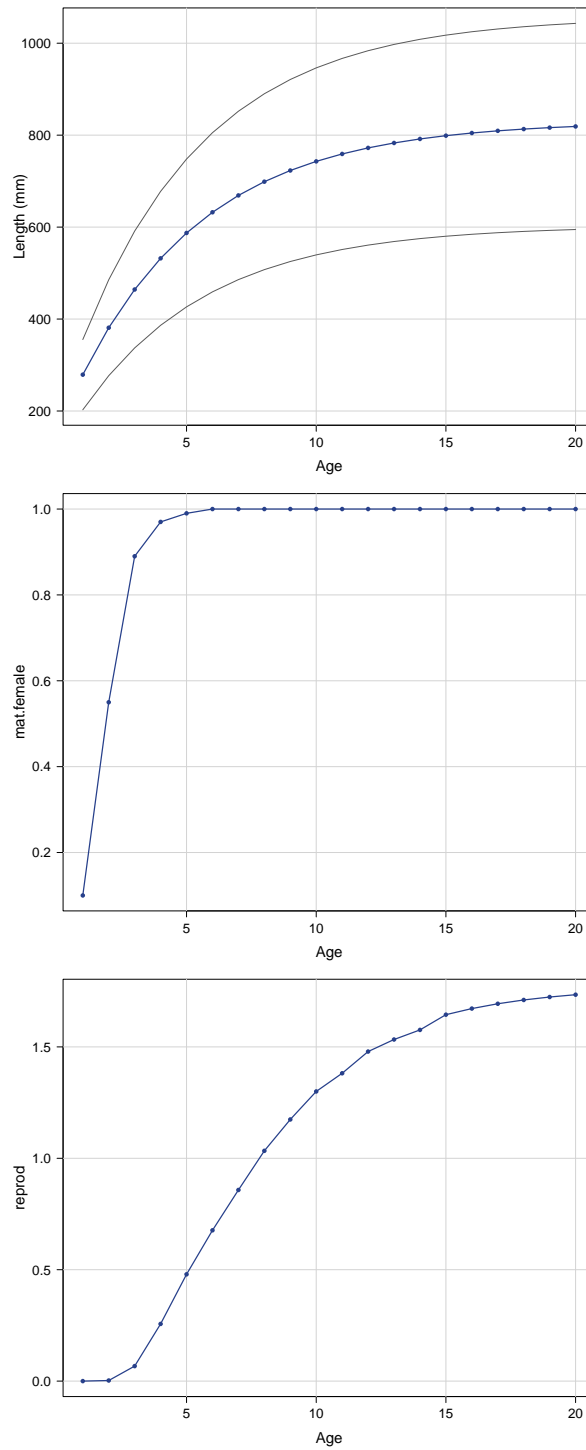


Figure 3. Observed (open circles) and estimated (solid line) annual age and length compositions by fleet. In panels indicating the data set: *acomp* = age compositions, *lcomp* = length compositions, *cH* = commercial handline, *cL* = commercial longline, *sM* = MARMAP longline survey, *rA* = general recreational. *N* indicates the number of trips from which individual fish samples were taken. The four digit number in upper right corner of each panel indicates year of sampling (e.g. 1997, 1998).

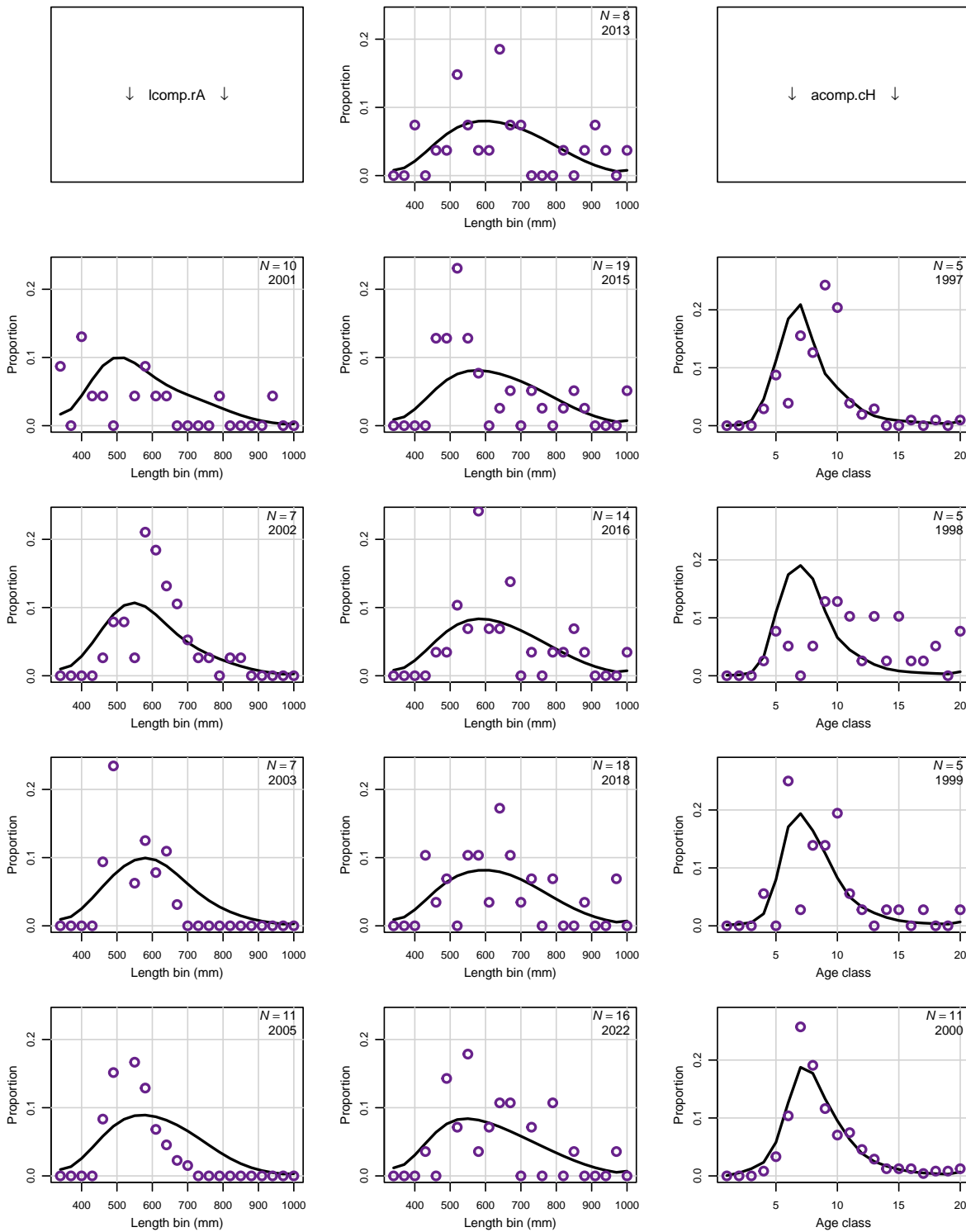


Figure 3. (cont.) Observed (open circles) and estimated (solid line) annual age and length compositions by fleet.

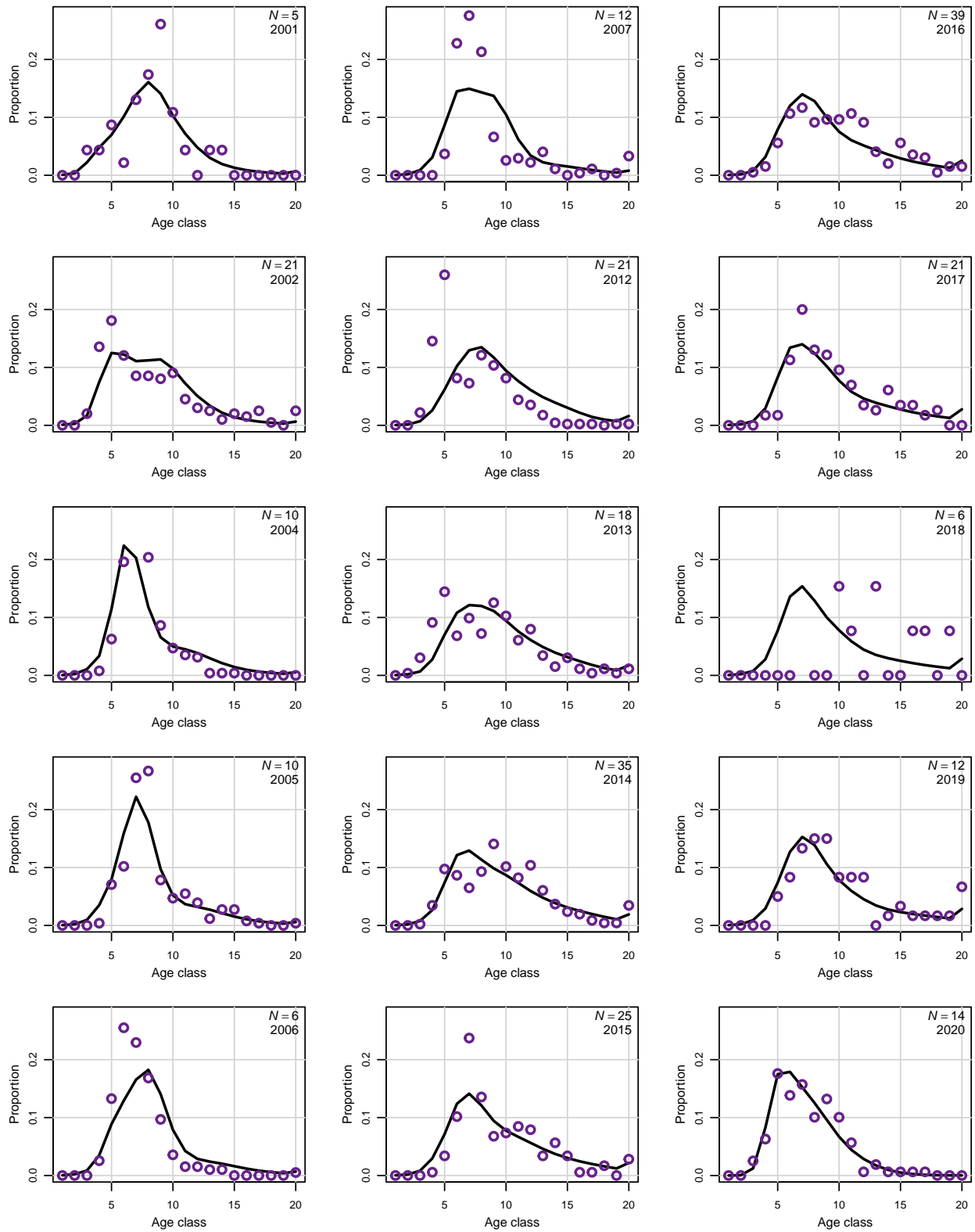


Figure 3. (cont.) Observed (open circles) and estimated (solid line) annual age and length compositions by fleet.

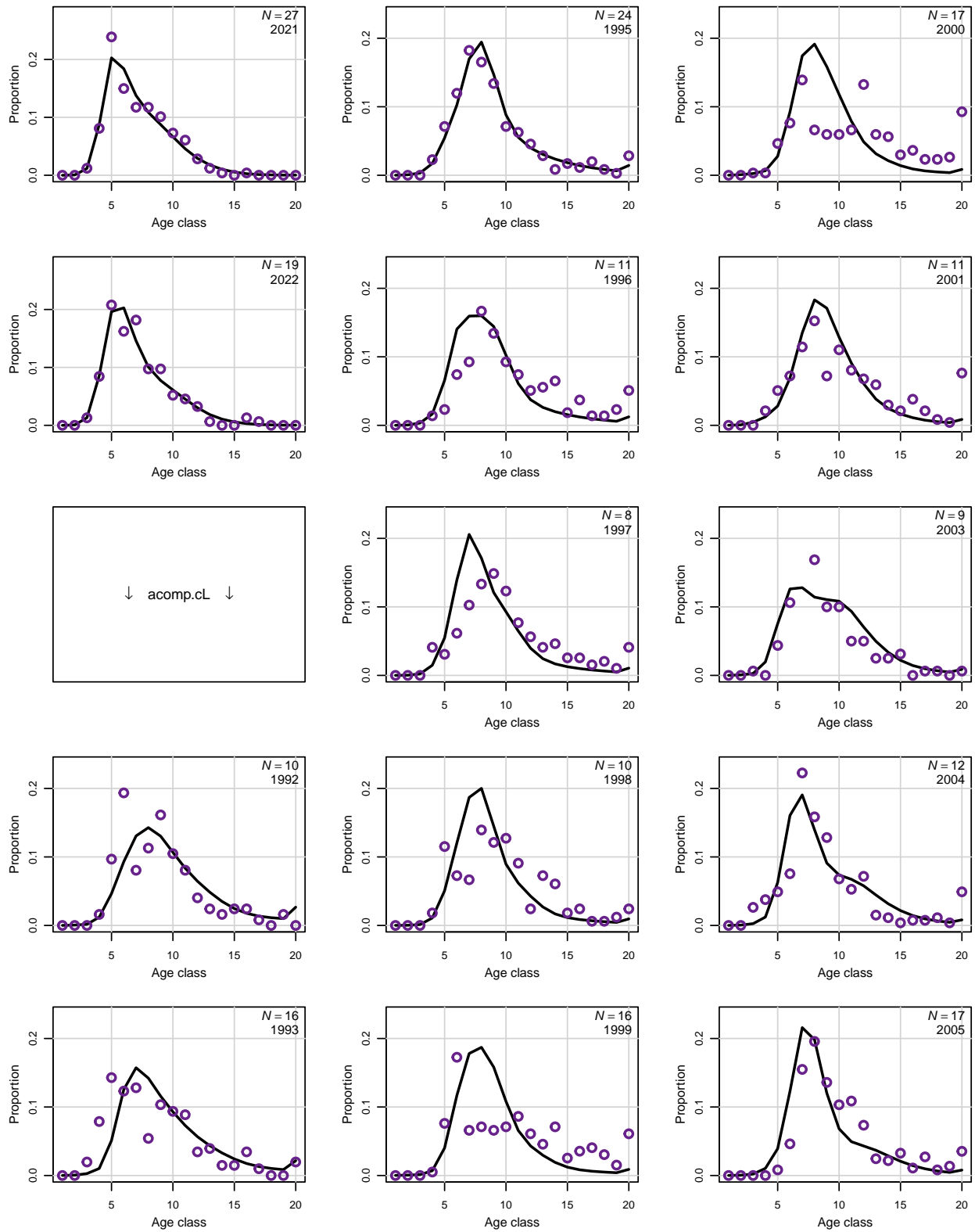


Figure 3. (cont.) Observed (open circles) and estimated (solid line) annual age and length compositions by fleet.

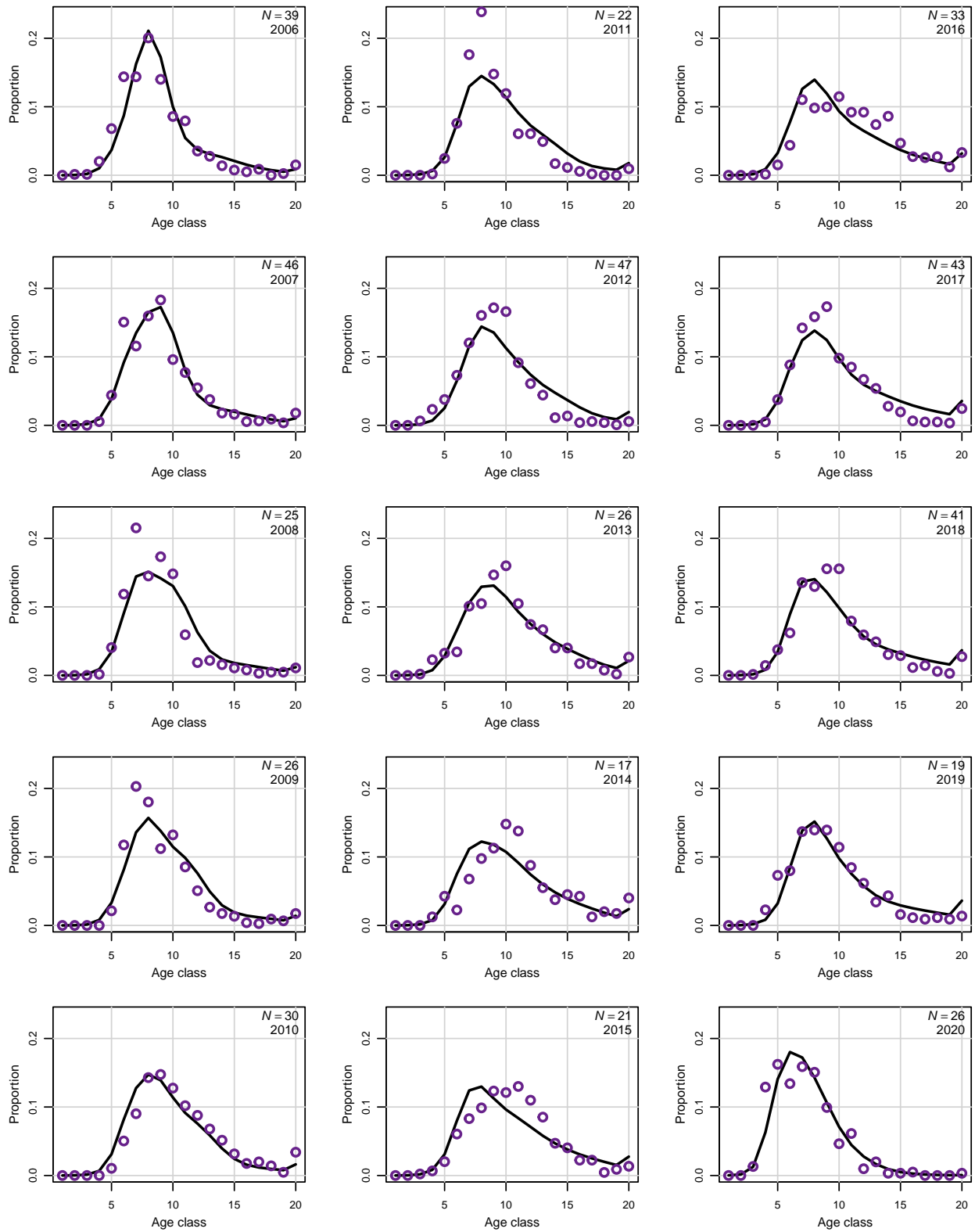


Figure 4. Observed (open circles) and estimated (line, solid circles) commercial handline landings (1000 lb gutted weight).

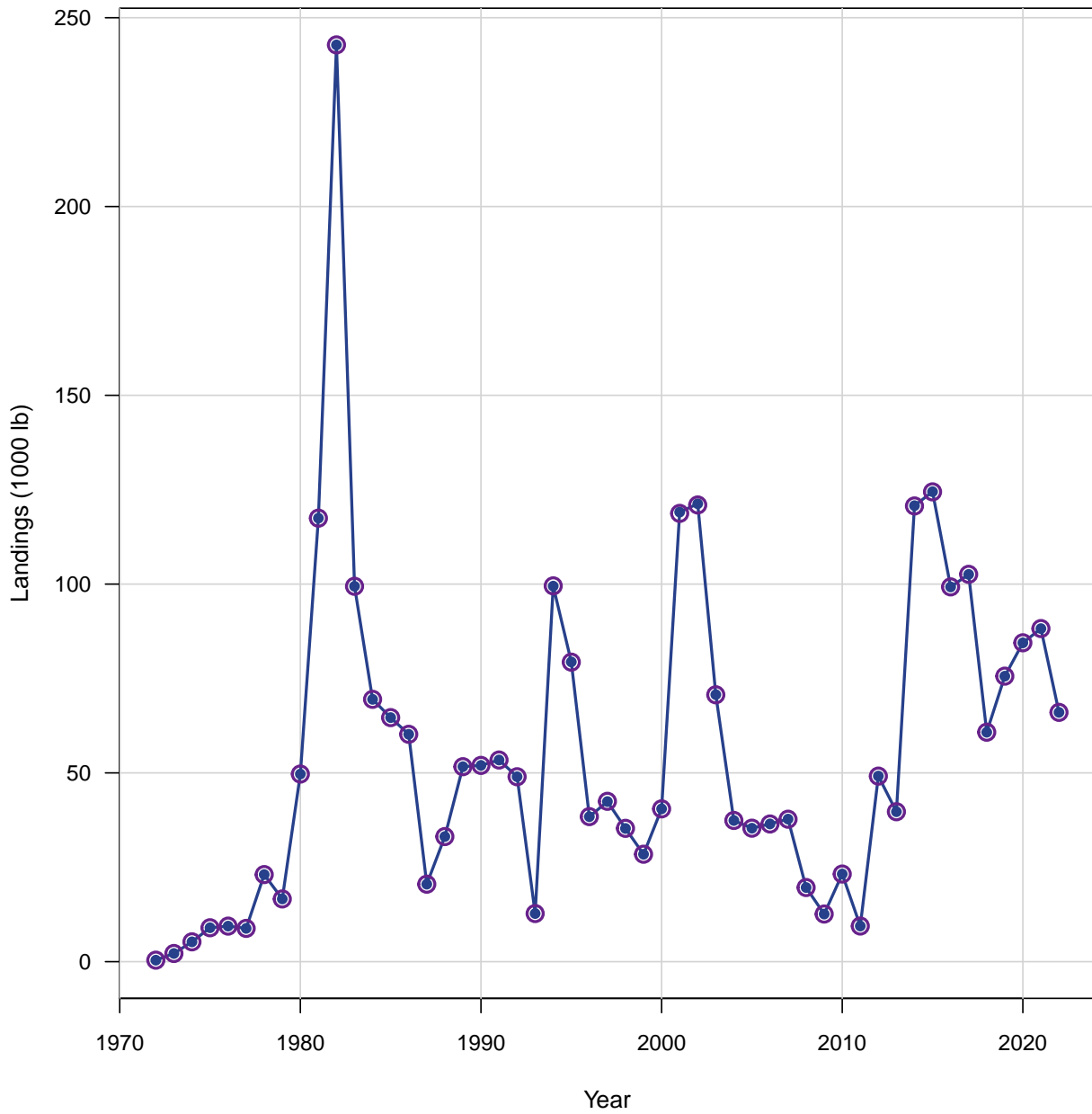


Figure 5. Observed (open circles) and estimated (line, solid circles) commercial longline landings (1000 lb gutted weight).

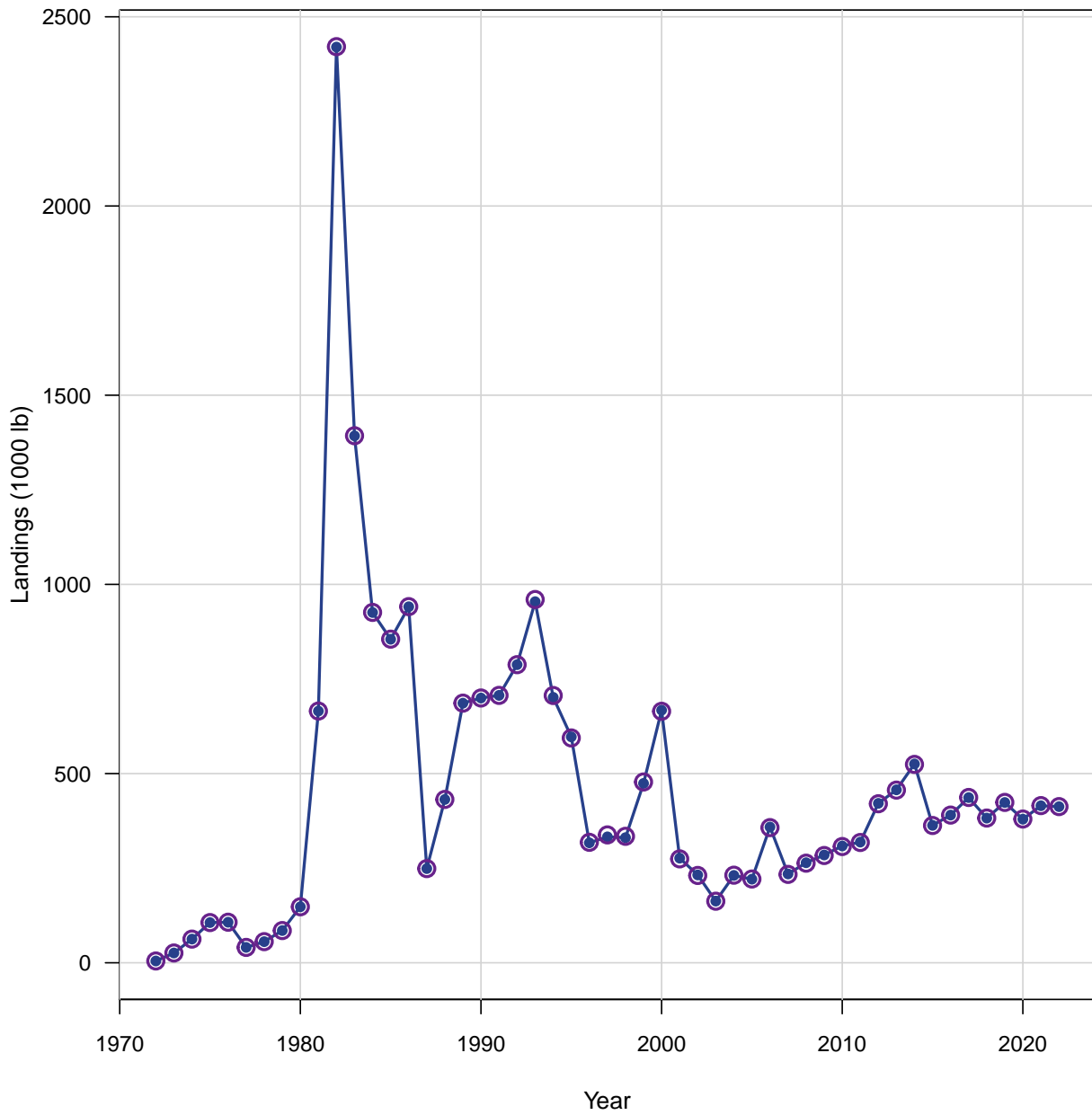


Figure 6. Observed (open circles) and estimated (line, solid circles) recreational landings (1000s fish).

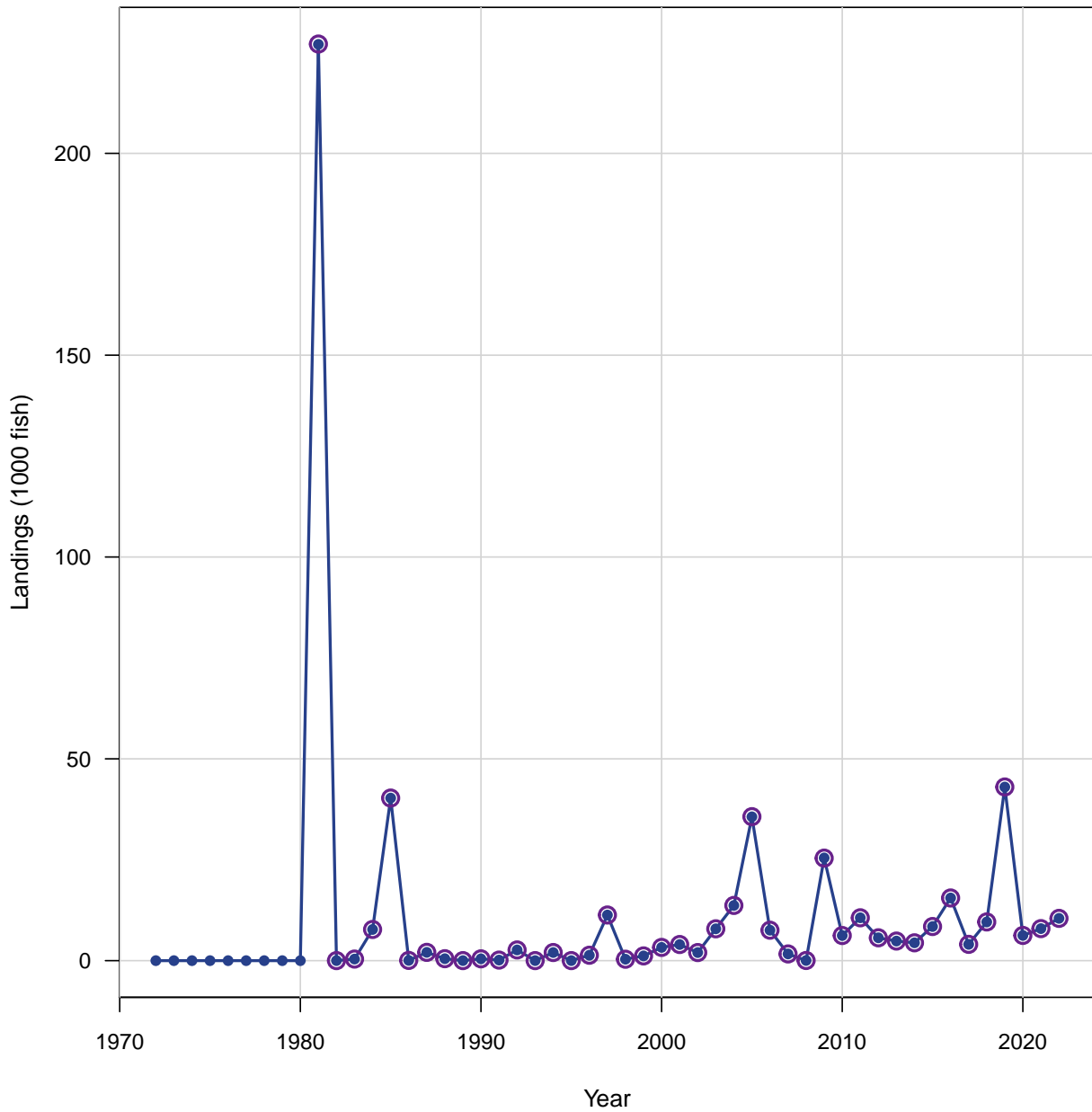


Figure 7. Observed (open circles) and estimated (line, solid circles) index of abundance from commercial longline. The bottom panel are the log residuals of the fit to the index and the color of the box indicates the p-value of the runs test (green > 0.05, orange ≤ 0.05 and >0.01, red < 0.01) and the width of the box is 3 times the standard error. Points that fall outside 3 standard errors are plotted in red.

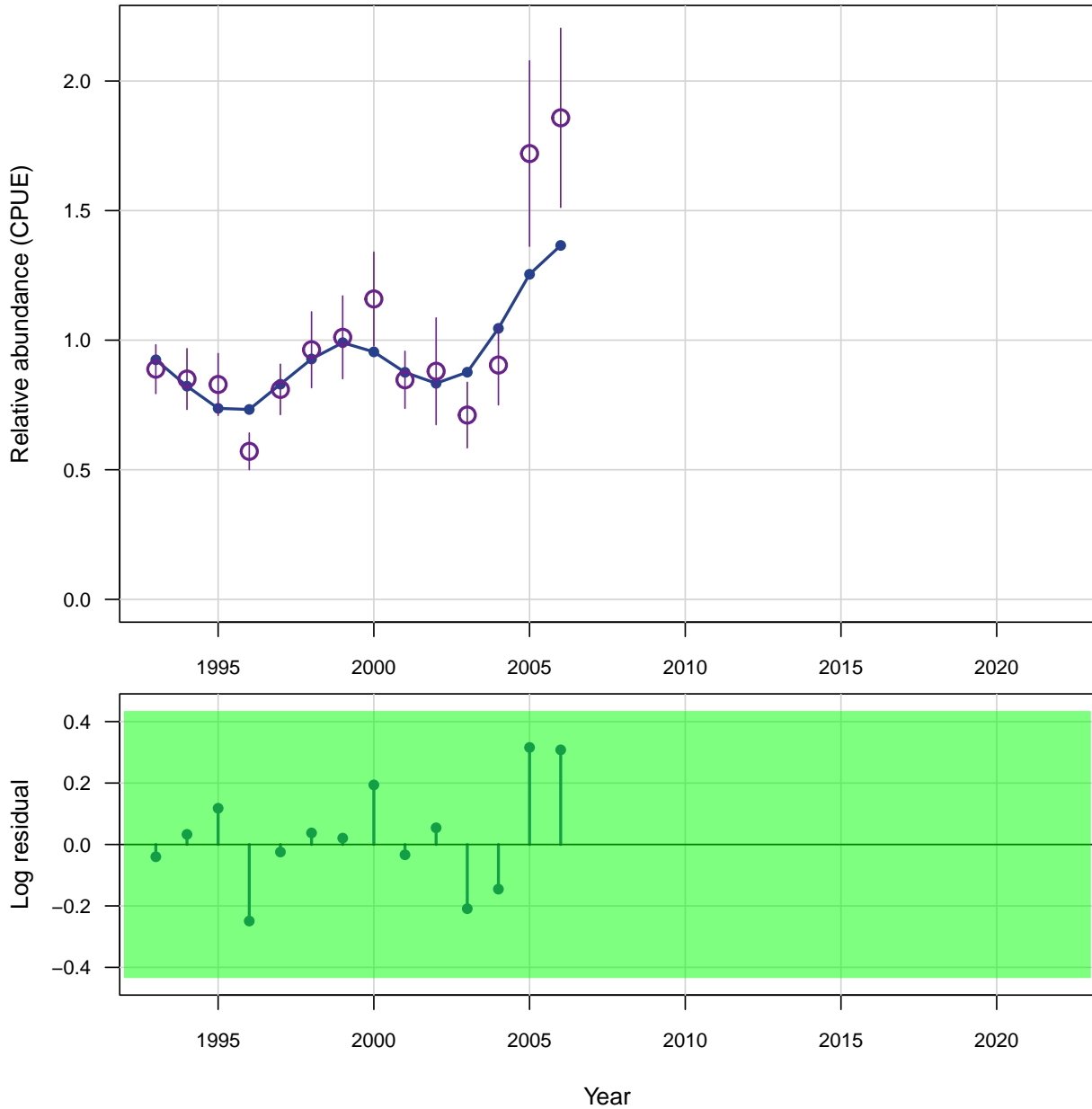


Figure 8. Observed (open circles) and estimated (line, solid circles) index of abundance from MARMAP longline survey. The bottom panel are the log residuals of the fit to the index and the color of the box indicates the p-value of the runs test (green > 0.05, orange ≤ 0.05 and >0.01, red < 0.01) and the width of the box is 3 times the standard error. Points that fall outside 3 standard errors are plotted in red.

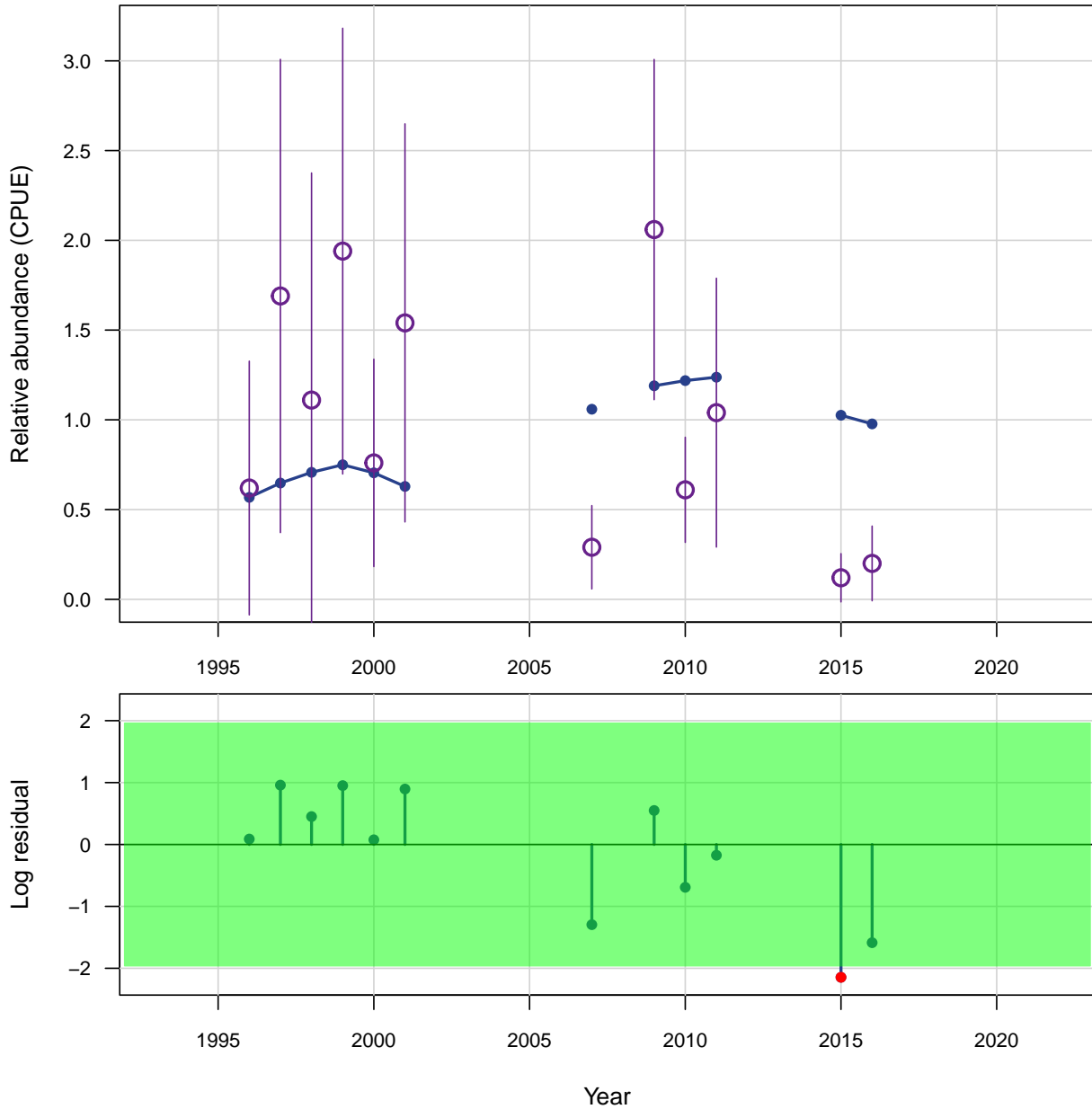


Figure 9. Estimated abundance at age at start of year

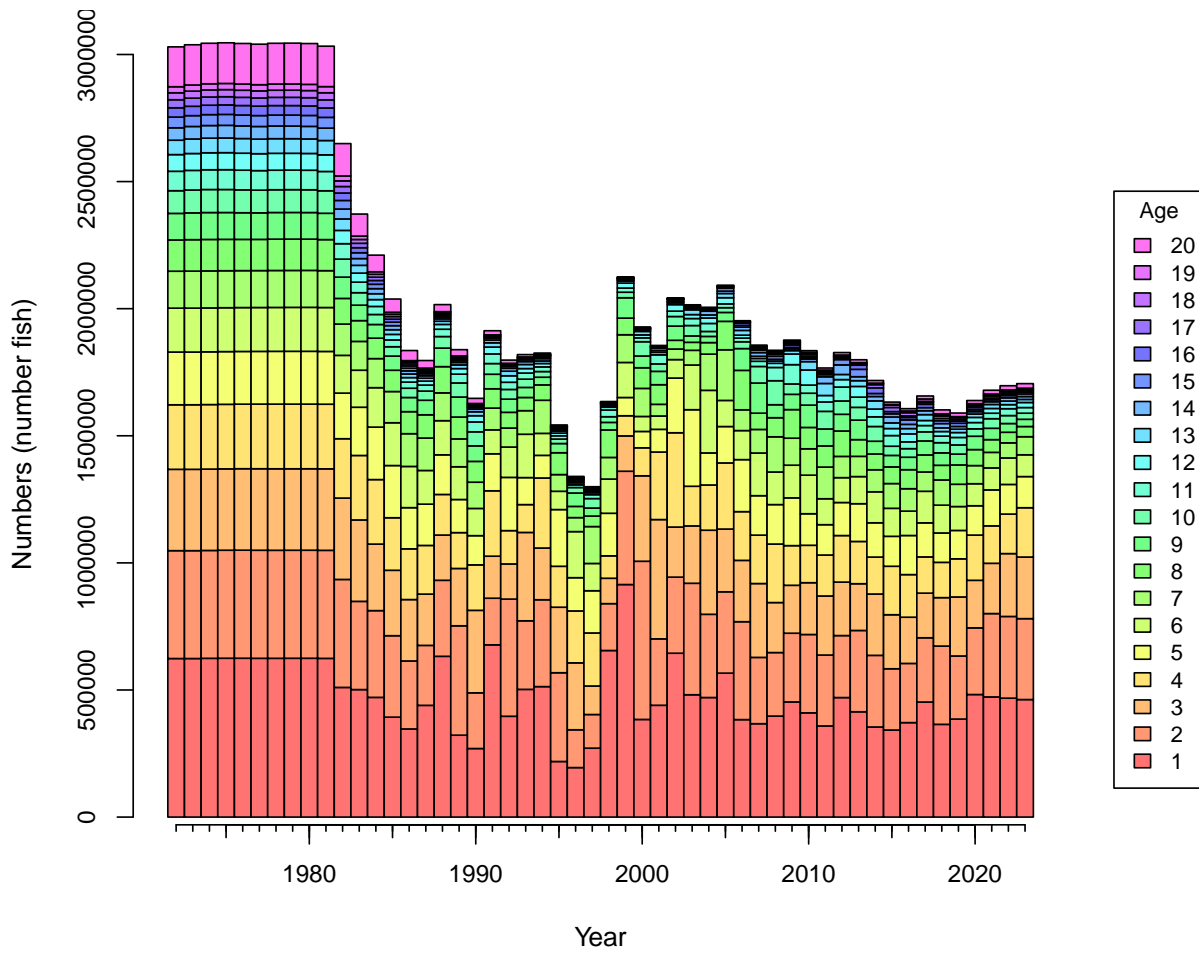


Figure 10. Estimated biomass at age at start of year.

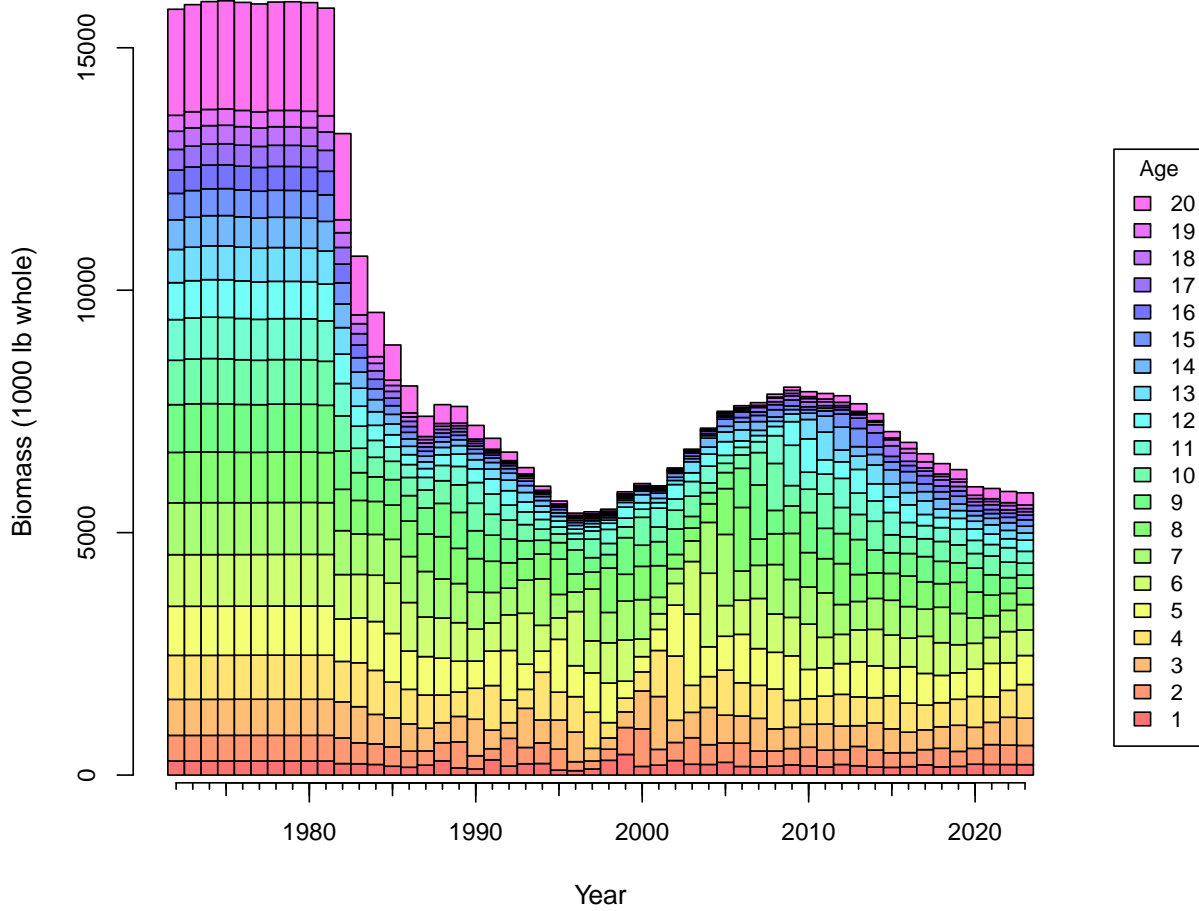


Figure 11. Estimated recruitment time series. Top panel: Estimated recruitment of age-1 fish. Horizontal dashed line indicates R_{MSY} . Bottom panel: log recruitment residuals (open circles). These are annual recruitment deviations (r_y) estimated within the model. The solid line is a lowess smoother fit to the residuals.

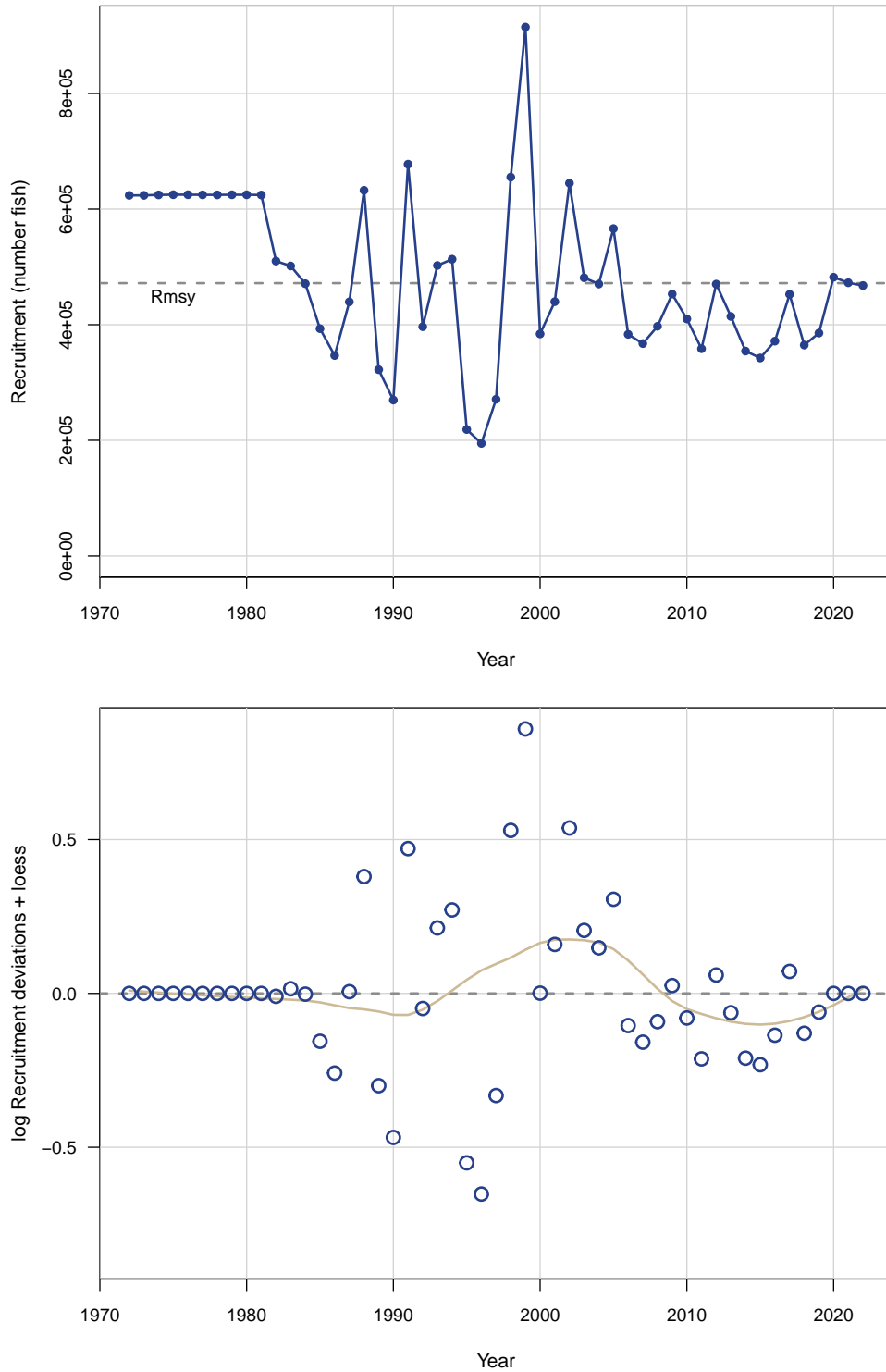


Figure 12. Estimated total biomass and spawning stock time series. Top panel: Estimated total biomass (1000 lb) at start of year. Horizontal dashed line indicates B_{MSY} . Bottom panel: Estimated spawning stock (trillion eggs) at time of peak spawning (May 15th; 0.37 yr). Note that B_{MSY} and MSST should only be compared to the last 3 years of the trend because of changes in selectivity in the time series.

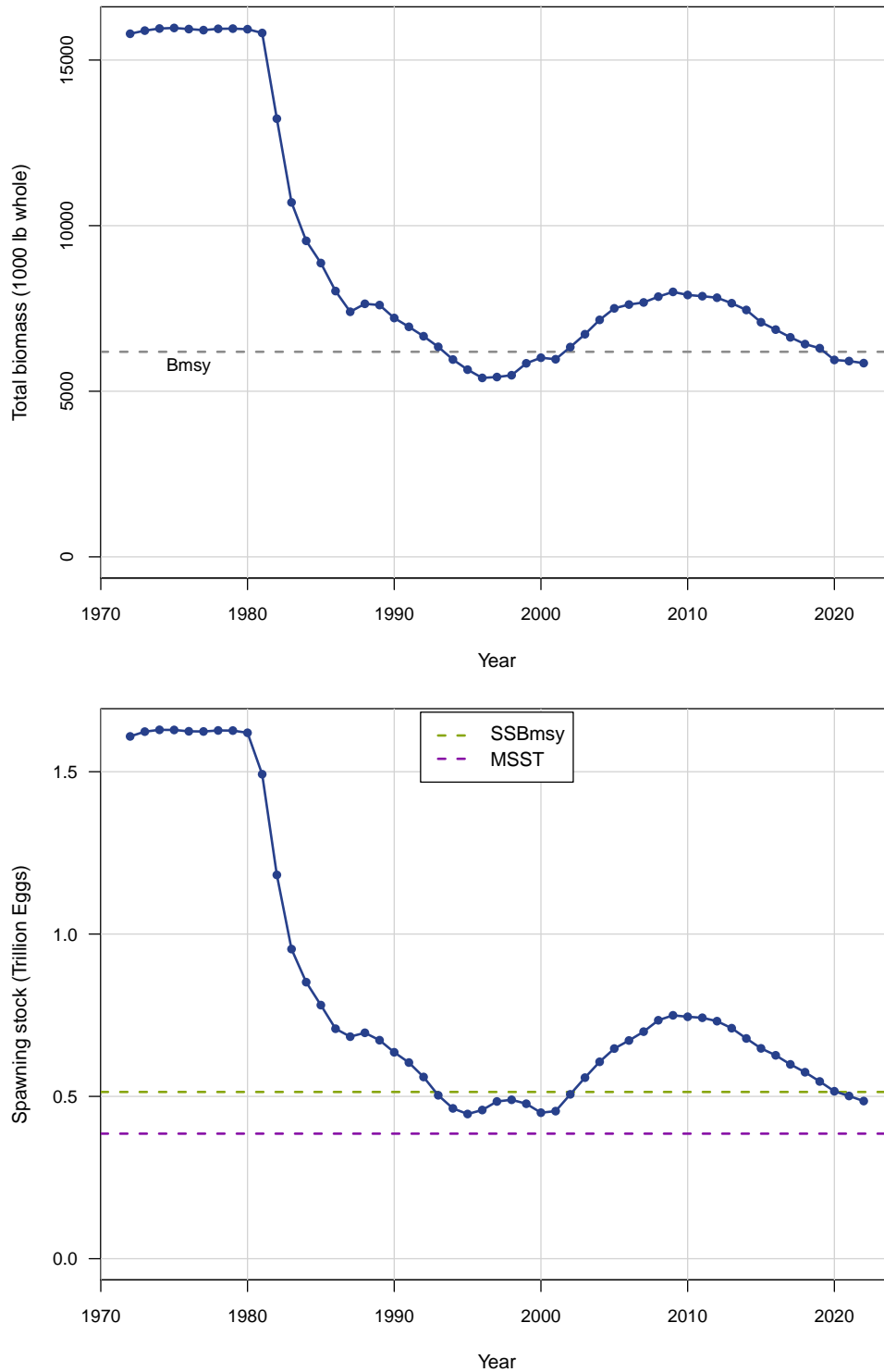


Figure 13. Selectivity of MARMAP longline index.

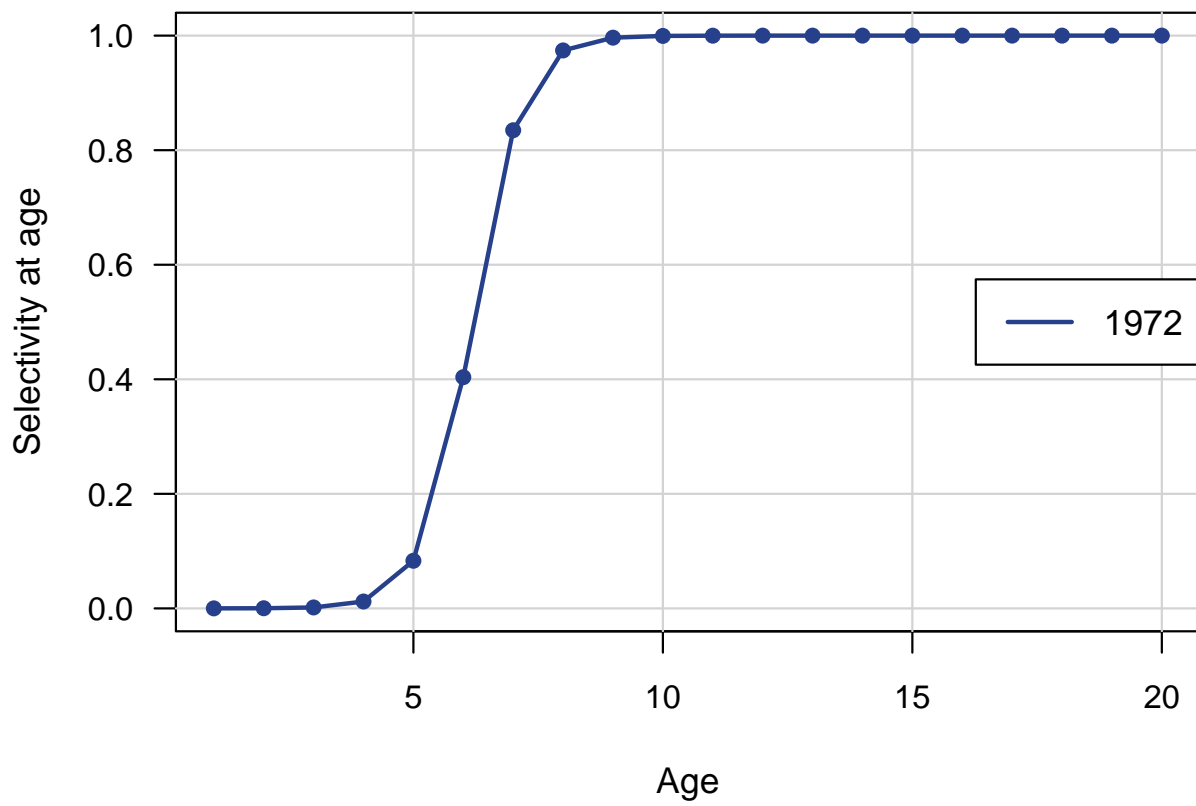


Figure 14. Selectivities of commercial handline landings (top) and commercial longline landings (bottom). Different colored lines indicate different selectivity blocks. The first year of each selectivity block is indicated in the legend.

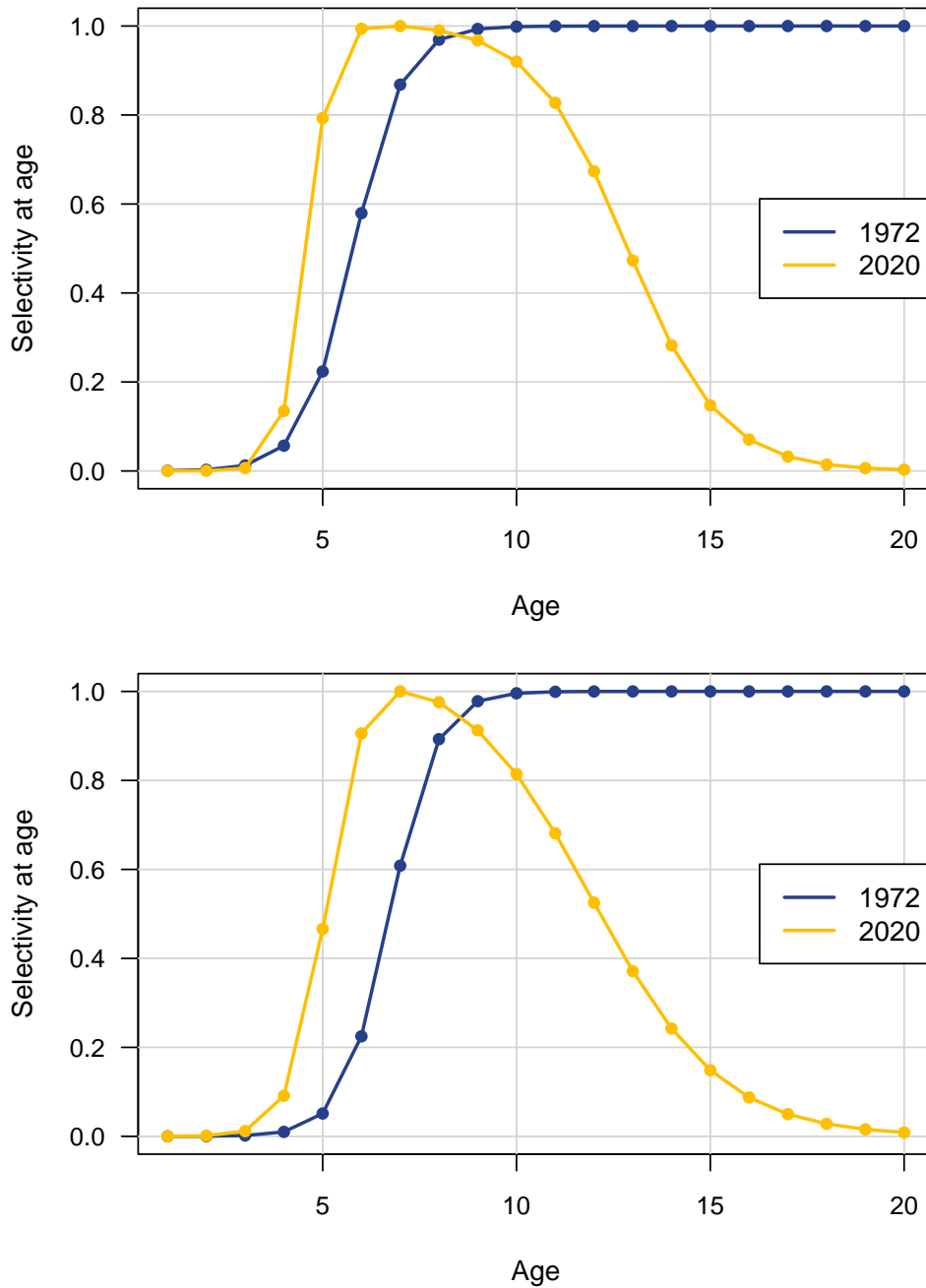


Figure 15. Selectivity of recreational landings.

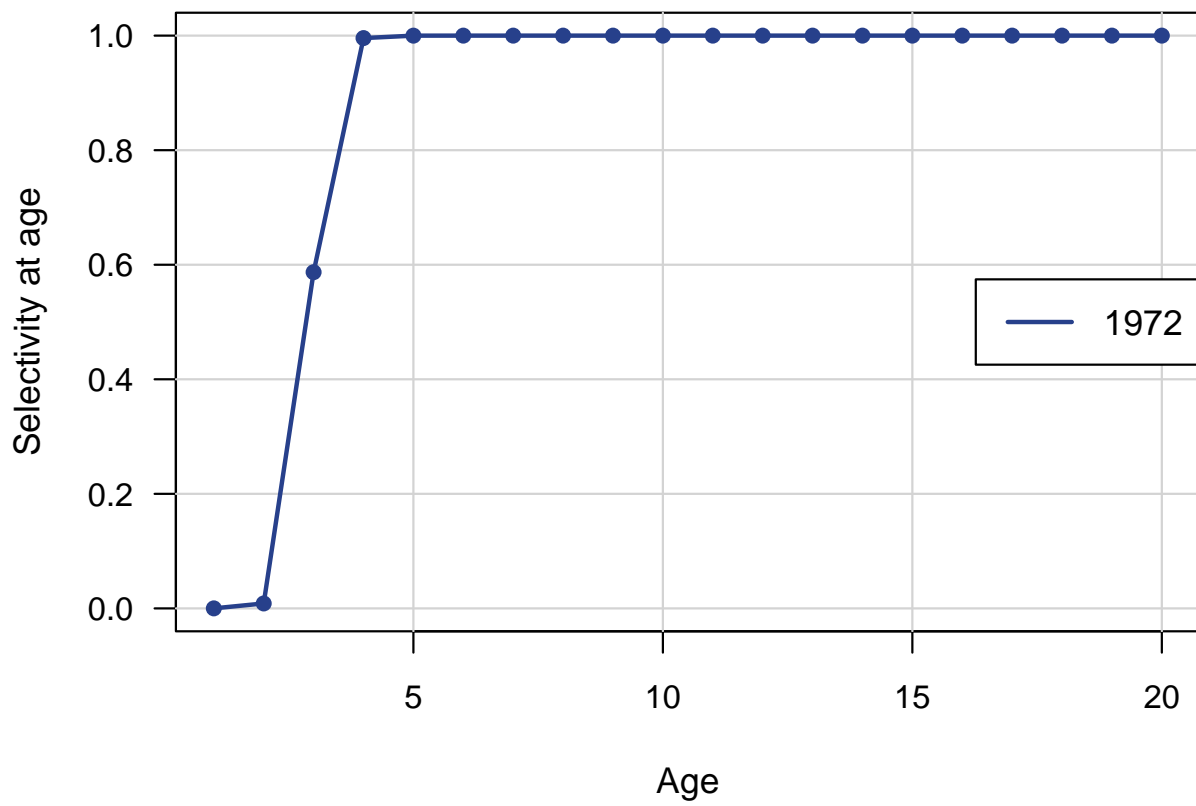


Figure 16. Average selectivity from the terminal assessment year weighted by geometric mean F s from the last three assessment years, for landings. This selectivity is used in computation of benchmarks and central-tendency projections.

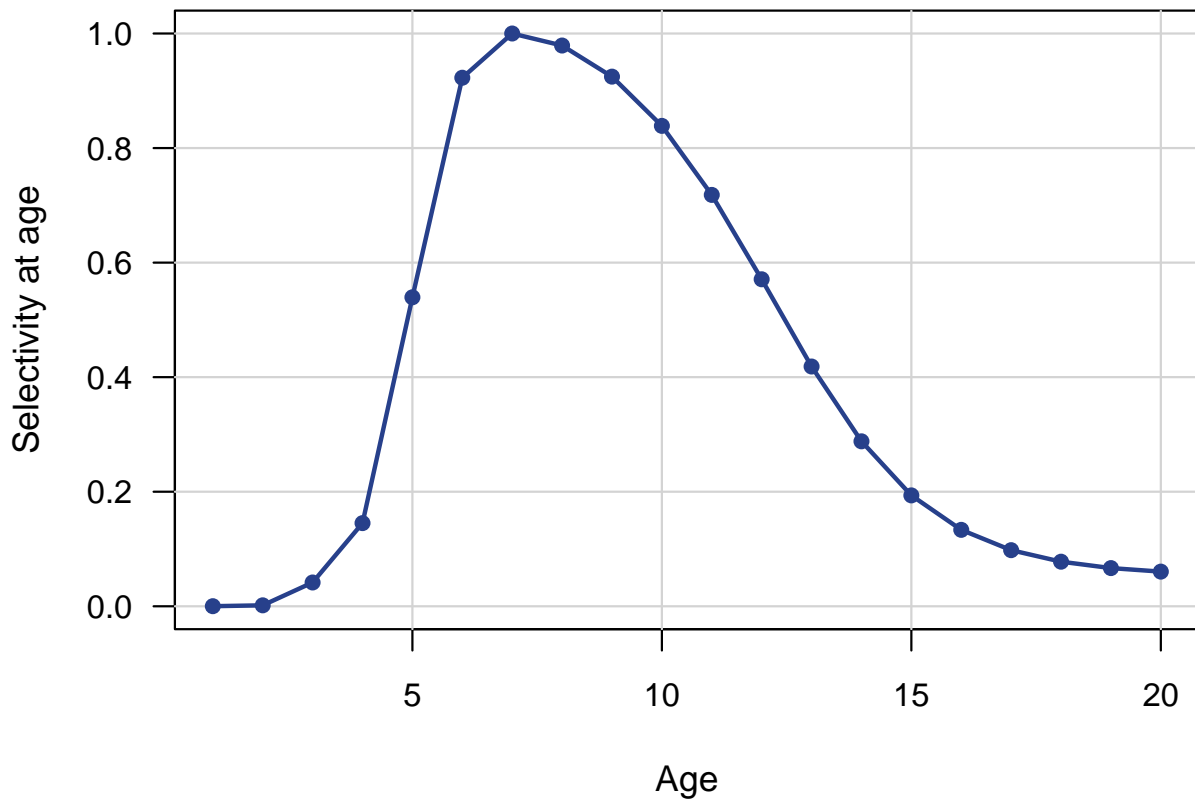


Figure 17. Estimated fully selected fishing mortality rate (per year) by fleet. rA = recreational, cL = commercial longline, and cH = commercial handline landings.

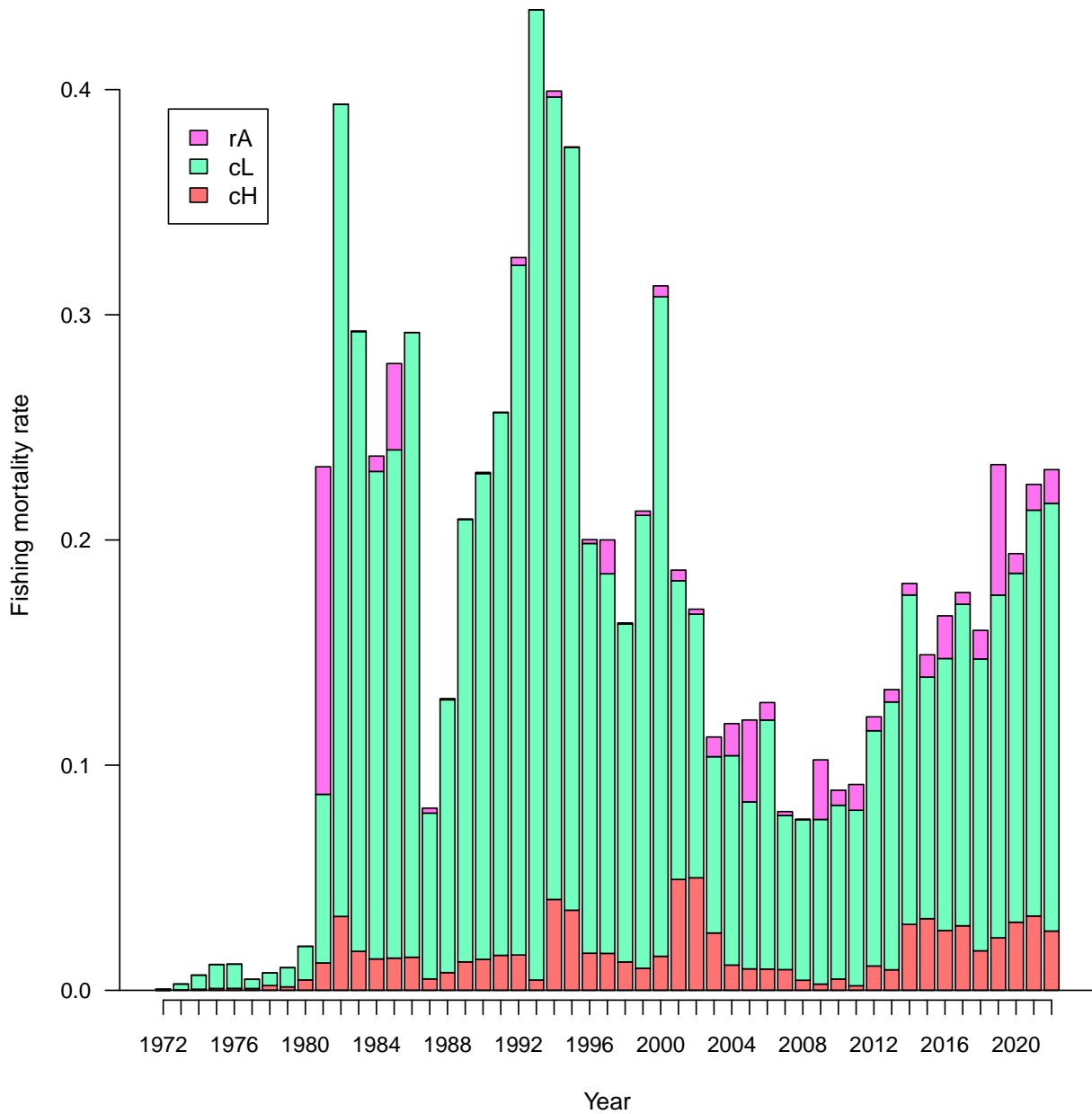


Figure 18. Estimated landings in absolute numbers (top) and proportion of total numbers (bottom) by fleet from the catch-at-age model. *rA* = recreational landings, *cL* = commercial longline landings, and *cH* = commercial handline landings

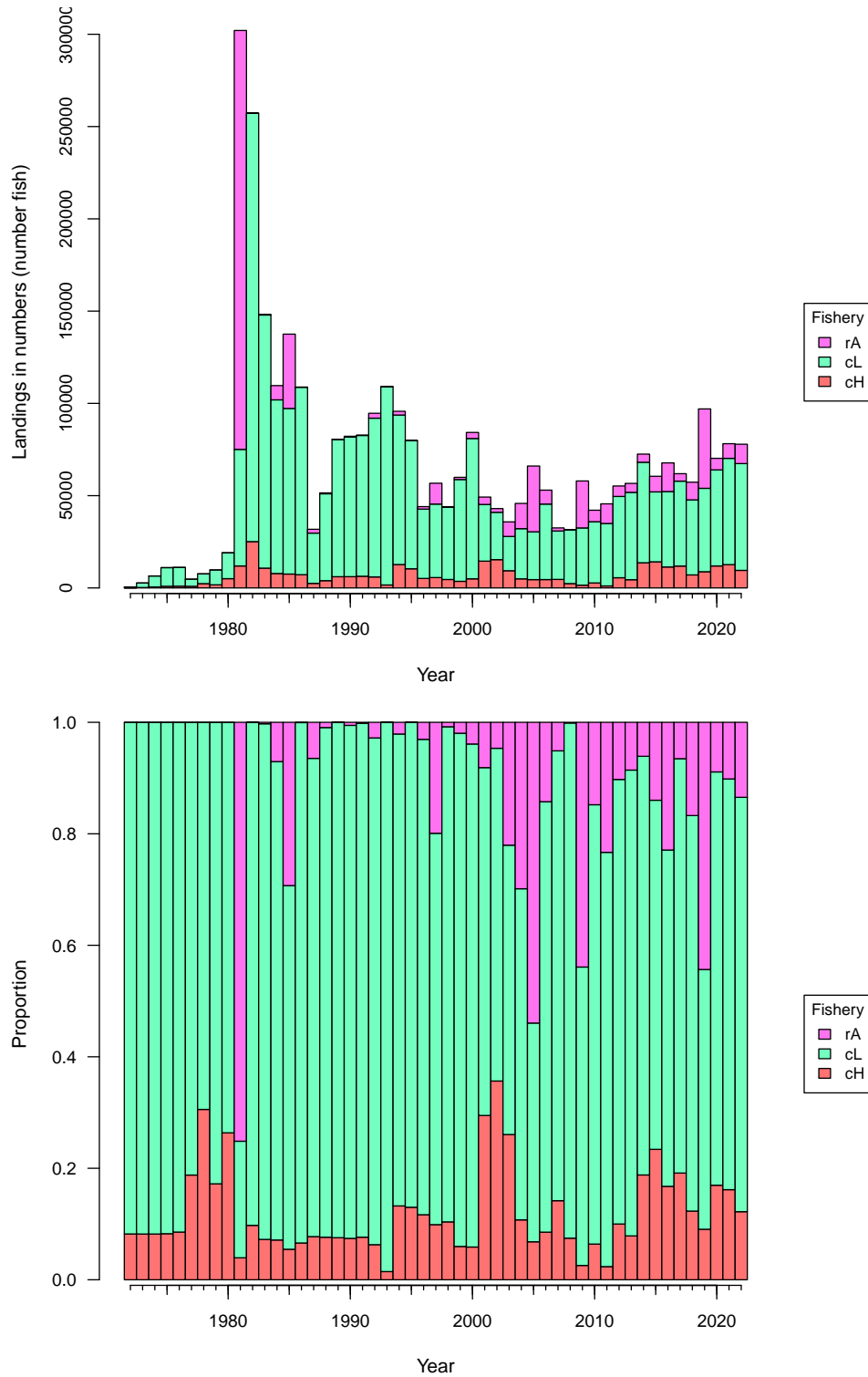


Figure 19. Estimated landings in absolute weight (top) and proportion of total weight (bottom) by fleet from the catch-at-age model. rA = recreational landings, cL = commercial longline landings, and cH = commercial handline landings

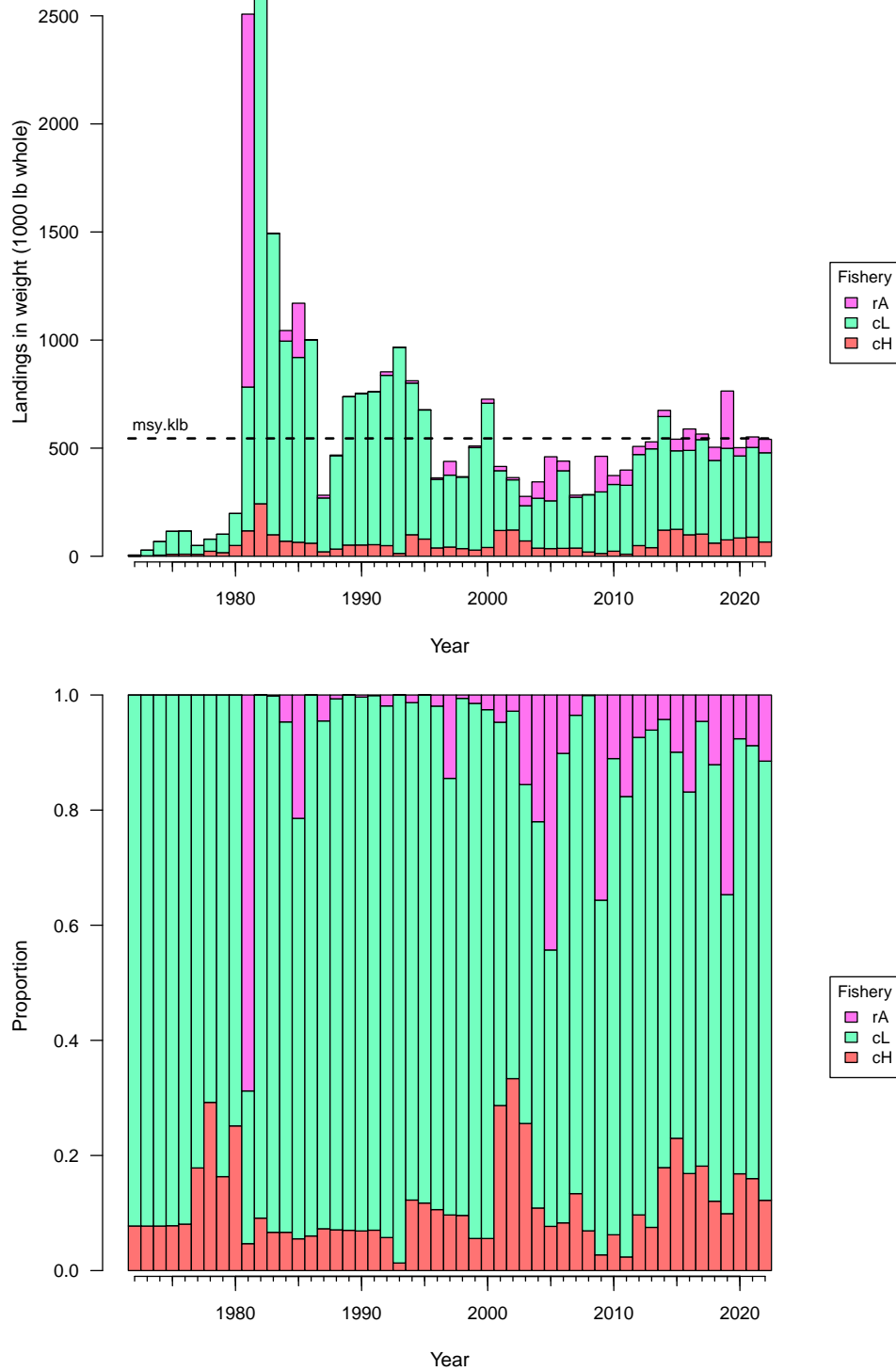


Figure 20. Beverton–Holt spawner-recruit curve (top) with and without lognormal bias correction. The expected (upper) curve was used for computing management benchmarks. Years within panel indicate year of recruitment generated from spawning biomass. Natural log of recruits (number of age-1 fish) per spawner is also plotted as function of the spawning stock (lower).

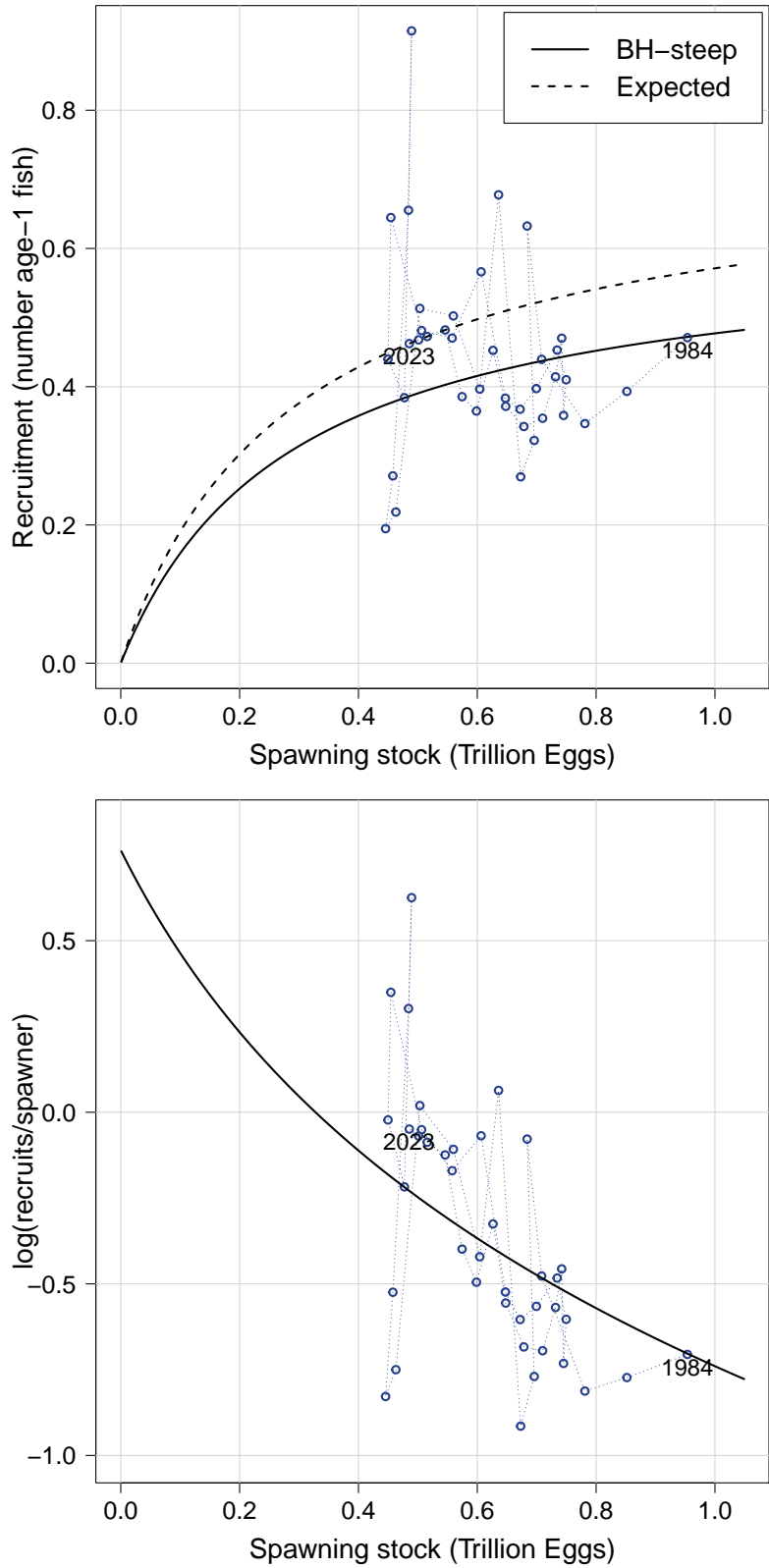


Figure 21. Probability densities of spawner-recruit quantities R_0 (unfished recruitment of age-1 fish), steepness, unfished spawners per recruit (million of eggs), and standard deviation of recruitment residuals in log space. Solid blue vertical lines represent point estimates or values from the BAM base run; dashed green vertical lines represent medians from the MCBE runs ($n = 3018$).

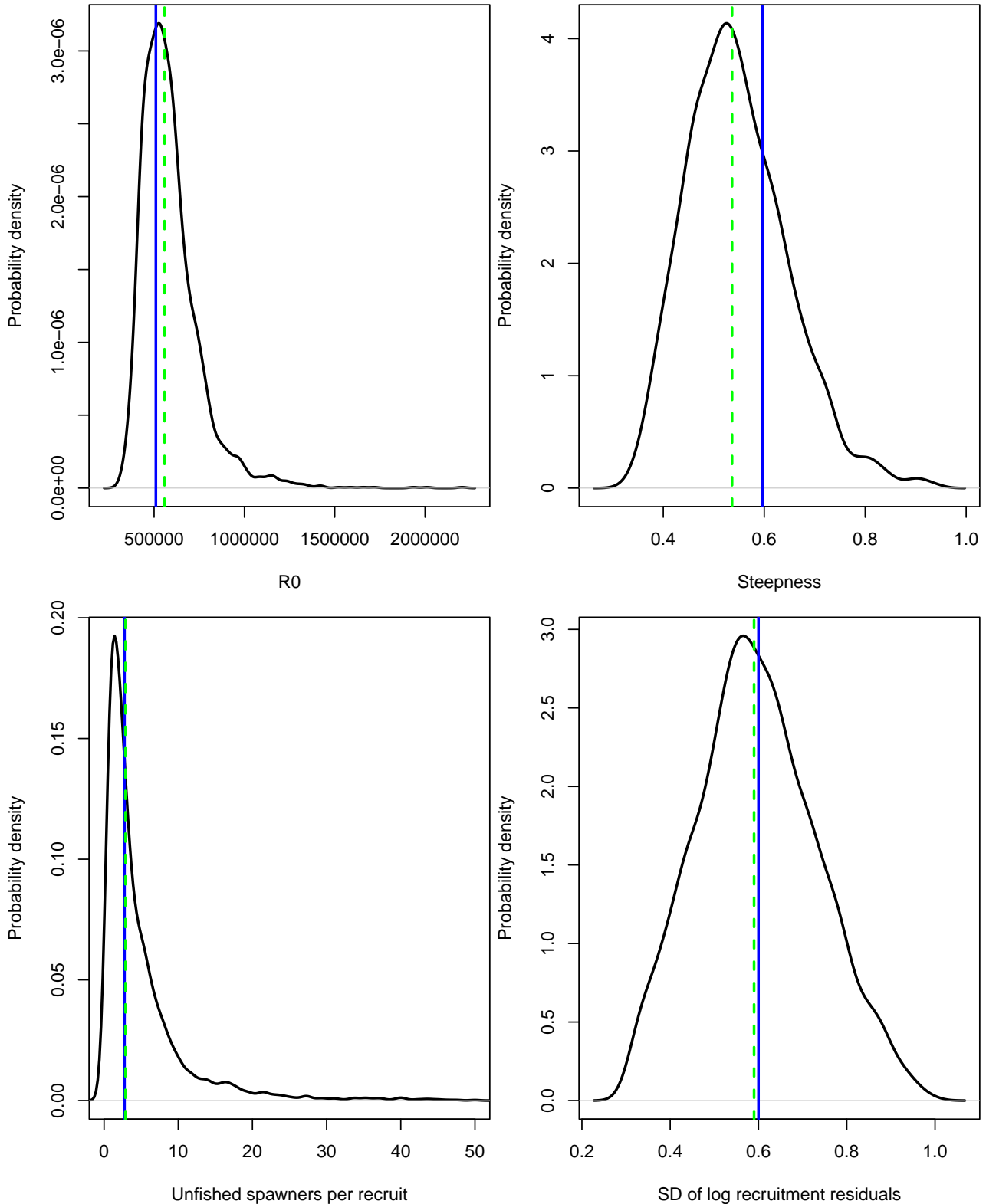


Figure 22. Yield per recruit (top; lb GW) and spawning potential ratio (bottom; spawning biomass per recruit relative to that at the unfished level) over a range of F . Both curves are based on average selectivity from the end of the assessment period.

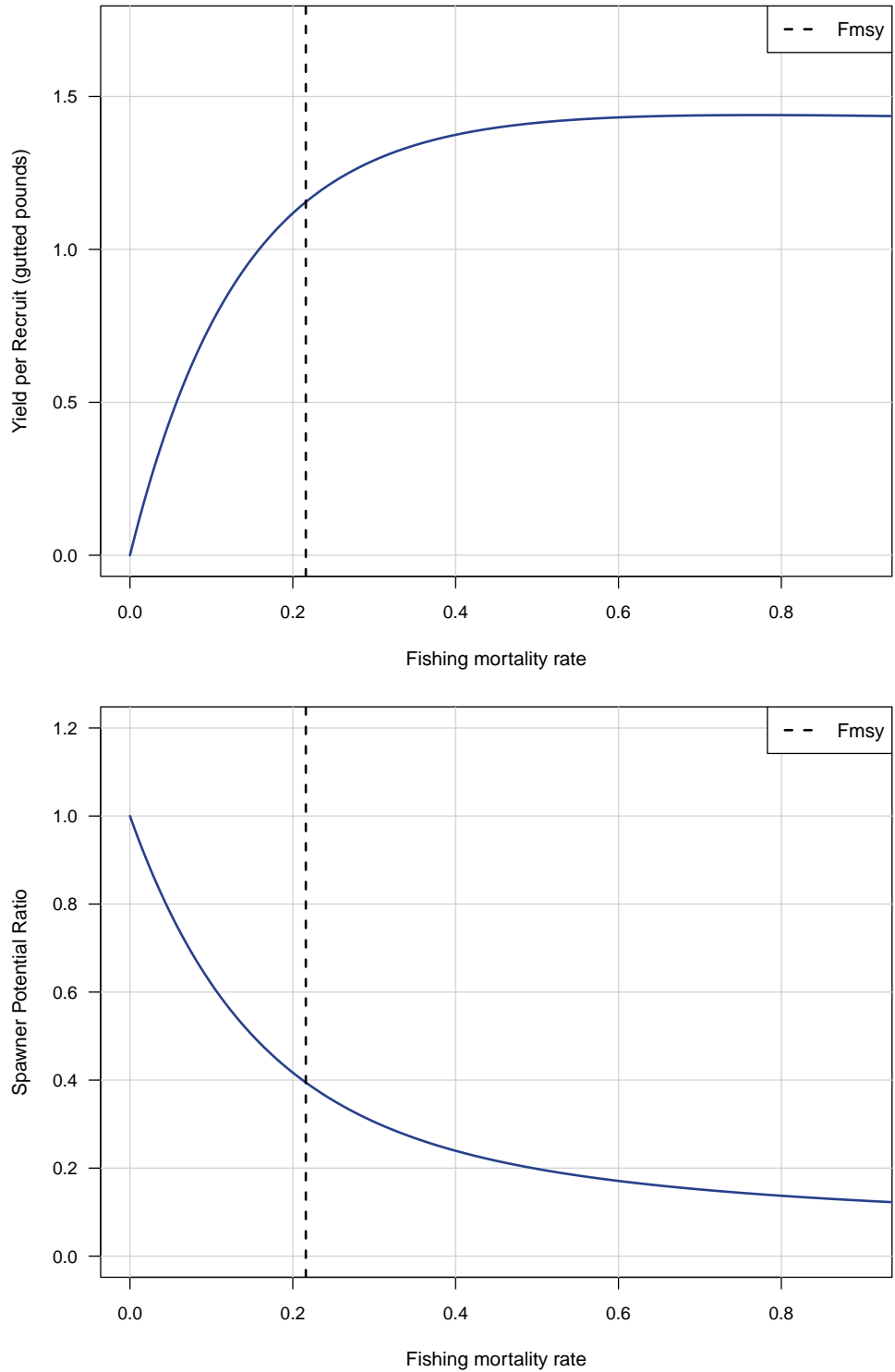


Figure 23. The top panel shows equilibrium landings at F . The peak occurs where fishing rate is $F_{MSY} = 0.216$ and equilibrium landings are $MSY = 545$ (1000 lb GW). The bottom panel shows equilibrium spawning biomass at F . Both curves are based on average selectivity from the end of the assessment period.

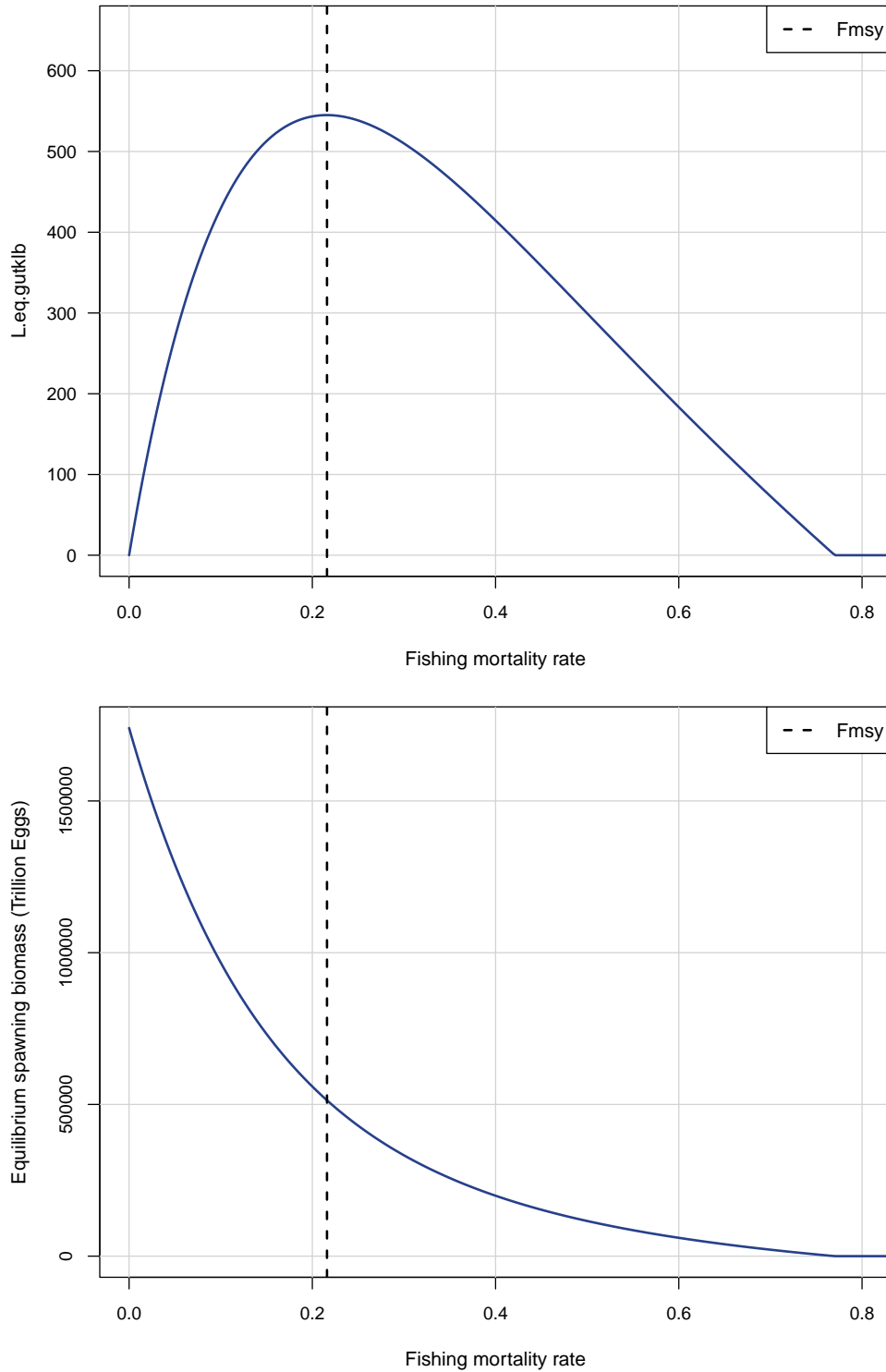


Figure 24. Probability densities of MSY-related benchmarks from MCBE analysis ($n = 3018$). The solid blue vertical line represent point estimates from the BAM base run; green dashed vertical line represent medians from the MCBE runs.

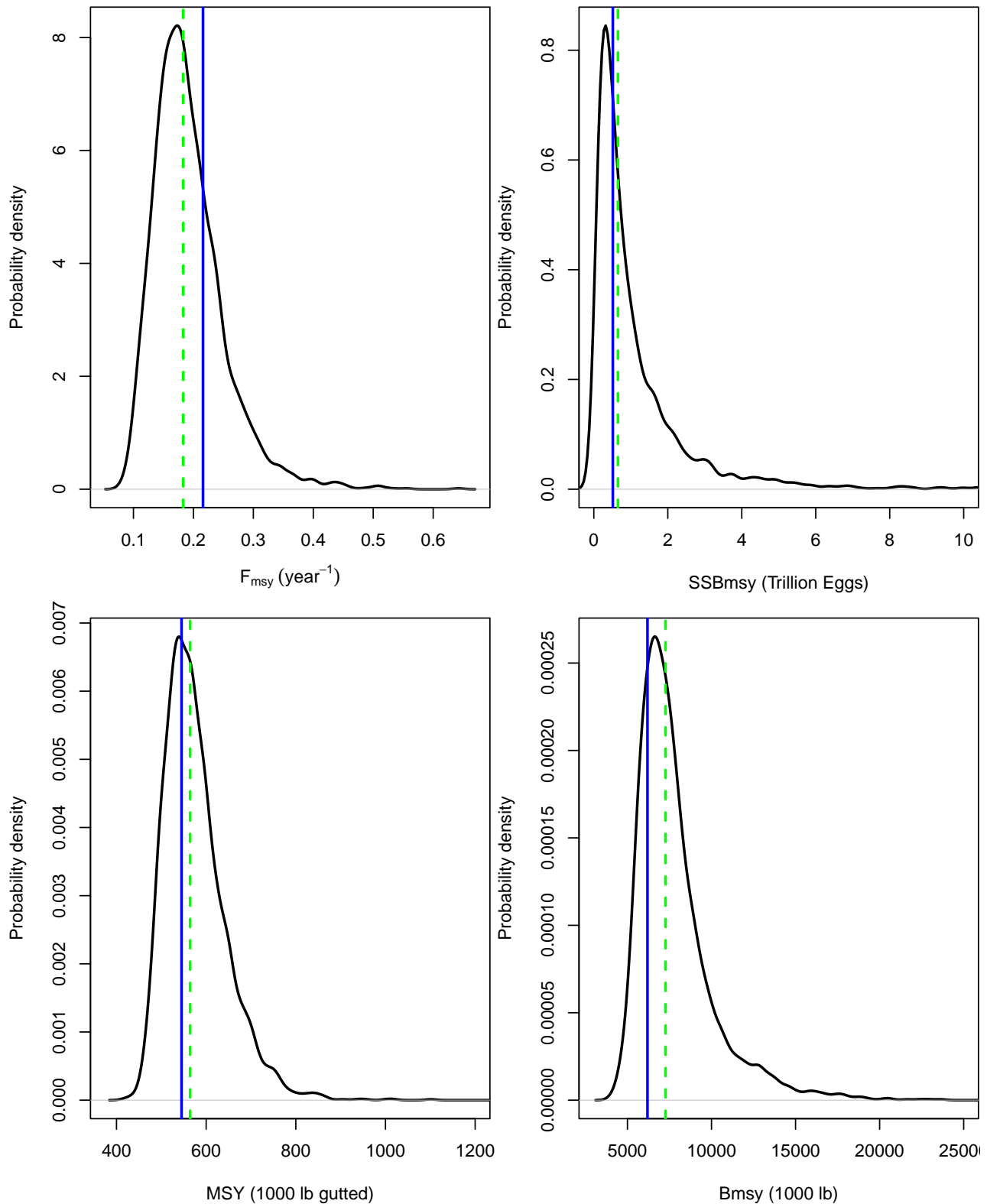


Figure 25. Estimated time series of SSB and F relative to benchmarks: (top) spawning biomass relative to the minimum stock size threshold (MSST), (middle) spawning biomass relative to the spawning stock as MSY (SSB_{MSY}), (bottom) F relative to F_{MSY} . Shaded region represents 90% confidence bands from the MCBE runs ($n = 3018$). The blue solid dotted line represents the estimate from the BAM base run, while the green dashed line represents the median across the MCBE runs for each year.

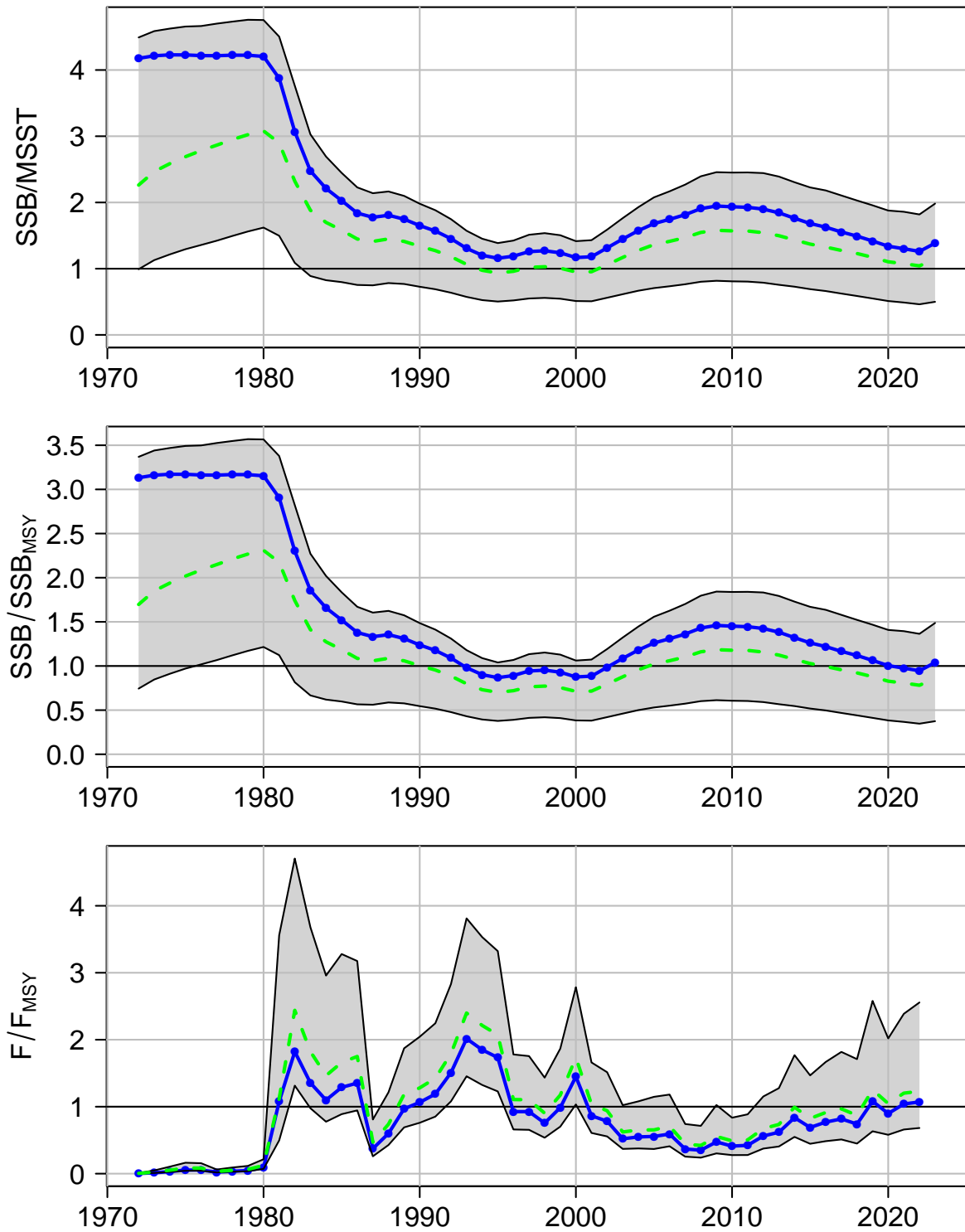


Figure 26. Estimated time series of SSB in million eggs at peak spawning. The solid blue dotted line is the estimate from the base BAM model, the dashed green line is the median of each year of the MCBE runs and the shaded region represents 90% confidence bands from the MCBE runs ($n = 3018$).

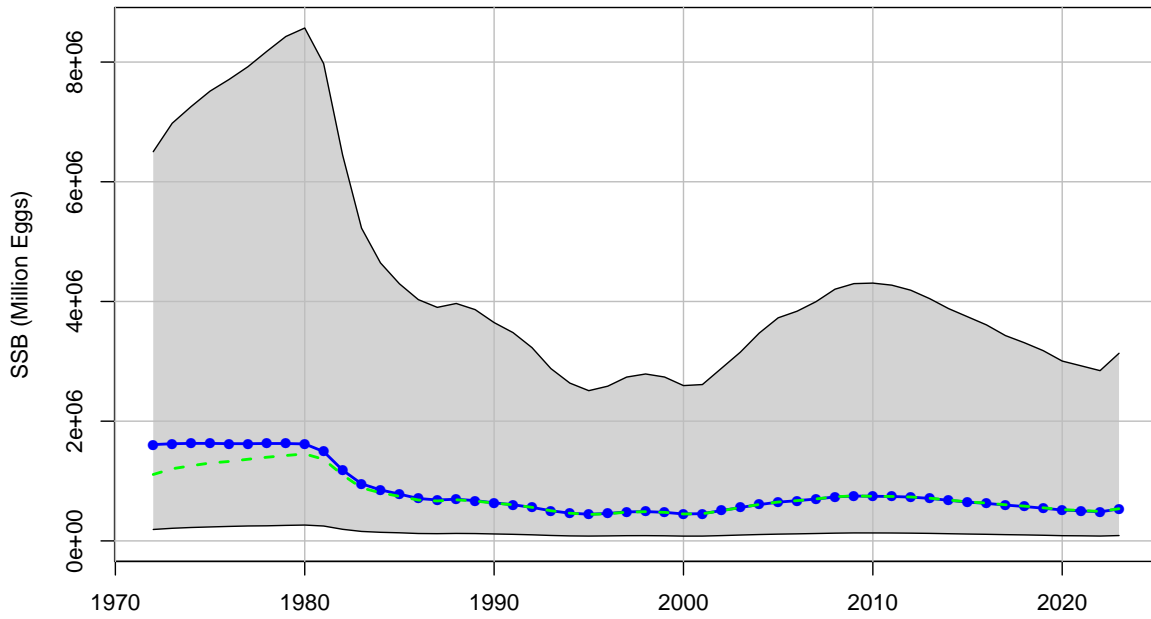


Figure 27. Probability densities of terminal status estimates from MCBE analysis of the Beaufort Assessment Model ($n = 3018$). The solid blue vertical line represent point estimates from the BAM base run; the dashed green vertical line represent medians from the MCBE runs.

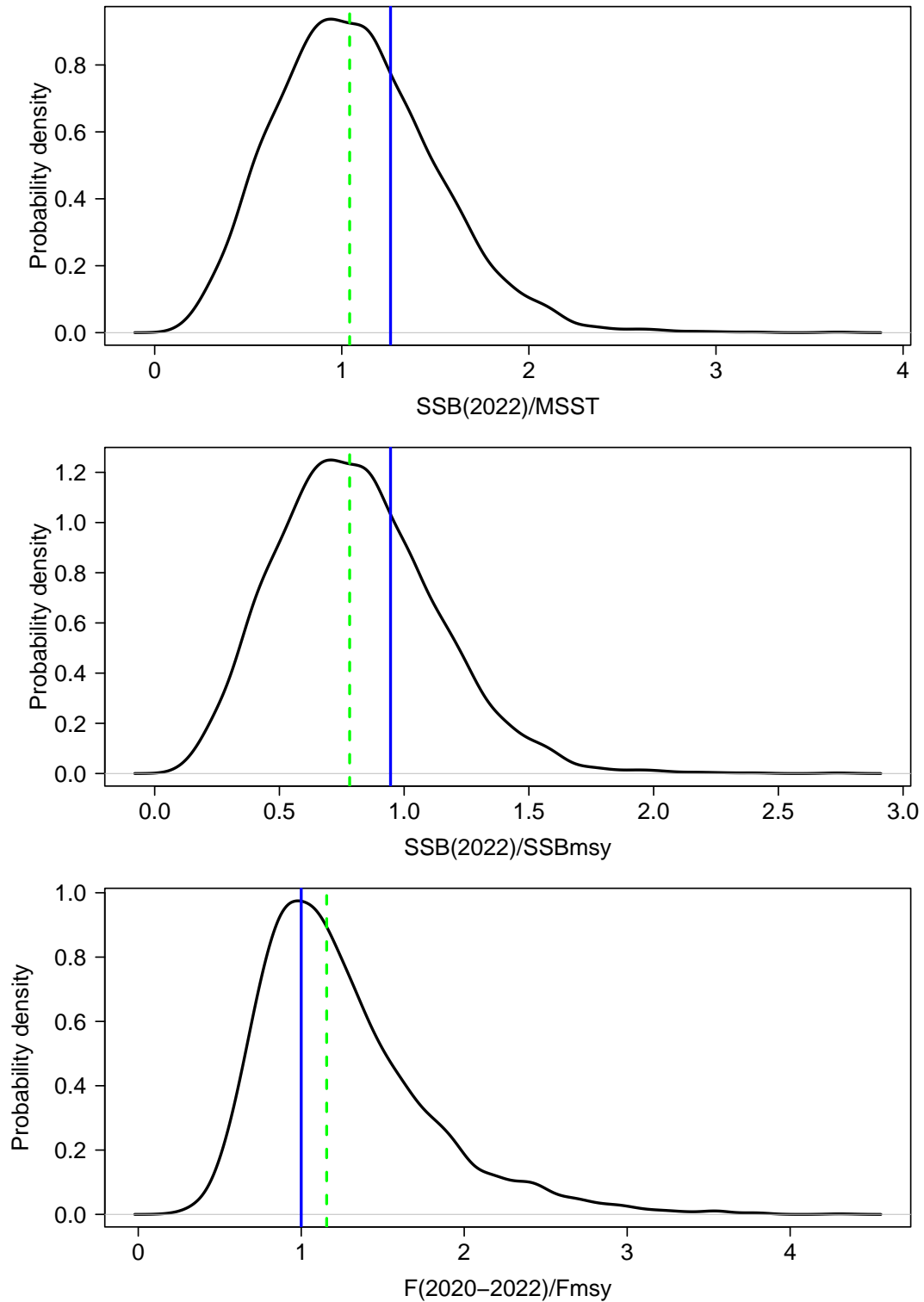


Figure 28. Phase plots of terminal status estimates from the MCBE of the Beaufort Assessment Model. Top panel is status relative to MSST, and the bottom panel is status relative to MSY. The filled black dot indicates the estimate from the base run; the purple filled triangle is the median of the MCBE analysis ($n = 3018$); the grey points indicate estimates from the MCBE runs and the shaded region is the 90th percentile of the two parameters.

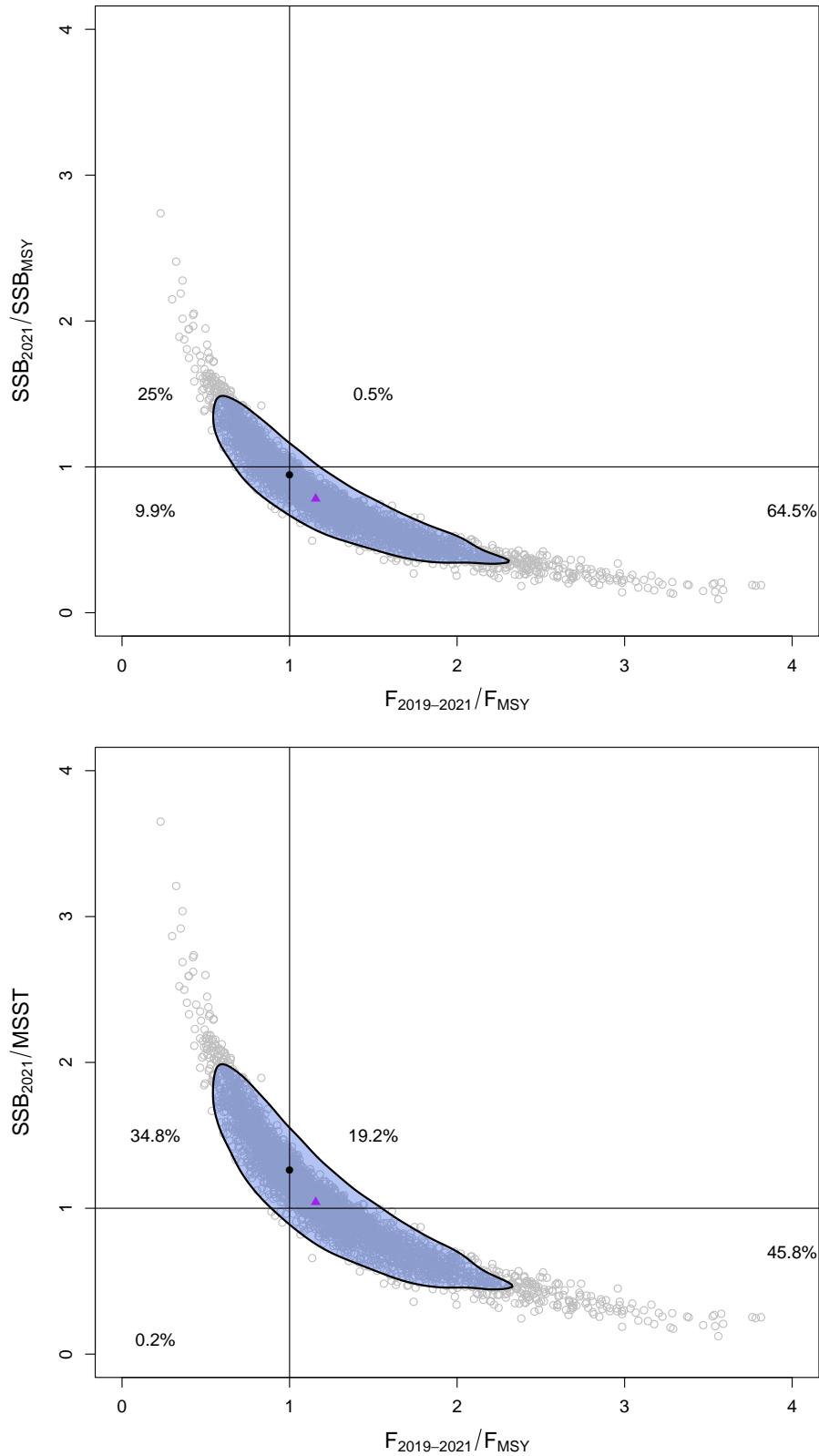


Figure 29. Estimated age structure from a series of individual years during the assessment, relative to the equilibrium expected at F_{MSY} .

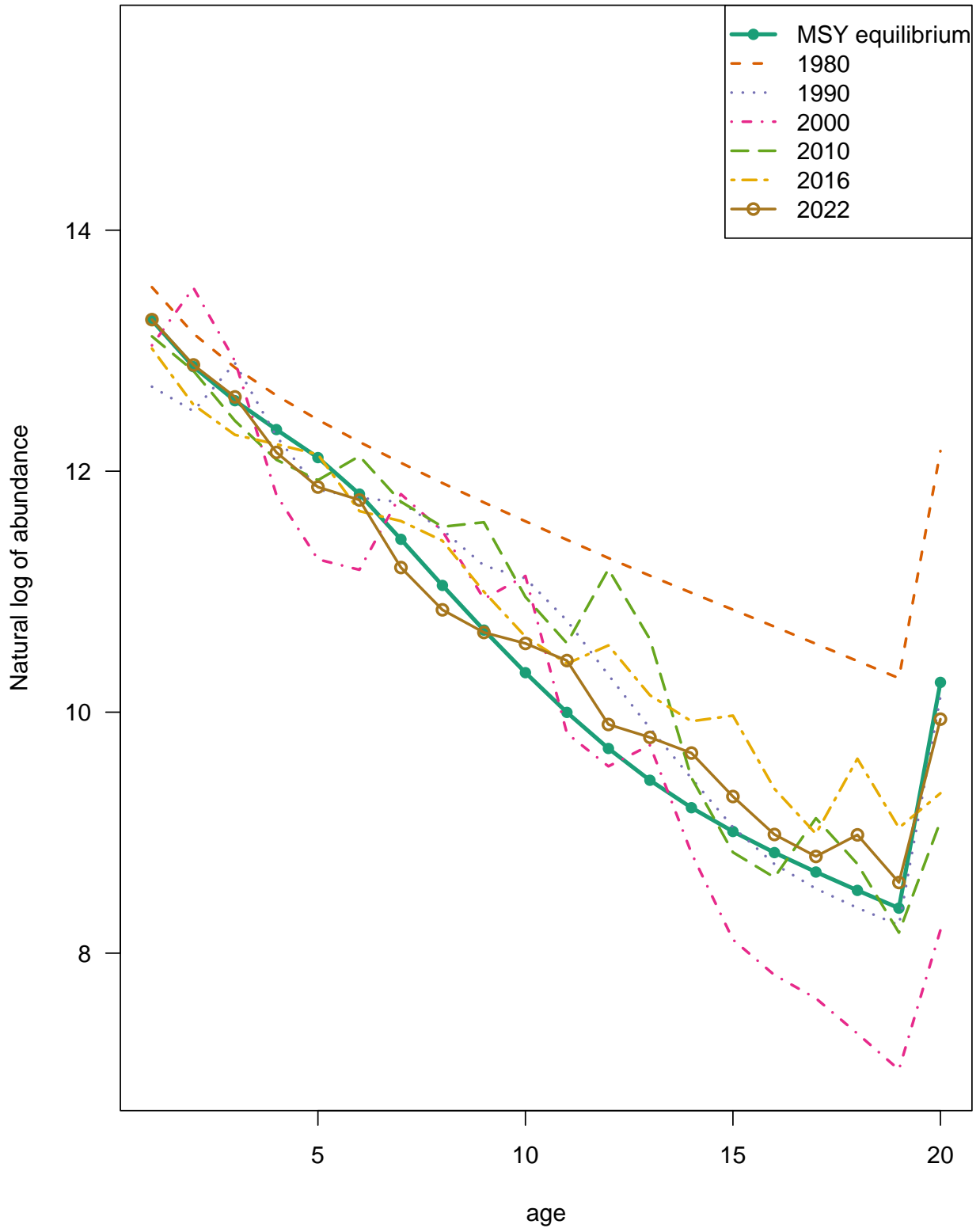


Figure 30. Sensitivity to low and high values of oldest and youngest ages used to calculate natural mortality at age: ($S1-S4$). Estimated time series of F and SSB relative to benchmarks. Sensitivity runs are indicated by colored broken lines, represented in the legend. Top panel: spawning stock biomass (SSB) relative to $MSST$. Bottom panel: F relative to F_{MSY} .

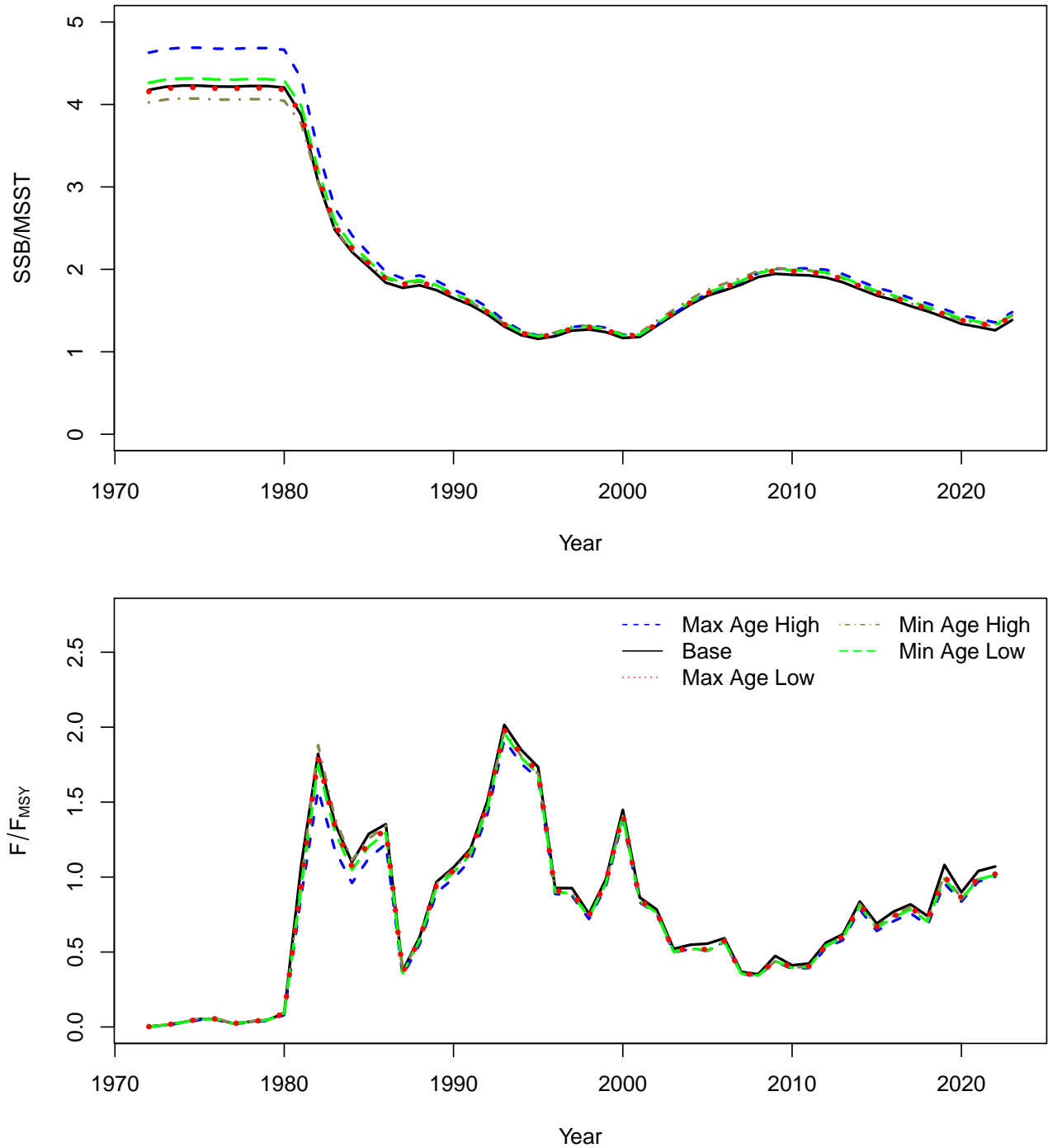


Figure 31. Sensitivity to low and high fixed values of steepness: (S5-S6). Estimated time series of F and SSB relative to benchmarks. Sensitivity runs are indicated by colored broken lines, represented in the legend. Top panel: spawning stock biomass (SSB) relative to $MSST$. Bottom panel: F relative to F_{MSY} .

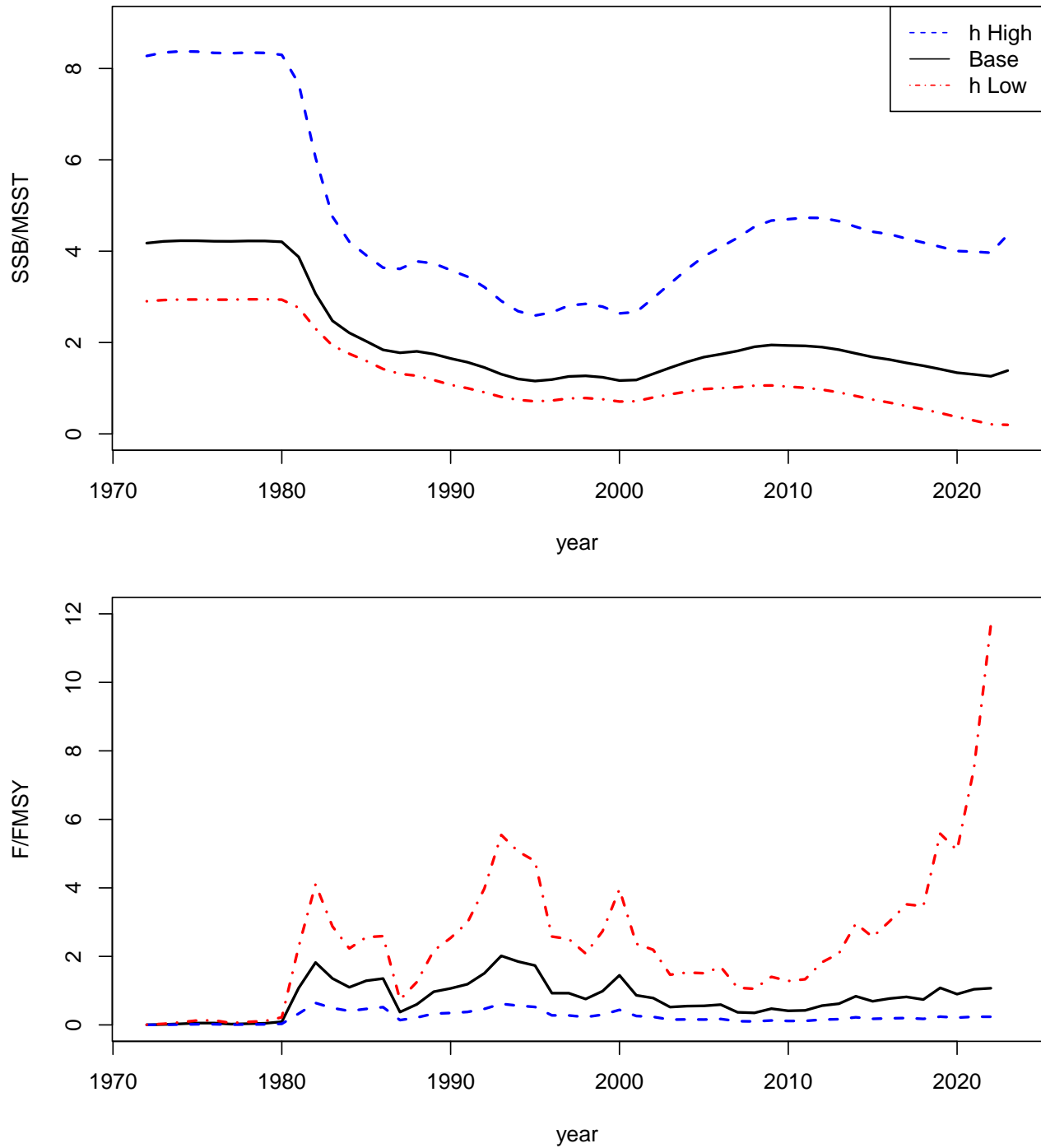


Figure 32. Sensitivity to low and high values of F_{init} : (S7-S8). Estimated time series of F and SSB relative to benchmarks. Sensitivity runs are indicated by colored broken lines, represented in the legend. Top panel: spawning stock biomass (SSB) relative to $MSST$. Bottom panel: F relative to F_{MSY} .

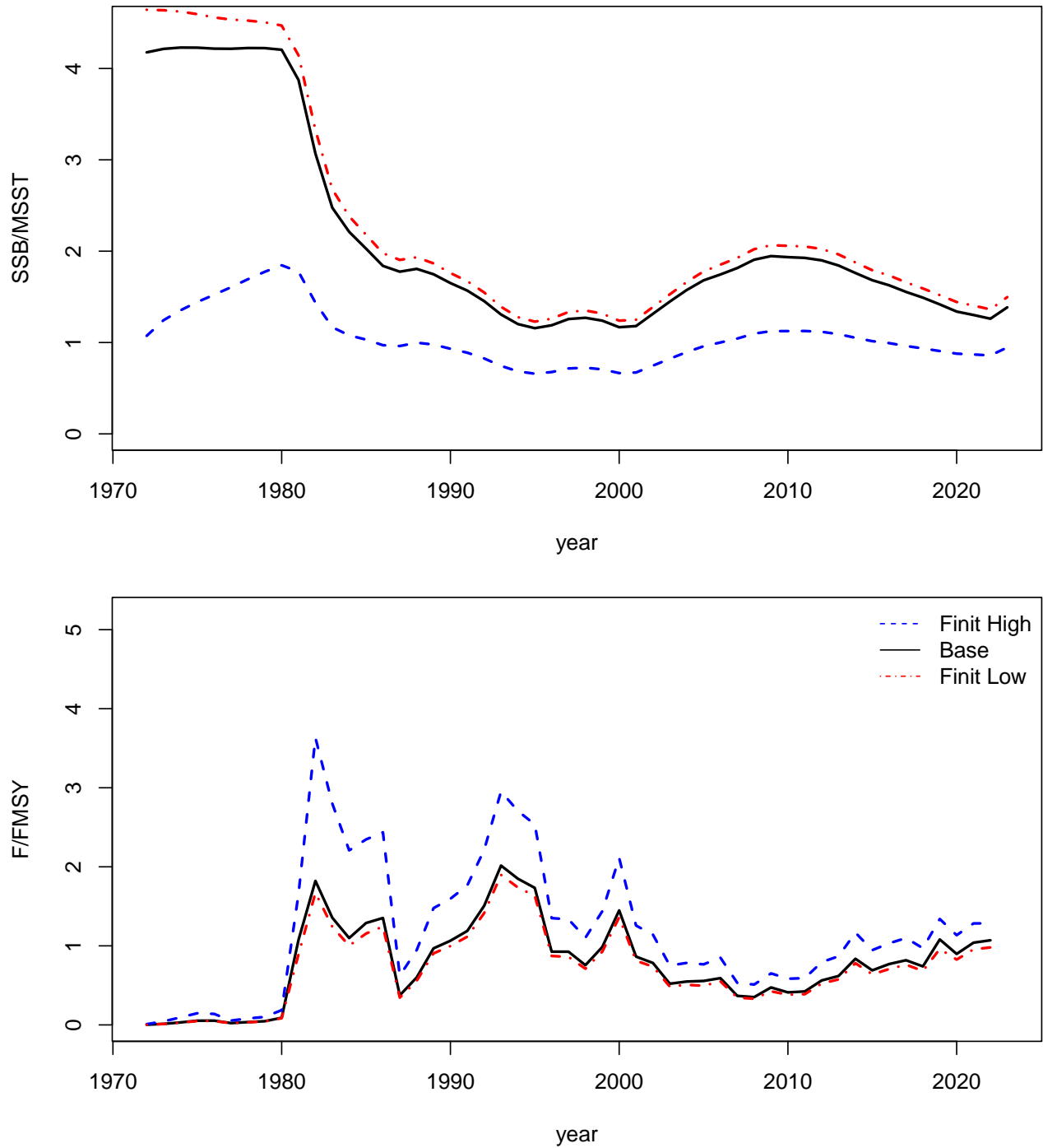


Figure 33. Sensitivity to low and high fixed t_0 values and estimated growth curves: (S9-S10). Estimated time series of F and SSB relative to benchmarks. Sensitivity runs are indicated by colored broken lines, represented in the legend. Top panel: spawning stock biomass (SSB) relative to $MSST$. Bottom panel: F relative to F_{MSY} .

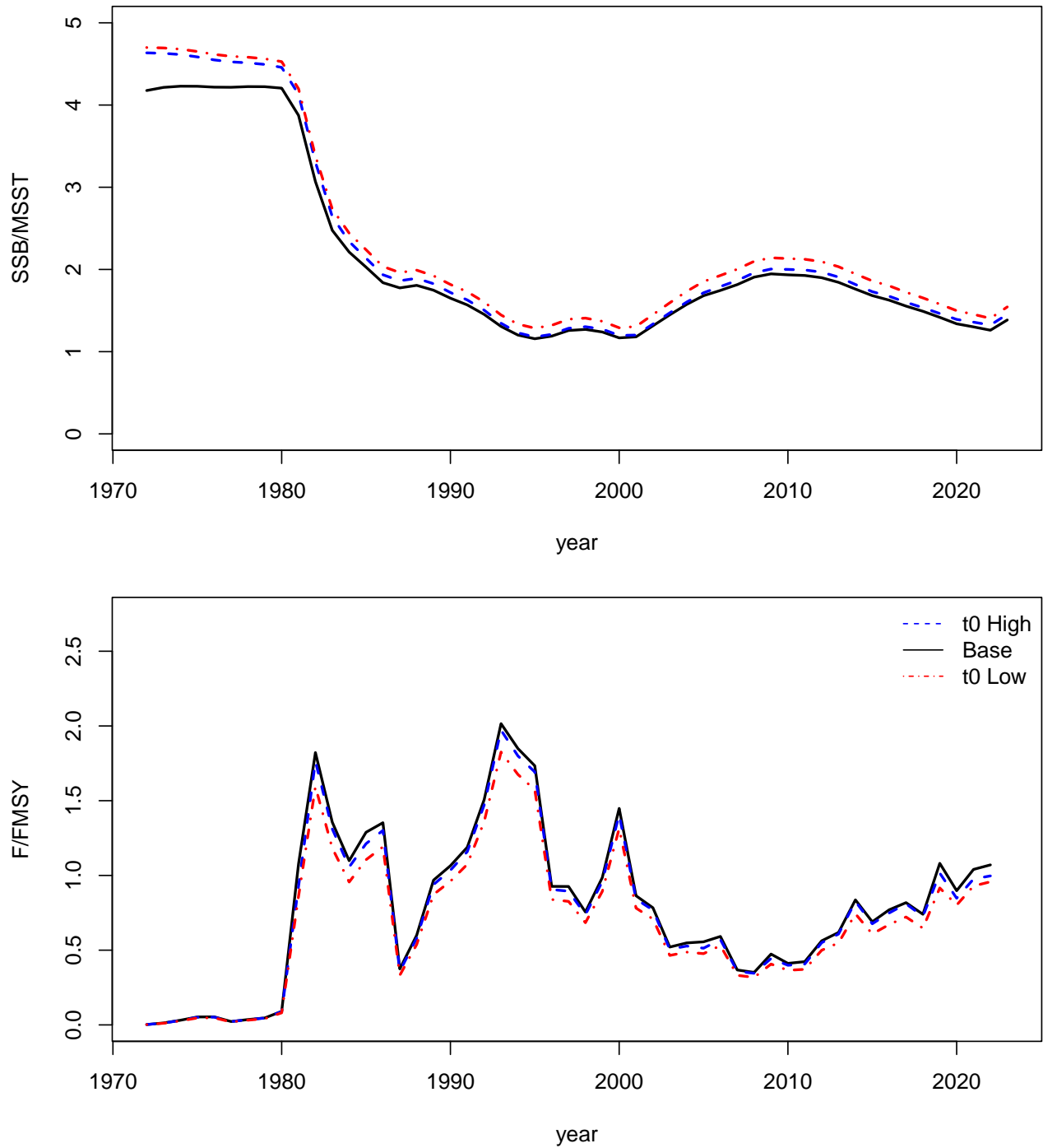


Figure 34. Retrospective analysis reducing the terminal year of the assessment from 2022 to values over a range from 2015 to 2021. Value at the top of each plot indicate the Mohn's rho value. Top left panel: Spawning Stock Biomass. Top right panel: Recruits. Bottom left panel: Biomass. Bottom right: Fishing mortality rates. Closed circles show terminal-year estimates.

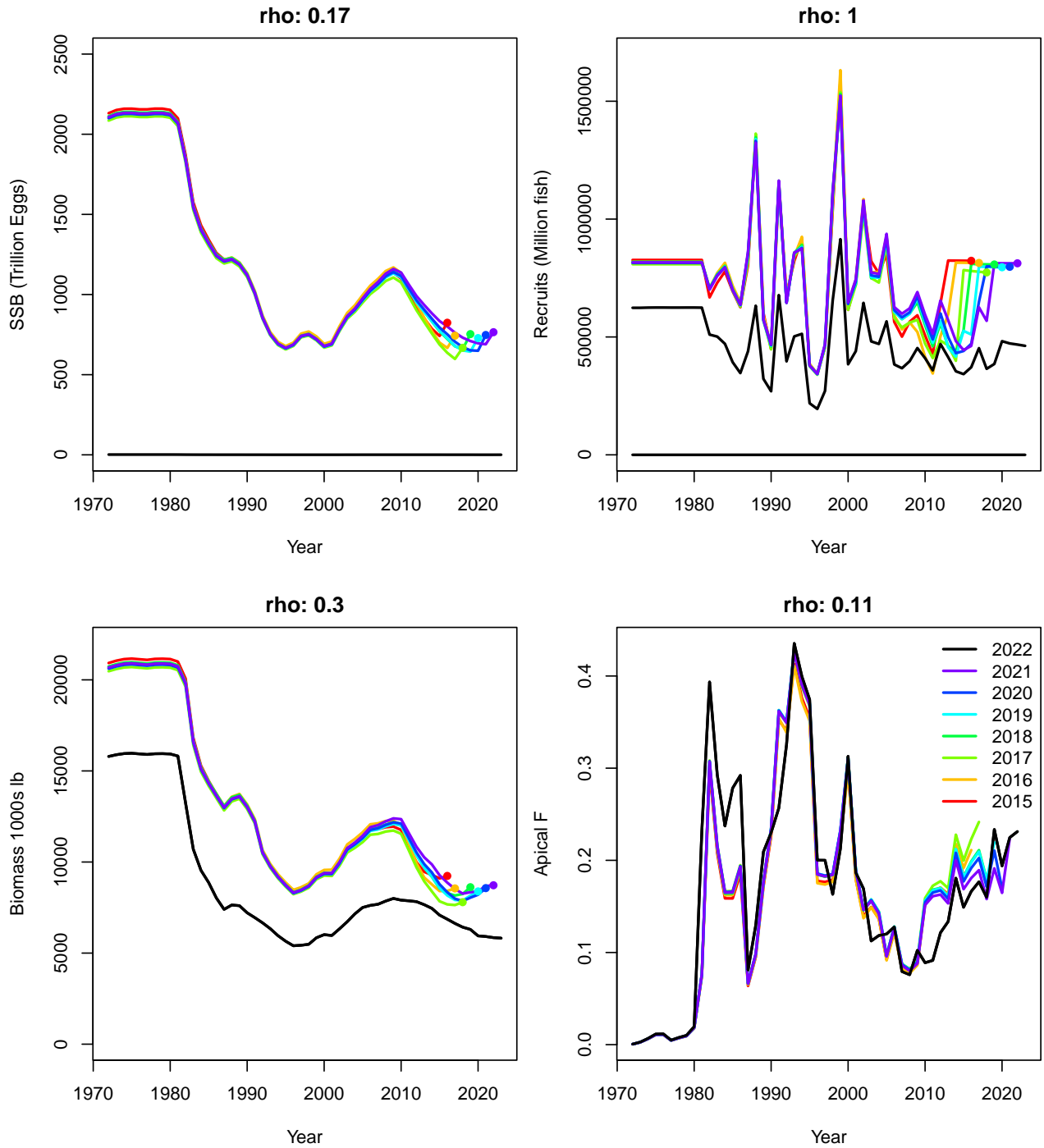


Figure 35. Plots of SSB, landings, recruits, F , and the probability that $SSB > MSST$ for projections with fishing mortality rate at fixed F that provides $P^* = 0.50$. In all panels except the bottom right, expected values (base run) represented by solid lines with solid circles, medians represented by dashed lines with open circles, and uncertainty represented by thin lines corresponding to 5th and 95th percentiles of replicate projections. Solid horizontal blue lines mark MSY-related quantities from the base model; dashed horizontal green lines represent corresponding medians from the MCBE analysis. Spawning stock (SSB) is at time of peak spawning. In the bottom right panel, the curve represents the proportion of projection replicates for which SSB exceeds the replicate-specific $MSST$.

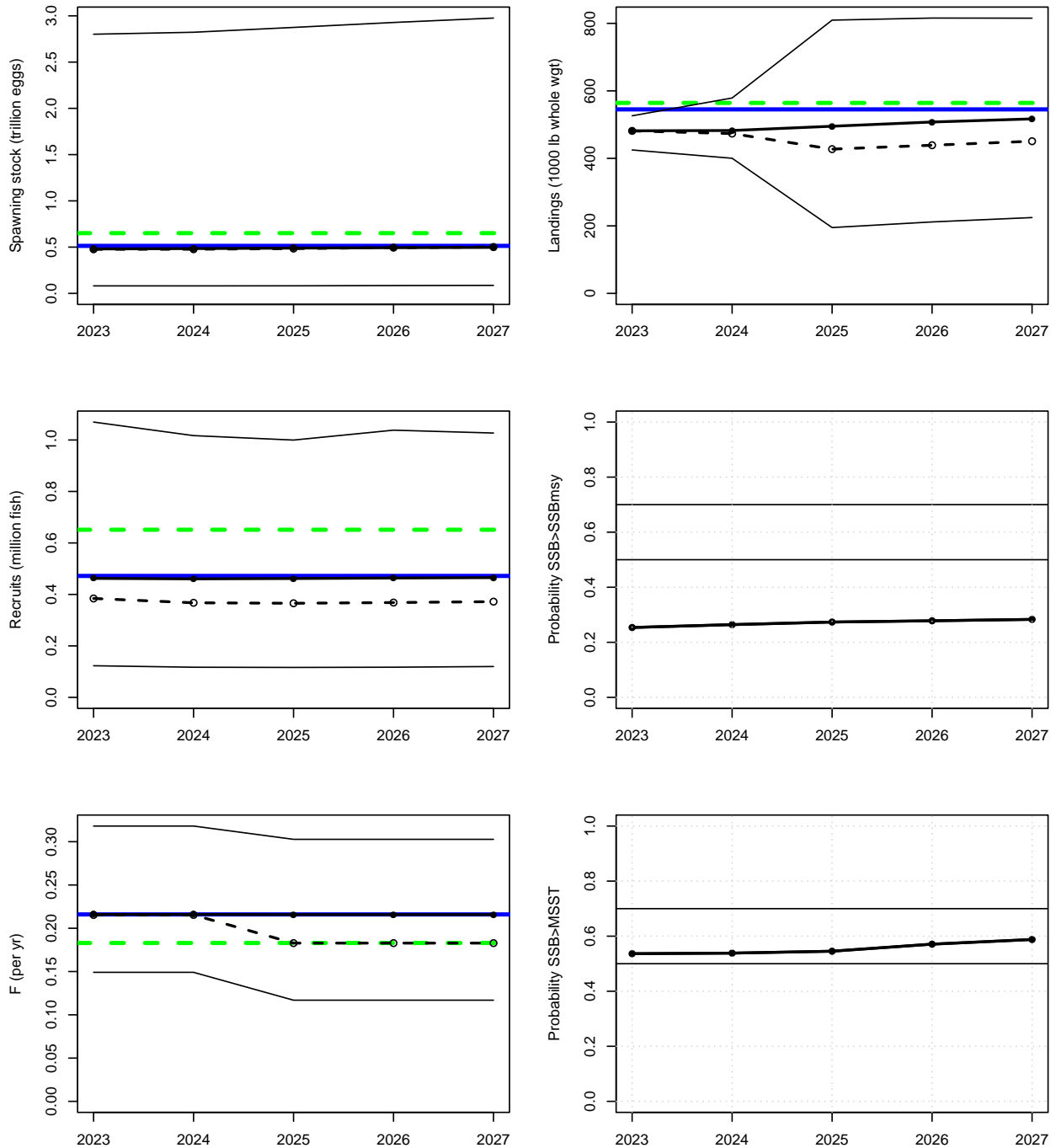


Figure 36. Plots of SSB, landings, recruits, F , and the probability that $SSB > MSST$ for projections with fishing mortality rate fixed at $F = F_{MSY}$. In all panels except the bottom right, expected values (base run) represented by solid lines with solid circles, medians represented by dashed lines with open circles, and uncertainty represented by thin lines corresponding to 5th and 95th percentiles of replicate projections. Solid horizontal blue lines mark MSY-related quantities from the base model; dashed horizontal green lines represent corresponding medians from the MCBE analysis. Spawning stock (SSB) is at time of peak spawning. In the bottom right panel, the curve represents the proportion of projection replicates for which SSB exceeds the replicate-specific $MSST$.

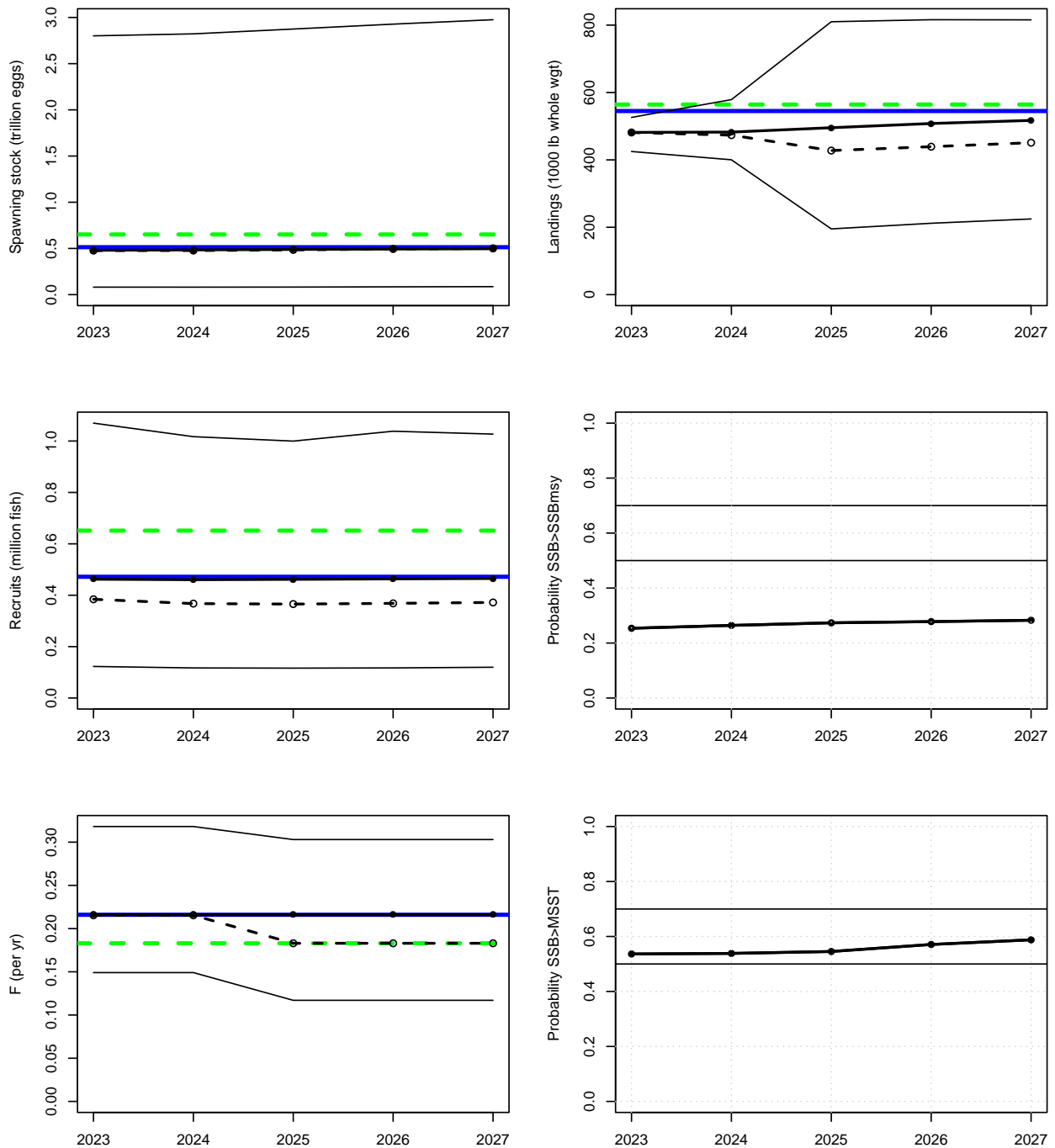


Figure 37. Plots of SSB, landings, recruits, F , and the probability that $SSB > MSST$ for projections with fishing mortality rate at fixed F that provides $P^* = 0.325$. In all panels except the bottom right, expected values (base run) represented by solid lines with solid circles, medians represented by dashed lines with open circles, and uncertainty represented by thin lines corresponding to 5th and 95th percentiles of replicate projections. Solid horizontal blue lines mark MSY-related quantities from the base model; dashed horizontal green lines represent corresponding medians from the MCBE analysis. Spawning stock (SSB) is at time of peak spawning. In the bottom right panel, the curve represents the proportion of projection replicates for which SSB exceeds the replicate-specific $MSST$.

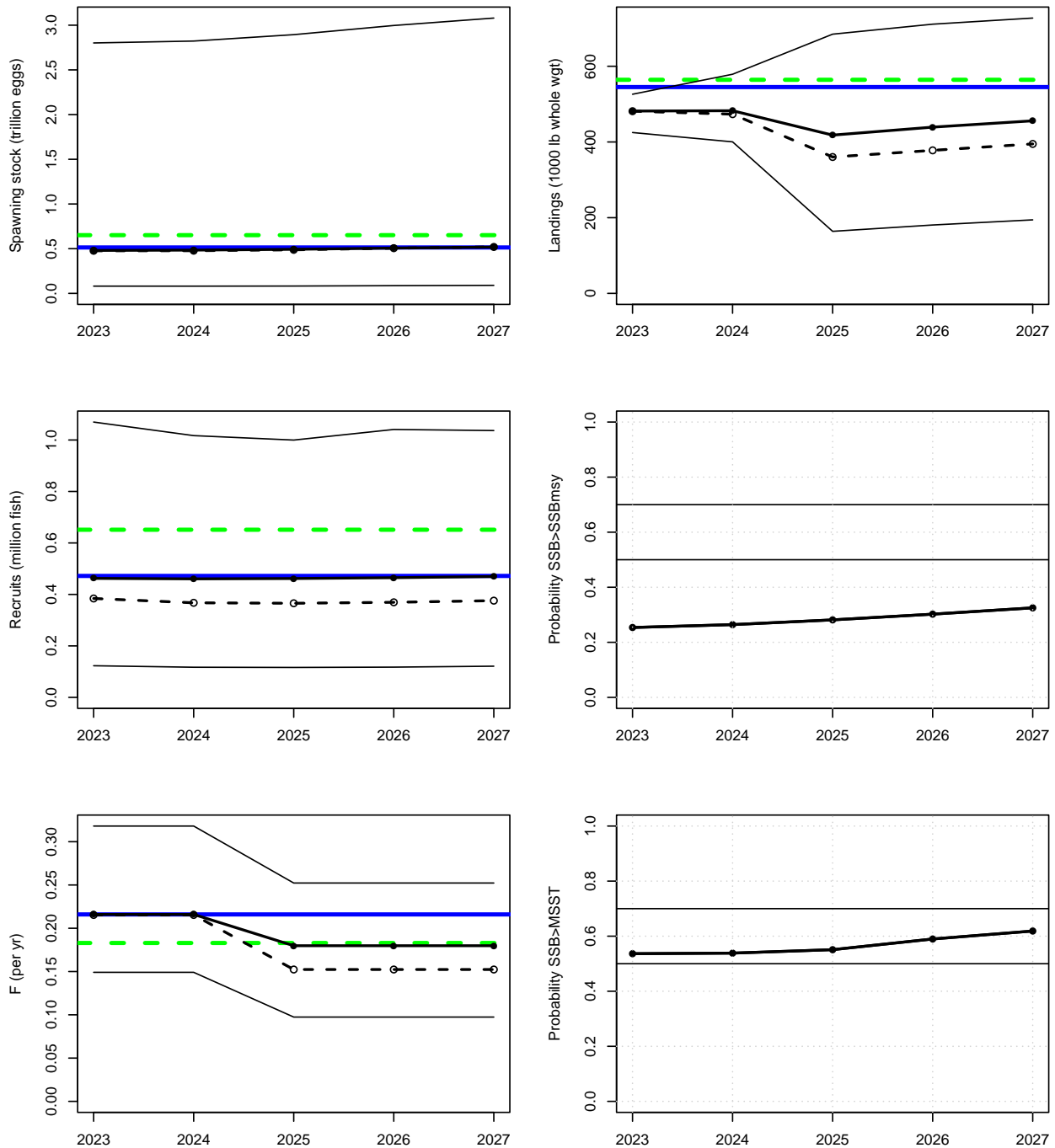


Figure 38. Plots of SSB, landings, recruits, F , and the probability that $SSB > MSST$ for projections with fishing mortality rate at fixed F that provides $P^* = 0.30$. In all panels except the bottom right, expected values (base run) represented by solid lines with solid circles, medians represented by dashed lines with open circles, and uncertainty represented by thin lines corresponding to 5th and 95th percentiles of replicate projections. Solid horizontal blue lines mark MSY-related quantities from the base model; dashed horizontal green lines represent corresponding medians from the MCBE analysis. Spawning stock (SSB) is at time of peak spawning. In the bottom right panel, the curve represents the proportion of projection replicates for which SSB exceeds the replicate-specific $MSST$.

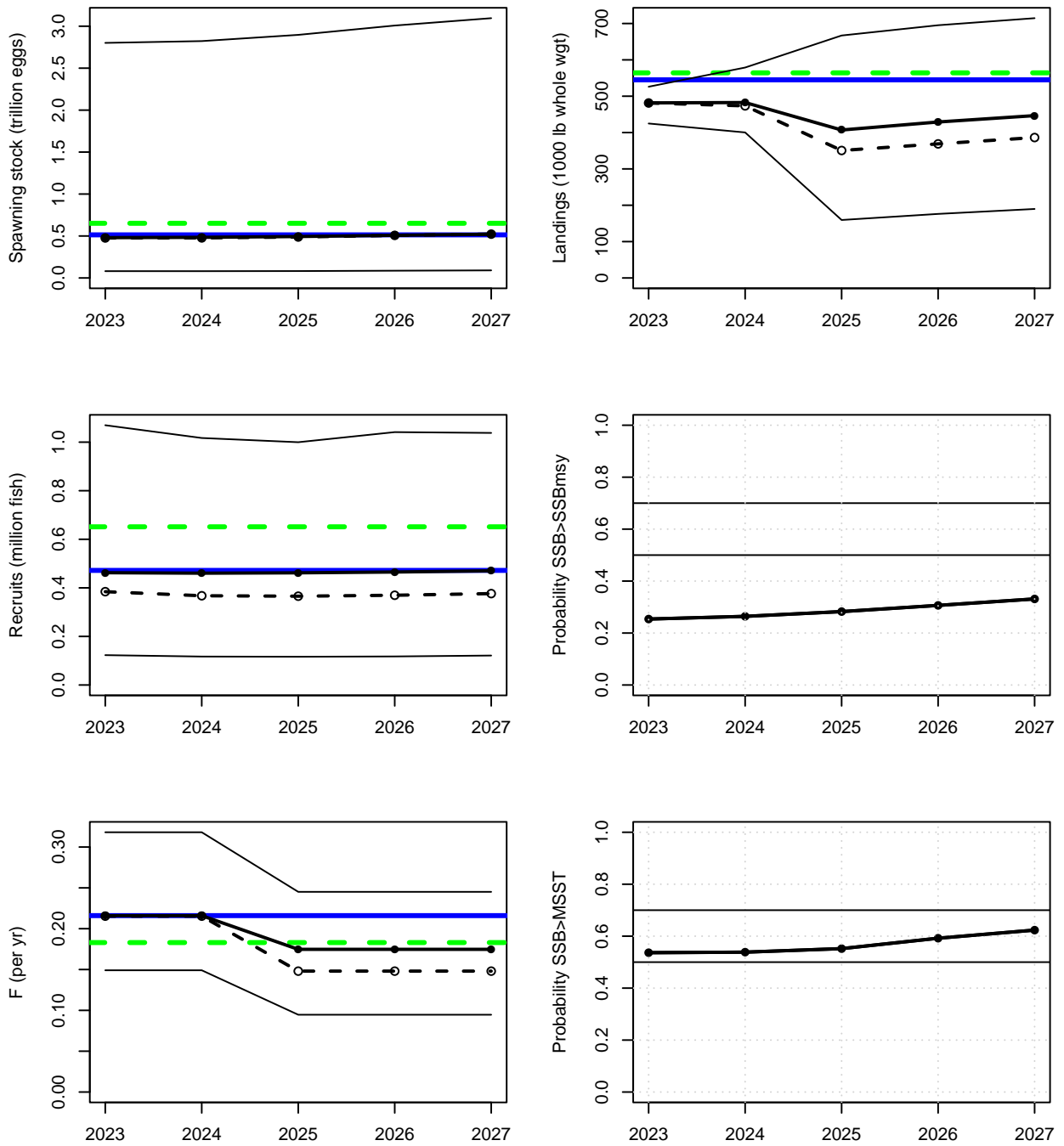
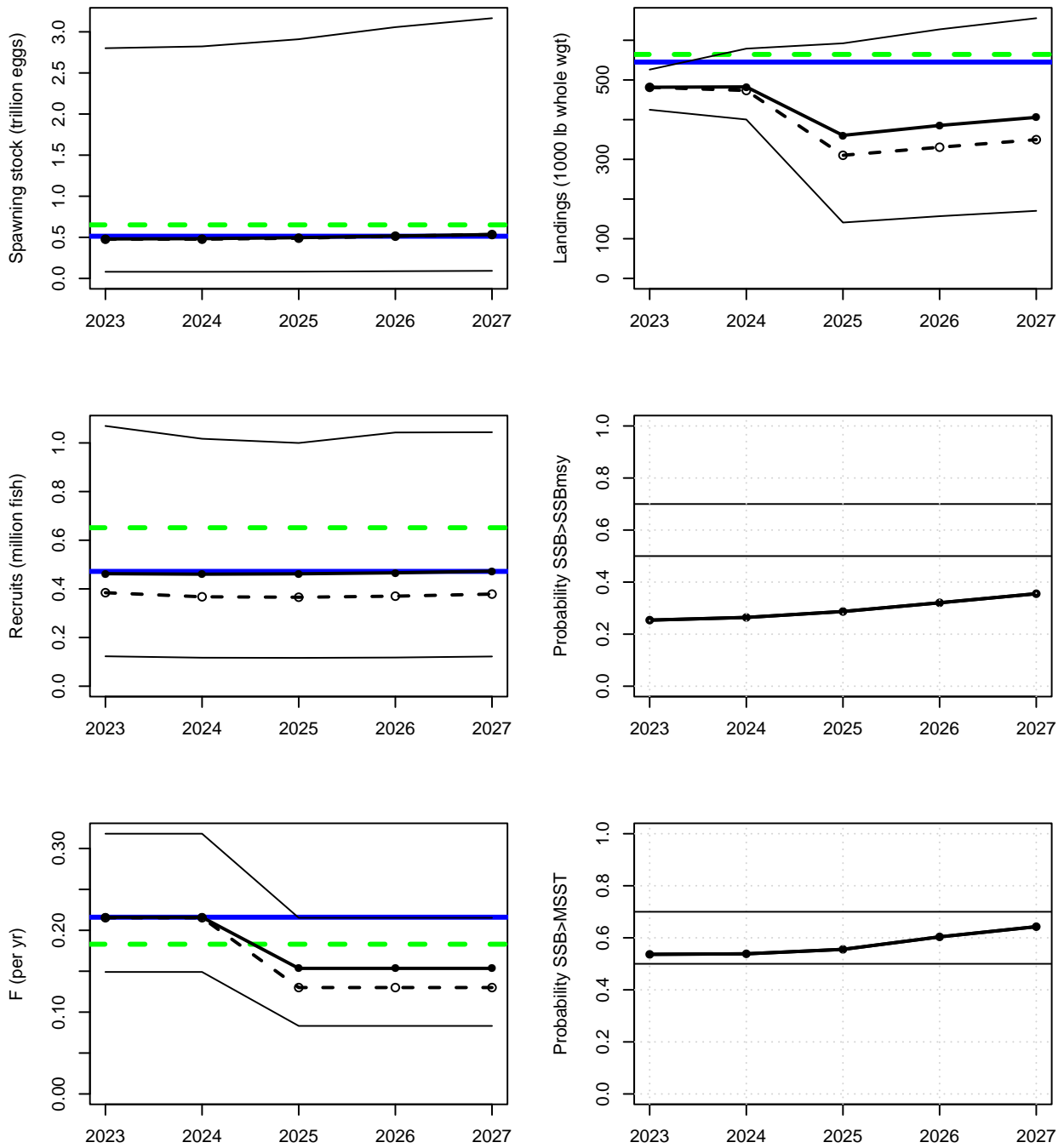


Figure 39. Plots of SSB, landings, recruits, F , and the probability that $SSB > MSST$ for projections with fishing mortality rate at fixed F that provides $P^* = 0.20$. In all panels except the bottom right, expected values (base run) represented by solid lines with solid circles, medians represented by dashed lines with open circles, and uncertainty represented by thin lines corresponding to 5th and 95th percentiles of replicate projections. Solid horizontal blue lines mark MSY-related quantities from the base model; dashed horizontal green lines represent corresponding medians from the MCBE analysis. Spawning stock (SSB) is at time of peak spawning. In the bottom right panel, the curve represents the proportion of projection replicates for which SSB exceeds the replicate-specific $MSST$.



Appendix A Abbreviations and symbols

Table 24. Acronyms and abbreviations used in this report

Symbol	Meaning
ABC	Acceptable Biological Catch
AW	Assessment Workshop (here, for tilefish)
ASY	Average Sustainable Yield
B	Total biomass of stock, conventionally on January 1
BAM	Beaufort Assessment Model (a statistical catch-age formulation)
CPUE	Catch per unit effort; used after adjustment as an index of abundance
CV	Coefficient of variation
CI	Confidence Interval
CVID	SERFS index combining sampling from chevron traps and video gear
DW	Data Workshop (here, for tilefish)
F	Instantaneous rate of fishing mortality
F_{MSY}	Fishing mortality rate at which MSY can be attained
FL	State of Florida
GA	State of Georgia
GLM	Generalized linear model
K	Average size of stock when not exploited by man; carrying capacity
kg	Kilogram(s); 1 kg is about 2.2 lb.
klb	Thousand pounds; thousands of pounds
lb	Pound(s); 1 lb is about 0.454 kg
m	Meter(s); 1 m is about 3.28 feet.
M	Instantaneous rate of natural (non-fishing) mortality
MARMAP	Marine Resources Monitoring, Assessment, and Prediction Program, a fishery-independent data collection program of SCDNR
MCBE	Monte Carlo/Bootstrap ensemble, an approach to quantifying uncertainty in model results
MFMT	Maximum fishing-mortality threshold; a limit reference point used in U.S. fishery management; often based on F_{MSY}
mm	Millimeter(s); 1 inch = 25.4 mm
MRFSS	Marine Recreational Fisheries Statistics Survey, a data-collection program of NMFS, predecessor of MRIP
MRIP	Marine Recreational Information Program, a data-collection program of NMFS, descended from MRFSS
MSST	Minimum stock-size threshold; a limit reference point used in U.S. fishery management. The SAFMC has defined MSST for tilefish as $(1 - M)SSB_{\text{MSY}} = 0.7SSB_{\text{MSY}}$.
MSY	Maximum sustainable yield (per year)
mt	Metric ton(s). One mt is 1000 kg, or about 2205 lb.
N	Number of fish in a stock, conventionally on January 1
NC	State of North Carolina
NMFS	National Marine Fisheries Service, same as “NOAA Fisheries Service”
NOAA	National Oceanic and Atmospheric Administration; parent agency of NMFS
OY	Optimum yield; SFA specifies that $OY \leq MSY$.
PSE	Proportional standard error
R	Recruitment
SAFMC	South Atlantic Fishery Management Council (also, Council)
SC	State of South Carolina
SCDNR	Department of Natural Resources of SC
SDNR	Standard deviation of normalized residuals
SEDAR	SouthEast Data Assessment and Review process
SEFIS	SouthEast Fishery-Independent Survey
SERFS	SouthEast Reef Fish Survey
SFA	Sustainable Fisheries Act; the Magnuson–Stevens Act, as amended
SL	Standard length (of a fish)
SPR	Spawning potential ratio
SSB	Spawning stock biomass; mature biomass of males and females
SSB_{MSY}	Level of SSB at which MSY can be attained
TIP	Trip Interview Program, a fishery-dependent biodata collection program of NMFS
TL	Total length (of a fish), as opposed to FL (fork length) or SL (standard length)
VPA	Virtual population analysis, an age-structured assessment
WW	Whole weight, as opposed to GW (gutted weight)
yr	Year(s)

Appendix B Parameter estimates from the Beaufort Assessment Model

```

# Number of parameters = 210 Objective function value = 3155.54834340810 Maximum gradient component = 0.000438841837565458
# Linf:
830.180000000
# K:
0.204830000000
# t0:
-0.500000000000
# Linf_f:
731.530000000
# K_f:
0.250730000000
# t0_f:
-0.500000000000
# len_cv_val:
0.139624637052
# log_Nage_dev:
0.0000000000 0.0000000000 0.0000000000 0.0000000000 0.0000000000 0.0000000000 0.0000000000 0.0000000000 0.0000000000 0.0000000000
0.0000000000 0.0000000000 0.0000000000 0.0000000000 0.0000000000 0.0000000000 0.0000000000 0.0000000000 0.0000000000 0.0000000000
# log_R0:
13.3252697609
# steep:
0.605261457828
# rec_sigma:
0.600000000000
# R_autocorr:
0.000000000000
# log_rec_dev:
-0.00466330801544 0.0216764128415 0.00542004428770 -0.148946763508 -0.255191658862 0.00656489955407 0.392558164886 -0.293040244494 -0.465442136094 0.471728329844
-0.0476821543183 0.213407990204 0.270330679099 -0.553147955508 -0.655098604979 -0.335974441206 0.522488767198 0.843119154500 -0.0101959112982 0.149225681482
0.522322883760 0.201124952241 0.146399958810 0.304880790896 -0.104099103480 -0.158109823146 -0.0901460078318 0.0291518963842 -0.0759460144725 -0.210286506176
0.0607470465199 -0.0613812538307 -0.212495036966 -0.231929874582 -0.137434304448 0.0728863567074 -0.126271146124 -0.0565879798733
# log_dm_lenc_rA:
3.01940106589
# log_dm_agec_cH:
4.19561881180
# log_dm_agec_cL:
4.58521652087
# log_dm_agec_sM:
2.91013199728
# selpar_L50_cH:
5.78896803165
# selpar_L50_cH2:
4.57853445752
# selpar_L502_cH2:
8.23188412053
# selpar_slope_cH:
1.56674043238
# selpar_slope_cH2:
3.20297221044
# selpar_slope2_cH2:
0.815776495128
# selpar_L50_cL:
6.73466069041
# selpar_L50_cL2:
5.10055130652
# selpar_L502_cL2:
6.79781303724
# selpar_slope_cL:
1.67767102877
# selpar_slope_cL2:
2.13852615314
# selpar_slope2_cL2:
0.595434963237
# selpar_L50_rA:
2.92470050478
# selpar_slope_rA:
5.10039126442
# selpar_L50_sM:
6.19242566384
# selpar_slope_sM:
2.01031372985
# log_q_cpue_cL:
-8.00483140256
# log_q_cpue_sM:
-8.42015654662
# M_constant:
0.135000000000
# log_avg_F_L_cH:
-4.76657759827
# log_F_dev_L_cH:
-5.414797971431 -3.72694425813 -2.84485210601 -2.30730644419 -2.25737384315 -2.32309929341 -1.36323731323 -1.69093203903 -0.589076367345 0.367597547078
1.34822672775 0.708853527185 0.491001440775 0.515603701244 0.541741979290 -0.521660054839 -0.0773670671198 0.396668228569 0.483251930473 0.605989327686
0.616178195992 -0.620712077141 1.56092788469 1.43552023501 0.666072125739 0.661432327823 0.398493794448 0.146818228733 0.581298355692 1.76340251382
1.77852671729 1.10490587560 0.285592162434 0.121535685565 0.107289320246 0.0849579916929 -0.633702112005 -1.11501006604 -0.525834452163 -1.43228339479
0.242881336739 1.0714165765702 1.23833365951 1.32190346565 1.13856467029 1.21403734923 0.722883316269 1.00142110577 1.25869147654 1.34483779754 1.11733402396
# log_avg_F_L_cL:
-2.48299176886
# log_F_dev_L_cL:
-5.13723580712 -3.44859758071 -2.56697381584 -2.03663212797 -2.02477581355 -2.99516907945 -2.67875938516 -2.25646758780 -1.69725652145 -0.0957989615756
1.46275036939 1.19148566725 0.950854683121 0.989735766661 1.19457785540 -0.128562045754 0.371654199263 0.857233699966 0.951928756191 1.06448428895
1.30547860953 1.64739155948 1.45758081124 1.40777522046 0.786772622028 0.709427515928 0.592009976039 0.885733340726 1.26237023095 0.471534631111
0.347540060658 -0.0547040084896 0.117189008950 -0.110380489275 0.287479744285 -0.191301825147 -0.148907575302 -0.125835906993 -0.0735792586092 -0.0644109361185
0.227873887703 0.357416398387 0.564364175456 0.253748159106 0.370769752836 0.536728072969 0.438858027061 0.594180463290 0.609237355761 0.759027997346 0.810155818805
# log_avg_F_L_rA:

```

```
-6.22409079649
# log_F_dev_L_rA:
4.10202061817 -5.59222351440 -2.00449881188 1.04179685149 2.76302053890 -3.67348302726 -0.0996648556891 -1.51213203529 -5.35472812767 -1.57447528357
-2.72290212899 0.357131479316 -5.23168794018 0.0868620369747 -5.20605100986 -0.348884419840 1.83041324382 -1.53041786030 -0.247775586303 0.696201551403
0.670819415377 -0.0823173155141 1.29538614385 1.78285273221 2.71646906660 1.17224481221 -0.370752110379 -4.12411833823 2.39588602069 1.01938456541
1.55452783833 0.937081167283 0.821722957455 0.746133011234 1.41043638795 2.05868973179 0.763022102129 1.65795216009 3.16953807882 1.27359172102
1.54327061316 1.80965751969
# F_init:
0.010000000000
```

Appendix C Additional diagnostic plots for the base model

C.1 Parameter bounding plots

Figure 40. Diagnostic plot of parameter estimates to check for bounding issues, where the red lines indicate the upper and lower parameter bounds, orange is the initial model parameter starting value and blue is the final model estimate.

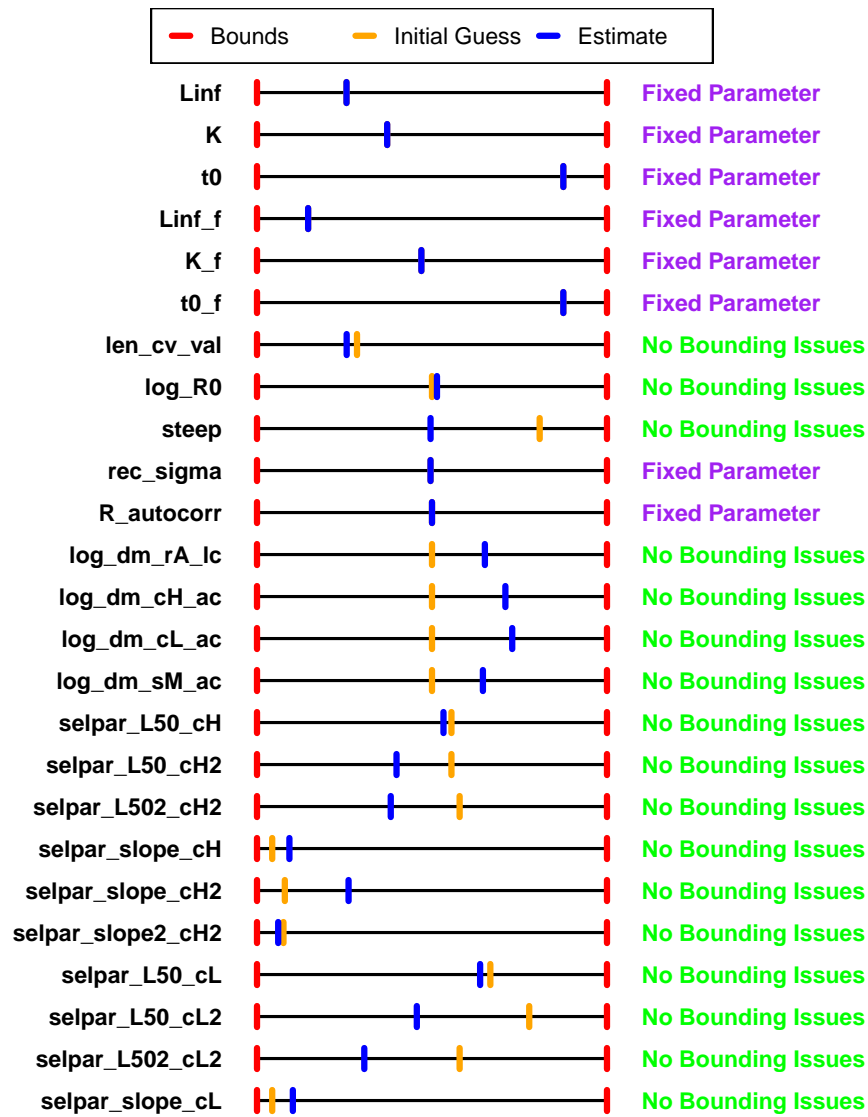
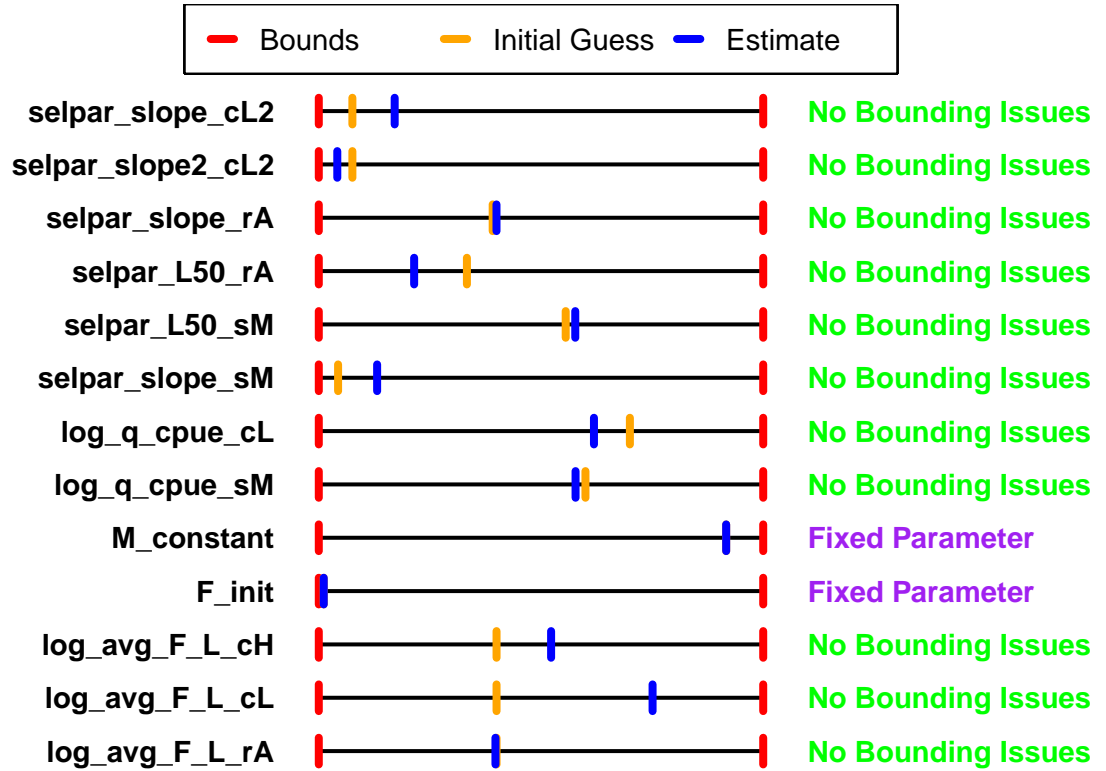


Figure 41. Continued: Diagnostic plot of parameter estimates to check for bounding issues, where the red lines indicate the upper and lower parameter bounds, orange is the initial model parameter starting value and blue is the final model estimate.



C.2 Composition fit plots

Figure 42. Top panel: One Step Ahead (OSA) residuals for the commercial handline age composition, where orange indicates an underestimate and blue is an overestimate and the size of the circle is the magnitude. Bottom panel: correlation between vectors of estimated and observed values.

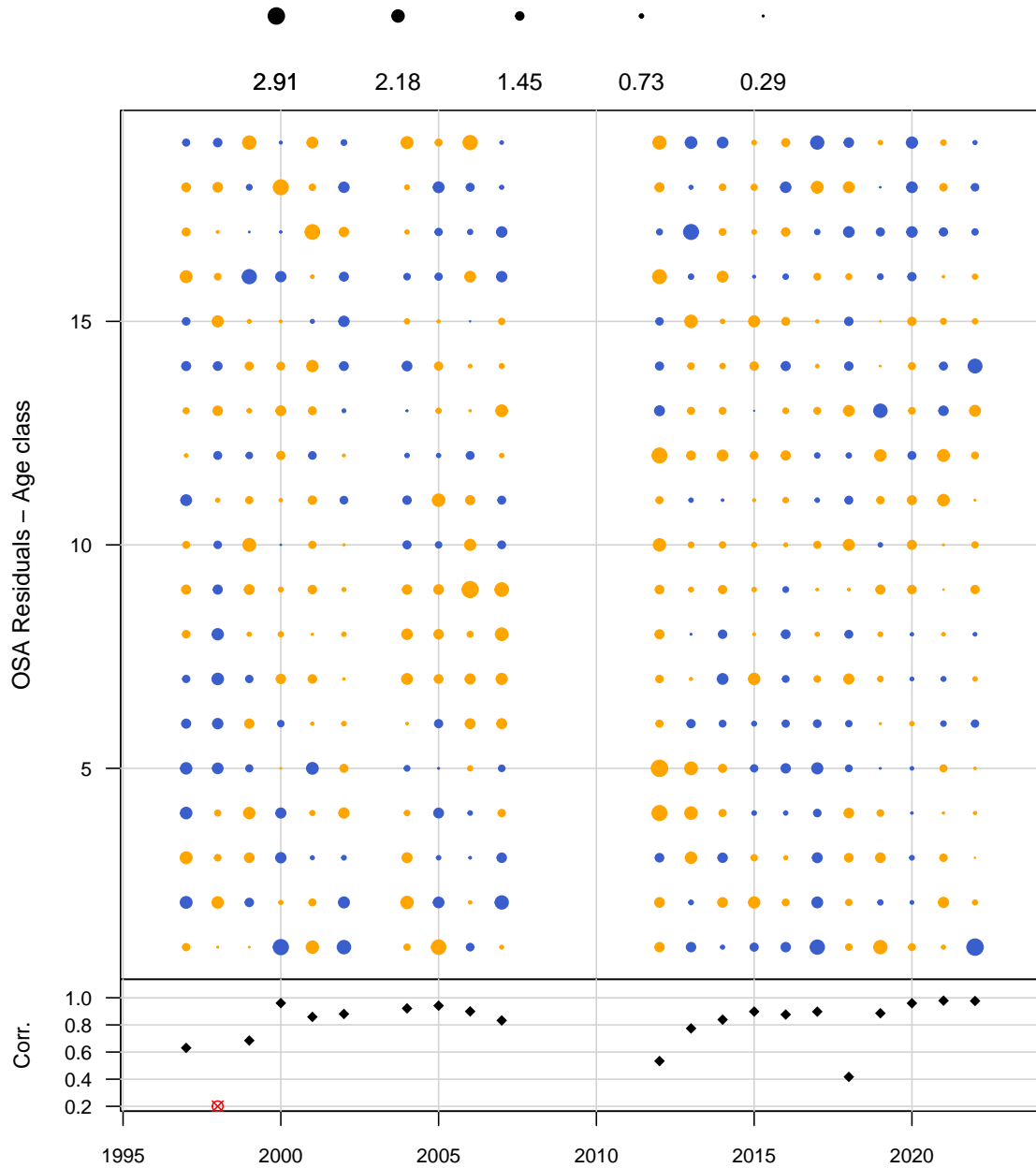


Figure 43. Top panel: One Step Ahead (OSA) residuals for the commercial longline age composition, where orange indicates an underestimate and blue is an overestimate and the size of the circle is the magnitude. Bottom panel: correlation between vectors of estimated and observed values.

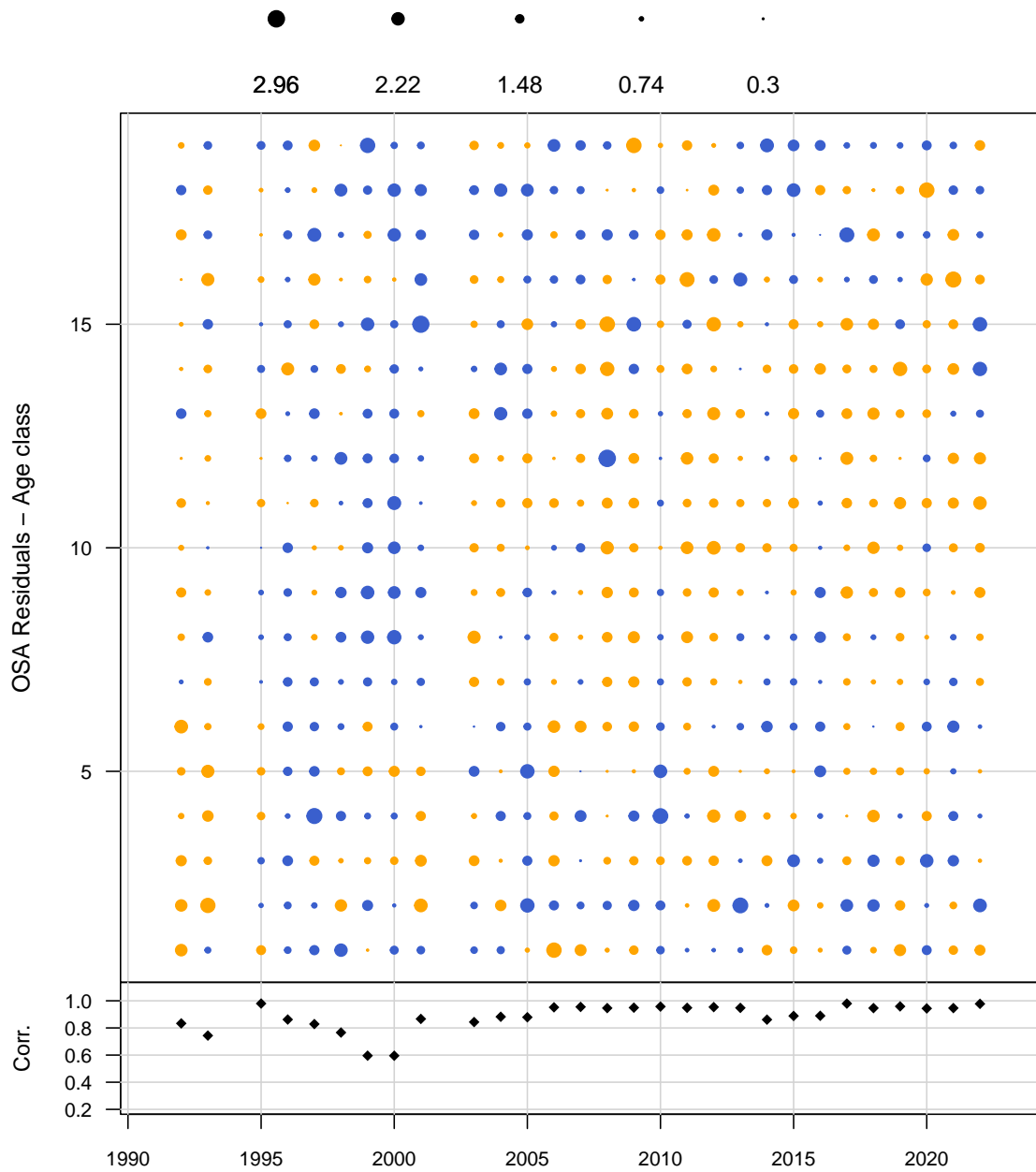


Figure 44. Top panel: One Step Ahead (OSA) residuals for the MARMAP survey age composition, where orange indicates an underestimate and blue is an overestimate and the size of the circle is the magnitude. Bottom panel: correlation between vectors of estimated and observed values.

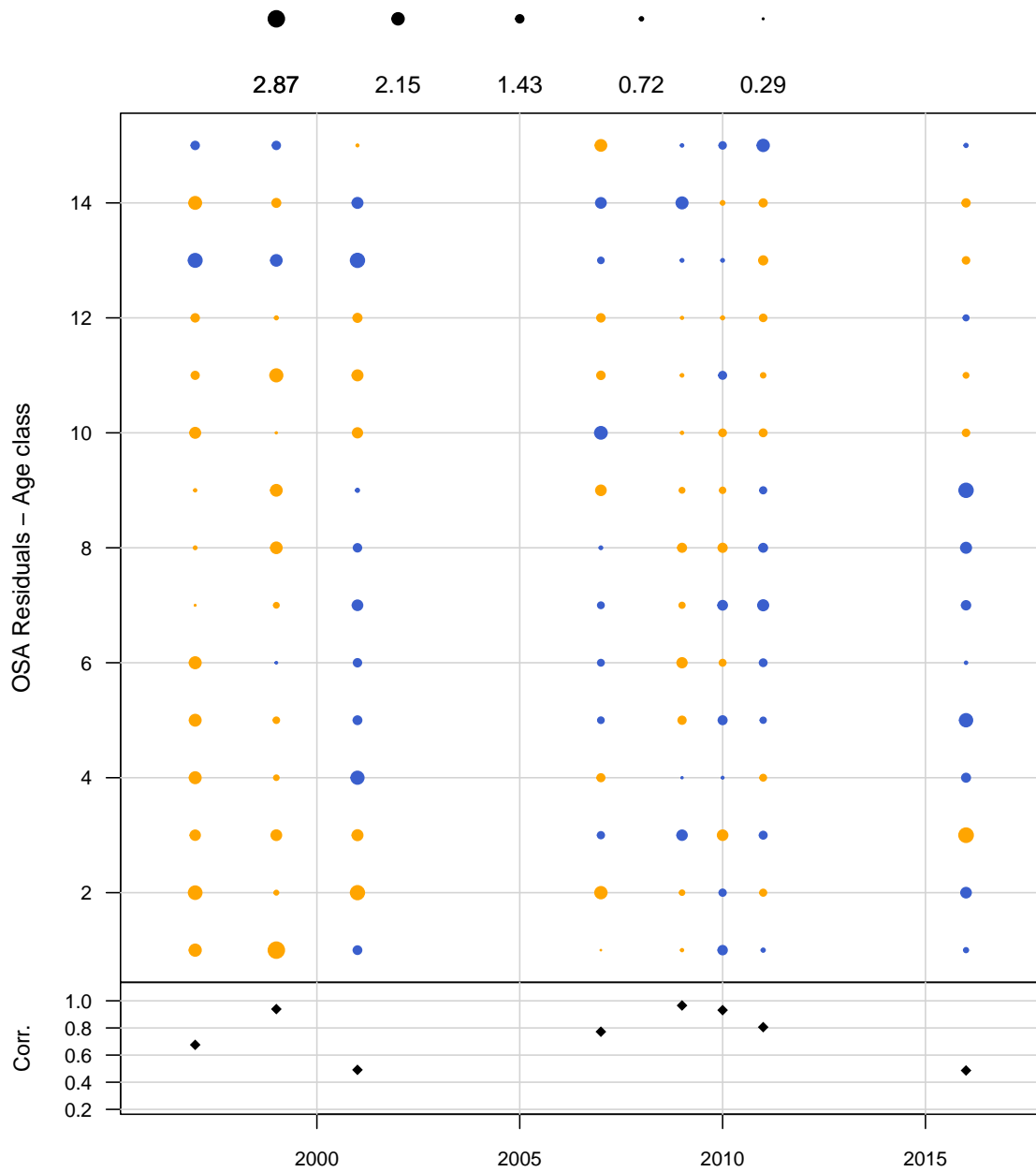
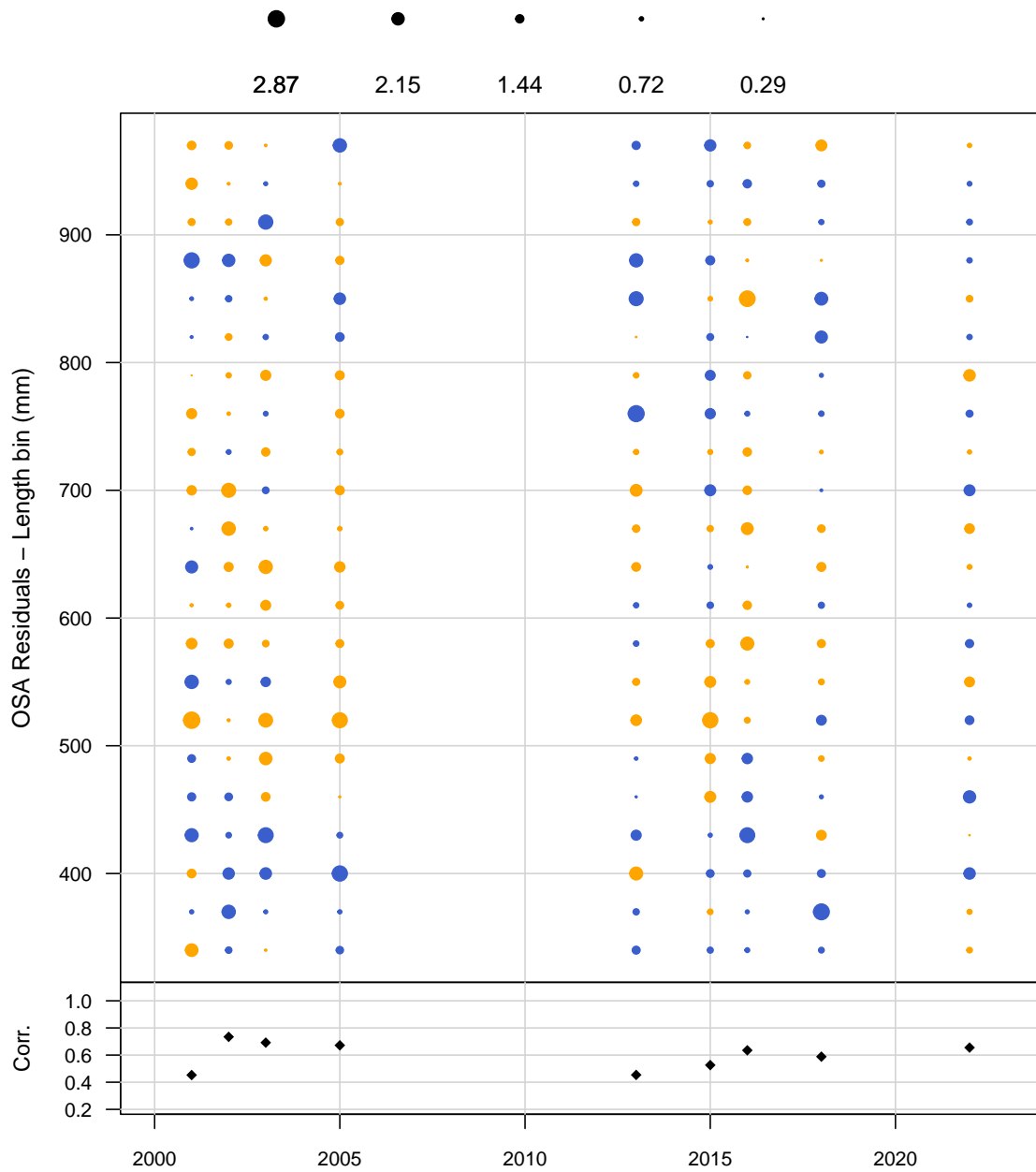


Figure 45. Top panel: One Step Ahead (OSA) residuals for the general recreation length composition, where orange indicates an underestimate and blue is an overestimate and the size of the circle is the magnitude. Bottom panel: correlation between vectors of estimated and observed values.



C.3 Pooled Composition fits

Figure 46. Observed (open circles) and estimated (solid line) pooled age compositions for the commercial longline fleet weighted by the effective sample size from the base run separated by the time block selectivities where the year range of the time block is in the top right corner of the plot.

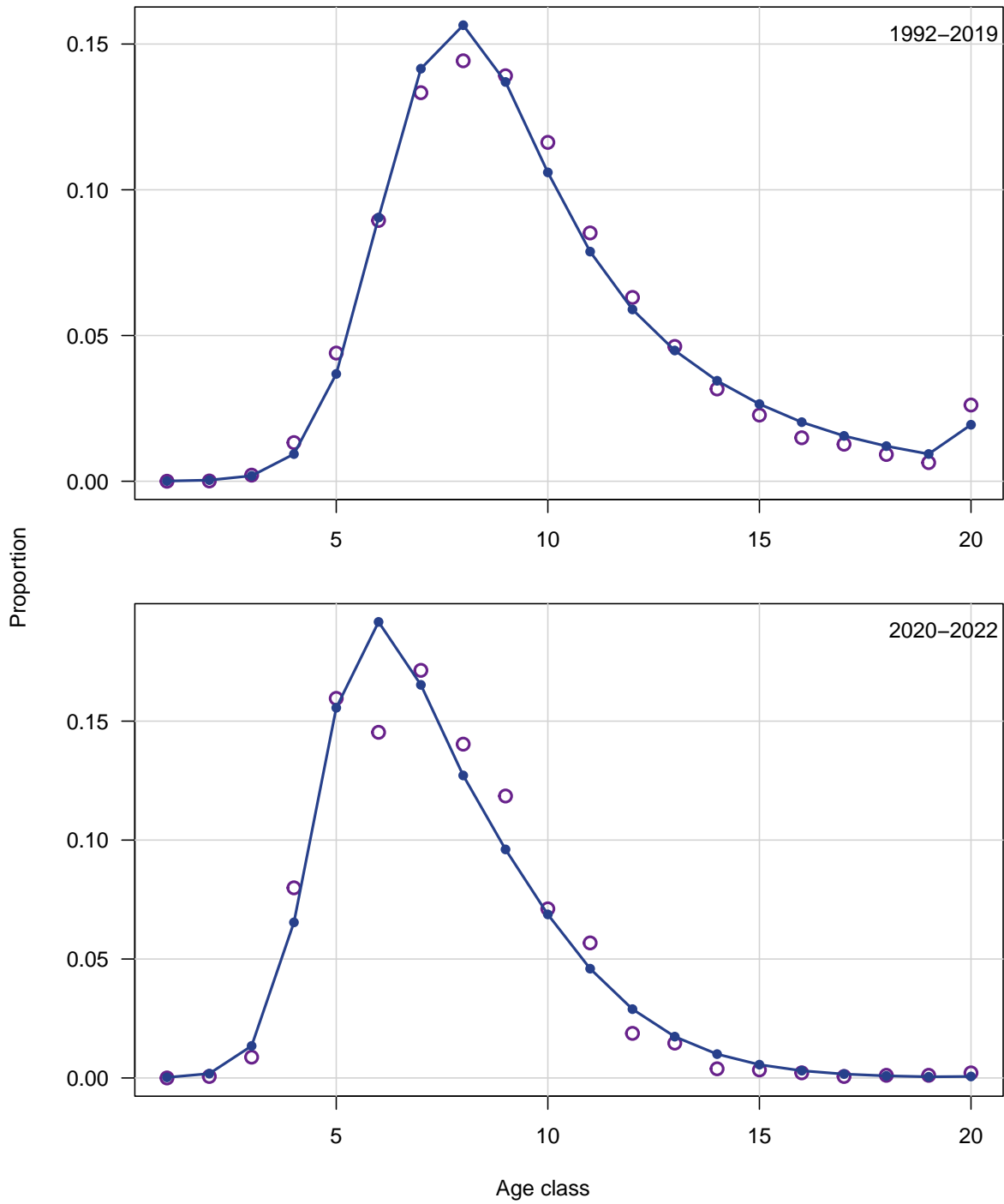


Figure 47. Observed (open circles) and estimated (solid line) pooled age compositions for the commercial handline fleet weighted by the effective sample size from the base run separated by the time block selectivities where the year range of the time block is in the top right corner of the plot.

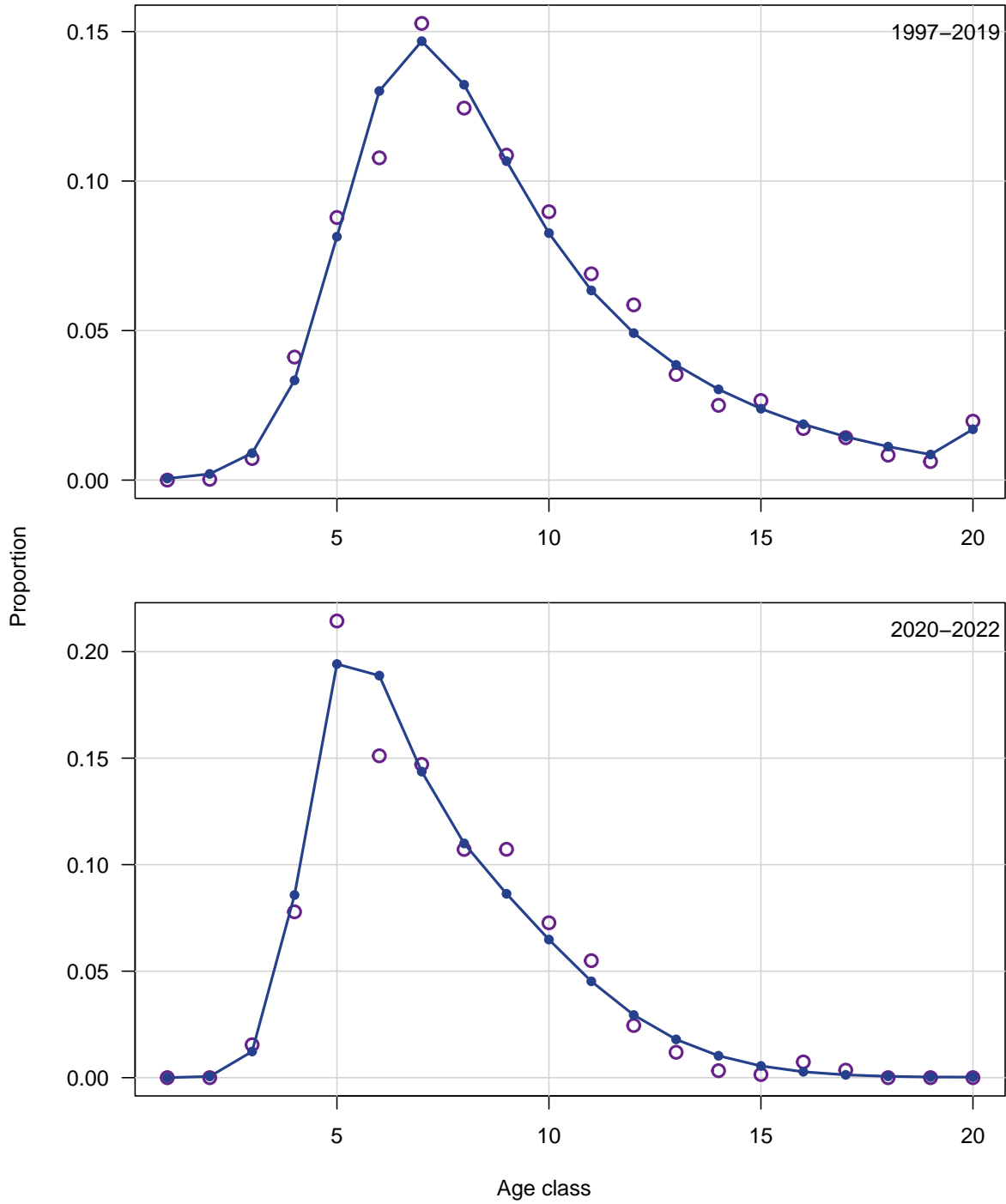


Figure 48. Observed (open circles) and estimated (solid line) age compositions for the MARMAP bottom long line survey from the base run.

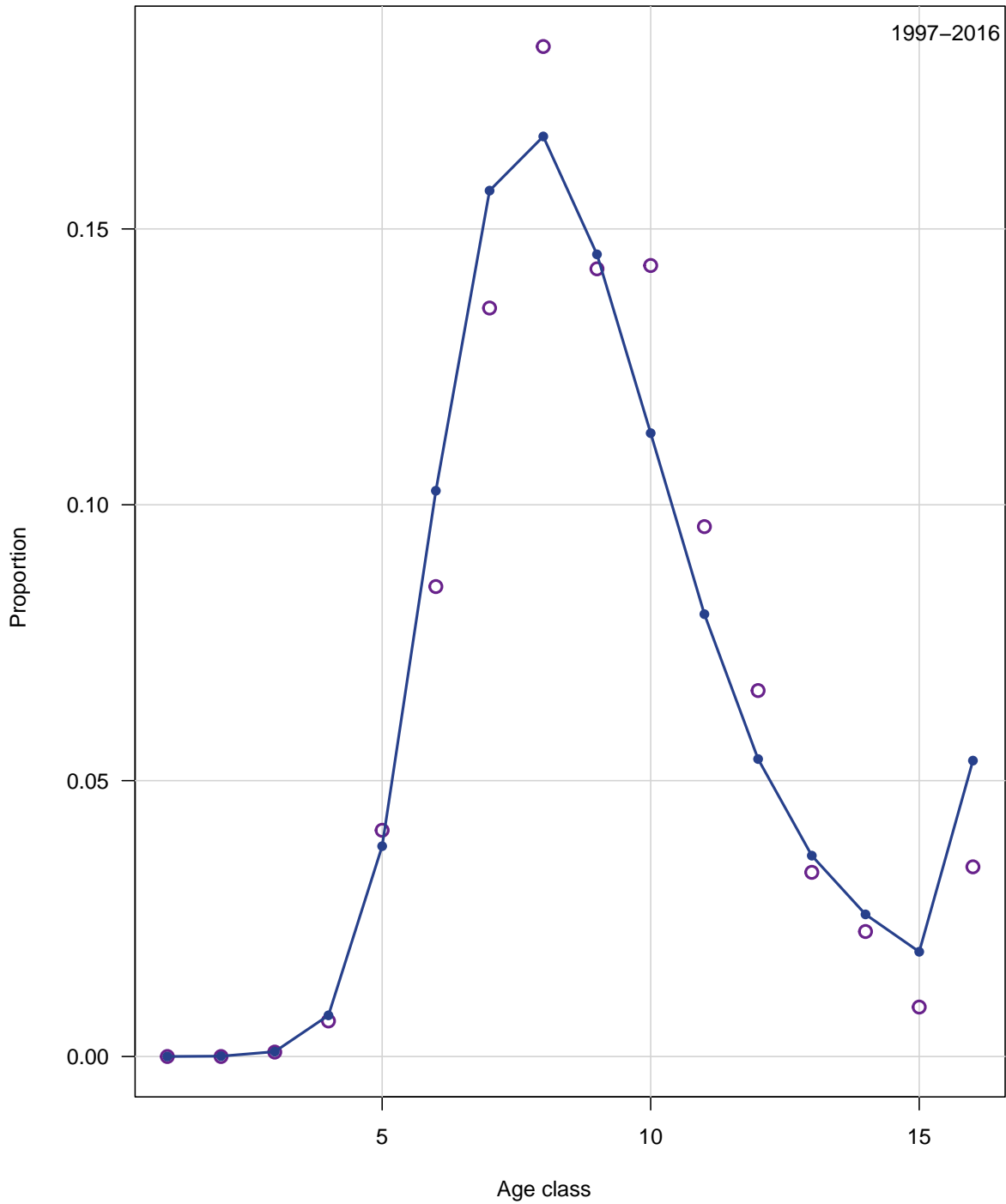
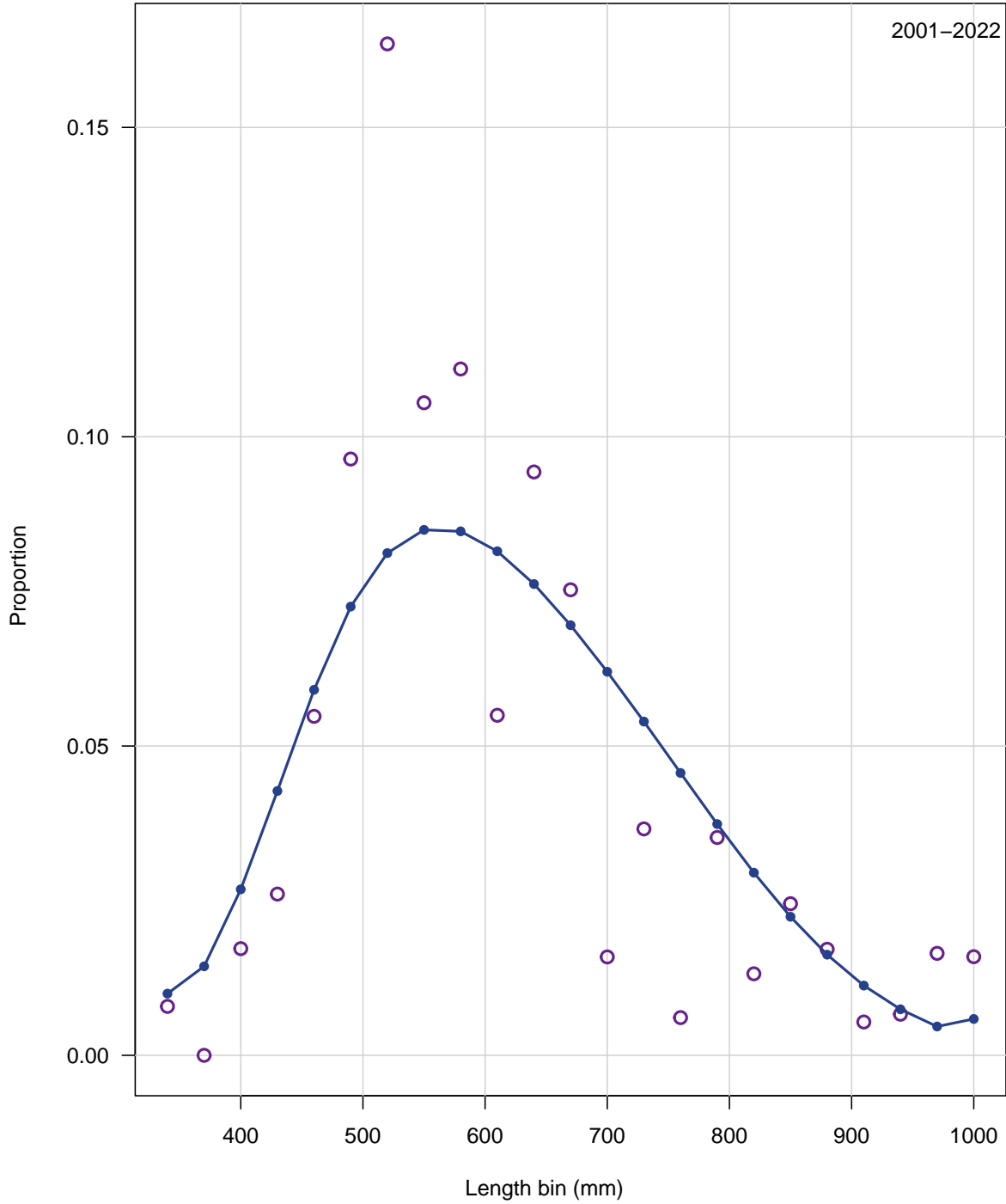


Figure 49. Observed (open circles) and estimated (solid line) pooled length compositions for the general recreational fleet weighted by the effective sample size from the base run separated by the time block selectivities where the year range of the time block is in the top right corner of the plot.



C.4 Likelihood Profiles

Figure 50. Scaled likelihood profile for Age 50 descending limb of commercial handline domed selectivity where the change in likelihood from the lowest observed value among values tested for each component. The color of the line indicates the data source of the change in likelihood where the black line is all data sources and prior penalties, the red line is from age compositions, the light green line is from indices of abundance, the dark green line is from landings, the brown line is from length composition, the orange line is from prior penalties, and the grey line is the recruitment deviate penalties and other stock recruitment related penalties.

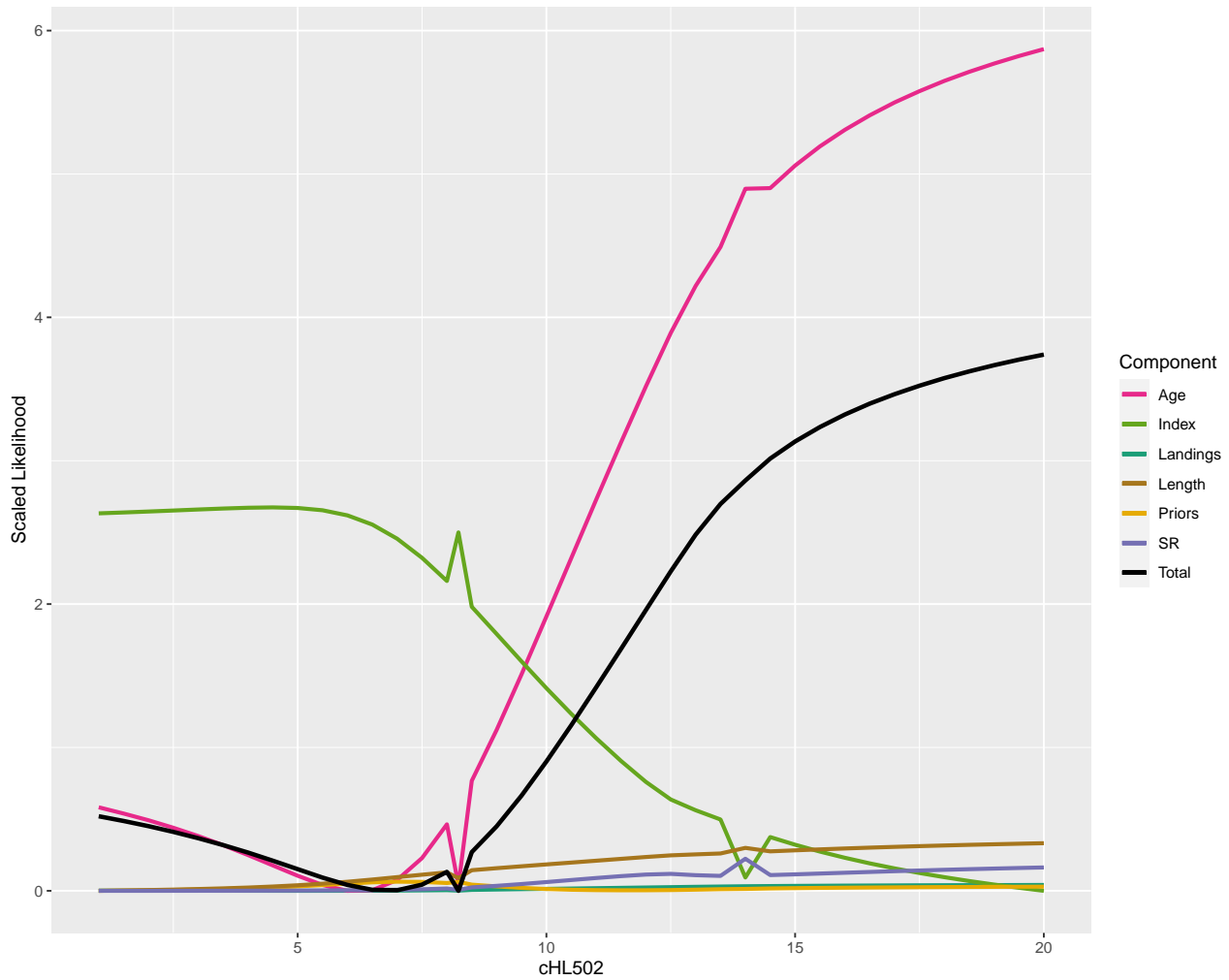


Figure 51. Scaled likelihood profile for Age 50 descending limb of commercial longline domed selectivity where the change in likelihood from the lowest observed value among values tested for each component. The color of the line indicates the data source of the change in likelihood where the black line is all data sources and prior penalties, the red line is from age compositions, the light green line is from indices of abundance, the dark green line is from landings, the brown line is from length composition, the orange line is from prior penalties, and the grey line is the recruitment deviate penalties and other stock recruitment related penalties.

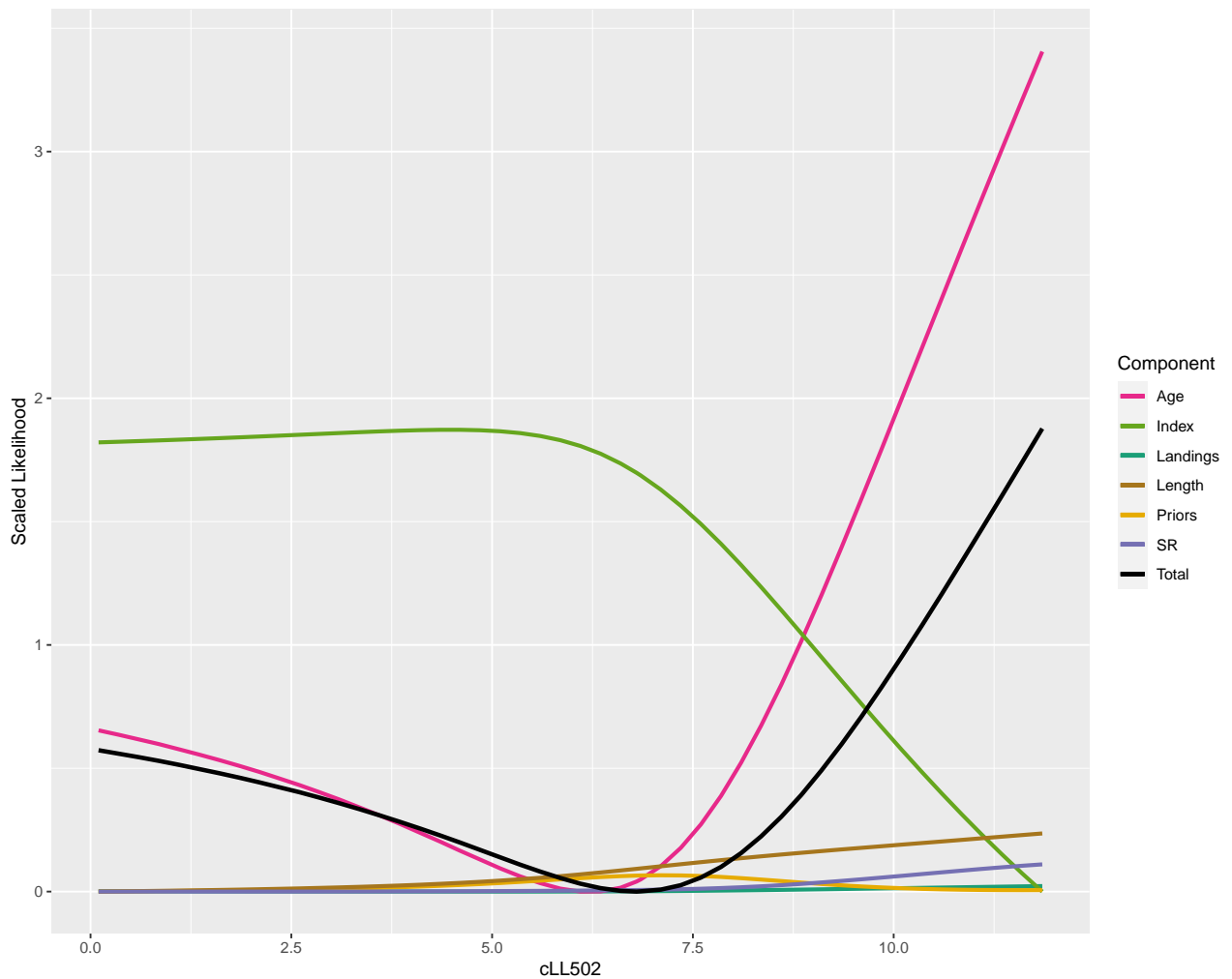


Figure 52. Scaled likelihood profile for slope descending limb of commercial handline domed selectivity where the change in likelihood from the lowest observed value among values tested for each component. The color of the line indicates the data source of the change in likelihood where the black line is all data sources and prior penalties, the red line is from age compositions, the light green line is from indices of abundance, the dark green line is from landings, the brown line is from length composition, the orange line is from prior penalties, and the grey line is the recruitment deviate penalties and other stock recruitment related penalties.

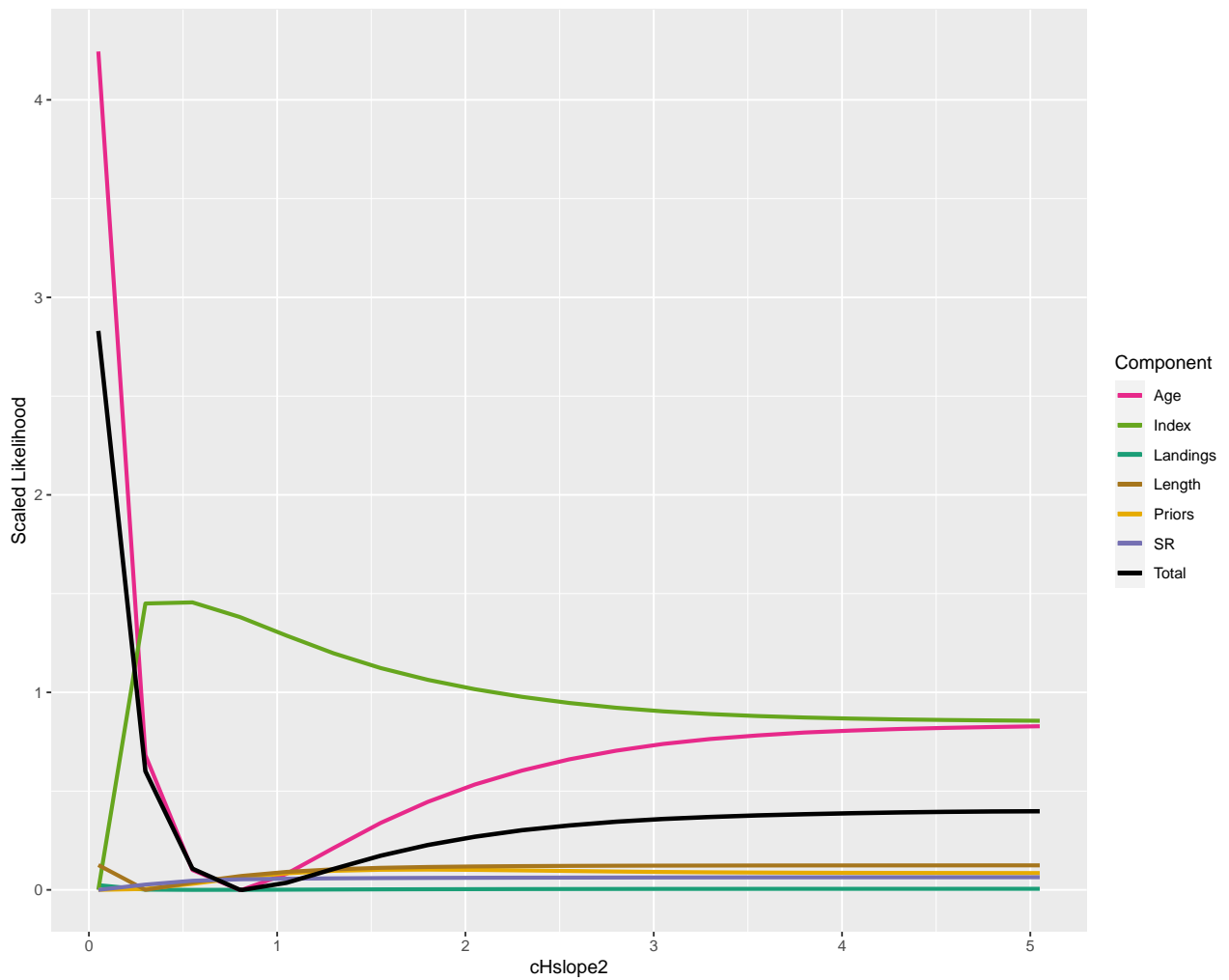


Figure 53. Scaled likelihood profile for slope descending limb of commercial longline domed selectivity where the change in likelihood from the lowest observed value among values tested for each component. The color of the line indicates the data source of the change in likelihood where the black line is all data sources and prior penalties, the red line is from age compositions, the light green line is from indices of abundance, the dark green line is from landings, the brown line is from length composition, the orange line is from prior penalties, and the grey line is the recruitment deviate penalties and other stock recruitment related penalties.

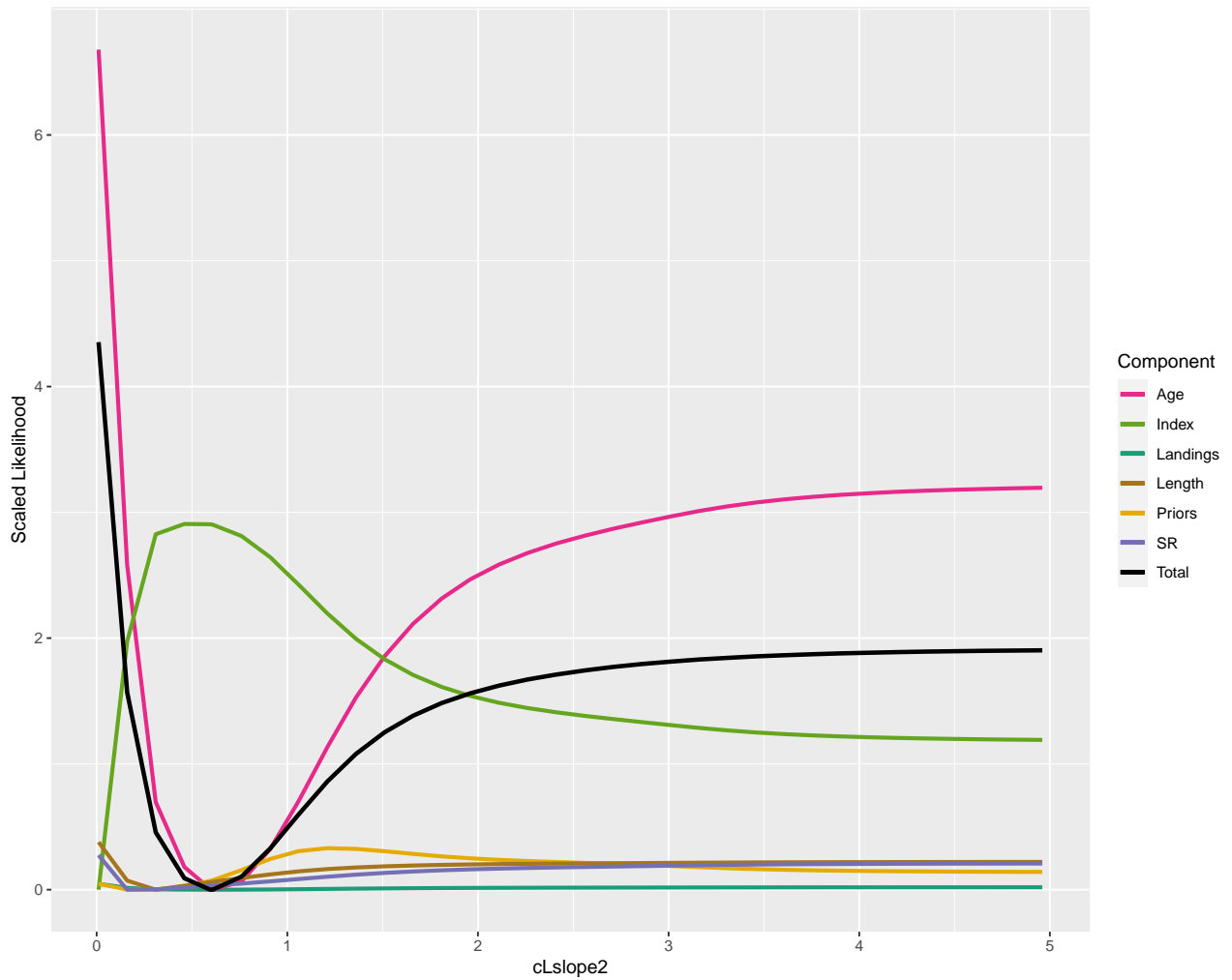


Figure 54. Scaled likelihood profile for Beverton-Holt steepness where the change in likelihood from the lowest observed value among values tested for each component. The color of the line indicates the data source of the change in likelihood where the black line is all data sources and prior penalties, the red line is from age compositions, the light green line is from indices of abundance, the dark green line is from landings, the brown line is from length composition, the orange line is from prior penalties, and the grey line is the recruitment deviate penalties and other stock recruitment related penalties.

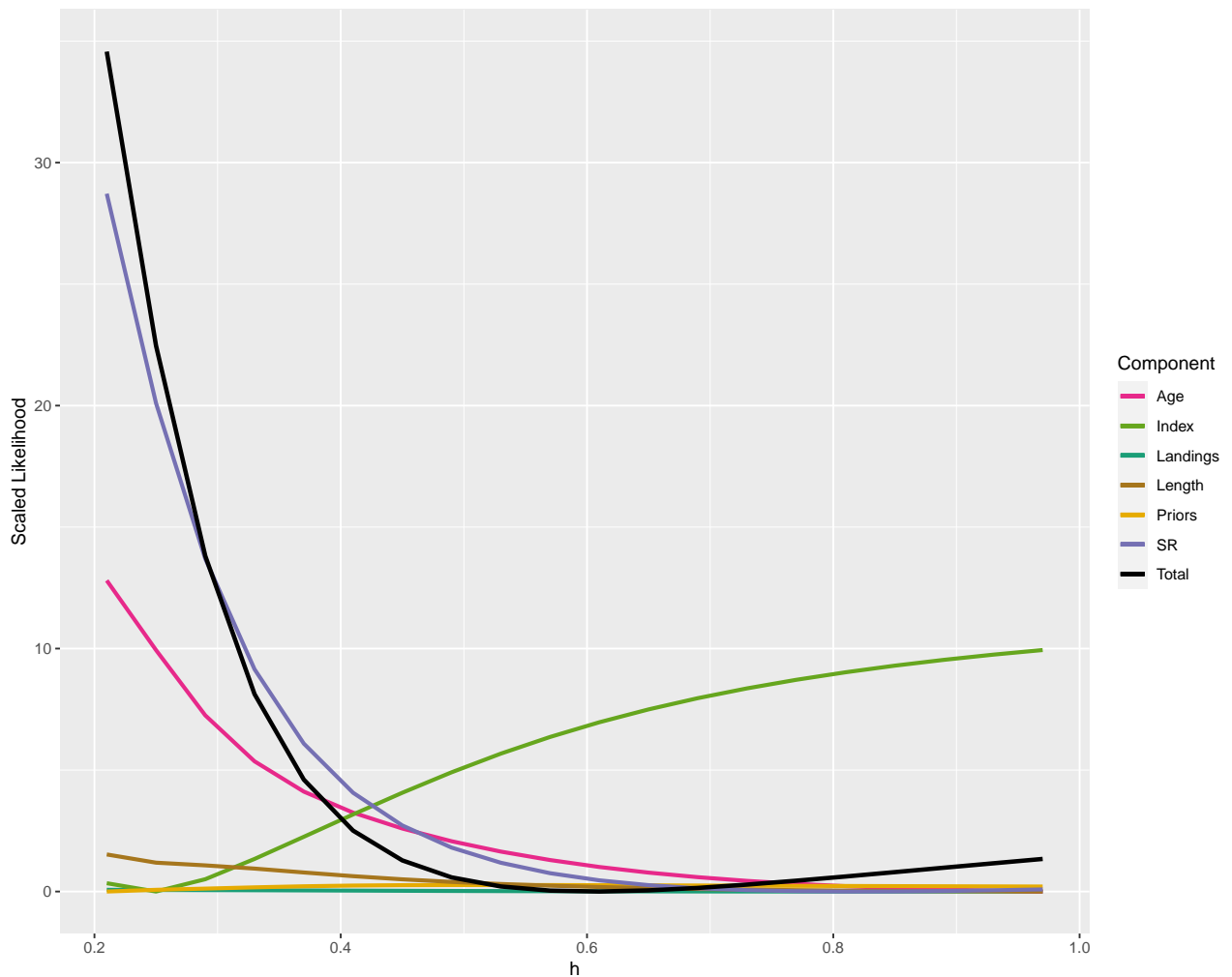


Figure 55. Scaled likelihood profile for initial fishing mortality rate F_{init} where the change in likelihood from the lowest observed value among values tested for each component. The color of the line indicates the data source of the change in likelihood where the black line is all data sources and prior penalties, the red line is from age compositions, the light green line is from indices of abundance, the dark green line is from landings, the brown line is from length composition, the orange line is from prior penalties, and the grey line is the recruitment deviate penalties and other stock recruitment related penalties.

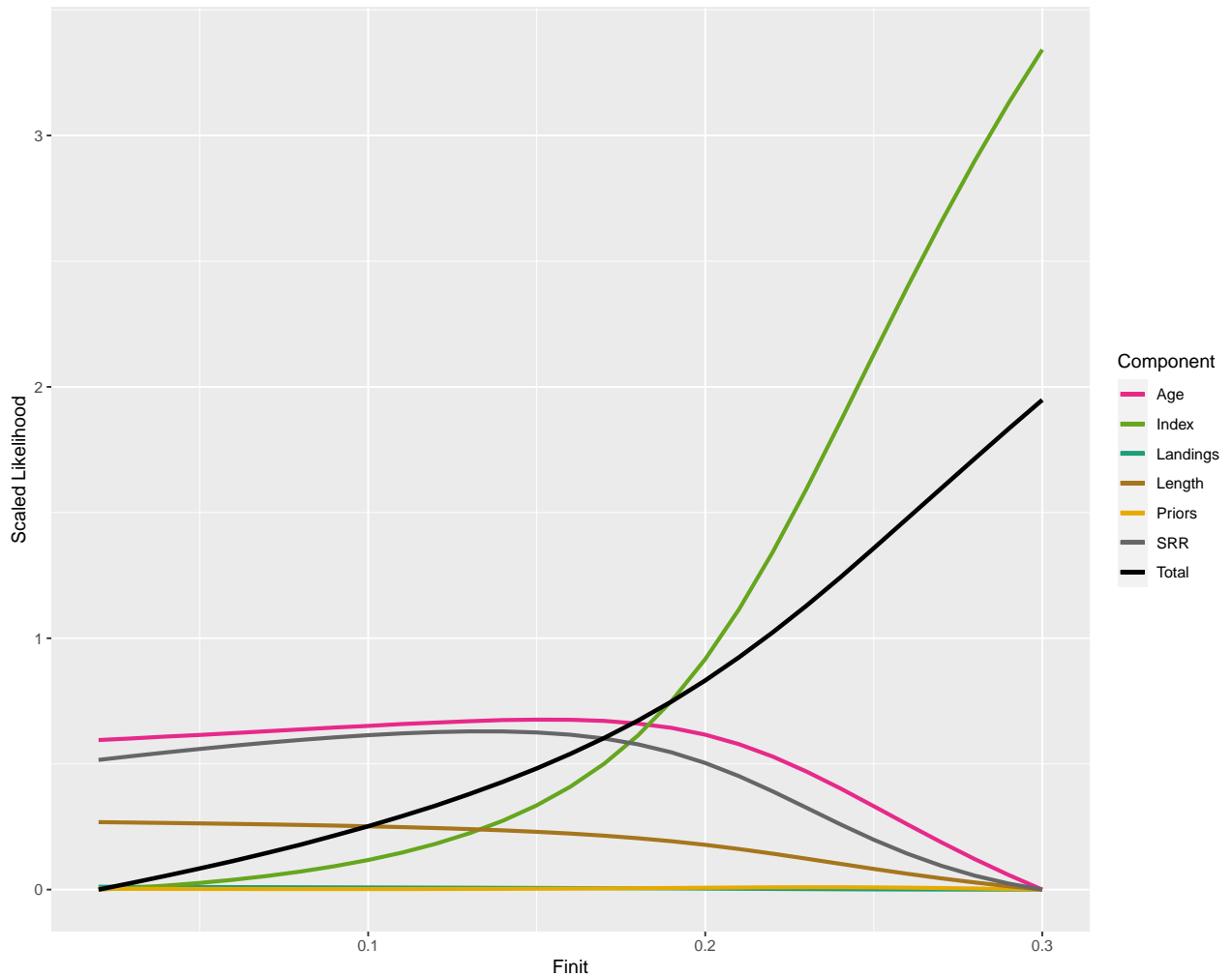


Figure 56. Scaled likelihood profile for Beverton-Holt R_0 where the change in likelihood from the lowest observed value among values tested for each component. The color of the line indicates the data source of the change in likelihood where the black line is all data sources and prior penalties, the red line is from age compositions, the light green line is from indices of abundance, the dark green line is from landings, the brown line is from length composition, the orange line is from prior penalties, and the grey line is the recruitment deviate penalties and other stock recruitment related penalties.

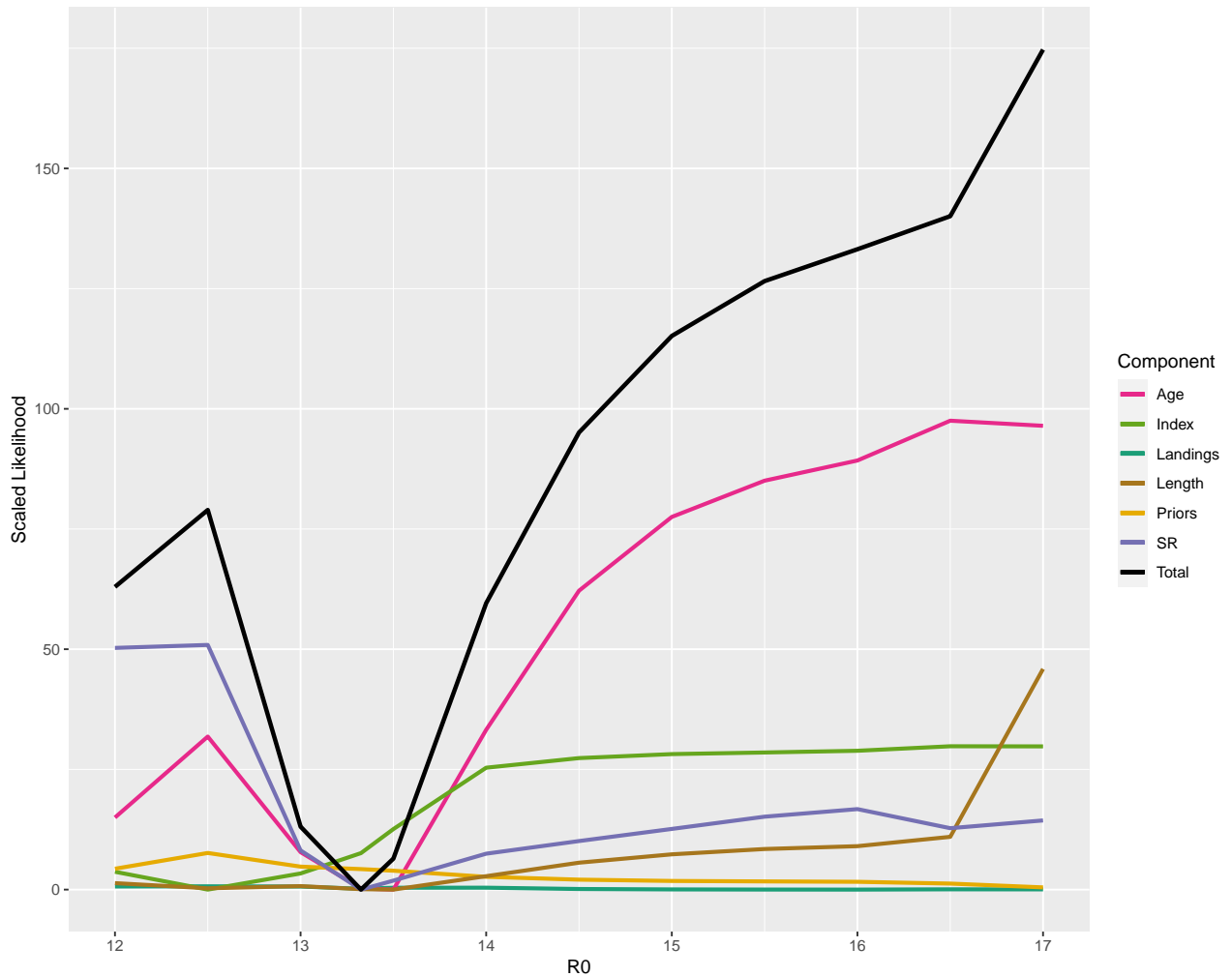


Figure 57. Scaled likelihood profile for the recruitment deviate in 2015, where the change in likelihood from the lowest observed value among values tested for each component. The color of the line indicates the data source of the change in likelihood where the black line is all data sources and prior penalties, the red line is from age compositions, the light green line is from indices of abundance, the dark green line is from landings, the brown line is from length composition, the orange line is from prior penalties, and the grey line is the recruitment deviate penalties and other stock recruitment related penalties.

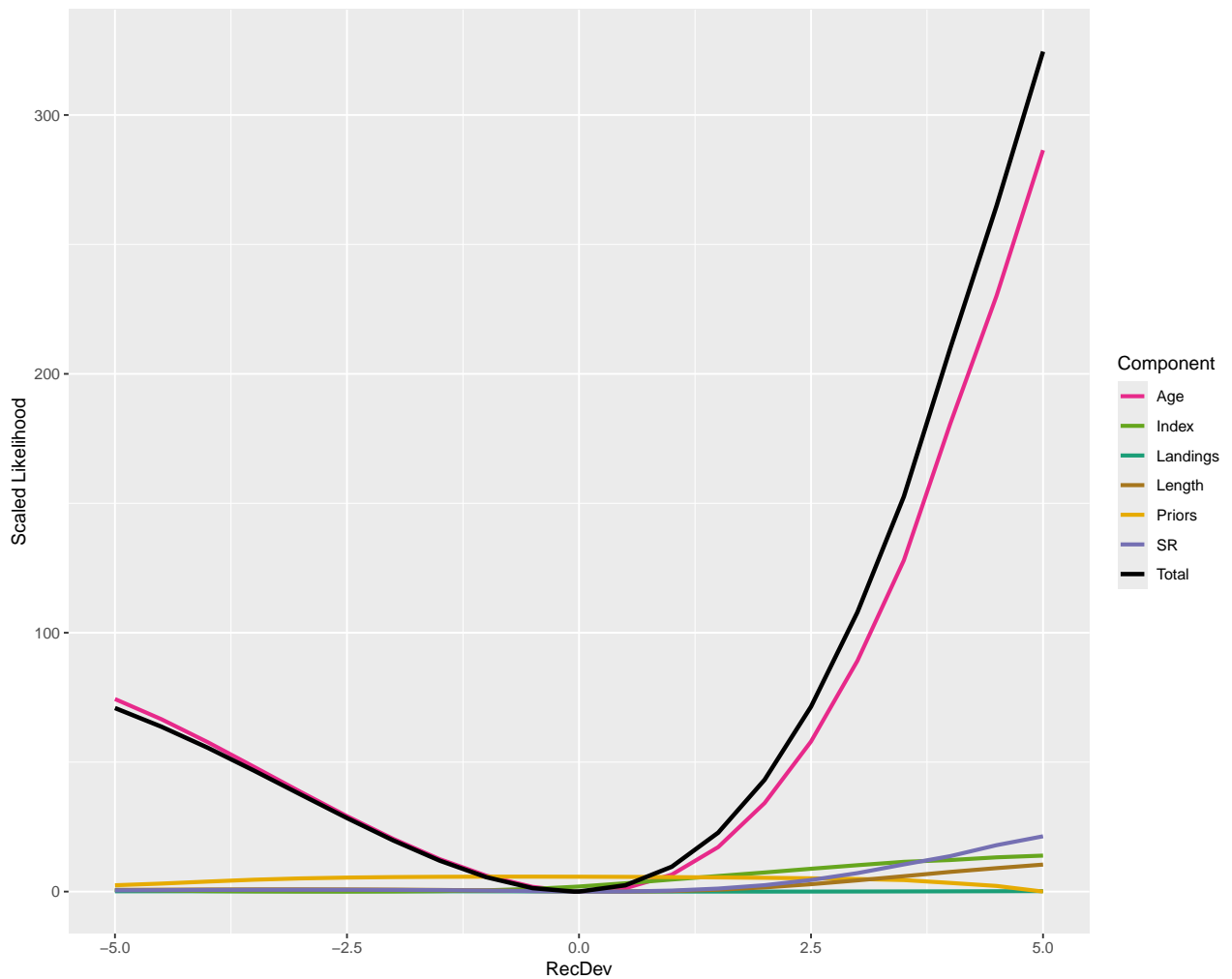


Figure 58. Scaled likelihood profile for the recruitment deviate in 2016, where the change in likelihood from the lowest observed value among values tested for each component. The color of the line indicates the data source of the change in likelihood where the black line is all data sources and prior penalties, the red line is from age compositions, the light green line is from indices of abundance, the dark green line is from landings, the brown line is from length composition, the orange line is from prior penalties, and the grey line is the recruitment deviate penalties and other stock recruitment related penalties.

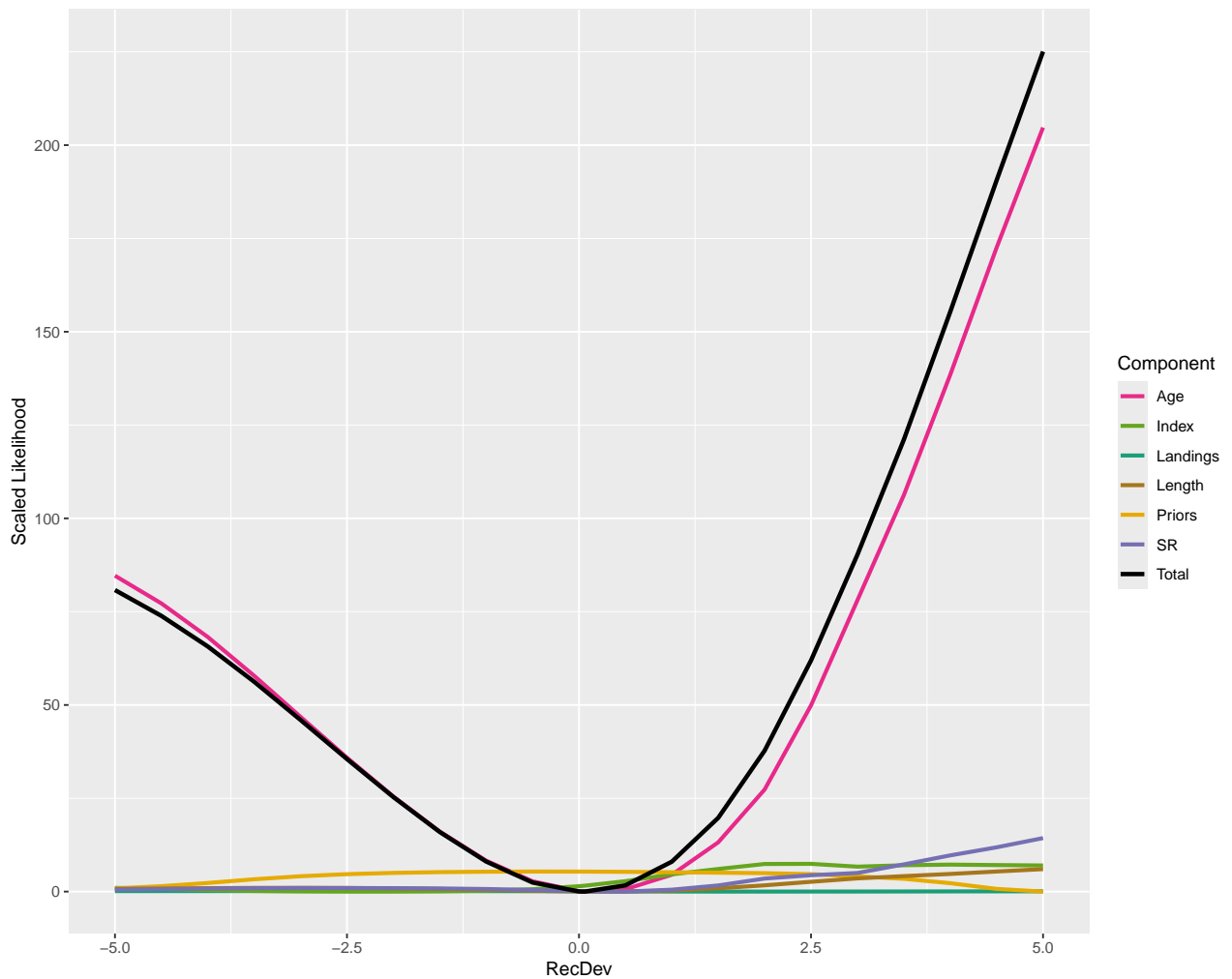


Figure 59. Scaled likelihood profile for the recruitment deviate in 2017, where the change in likelihood from the lowest observed value among values tested for each component. The color of the line indicates the data source of the change in likelihood where the black line is all data sources and prior penalties, the red line is from age compositions, the light green line is from indices of abundance, the dark green line is from landings, the brown line is from length composition, the orange line is from prior penalties, and the grey line is the recruitment deviate penalties and other stock recruitment related penalties.

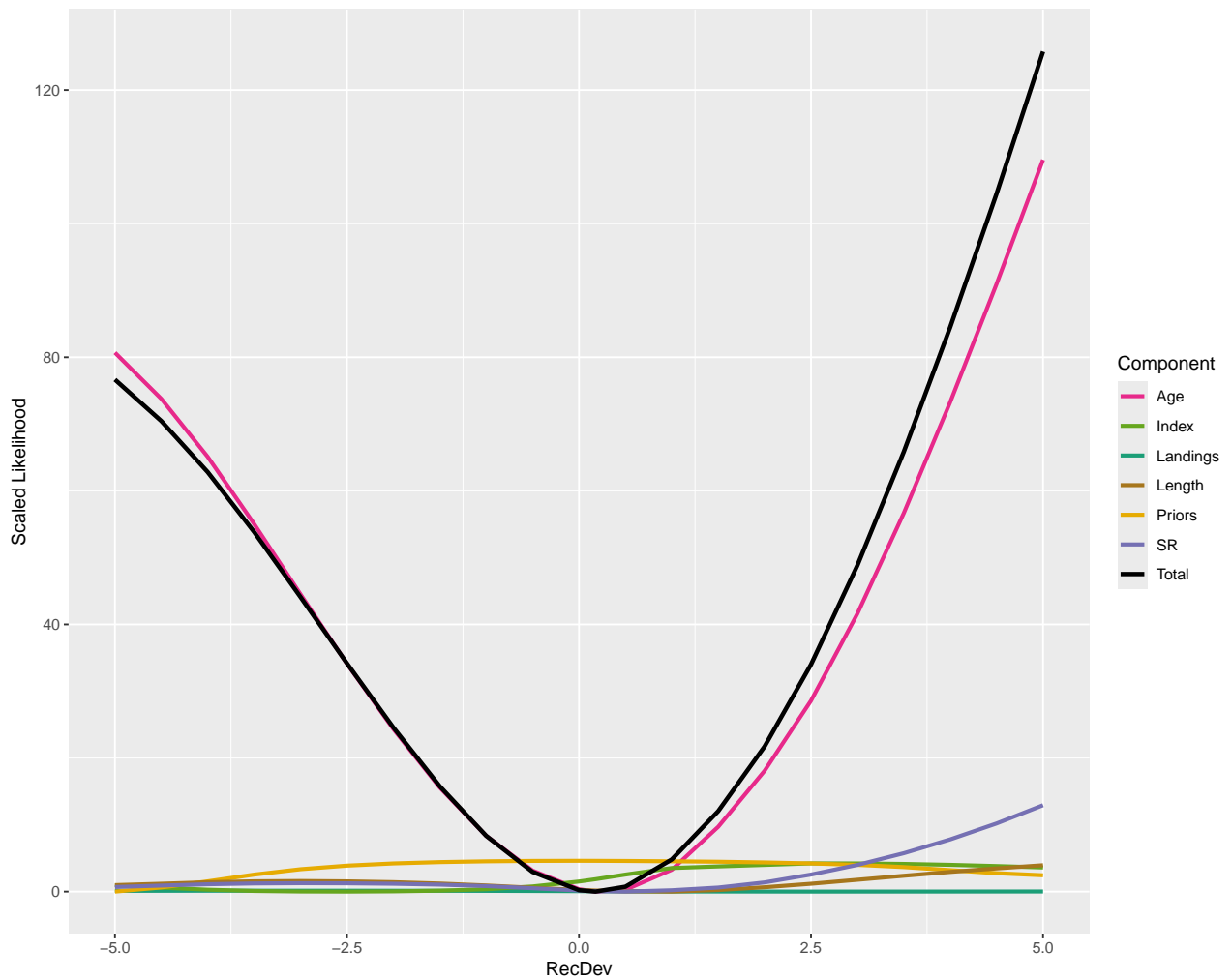


Figure 60. Scaled likelihood profile for the recruitment deviate in 2018, where the change in likelihood from the lowest observed value among values tested for each component. The color of the line indicates the data source of the change in likelihood where the black line is all data sources and prior penalties, the red line is from age compositions, the light green line is from indices of abundance, the dark green line is from landings, the brown line is from length composition, the orange line is from prior penalties, and the grey line is the recruitment deviate penalties and other stock recruitment related penalties.

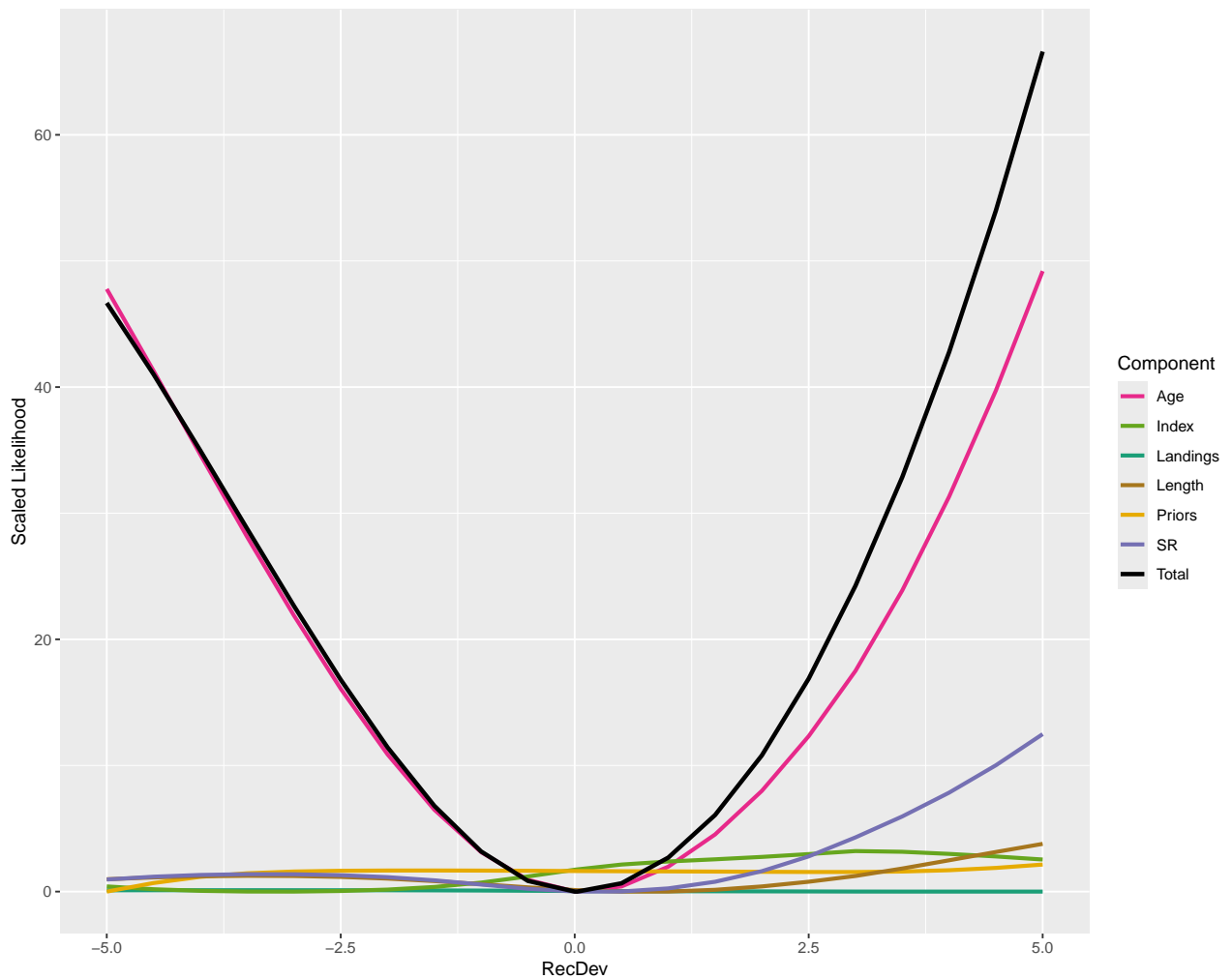


Figure 61. Scaled likelihood profile for the recruitment deviate in 2019, where the change in likelihood from the lowest observed value among values tested for each component. The color of the line indicates the data source of the change in likelihood where the black line is all data sources and prior penalties, the red line is from age compositions, the light green line is from indices of abundance, the dark green line is from landings, the brown line is from length composition, the orange line is from prior penalties, and the grey line is the recruitment deviate penalties and other stock recruitment related penalties.

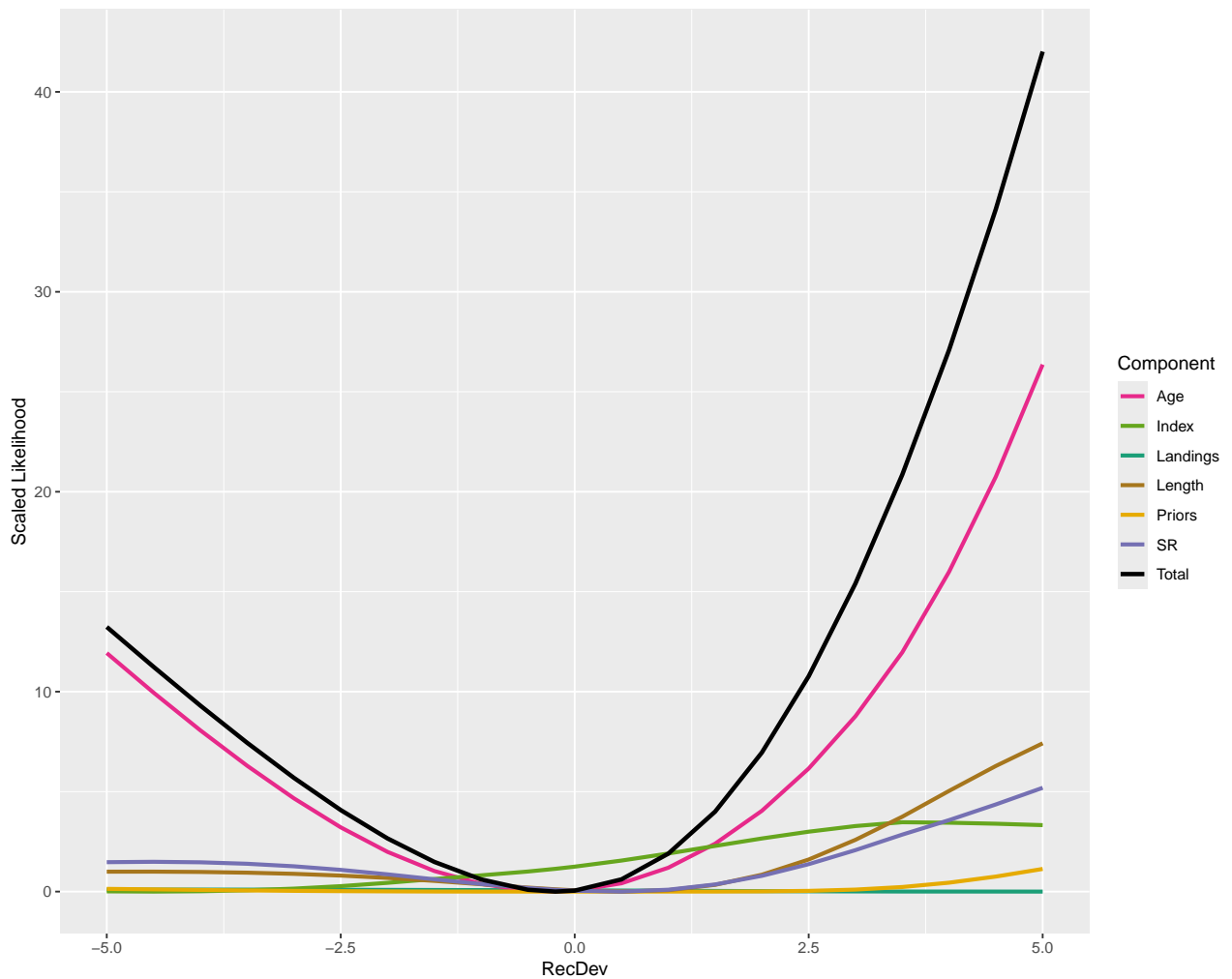
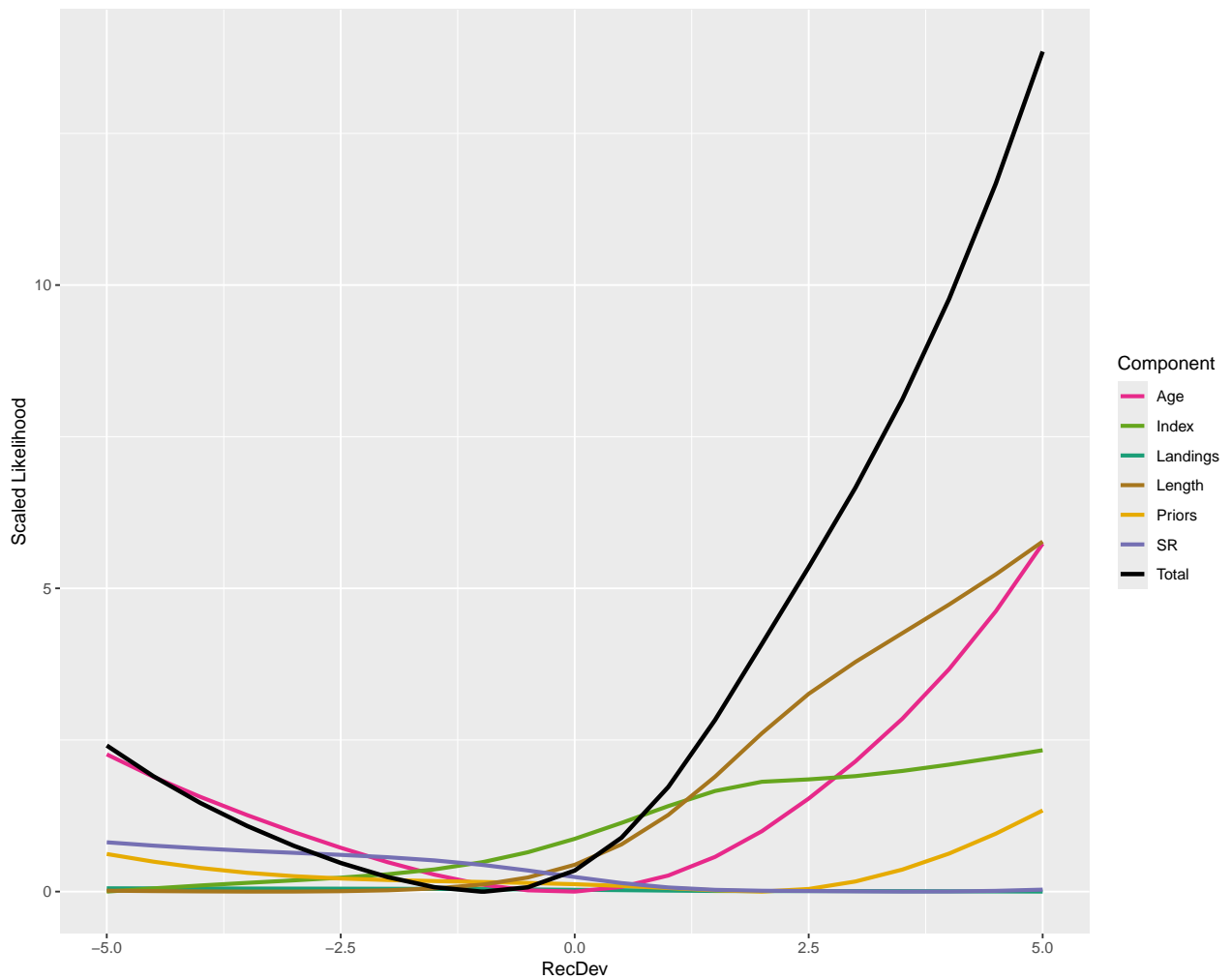


Figure 62. Scaled likelihood profile for the recruitment deviate in 2020, where the change in likelihood from the lowest observed value among values tested for each component. The color of the line indicates the data source of the change in likelihood where the black line is all data sources and prior penalties, the red line is from age compositions, the light green line is from indices of abundance, the dark green line is from landings, the brown line is from length composition, the orange line is from prior penalties, and the grey line is the recruitment deviate penalties and other stock recruitment related penalties.



C.5 Fixed MCBE parameters

Figure 63. Density plots of fixed parameters in the MCBE models where the solid blue vertical lines are the value in the base BAM model, the green vertical lines are the median of the MCBE model runs ($n = 3018$). Top left panel: fixed constant natural mortality used to calculate M_a , Top right panel: Fishing mortality in the initial year, Bottom left panel: fraction of year of peak spawning, Bottom right panel: standard deviation of recruitment deviates.

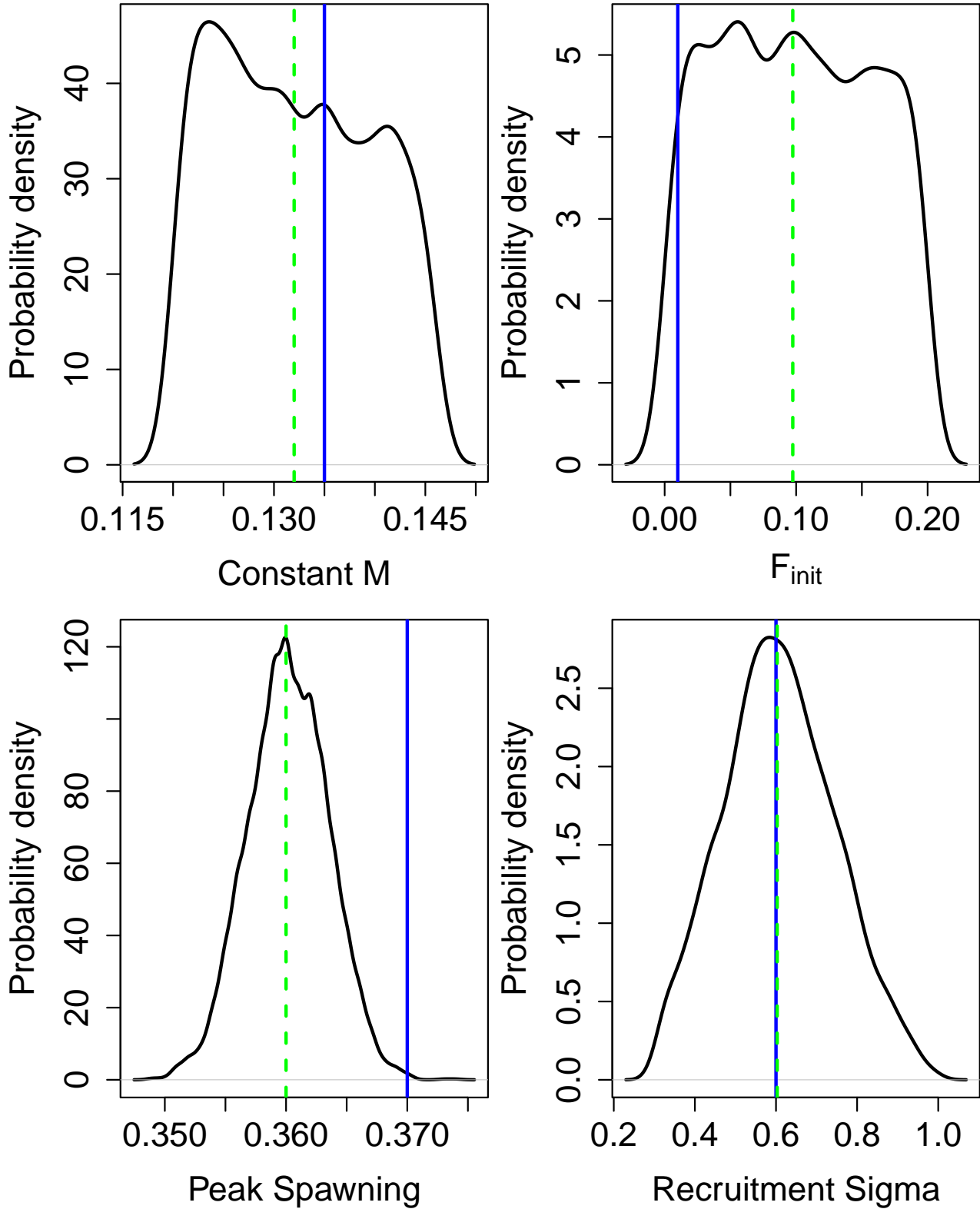


Figure 64. Density plots of fixed age vectors in the MCBE models where the solid blue lines are the value in the base BAM model, the green lines are the median of the MCBE model runs and the shaded region represents 90% confidence bands from the MCBE runs ($n = 3018$). Top panel: Total reproductive output at age in millions of eggs produced (is the product of batch fecundity at age, number of batches at age and maturity at age), Middle panel: Maximum total length in millimeters, Bottom panel: natural mortality at age.

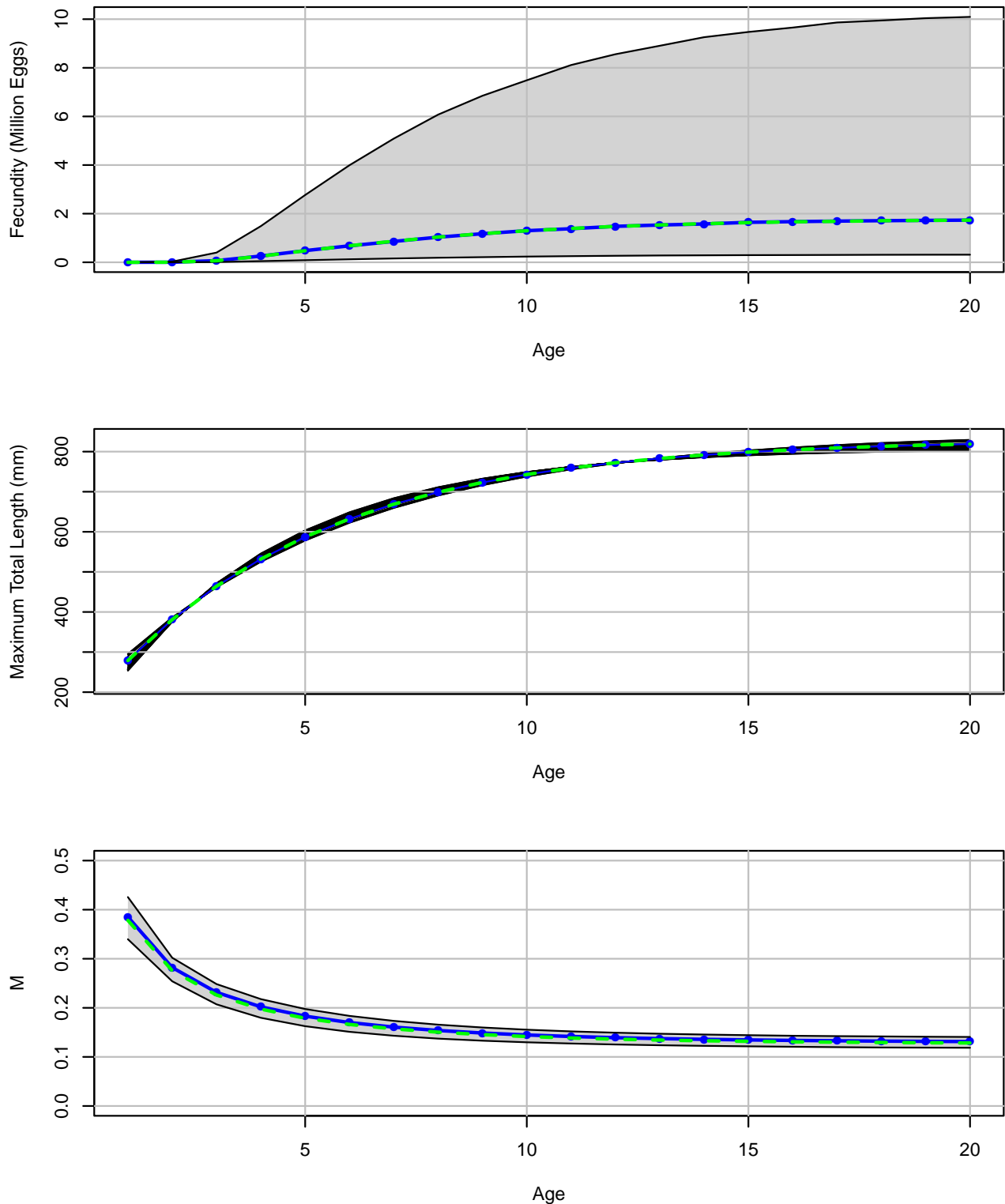


Figure 65. Density plots of fixed age vectors used to calculate reproductive output (i.e., fecundity) in the MCBE models where the solid blue lines are the value in the base BAM model, the green lines are the median of the MCBE model runs and the shaded region represents 90% confidence bands from the MCBE runs (n = 3018). Top panel: Proportion mature at age, Middle panel: Batch fecundity at age, Bottom panel: number of spawns per year by age.

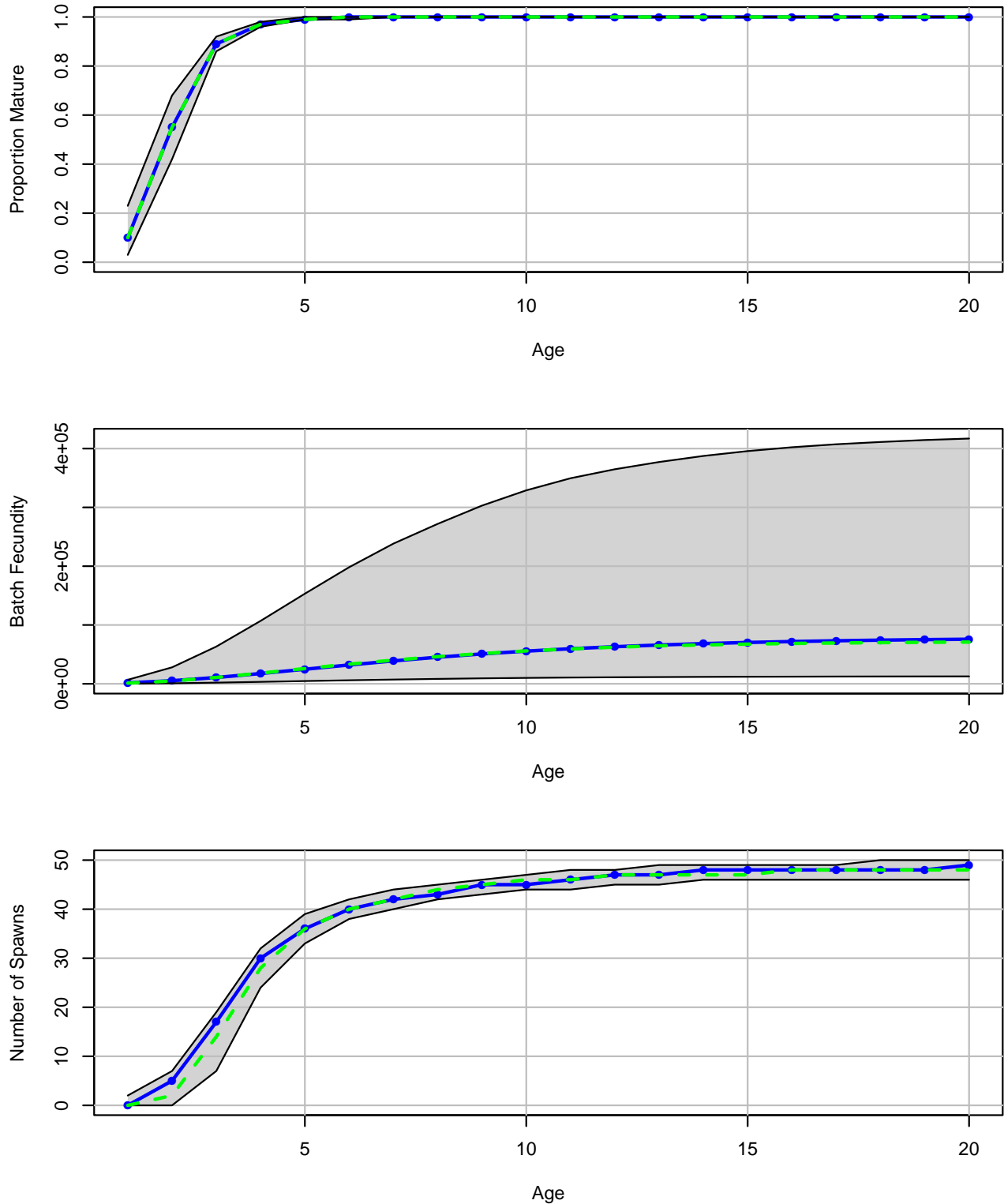
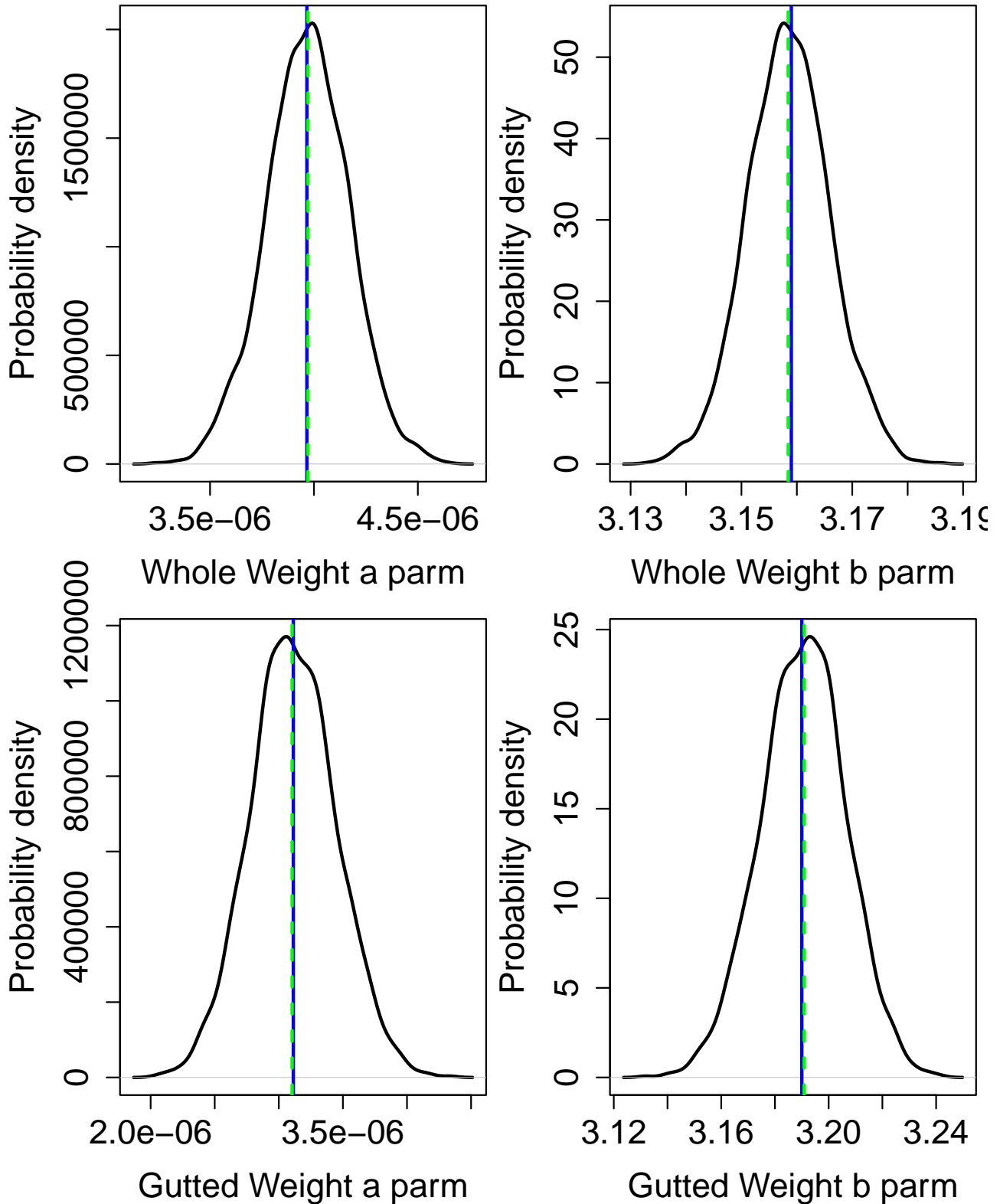


Figure 66. Density plots of fixed parameters in the MCBE models where the solid blue vertical lines are the value in the base BAM model, the green vertical lines are the median of the MCBE model runs ($n = 3018$). Top left panel: a parameter of total length to whole weight relationship, Top right panel: b parameter of total length to whole weight relationship, Bottom left panel: a parameter of total length to gutted weight relationship, Bottom right panel: b parameter of total length to gutted weight relationship.




```

init_vector set_len_cv(1,7);

//Scalar used only for computing MSST.
init_vector set_M_constant(1,7);

//Spawner-recruit parameters (Initial guesses or fixed values)
init_vector set_steep(1,7); //recruitment steepness
init_vector set_log_R0(1,7); //recruitment R0
init_vector set_R_autocorr(1,7); //recruitment autocorrelation
init_vector set_rec_sigma(1,7); //recruitment standard deviation in log space

init_vector set_log_dm_lenc_rA(1,7); //Dirichlet-multinomial overdispersion parameter
init_vector set_log_dm_agec_ch(1,7); //Dirichlet-multinomial overdispersion parameter
init_vector set_log_dm_agec_cL(1,7); //Dirichlet-multinomial overdispersion parameter
init_vector set_log_dm_agec_sM(1,7); //Dirichlet-multinomial overdispersion parameter

//Initial guesses or fixed values of estimated selectivity parameters

init_vector set_selpar_L50_ch(1,7);
init_vector set_selpar_L50_ch2(1,7);
init_vector set_selpar_L502_ch2(1,7);
init_vector set_selpar_slope_ch(1,7);
init_vector set_selpar_slope_ch2(1,7);
init_vector set_selpar_slope2_ch2(1,7);

init_vector set_selpar_L50_cL(1,7);
init_vector set_selpar_L50_cL2(1,7);
init_vector set_selpar_L502_cL2(1,7);
init_vector set_selpar_slope_cL(1,7);
init_vector set_selpar_slope_cL2(1,7);
init_vector set_selpar_slope2_cL2(1,7);

init_vector set_selpar_L50_rA(1,7);
init_vector set_selpar_slope_rA(1,7);

init_vector set_selpar_L50_sM(1,7);
init_vector set_selpar_slope_sM(1,7);

/--index catchability-----
init_vector set_log_q_cpue_cL(1,7); //catchability coefficient (log) for comm longline index
init_vector set_log_q_cpue_sM(1,7); //catchability coefficient (log) for MARMAP index

//initial F
init_vector set_F_init(1,7); //scales initial F
/--mean F's in log space -----
init_vector set_log_avg_F_L_ch(1,7);
init_vector set_log_avg_F_L_cL(1,7);
init_vector set_log_avg_F_L_rA(1,7);
init_number test6;
!!if (test6 != 1234567890){cout << "DAT selectivities, q, and F not read correctly" << endl << "test6: " << test6 << endl; exit(16);}

/*****Dev Vector Parameter values (vals) and bounds *****/
/--F vectors-----
init_vector set_log_F_dev_L_ch(1,3);
init_vector set_log_F_dev_L_cL(1,3);
init_vector set_log_F_dev_L_rA(1,3);
init_vector set_log_rec_dev(1,3);
init_vector set_log_Nage_dev(1,3);

init_vector set_log_F_dev_vals_L_ch(styr_L_ch, endyr_L_ch);
init_vector set_log_F_dev_vals_L_cL(styr_L_cL, endyr_L_cL);
init_vector set_log_F_dev_vals_L_rA(styr_L_rA, endyr_L_rA);
init_vector set_log_rec_dev_vals(styr_rec_dev, endyr_rec_dev);
init_vector set_log_Nage_dev_vals(2, nages);
init_number test7;
!!if (test7 != 1234567890){cout << "DAT Dev vectors not read correctly" << endl << "test7: " << test7 << endl; exit(17);}

/-- BAM DATA_SECTION: likelihood weights section
init_number set_w_L; //weight for landings
init_number set_w_cpue_cL; //weight for comm handline index
init_number set_w_cpue_sM; //weight for MARMAP index
init_number set_w_lenc_rA; //weight for rA len comps
init_number set_w_agec_ch; //weight for comm handline age comps
init_number set_w_agec_cL; //weight for comm longline age comps
init_number set_w_agec_sM; //weight for MARMAP age comps
init_number set_w_Nage_init; //for fitting initial abundance at age (excluding first age)
init_number set_w_rec; //for fitting S-R curve
init_number set_w_rec_early; //additional constraint on early years recruitment
init_number set_w_rec_end; //additional constraint on ending years recruitment
init_number set_w_fullF; //penalty for any Fapex>3 (removed in final phase of optimization)
init_number set_w_Ftune; //weight applied to tuning F (removed in final phase of optimization)
init_number test8;
!!if (test8 != 1234567890){cout << "DAT likelihoods not read correctly" << endl << "test8: " << test8 << endl; exit(18);}

/-- BAM DATA_SECTION: miscellaneous stuff section

//TL(mm)-weight(whole weight in g) relationship: W=aL^b
init_number wgtpar_a;
init_number wgtpar_b;

//Reproductive output vector in total eggs at age in millions to be multiplied by the maturity at age
init_vector fecundity(1, nages);

//TL(mm)- weight(whole weight in g) relationship: W=aL^b

```

```

init_number gutwtgpar_a;
init_number gutwtgpar_b;

//Maturity and proportion female at age
init_vector maturity_f_obs(1,nages); //proportion females mature at age
init_vector maturity_m_obs(1,nages); //proportion males mature at age
init_vector prop_f_obs(1,nages); //proportion female at age

init_number spawn_time_frac; //time of year of peak spawning, as a fraction of the year

// init_number min_M_age; //max observed age, used to scale M
// Natural mortality
init_number min_M_age; //minimum age to start calculating average M from for older ages
init_number max_M_age; //maximum age to sum over M from Lorenzen scaling
// init_vector set_M(1,nages); //age-dependent: used in model
// init_number max_obs_age; //max observed age, used to scale M, if estimated

//Spawner-recruit parameters (Initial guesses or fixed values)
init_int SR_switch;

//rate of increase on q
init_int set_q_rate_phase; //value sets estimation phase of rate increase, negative value turns it off
init_number set_q_rate;
//density dependence on fishery q's
init_int set_q_DD_phase; //value sets estimation phase of random walk, negative value turns it off
init_number set_q_DD_beta; //value of 0.0 is density independent
init_number set_q_DD_beta_se;
init_int set_q_DD_stage; //age to begin counting biomass, should be near full exploitation

//random walk on fishery q's
init_int set_q_RW_phase; //value sets estimation phase of random walk, negative value turns it off
init_number set_q_RW_rec_var; //assumed variance of RW q

//Tune Fapex (tuning removed in final year of optimization)
init_number set_Ftune;
init_int set_Ftune_yr;

//threshold sample sizes for length comps
init_number minSS_lenc_rA;

//threshold sample sizes for age comps
init_number minSS_agec_ch;
init_number minSS_agec_cl;
init_number minSS_agec_sM;

//ageing error matrix (columns are true ages, rows are ages as read for age comps: columns should sum to one)
init_matrix age_error(1,nages,1,nages);

// #####Indexing integers for year(iyear), age(iage),length(ilen) #####
int iyear;
int jyear;
int iage;
int ilen;
int ff;

number sqrt2pi;
number g2mt; //conversion of grams to metric tons
// number g2kg; //conversion of grams to kg
number g2klb; //conversion of grams to 1000 lb
// number mt2klb; //conversion of metric tons to 1000 lb
// number mt2lb; //conversion of metric tons to lb
number dzero; //small additive constant to prevent division by zero
number huge_number; //huge number, to avoid irregular parameter space

init_number end_of_data_file;

//this section MUST BE INDENTED!!!
LOCAL_CALCS
  if(end_of_data_file!=999)
  {
    cout << "**** WARNING: Data File NOT READ CORRECTLY ****" << endl;
    exit(0);
  }
  else
  {cout << "Data File read correctly" << endl;}
END_CALCS

PARAMETER_SECTION

LOCAL_CALCS
const double Linf_LO=set_Linf(2); const double Linf_HI=set_Linf(3); const double Linf_PH=set_Linf(4);
const double K_LO=set_K(2); const double K_HI=set_K(3); const double K_PH=set_K(4);
const double t0_LO=set_t0(2); const double t0_HI=set_t0(3); const double t0_PH=set_t0(4);
const double Linf_f_LO=set_Linf_f(2); const double Linf_f_HI=set_Linf_f(3); const double Linf_f_PH=set_Linf_f(4);
const double K_f_LO=set_K_f(2); const double K_f_HI=set_K_f(3); const double K_f_PH=set_K_f(4);
const double t0_f_LO=set_t0_f(2); const double t0_f_HI=set_t0_f(3); const double t0_f_PH=set_t0_f(4);
const double len_cv_LO=set_len_cv(2); const double len_cv_HI=set_len_cv(3); const double len_cv_PH=set_len_cv(4);
const double M_constant_LO=set_M_constant(2); const double M_constant_HI=set_M_constant(3); const double M_constant_PH=set_M_constant(4);
const double steep_LO=set_steep(2); const double steep_HI=set_steep(3); const double steep_PH=set_steep(4);
const double log_R0_LO=set_log_R0(2); const double log_R0_HI=set_log_R0(3); const double log_R0_PH=set_log_R0(4);
const double R_autocorr_LO=set_R_autocorr(2); const double R_autocorr_HI=set_R_autocorr(3); const double R_autocorr_PH=set_R_autocorr(4);
const double rec_sigma_LO=set_rec_sigma(2); const double rec_sigma_HI=set_rec_sigma(3); const double rec_sigma_PH=set_rec_sigma(4);

const double log_dm_lenc_rA_LO=set_log_dm_lenc_rA(2); const double log_dm_lenc_rA_HI=set_log_dm_lenc_rA(3); const double log_dm_lenc_rA_PH=set_log_dm_lenc_rA(4);
const double log_dm_agec_ch_LO=set_log_dm_agec_ch(2); const double log_dm_agec_ch_HI=set_log_dm_agec_ch(3); const double log_dm_agec_ch_PH=set_log_dm_agec_ch(4);
const double log_dm_agec_cl_LO=set_log_dm_agec_cl(2); const double log_dm_agec_cl_HI=set_log_dm_agec_cl(3); const double log_dm_agec_cl_PH=set_log_dm_agec_cl(4);
const double log_dm_agec_sM_LO=set_log_dm_agec_sM(2); const double log_dm_agec_sM_HI=set_log_dm_agec_sM(3); const double log_dm_agec_sM_PH=set_log_dm_agec_sM(4);

```

```

const double selpar_L50_ch_L0=set_selpar_L50_ch(2); const double selpar_L50_ch_HI=set_selpar_L50_ch(3); const double selpar_L50_ch_PH=set_selpar_L50_ch(4);
const double selpar_L50_ch2_L0=set_selpar_L50_ch2(2); const double selpar_L50_ch2_HI=set_selpar_L50_ch2(3); const double selpar_L50_ch2_PH=set_selpar_L50_ch2(4);
const double selpar_L502_ch2_L0=set_selpar_L502_ch2(2); const double selpar_L502_ch2_HI=set_selpar_L502_ch2(3); const double selpar_L502_ch2_PH=set_selpar_L502_ch2(4);
const double selpar_slope_ch_L0=set_selpar_slope_ch(2); const double selpar_slope_ch_HI=set_selpar_slope_ch(3); const double selpar_slope_ch_PH=set_selpar_slope_ch(4);
const double selpar_slope_ch2_L0=set_selpar_slope_ch2(2); const double selpar_slope_ch2_HI=set_selpar_slope_ch2(3); const double selpar_slope_ch2_PH=set_selpar_slope_ch2(4);
const double selpar_slope2_ch2_L0=set_selpar_slope2_ch2(2); const double selpar_slope2_ch2_HI=set_selpar_slope2_ch2(3); const double selpar_slope2_ch2_PH=set_selpar_slope2_ch2(4);
const double selpar_L50_cl_L0=set_selpar_L50_cl(2); const double selpar_L50_cl_HI=set_selpar_L50_cl(3); const double selpar_L50_cl_PH=set_selpar_L50_cl(4);
const double selpar_L50_cl2_L0=set_selpar_L50_cl2(2); const double selpar_L50_cl2_HI=set_selpar_L50_cl2(3); const double selpar_L50_cl2_PH=set_selpar_L50_cl2(4);
const double selpar_L502_cl2_L0=set_selpar_L502_cl2(2); const double selpar_L502_cl2_HI=set_selpar_L502_cl2(3); const double selpar_L502_cl2_PH=set_selpar_L502_cl2(4);
const double selpar_slope_cl_L0=set_selpar_slope_cl(2); const double selpar_slope_cl_HI=set_selpar_slope_cl(3); const double selpar_slope_cl_PH=set_selpar_slope_cl(4);
const double selpar_slope_cl2_L0=set_selpar_slope_cl2(2); const double selpar_slope_cl2_HI=set_selpar_slope_cl2(3); const double selpar_slope_cl2_PH=set_selpar_slope_cl2(4);
const double selpar_slope2_cl2_L0=set_selpar_slope2_cl2(2); const double selpar_slope2_cl2_HI=set_selpar_slope2_cl2(3); const double selpar_slope2_cl2_PH=set_selpar_slope2_cl2(4);

//const double selpar_afull_cl_L0=set_selpar_afull_cl(2); const double selpar_afull_cl_HI=set_selpar_afull_cl(3); const double selpar_afull_cl_PH=set_selpar_afull_cl(4);
//const double selpar_sigma_cl_L0=set_selpar_afull_cl(2); const double selpar_sigma_cl_HI=set_selpar_afull_cl(3); const double selpar_sigma_cl_PH=set_selpar_afull_cl(4);

const double selpar_L50_ra_L0=set_selpar_L50_ra(2); const double selpar_L50_ra_HI=set_selpar_L50_ra(3); const double selpar_L50_ra_PH=set_selpar_L50_ra(4);
const double selpar_slope_ra_L0=set_selpar_slope_ra(2); const double selpar_slope_ra_HI=set_selpar_slope_ra(3); const double selpar_slope_ra_PH=set_selpar_slope_ra(4);

const double selpar_L50_sm_L0=set_selpar_L50_sm(2); const double selpar_L50_sm_HI=set_selpar_L50_sm(3); const double selpar_L50_sm_PH=set_selpar_L50_sm(4);
const double selpar_slope_sm_L0=set_selpar_slope_sm(2); const double selpar_slope_sm_HI=set_selpar_slope_sm(3); const double selpar_slope_sm_PH=set_selpar_slope_sm(4);

const double log_q_cpue_cl_L0=set_log_q_cpue_cl(2); const double log_q_cpue_cl_HI=set_log_q_cpue_cl(3); const double log_q_cpue_cl_PH=set_log_q_cpue_cl(4);
const double log_q_cpue_sm_L0=set_log_q_cpue_sm(2); const double log_q_cpue_sm_HI=set_log_q_cpue_sm(3); const double log_q_cpue_sm_PH=set_log_q_cpue_sm(4);

const double F_init_L0=set_F_init(2); const double F_init_HI=set_F_init(3); const double F_init_PH=set_F_init(4);
const double log_avg_F_L_ch_L0=set_log_avg_F_L_ch(2); const double log_avg_F_L_ch_HI=set_log_avg_F_L_ch(3); const double log_avg_F_L_ch_PH=set_log_avg_F_L_ch(4);
const double log_avg_F_L_cl_L0=set_log_avg_F_L_cl(2); const double log_avg_F_L_cl_HI=set_log_avg_F_L_cl(3); const double log_avg_F_L_cl_PH=set_log_avg_F_L_cl(4);
const double log_avg_F_L_ra_L0=set_log_avg_F_L_ra(2); const double log_avg_F_L_ra_HI=set_log_avg_F_L_ra(3); const double log_avg_F_L_ra_PH=set_log_avg_F_L_ra(4);

//--dev vectors-----
const double log_F_dev_L_ch_L0=set_log_F_dev_L_ch(1); const double log_F_dev_L_ch_HI=set_log_F_dev_L_ch(2); const double log_F_dev_L_ch_PH=set_log_F_dev_L_ch(3);
const double log_F_dev_L_cl_L0=set_log_F_dev_L_cl(1); const double log_F_dev_L_cl_HI=set_log_F_dev_L_cl(2); const double log_F_dev_L_cl_PH=set_log_F_dev_L_cl(3);
const double log_F_dev_L_ra_L0=set_log_F_dev_L_ra(1); const double log_F_dev_L_ra_HI=set_log_F_dev_L_ra(2); const double log_F_dev_L_ra_PH=set_log_F_dev_L_ra(3);

const double log_rec_dev_L0=set_log_rec_dev(1); const double log_rec_dev_HI=set_log_rec_dev(2); const double log_rec_dev_PH=set_log_rec_dev(3);
const double log_Nage_dev_L0=set_log_Nage_dev(1); const double log_Nage_dev_HI=set_log_Nage_dev(2); const double log_Nage_dev_PH=set_log_Nage_dev(3);

END_CALCUS

////-----Growth-----
init_bounded_number Linf(Linf_L0,Linf_HI,Linf_PH);
init_bounded_number K(K_L0,K_HI,K_PH);
init_bounded_number t0(t0_L0,t0_HI,t0_PH);
init_bounded_number Linf_f(Linf_f_L0,Linf_f_HI,Linf_f_PH);
init_bounded_number K_f(K_f_L0,K_f_HI,K_f_PH);
init_bounded_number t0_f(t0_f_L0,t0_f_HI,t0_f_PH);
init_bounded_number len_cv_val(len_cv_L0,len_cv_HI,len_cv_PH);
vector Linf_out(1,8);
vector K_out(1,8);
vector t0_out(1,8);
vector Linf_f_out(1,8);
vector K_f_out(1,8);
vector t0_f_out(1,8);
vector len_cv_val_out(1,8);

vector meanlen_TL(1,nages); //mean total length (mm) at age all fish
vector meanlen_TL_f(1,nages); //mean total length (mm) at age females

vector wgt_g(1,nages); //whole wgt in g
// vector wgt_kg(1,nages); //whole wgt in kg
// vector wgt_mt(1,nages); //whole wgt in mt
vector wgt_klb(1,nages); //whole wgt in 1000 lb
vector wgt_lb(1,nages); //whole wgt in lb
vector wgt_lb_gut(1,nages); //gutted wgt in lb
vector wgt_klb_gut(1,nages); //gutted wgt in 1000 lb
vector wgt_g_gut(1,nages); //gutted wgt in lb
// vector wgt_mt_gut(1,nages); //gutted wgt in lb

vector wgt_g_f(1,nages); //whole wgt in g
// vector wgt_kg_f(1,nages); //whole wgt in kg
// vector wgt_mt_f(1,nages); //whole wgt in mt
vector wgt_klb_f(1,nages); //whole wgt in 1000 lb
vector wgt_lb_f(1,nages); //whole wgt in lb
// vector gonad_wgt_mt(1,nages); //gonad wgt in mt

matrix len_cl_mm(styr,endyr,1,nages); //mean length at age of commercial longline landings in mm (may differ from popn mean)
matrix wholewgt_cl_klb(styr,endyr,1,nages); //whole wgt of commercial longline landings in 1000 lb
matrix gutwgt_cl_klb(styr,endyr,1,nages); //gutted wgt of commercial longline landings in 1000 lb

matrix len_ch_mm(styr,endyr,1,nages); //mean length at age of commercial handline landings in mm (may differ from popn mean)
matrix gutwgt_ch_klb(styr,endyr,1,nages); //gutted wgt of commercial handline landings in 1000 lb

matrix len_ra_mm(styr,endyr,1,nages); //mean length at age of rA landings in mm (may differ from popn mean)
matrix gutwgt_ra_klb(styr,endyr,1,nages); //gutted wgt of rA landings in 1000 lb

matrix len_sm_mm(styr,endyr,1,nages); //mean length at age of MARMAP landings in mm (may differ from popn mean)
matrix wgt_sm_klb(styr,endyr,1,nages); //whole wgt of MARMAP landings in 1000 lb

matrix lenprob(1,nages,1,nlenbins); //distn of size at age (age-length key, 3 cm bins) in population
number zscore_len; //standardized normal values used for computing lenprob
vector cprob_lenvec(1,nlenbins); //cumulative probabilities used for computing lenprob
number zscore_lzero; //standardized normal values for length = 0
number cprob_lzero; //length probability mass below zero, used for computing lenprob

//matrices below are used to match length comps
matrix lenprob_ch(1,nages,1,nlenbins); //distn of size at age in ch
matrix lenprob_cl(1,nages,1,nlenbins); //distn of size at age in cl
matrix lenprob_ra(1,nages,1,nlenbins); //distn of size at age in rA

```

```

// //init_bounded_dev_vector log_len_cv_dev(1,nages,-2,2,3)
// number log_len_cv
// vector len_sd(1,nages);
// vector len_cv(1,nages); //for fishgraph

//----Predicted length compositions
matrix pred_lenc_rA(1,nyr_lenc_rA,1,nlenbins);

//----Predicted age compositions
matrix pred_agec_ch(1,nyr_agec_ch,1,nages_agec);
matrix pred_agec_ch_allages(1,nyr_agec_ch,1,nages);
matrix ErrorFree_agec_ch(1,nyr_agec_ch,1,nages);
matrix pred_agec_cl(1,nyr_agec_cl,1,nages_agec);
matrix pred_agec_cl_allages(1,nyr_agec_cl,1,nages);
matrix ErrorFree_agec_cl(1,nyr_agec_cl,1,nages);
matrix pred_agec_sM(1,nyr_agec_sM,1,nages_agec_sM);
matrix pred_agec_sM_allages(1,nyr_agec_sM,1,nages);
matrix ErrorFree_agec_sM(1,nyr_agec_sM,1,nages);

//effective sample size applied in multinomial distributions
vector nsamp_lenc_rA_allyr(styr,endyr);

vector nsamp_agec_ch_allyr(styr,endyr);
vector nsamp_agec_cl_allyr(styr,endyr);
vector nsamp_agec_sM_allyr(styr,endyr);

//Nfish used in MCB analysis (not used in fitting)
vector nfish_lenc_rA_allyr(styr,endyr);
vector nfish_agec_ch_allyr(styr,endyr);
vector nfish_agec_cl_allyr(styr,endyr);
vector nfish_agec_sM_allyr(styr,endyr);

//Computed effective sample size for output (not used in fitting)
vector neff_lenc_rA_allyr_out(styr,endyr);
vector neff_agec_ch_allyr_out(styr,endyr);
vector neff_agec_cl_allyr_out(styr,endyr);
vector neff_agec_sM_allyr_out(styr,endyr);

//----Population-----
matrix N(styr,endyr+1,1,nages); //Population numbers by year and age at start of yr
matrix N_mdyr(styr,endyr,1,nages); //Population numbers by year and age at mdpt of yr: used for comps and cpe
matrix N_spawn(styr,endyr+1,1,nages); //Population numbers by year and age at peaking spawning: used for SSB (proj yr ok bc of ssb on Jan1)
init_bounded_vector log_Nage_dev(2,nages,log_Nage_dev_L0,log_Nage_dev_HI,log_Nage_dev_PH);
vector log_Nage_dev_output(1,nages); //used in output. equals zero for first age
matrix B(styr,endyr+1,1,nages); //Population biomass by year and age at start of yr
vector totB(styr,endyr+1); //Total biomass by year
vector totN(styr,endyr+1); //Total abundance by year
vector SSB(styr,endyr+1); //Total spawning biomass by year (female + male mature biomass) (proj yr ok bc of ssb on Jan1)
vector MatFemB(styr,endyr+1); //Total spawning biomass by year (mature female biomass) (proj yr ok bc of ssb on Jan1)
vector rec(styr,endyr+1); //Recruits by year
vector prop_m(1,nages); //Year-dependent proportion male by age
vector prop_f(1,nages); //Proportion female by age
vector maturity_f(1,nages); //Proportion of female mature at age
vector maturity_m(1,nages); //Proportion of male mature at age
vector reprod(1,nages); //vector used to compute spawning biomass (total mature biomass - males + females)
vector reprod2(1,nages); //vector used to compute mature female biomass

//---Stock-Recruit Function (Beverton-Holt, steepness parameterization)-----
init_bounded_number log_RO(log_RO_L0,log_RO_HI,log_RO_PH); //log(virgin Recruitment)
vector log_RO_out(1,8);
number R0; //virgin recruitment
init_bounded_number steep(steep_L0,steep_HI,steep_PH); //steepness
vector steep_out(1,8);
init_bounded_number rec_sigma(rec_sigma_L0,rec_sigma_HI,rec_sigma_PH); //sd recruitment residuals //KC comment out; this should fix it at the initial value
vector rec_sigma_out(1,8);
init_bounded_number R_autocorr(R_autocorr_L0,R_autocorr_HI,R_autocorr_PH); //autocorrelation in SR KC commented out since not estimated
vector R_autocorr_out(1,8);

number rec_sigma_sq; //square of rec_sigma
number rec_logL_add; //additive term in -logL term

init_bounded_dev_vector log_rec_dev(styr_rec_dev,endyr_rec_dev,log_rec_dev_L0,log_rec_dev_HI,log_rec_dev_PH);
vector log_rec_dev_output(styr,endyr+1); //used in t.series output. equals zero except for yrs in log_rec_dev
vector log_rec_dev_out(styr_rec_dev,endyr_rec_dev); //used in output for bound checking

number var_rec_dev; //variance of log recruitment deviations, from yrs with unconstrained S-R(XXXX-XXXX)
number sigma_rec_dev; //sample SD of log residuals (may not equal rec_sigma

number rec_mean_alt1_temp //intermediate calc for geometric mean of recruitment values during alternative period
number rec_mean_alt1 //geometric mean of recruitment values during alternative period
number nyrs_rec_alt1 //number of years during alternative period

number BiasCor; //Bias correction in equilibrium recruits
number S0; //equal to spr_F0*R0 = virgin SSB
number B0; //equal to bpr_F0*R0 = virgin B
number R1; //Recruits in styr
number R_virgin; //unfished recruitment with bias correction
vector SdS0(styr,endyr+1); //SSB / virgin SSB (projection yr possible bc of SSB on Jan1

init_bounded_number log_dm_lenc_rA(log_dm_lenc_rA_L0,log_dm_lenc_rA_HI,log_dm_lenc_rA_PH);
init_bounded_number log_dm_agec_ch(log_dm_agec_ch_L0,log_dm_agec_ch_HI,log_dm_agec_ch_PH);
init_bounded_number log_dm_agec_cl(log_dm_agec_cl_L0,log_dm_agec_cl_HI,log_dm_agec_cl_PH);
init_bounded_number log_dm_agec_sM(log_dm_agec_sM_L0,log_dm_agec_sM_HI,log_dm_agec_sM_PH);

vector log_dm_lenc_rA_out(1,8);
vector log_dm_agec_ch_out(1,8);
vector log_dm_agec_cl_out(1,8);
vector log_dm_agec_sM_out(1,8);

```

```

-----
////---Selectivity-----
//Commercial headline-----
matrix sel_ch(styr,endyr,1,nages);
init_bounded_number selpar_L50_ch(selpar_L50_ch_L0,selpar_L50_ch_HI,selpar_L50_ch_PH);
init_bounded_number selpar_L50_ch2(selpar_L50_ch2_L0,selpar_L50_ch2_HI,selpar_L50_ch2_PH);
init_bounded_number selpar_L502_ch2(selpar_L502_ch2_L0,selpar_L502_ch2_HI,selpar_L502_ch2_PH);
init_bounded_number selpar_slope_ch(selpar_slope_ch_L0,selpar_slope_ch_HI,selpar_slope_ch_PH);
init_bounded_number selpar_slope_ch2(selpar_slope_ch2_L0,selpar_slope_ch2_HI,selpar_slope_ch2_PH);
init_bounded_number selpar_slope2_ch2(selpar_slope2_ch2_L0,selpar_slope2_ch2_HI,selpar_slope2_ch2_PH);
vector selpar_L50_ch_out(1,8);
vector selpar_L50_ch2_out(1,8);
vector selpar_L502_ch2_out(1,8);
vector selpar_slope_ch_out(1,8);
vector selpar_slope_ch2_out(1,8);
vector selpar_slope2_ch2_out(1,8);

//Commercial longline-----
matrix sel_cl(styr,endyr,1,nages);
init_bounded_number selpar_L50_cl(selpar_L50_cl_L0,selpar_L50_cl_HI,selpar_L50_cl_PH);
init_bounded_number selpar_L50_cl2(selpar_L50_cl2_L0,selpar_L50_cl2_HI,selpar_L50_cl2_PH);
init_bounded_number selpar_L502_cl2(selpar_L502_cl2_L0,selpar_L502_cl2_HI,selpar_L502_cl2_PH);
init_bounded_number selpar_slope_cl(selpar_slope_cl_L0,selpar_slope_cl_HI,selpar_slope_cl_PH);
init_bounded_number selpar_slope_cl2(selpar_slope_cl2_L0,selpar_slope_cl2_HI,selpar_slope_cl2_PH);
init_bounded_number selpar_slope2_cl2(selpar_slope2_cl2_L0,selpar_slope2_cl2_HI,selpar_slope2_cl2_PH);
//init_bounded_number selpar_afull_cl(selpar_afull_cl_L0,selpar_afull_cl_HI,selpar_afull_cl_PH);
//init_bounded_number selpar_sigma_cl(selpar_sigma_cl_L0,selpar_sigma_cl_HI,selpar_sigma_cl_PH);
vector selpar_L50_cl_out(1,8);
vector selpar_L50_cl2_out(1,8);
vector selpar_L502_cl2_out(1,8);
vector selpar_slope_cl_out(1,8);
vector selpar_slope_cl2_out(1,8);
vector selpar_slope2_cl2_out(1,8);
//vector selpar_afull_cl_out(1,8);
//vector selpar_sigma_cl_out(1,8);

//Recreational (rA)-----
matrix sel_rA(styr,endyr,1,nages);
init_bounded_number selpar_L50_rA(selpar_L50_rA_L0,selpar_L50_rA_HI,selpar_L50_rA_PH);
init_bounded_number selpar_slope_rA(selpar_slope_rA_L0,selpar_slope_rA_HI,selpar_slope_rA_PH);
vector selpar_L50_rA_out(1,8);
vector selpar_slope_rA_out(1,8);

//MARMAP (sM)-----
matrix sel_sM(styr,endyr,1,nages);
init_bounded_number selpar_L50_sM(selpar_L50_sM_L0,selpar_L50_sM_HI,selpar_L50_sM_PH);
init_bounded_number selpar_slope_sM(selpar_slope_sM_L0,selpar_slope_sM_HI,selpar_slope_sM_PH);
vector selpar_L50_sM_out(1,8);
vector selpar_slope_sM_out(1,8);

//Weighted total selectivity-----
//effort-weighted, recent selectivities
vector sel_wgtd_L(1,nages); //toward landings
vector sel_wgtd_tot(1,nages); //toward Z, landings plus dead discards (none in this asmt, but kept structure)

//-----CPUE Predictions-----
vector pred_cl_cpue(styr_cpue_cl,endyr_cpue_cl); //predicted cl index (weight fish per effort)
matrix N_cl(styr_cpue_cl,endyr_cpue_cl,1,nages); //used to compute cl index

vector pred_sM_cpue(1,nyr_cpue_sM); //predicted sM index (number fish per effort)
matrix N_sM(1,nyr_cpue_sM,1,nages); //used to compute sM index
vector pred_sM_cpue_allyr(styr,endyr); // used for graphing purposes, fills in consec years
vector obs_cpue_sM_allyr(styr,endyr); // used for graphing purposes, fills in consec years
vector cv_cpue_sM_allyr(styr,endyr); // used for graphing purposes, fills in consec years

//---Catchability (CPUE q's)-----
init_bounded_number log_q_cpue_cl(log_q_cpue_cl_L0,log_q_cpue_cl_HI,log_q_cpue_cl_PH);
init_bounded_number log_q_cpue_sM(log_q_cpue_sM_L0,log_q_cpue_sM_HI,log_q_cpue_sM_PH);
vector log_q_cpue_cl_out(1,8);
vector log_q_cpue_sM_out(1,8);

//init_bounded_number q_rate(0.001,0.1,set_q_rate_phase); //not estimated so commented out, declared as number
number q_rate;
vector q_rate_fcn_cl(styr_cpue_cl,endyr_cpue_cl); //increase due to technology creep (saturates in 2003)

// init_bounded_number q_DD_beta(0.1,0.9,set_q_DD_phase); //not estimated so commented out and declared as number (below)
number q_DD_beta;
vector q_DD_fcn(styr,endyr); //density dependent function as a multiple of q (scaled a la Katsukawa and Matsuda. 2003)
number B0_q_DD; //B0 of ages q_DD_age plus
vector B_q_DD(styr,endyr); //annual biomass of ages q_DD_age plus

//Fishery dependent random walk catchability
// init_bounded_vector q_RW_log_dev_HB(styr_HB_cpue,endyr_HB_cpue-1,-3.0,3.0,set_q_RW_phase); //NOT estimated in this model
vector q_RW_log_dev_cl(styr_cpue_cl,endyr_cpue_cl-1);

//Catchability vector over time, may be constant
vector q_cl(styr_cpue_cl,endyr_cpue_cl);
number q_sM;

//-----Landings in numbers (total or 1000 fish) and in wgt (guttet klb)-----
matrix L_ch_num(styr,endyr,1,nages); //landings (numbers) at age
matrix L_ch_klb(styr,endyr,1,nages); //landings (1000 lb gutted weight) at age
vector pred_ch_L_knum(styr,endyr); //yearly landings in 1000 fish summed over ages

```



```

vector pred_ch_L_klb(styr,endyr); //yearly landings in 1000 lb gutted summed over ages
//vector obs_L_ch_wbias(styr,endyr); //yearly landings observed, perhaps adjusted for multiplicative bias

matrix L_cL_num(styr,endyr,1,nages); //landings (numbers) at age
matrix L_cL_klb(styr,endyr,1,nages); //landings (1000 lb gutted weight) at age
vector pred_cl_L_knum(styr,endyr); //yearly landings in 1000 fish summed over ages
vector pred_cl_L_klb(styr,endyr); //yearly landings in 1000 lb gutted summed over ages

matrix L_rA_num(styr,endyr,1,nages); //landings (numbers) at age
matrix L_rA_klb(styr,endyr,1,nages); //landings (1000 lb gutted weight) at age
vector pred_rA_L_knum(styr,endyr); //yearly landings in 1000 fish summed over ages
vector pred_rA_L_klb(styr,endyr); //yearly landings in 1000 lb gutted summed over ages

matrix L_total_num(styr,endyr,1,nages); //total landings in number at age
matrix L_total_klb(styr,endyr,1,nages); //landings in klb gutted wgt at age
vector L_total_knum_yr(styr,endyr); //total landings in 1000 fish by yr summed over ages
vector L_total_klb_yr(styr,endyr); //total landings (klb gutted wgt) by yr summed over ages

////---MSY calcs-----
number F_ch_prop; //proportion of F_sum attributable to ch, last X=selpar_n_yrs_wgtd yrs
number F_cL_prop; //proportion of F_sum attributable to cL, last X=selpar_n_yrs_wgtd yrs
number F_rA_prop; //proportion of F_sum attributable to rA, last X=selpar_n_yrs_wgtd yrs

number F_init_ch_prop; //proportion of F_init attributable to ch, first X yrs, No diving or discards in initial yrs
number F_init_cL_prop; //proportion of F_init attributable to cL, first X yrs
number F_init_rA_prop; //proportion of F_init attributable to rA, first X yrs

number F_temp_sum; //sum of geom mean Fsum's in last X yrs, used to compute F_fishery_prop

vector F_end(1,nages);
vector F_end_L(1,nages);
vector F_end_D(1,nages);
number F_end_apex;

number SSB_msy_out; //SSB (total mature biomass) at msy
number F_msy_out; //F at msy
number msy_klb_out; //max sustainable yield (1000 lb gutted wgt)
number msy_knum_out; //max sustainable yield (1000 fish)
number B_msy_out; //total biomass at MSY
number R_msy_out; //equilibrium recruitment at F=Fmsy
number spr_msy_out; //spr at F=Fmsy

// Stuff that goes into spr.brps matrix in cxx file
number F20_dum; //intermediate calculation for F20
number F30_dum; //intermediate calculation for F30
number F40_dum; //intermediate calculation for F40
number F20_out; //F20
number F30_out; //F30
number F40_out; //F40
number SSB_F30_out;
number B_F30_out;
number R_F30_out;
number L_F30_knum_out;
number L_F30_klb_out;
number D_F30_knum_out;
number D_F30_klb_out;
number rec_mean; //arithmetic average recruitment used in SPR-related quantities

vector N_age_msy(1,nages); //numbers at age for MSY calculations: beginning of yr
vector N_age_msy_spawn(1,nages); //numbers at age for MSY calculations: time of peak spawning
vector L_age_msy(1,nages); //landings at age for MSY calculations
vector Z_age_msy(1,nages); //total mortality at age for MSY calculations
vector F_L_age_msy(1,nages); //fishing mortality landings (not discards) at age for MSY calculations
vector F_msy(1,n_iter_msy); //values of full F to be used in equilibrium calculations
vector spr_msy(1,n_iter_msy); //reproductive capacity-per-recruit values corresponding to F values in F_msy
vector R_eq(1,n_iter_msy); //equilibrium recruitment values corresponding to F values in F_msy
vector L_eq_klb(1,n_iter_msy); //equilibrium landings(klb gutted wgt) values corresponding to F values in F_msy
vector L_eq_knum(1,n_iter_msy); //equilibrium landings(1000 fish) values corresponding to F values in F_msy
vector SSB_eq(1,n_iter_msy); //equilibrium reproductive capacity values corresponding to F values in F_msy
vector B_eq(1,n_iter_msy); //equilibrium biomass values corresponding to F values in F_msy

vector FdF_msy(styr,endyr);
vector FdF30(styr,endyr);
vector SdSSB_msy(styr,endyr+1); //proj yr ok bc of ssb on Jan1
number SdSSB_msy_end;
number FdF_msy_end;
number FdF_msy_end_mean; //geometric mean of last X yrs
vector SdSSB_F30(styr,endyr+1); //proj yr ok bc of ssb on Jan1
vector Sdmsst_F30(styr,endyr+1); //proj yr ok bc of ssb on Jan1
number SdSSB_F30_end;
number Sdmsst_F30_end;
number FdF30_end_mean; //geometric mean of last selpar_n_yrs_wgtd yrs
number Fend_mean_temp; //intermediate calc for geometric mean of last selpar_n_yrs_wgtd yrs
number Fend_mean; //geometric mean of last selpar_n_yrs_wgtd yrs
vector L_age_F30(1,nages); //landings at age for F30 calculations
//vector D_age_F30(1,nages); //discard mortality (dead discards) at age for F30 calculations

vector wgt_wgtd_L_klb(1,nages); //fishery-weighted average weight at age of landings in gutted weight
number wgt_wgtd_L_denom; //used in intermediate calculations

number iter_inc_msy; //increments used to compute msy, equals 1/(n_iter_msy-1)

////-----Mortality-----
vector M(1,nages); //age-dependent natural mortality
vector Mscale_len(1,max_M_age);
vector M_lorenzen(1,max_M_age);
number cum_surv_lplus;
number nages_M_sum;

```

```

init_bounded_number M_constant(M_constant_LO,M_constant_HI,M_constant_PH);           //age-independent: used only for MSST
vector M_constant_out(1,8);

number smy2msst;           //scales Smsy to get msst using (1-M). Used only in output.
number smy2msst75;       //scales Smsy to get msst using 75%. Used only in output.

matrix F(styr,endyr,1,nages);
vector Fsum(styr,endyr);           //Full fishing mortality rate by year
vector Papex(styr,endyr);         //Max across ages, fishing mortality rate by year (may differ from Fsum bc of dome-shaped sel
matrix Z(styr,endyr,1,nages);

init_bounded_number log_avg_F_L_cH(log_avg_F_L_cH_LO,log_avg_F_L_cH_HI,log_avg_F_L_cH_PH);
vector log_avg_F_L_cH_out(1,8);
init_bounded_dev_vector log_F_dev_L_cH(styr_L_cH,endyr_L_cH,log_F_dev_L_cH_LO,log_F_dev_L_cH_HI,log_F_dev_L_cH_PH);
vector log_F_dev_L_cH_out(styr_L_cH,endyr_L_cH);
matrix F_cH(styr,endyr,1,nages);
vector F_cH_out(styr,endyr);       //used for intermediate calculations in fcn get_mortality
number log_F_dev_init_cH;
number log_F_dev_end_cH;

init_bounded_number log_avg_F_L_cL(log_avg_F_L_cL_LO,log_avg_F_L_cL_HI,log_avg_F_L_cL_PH);
vector log_avg_F_L_cL_out(1,8);
init_bounded_dev_vector log_F_dev_L_cL(styr_L_cL,endyr_L_cL,log_F_dev_L_cL_LO,log_F_dev_L_cL_HI,log_F_dev_L_cL_PH);
vector log_F_dev_L_cL_out(styr_L_cL,endyr_L_cL);
matrix F_cL(styr,endyr,1,nages);
vector F_cL_out(styr,endyr);       //used for intermediate calculations in fcn get_mortality
number log_F_dev_init_cL;         //cL landings do not extend to beginning of time series
number log_F_dev_end_cL;

init_bounded_number log_avg_F_L_rA(log_avg_F_L_rA_LO,log_avg_F_L_rA_HI,log_avg_F_L_rA_PH);
vector log_avg_F_L_rA_out(1,8);
init_bounded_dev_vector log_F_dev_L_rA(styr_L_rA,endyr_L_rA,log_F_dev_L_rA_LO,log_F_dev_L_rA_HI,log_F_dev_L_rA_PH);
vector log_F_dev_L_rA_out(styr_L_rA,endyr_L_rA);
matrix F_rA(styr,endyr,1,nages);
vector F_rA_out(styr,endyr);       //used for intermediate calculations in fcn get_mortality
number log_F_dev_init_rA;
number log_F_dev_end_rA;

init_bounded_number F_init(F_init_LO,F_init_HI,F_init_PH); //scales early F for initialization
vector F_init_out(1,8);
number F_init_denom; //interim calculation
vector sel_initial(1,nages);       //initial selectivity (a combination of for-hire and commercial selectivities)

//---Per-recruit stuff-----
vector N_age_spr(1,nages);           //numbers at age for SPR calculations: beginning of year
vector N_age_spr_spawn(1,nages);     //numbers at age for SPR calculations: time of peak spawning
vector L_age_spr(1,nages);           //catch at age for SPR calculations
vector Z_age_spr(1,nages);           //total mortality at age for SPR calculations
vector spr_static(styr,endyr);       //vector of static SPR values by year
vector F_L_age_spr(1,nages);         //fishing mortality of landings (not discards) at age for SPR calculations
vector F_spr(1,n_iter_spr);         //values of full F to be used in per-recruit calculations
vector spr_spr(1,n_iter_spr);       //reproductive capacity-per-recruit values corresponding to F values in F_spr
vector spr_ratio(1,n_iter_spr);     //reproductive capacity-per-recruit relative to spr_F0 values corresponding to F values in F_spr
vector L_spr(1,n_iter_spr);         //landings(lb gutted)-per-recruit (ypr) values corresponding to F values in F_spr

vector N_spr_F0(1,nages);           //Used to compute spr at F=0: at time of peak spawning
vector N_bpr_F0(1,nages);           //Used to compute bpr at F=0: at start of year
vector N_spr_initial(1,nages);       //Initial spawners per recruit at age given initial F
vector N_initial_eq(1,nages);       //Initial equilibrium abundance at age
vector F_initial(1,nages);          //initial F at age
vector Z_initial(1,nages);          //initial Z at age
number spr_initial;                 //initial spawners per recruit
number spr_F0;                       //Spawning biomass per recruit at F=0
number bpr_F0;                       //Biomass per recruit at F=0

number iter_inc_spr;                 //increments used to compute msy, equals max_F_spr_msy/(n_iter_spr-1)

//-----SDNR output-----
number sdnr_lc_cH;
number sdnr_lc_cL;
number sdnr_lc_rA;

number sdnr_ac_cH;
number sdnr_ac_cL;
number sdnr_ac_sM;

number sdnr_I_cL;
number sdnr_I_sM;

//-----Objective function components-----
number w_L;

number w_cpue_cL;
number w_cpue_sM;

number w_lenc_rA;

number w_agec_cH;
number w_agec_cL;
number w_agec_sM;

number w_Nage_init;
number w_rec;
number w_rec_early;
number w_rec_end;
number w_fullF;
number w_Ftune;

```



```

    }
    if (iyear>2003) {q_rate_fcn_cl(iyear)=q_rate_fcn_cl(iyear-1);}
  }
} //end q_rate conditional

w_L=set_w_L;

w_cpue_cl=set_w_cpue_cl;
w_cpue_sM=set_w_cpue_sM;

w_lenc_rA=set_w_lenc_rA;

w_agec_ch=set_w_agec_ch;
w_agec_cl=set_w_agec_cl;
w_agec_sM=set_w_agec_sM;

w_Nage_init=set_w_Nage_init;
w_rec=set_w_rec;
w_rec_early=set_w_rec_early;
w_rec_end=set_w_rec_end;
w_fullF=set_w_fullF;
w_Ftune=set_w_Ftune;

F_init=set_F_init(1);

log_avg_F_L_ch=set_log_avg_F_L_ch(1);
log_avg_F_L_cl=set_log_avg_F_L_cl(1);
log_avg_F_L_rA=set_log_avg_F_L_rA(1);

log_F_dev_L_ch=set_log_F_dev_vals_L_ch;
log_F_dev_L_cl=set_log_F_dev_vals_L_cl;
log_F_dev_L_rA=set_log_F_dev_vals_L_rA;

selpar_L50_ch=set_selpar_L50_ch(1);
selpar_L50_ch2=set_selpar_L50_ch2(1);
selpar_L502_ch2=set_selpar_L502_ch2(1);
selpar_slope_ch=set_selpar_slope_ch(1);
selpar_slope_ch2=set_selpar_slope_ch2(1);
selpar_slope2_ch2=set_selpar_slope2_ch2(1);

selpar_L50_cl=set_selpar_L50_cl(1);
selpar_L50_cl2=set_selpar_L50_cl2(1);
selpar_L502_cl2=set_selpar_L502_cl2(1);
selpar_slope_cl=set_selpar_slope_cl(1);
selpar_slope_cl2=set_selpar_slope_cl2(1);
selpar_slope2_cl2=set_selpar_slope2_cl2(1);
//selpar_afull_cl=set_selpar_afull_cl(1);
//selpar_sigma_cl=set_selpar_sigma_cl(1);

selpar_L50_rA=set_selpar_L50_rA(1);
selpar_slope_rA=set_selpar_slope_rA(1);

selpar_L50_sM=set_selpar_L50_sM(1);
selpar_slope_sM=set_selpar_slope_sM(1);

sqrt2pi=sqrt(2.*3.14159265);
g2mt=0.000001; //conversion of grams to metric tons
// g2kg=0.001; //conversion of grams to kg
// mt2klb=2.20462; //conversion of metric tons to 1000 lb
// nt2lb=mt2klb*1000.0; //conversion of metric tons to lb
// g2klb=g2mt*mt2klb; //conversion of grams to 1000 lb
g2klb=g2mt*2.20462; //conversion of grams to 1000 lb
dzero=0.00001;
huge_number=1.0e+10;

SSB_msy_out=0.0;

iter_inc_msy=max_F_spr_msy/(n_iter_msy-1);
iter_inc_spr=max_F_spr_msy/(n_iter_spr-1);

maturity_f=maturity_f_obs;
maturity_m=maturity_m_obs;
prop_f=prop_f_obs;

//lbins=lenbins; //NOT NEEDED

//Fill in sample sizes of comps, possibly sampled in nonconsec yrs
//Used primarily for output in R object

nsamp_lenc_rA_allyr=missing;
nsamp_agec_ch_allyr=missing;
nsamp_agec_cl_allyr=missing;
nsamp_agec_sM_allyr=missing;

nfish_lenc_rA_allyr=missing;
nfish_agec_ch_allyr=missing;
nfish_agec_cl_allyr=missing;
nfish_agec_sM_allyr=missing;

pred_sM_cpue_allyr=missing;
obs_cpue_sM_allyr=missing;
cv_cpue_sM_allyr=missing;

for (iyear=1; iyear<=nyr_lenc_rA; iyear++)
  {if (nsamp_lenc_rA(iyear)>=minSS_lenc_rA)
    {nsamp_lenc_rA_allyr(yrs_lenc_rA(iyear))=nsamp_lenc_rA(iyear);

```



```

//cout<< "got weight at age of landings"<<endl;
get_spr_F0();
//cout << "got F0 spr" << endl;
get_selectivity();
//cout << "got selectivity" << endl;
get_mortality();
//cout << "got mortalities" << endl;
get_bias_corr();
//cout<< "got recruitment bias correction" << endl;
get_numbers_at_age();
//cout << "got numbers at age" << endl;
get_landings_numbers();
//cout << "got landings in numbers" << endl;
get_landings_wgt();
//cout << "got landings in wgt" << endl;
get_catchability_fcns();
//cout << "got catchability_fcns" << endl;
get_indices();
//cout << "got indices" << endl;
get_length_comps();
//cout<< "got length comps"<< endl;
get_age_comps();
//cout<< "got age comps"<< endl;
evaluate_objective_function();
//cout << "objective function calculations complete" << endl;

FUNCTION get_M_at_age
  cum_surv_1plus=nages*M_sum*M_constant;
  M=M_lorenzen(1,nages)*(cum_surv_1plus/sum(M_lorenzen(min_M_age,max_M_age)));

FUNCTION get_length_weight_at_age
  meanlen_TL=Linf*(1.0-mfexp(-K*(agebins-t0+0.5))); //mean total length at age in mm
  wgt_g=wtgtpar_a*pow(meanlen_TL,wtgtpar_b); //mean whole wgt at age in grams
  // wgt_mt=wtgt_g*g2mt; //mean whole wgt at age in mts
  // wgt_kg=g2kg*wtgt_g; //mean whole wgt at age in kilograms
  wgt_klb=g2klb*wtgt_g; //mean whole weight at age in 1000 lbs
  wgt_lb=wtgt_klb*1000.; //mean whole weight at age in lbs
  wgt_g_gut=wtgtgtpar_a*pow(meanlen_TL,wtgtgtpar_b); //mean gutted wgt at age in g
  wgt_klb_gut=wtgt_g_gut*g2klb; //mean gutted weight at age in 1000 lbs

  meanlen_TL_f=Linf*(1.0-mfexp(-K*(agebins-t0_f+0.5))); //total length in mm
  wgt_g_f=wtgtpar_a*pow(meanlen_TL_f,wtgtpar_b); //wgt in grams
  // wgt_mt_f=wtgt_mt_f*g2mt; //wgt in mt
  // wgt_kg_f=g2kg*wtgt_g_f; //wgt in kilograms
  wgt_klb_f=g2klb*wtgt_g_f; //1000 lb of whole wgt
  wgt_lb_f=wtgt_klb_f*1000.; //lb of whole wgt

FUNCTION get_reprod
  //reprod is product of stuff going into reproductive capacity calcs
  //for (iyear=styr; iyear<=endyr; iyear++)
  //t
  //reprod(iyear)=elem_prod((elem_prod(prop_f(iyear),maturity_f)+elem_prod((prop_m(iyear),maturity_m)),wgt_mt);
  //reprod2(iyear)=elem_prod(elem_prod(prop_f(iyear),maturity_f),wgt_mt);
  //t
  reprod=elem_prod(elem_prod(prop_f,maturity_f),fecundity);
  reprod2=elem_prod(elem_prod(prop_f,maturity_f),wgt_klb_f);

FUNCTION get_length_at_age_dist
  //compute matrix of length at age, based on the normal distribution

  for (iage=1;iage<=nages;iage++)
  {
    //len_cv(iage)=mfexp(log_len_cv+log_len_cv_dev(iage));
    len_cv(iage)=len_cv_val;
    len_sd(iage)=meanlen_TL(iage)*len_cv(iage);

    zscore_lzero=(0.0-meanlen_TL(iage))/len_sd(iage);
    cprob_lzero=cumd_norm(zscore_lzero);

    //first length bin
    zscore_len=((lenbins(1)+0.5*lenbins_width)-meanlen_TL(iage)) / len_sd(iage);
    cprob_lenvec(1)=cumd_norm(zscore_len); //includes any probability mass below zero
    lenprob(iage,1)=cprob_lenvec(1)-cprob_lzero; //removes any probability mass below zero

    //most other length bins
    for (ilen=2;ilen<=lenbins;ilen++)
    {
      zscore_len=((lenbins(ilen)+0.5*lenbins_width)-meanlen_TL(iage)) / len_sd(iage);
      cprob_lenvec(ilen)=cumd_norm(zscore_len);
      lenprob(iage,ilen)=cprob_lenvec(ilen)-cprob_lenvec(ilen-1);
    }

    //last length bin is a plus group
    zscore_len=((lenbins(nlenbins)-0.5*lenbins_width)-meanlen_TL(iage)) / len_sd(iage);
    lenprob(iage,nlenbins)=1.0-cumd_norm(zscore_len);

    lenprob(iage)=lenprob(iage)/(1.0-cprob_lzero); //renormalize to account for any prob mass below size=0
  }

  //fleet and survey specific length probs, all assumed here to equal the popn
  lenprob_ch=lenprob;
  lenprob_cl=lenprob;
  lenprob_ra=lenprob;

FUNCTION get_weight_at_age_landings

  for (iyear=styr; iyear<=endyr; iyear++)

```

```

{
  len_ch_mm(iyear)=meanlen_TL;
  gutwgt_ch_klb(iyear)=wgt_klb_gut;

len_cl_mm(iyear)=meanlen_TL;
  gutwgt_cl_klb(iyear)=wgt_klb_gut;
wholewgt_cl_klb(iyear)=wgt_klb; //wholeweight used to match index

  len_ra_mm(iyear)=meanlen_TL;
  gutwgt_ra_klb(iyear)=wgt_klb_gut;

len_sM_mm(iyear)=meanlen_TL;
  wgt_sM_klb(iyear)=wgt_klb;

}

FUNCTION get_spr_FO
//at mdyr, apply half this yr's mortality, half next yr's
N_spr_FO(1)=1.0*mfexp(-1.0*M(1)*spawn_time_frac); //at peak spawning time
N_bpr_FO(1)=1.0; //at start of year
for (iages=2; iage<=nages; iage++)
{ N_spr_FO(iage)=N_spr_FO(iage-1)*mfexp(-1.0*(M(iage-1)*(1.0-spawn_time_frac) + M(iage)*spawn_time_frac));
  N_bpr_FO(iage)=N_bpr_FO(iage-1)*mfexp(-1.0*(M(iage-1)));
}
N_spr_FO(nages)=N_spr_FO(nages)/(1.0-mfexp(-1.0*M(nages))); //plus group (sum of geometric series)
N_bpr_FO(nages)=N_bpr_FO(nages)/(1.0-mfexp(-1.0*M(nages)));

spr_FO=sum(elem_prod(N_spr_FO, reprod));
bpr_FO=sum(elem_prod(N_bpr_FO, wgt_klb));

FUNCTION get_selectivity
for (iyear=styr; iyear<=endyr_selphase1; iyear++)
{sel_ch(iyear)=logistic(agebins, selpar_L50_ch, selpar_slope_ch);
 sel_cl(iyear)=logistic(agebins, selpar_L50_cl, selpar_slope_cl);}

for (iyear=(endyr_selphase1+1); iyear<=endyr; iyear++)
{sel_ch(iyear)=logistic_double(agebins, selpar_L50_ch2, selpar_slope_ch2, selpar_L502_ch2, selpar_slope2_ch2);
 sel_cl(iyear)=logistic_double(agebins, selpar_L50_cl2, selpar_slope_cl2, selpar_L502_cl2, selpar_slope2_cl2);}

for (iyear=styr; iyear<=endyr; iyear++)
{sel_ra(iyear)=logistic(agebins, selpar_L50_ra, selpar_slope_ra);
 sel_sM(iyear)=logistic(agebins, selpar_L50_sM, selpar_slope_sM); }

sel_initial=sel_cl(styr);

FUNCTION get_mortality
Fsum.initialize();
Fapex.initialize();
F.initialize();
//initialization F is avg from first 3 yrs of observed landings
log_F_dev_init_ch=sum(log_F_dev_L_ch(styr_L_ch, (styr_L_ch+2)))/3.0;
log_F_dev_init_cl=sum(log_F_dev_L_cl(styr_L_cl, (styr_L_cl+2)))/3.0;
log_F_dev_init_ra=sum(log_F_dev_L_ra(styr_L_ra, (styr_L_ra+2)))/3.0;

for (iyear=styr; iyear<=endyr; iyear++)
{
  if (iyear>=styr_L_ch & iyear<=endyr_L_ch)
  { F_ch_out(iyear)=mfexp(log_avg_F_L_ch+log_F_dev_L_ch(iyear)); //}
  // if (iyear<styr_L_ch){F_ch_out(iyear)=mfexp(log_avg_F_L_ch+log_F_dev_init_ch);}
  F_ch(iyear)=sel_ch(iyear)*F_ch_out(iyear);
  Fsum(iyear)+=F_ch_out(iyear);
}

  if (iyear>=styr_L_cl & iyear<=endyr_L_cl)
  { F_cl_out(iyear)=mfexp(log_avg_F_L_cl+log_F_dev_L_cl(iyear)); //}
  // if (iyear<styr_L_cl){F_cl_out(iyear)=mfexp(log_avg_F_L_cl+log_F_dev_init_cl);}
  F_cl(iyear)=sel_cl(iyear)*F_cl_out(iyear);
  Fsum(iyear)+=F_cl_out(iyear);
}

  if (iyear>=styr_L_ra & iyear<=endyr_L_ra)
  { F_ra_out(iyear)=mfexp(log_avg_F_L_ra+log_F_dev_L_ra(iyear)); //}
  // if (iyear<styr_L_ra){F_ra_out(iyear)=mfexp(log_avg_F_L_ra+log_F_dev_init_ra);}
  F_ra(iyear)=sel_ra(iyear)*F_ra_out(iyear);
  Fsum(iyear)+=F_ra_out(iyear);
}

//Total F at age
F(iyear)=F_ch(iyear); //first in additive series (NO +=)
F(iyear)+=F_cl(iyear);
F(iyear)+=F_ra(iyear);

Fapex(iyear)=max(F(iyear));
Z(iyear)=M+F(iyear);
} //end iyear

FUNCTION get_bias_corr
var_rec_dev=norm2(log_rec_dev(styr_rec_dev, endyr_rec_dev)-
  sum(log_rec_dev(styr_rec_dev, endyr_rec_dev))/nyrs_rec)
  /(nyrs_rec-1.0);
//if (set_BiasCor <= 0.0) {BiasCor=mfexp(var_rec_dev/2.0);} //bias correction based on empirical residuals
rec_sigma_sq=square(rec_sigma);
if (set_BiasCor <= 0.0) {BiasCor=mfexp(rec_sigma_sq/2.0);} //bias correction based on Rsigma
else {BiasCor=set_BiasCor;}

FUNCTION get_numbers_at_age

```

```

//Initialization
R0=mfexp(log_R0);
S0=spr_F0*R0;
//R_virgin=(R0/((5.0*steep-1.0)*spr_F0))*
//      (BiasCor*4.0*steep*spr_F0-spr_F0*(1.0-steep));
//R_virgin=R0/(spr_F0/spr_F0)+BiasCor*(1.0+log(spr_F0/spr_F0)/steep); //Ricker

R_virgin=SR_eq_func(R0, steep, spr_F0, spr_F0, BiasCor, SR_switch);

B0=bpr_F0*R_virgin;
B0_q_DD=R_virgin*sum(elem_prod(N_bpr_F0(set_q_DD_stage,nages),wgt_klb(set_q_DD_stage,nages)));

//F_init_denom=mfexp(log_avg_F_L_ch+log_F_dev_init_ch)+mfexp(log_avg_F_HB+log_F_dev_init_HB)+mfexp(log_avg_F_L_rA+log_F_dev_init_rA);
//F_init_ch_prop=mfexp(log_avg_F_L_ch+log_F_dev_init_ch)/F_init_denom;
//F_init_HB_prop=mfexp(log_avg_F_HB+log_F_dev_init_HB)/F_init_denom;
//F_init_rA_prop=mfexp(log_avg_F_L_rA+log_F_dev_init_rA)/F_init_denom;

F_initial=sel_initial*F_init;

//F_initial=sel_ch(styr)*F_init*F_init_ch_prop+
//sel_HB(styr)*F_init*F_init_HB_prop+
//sel_rA(styr)*F_init*F_init_rA_prop; //rA uses HB selex
Z_initial=M*F_initial;

//Initial equilibrium age structure
N_spr_initial(1)=1.0*mfexp(-1.0*Z_initial(1)*spawn_time_frac); //at peak spawning time;
for (iage=2; iage<=nages; iage++)
{
  N_spr_initial(iage)=N_spr_initial(iage-1)*
    mfexp(-1.0*(Z_initial(iage-1)*(1.0-spawn_time_frac) + Z_initial(iage)*spawn_time_frac));
}
N_spr_initial(nages)=N_spr_initial(nages)/(1.0-mfexp(-1.0*Z_initial(nages))); //plus group
spr_initial=sum(elem_prod(N_spr_initial,reprod));

//if (styr==styr_rec_dev) {R1=(R0/((5.0*steep-1.0)*spr_initial))*
//      (4.0*steep*spr_initial-spr_F0*(1.0-steep));} //without bias correction (deviation added later)
//else {R1=(R0/((5.0*steep-1.0)*spr_initial))*
//      (BiasCor*4.0*steep*spr_initial-spr_F0*(1.0-steep));} //with bias correction

if (styr==styr_rec_dev) {R1=SR_eq_func(R0, steep, spr_F0, spr_initial, 1.0, SR_switch);} //without bias correction (deviation added later)
else {R1=SR_eq_func(R0, steep, spr_F0, spr_initial, BiasCor, SR_switch);} //with bias correction
if(R1<10.0) {R1=10.0;} //Avoid unrealistically low popn sizes during search algorithm

//Compute equilibrium age structure for first year
N_initial_eq(1)=R1;
for (iage=2; iage<=nages; iage++)
{
  N_initial_eq(iage)=N_initial_eq(iage-1)*
    mfexp(-1.0*(Z_initial(iage-1)));
}
//plus group calculation
N_initial_eq(nages)=N_initial_eq(nages)/(1.0-mfexp(-1.0*Z_initial(nages))); //plus group

//Add deviations to initial equilibrium N
N(styr)(2,nages)=elem_prod(N_initial_eq(2,nages),mfexp(log_Nage_dev));

if (styr==styr_rec_dev) {N(styr,1)=N_initial_eq(1)*mfexp(log_rec_dev(styr_rec_dev));}
else {N(styr,1)=N_initial_eq(1);}

N_mdyr(styr)(1,nages)=elem_prod(N(styr)(1,nages), (mfexp(-1.*(Z_initial(1,nages))*0.5))); //mid year
N_spawn(styr)(1,nages)=elem_prod(N(styr)(1,nages), (mfexp(-1.*(Z_initial(1,nages))*spawn_time_frac))); //peak spawning time

SSB(styr)=sum(elem_prod(N_spawn(styr),reprod));
MatFemB(styr)=sum(elem_prod(N_spawn(styr),reprod2));
B_q_DD(styr)=sum(elem_prod(N(styr)(set_q_DD_stage,nages),wgt_klb(set_q_DD_stage,nages)));

//Rest of years
nyrs_rec_alt1 = endyr_rec_alt1-styr_rec_alt1+1.0; // Number of years in time period for estimated alternative recruitment value

for (iyear=styr; iyear<=endyr; iyear++)
{
  if (iyear<(styr_rec_dev-1) || iyear>(endyr_rec_dev-1)) //recruitment follows S-R curve (with bias correction) exactly
  {
    N(iyear+1,1)=SR_func(R0, steep, spr_F0, SSB(iyear),SR_switch)*BiasCor;
  }
  if (rec_alt1_switch==1 && iyear>(endyr_rec_dev-1)) // recruitment is estimated as geometric mean of a specified set of years
  {
    rec_mean_alt1_temp=1.0;
    for (jyear=1; jyear<=nyrs_rec_alt1; jyear++) {rec_mean_alt1_temp*=mfexp(log_rec_dev(styr_rec_alt1+jyear-1));}
    rec_mean_alt1=log(pow(rec_mean_alt1_temp, (1.0/nyrs_rec_alt1)));
    log_rec_dev_output(iyear+1)=rec_mean_alt1;
    N(iyear+1,1)=SR_func(R0, steep, spr_F0, SSB(iyear),SR_switch)*mfexp(rec_mean_alt1);
  }
  else //recruitment follows S-R curve with lognormal deviation
  {
    N(iyear+1,1)=SR_func(R0, steep, spr_F0, SSB(iyear),SR_switch)*mfexp(log_rec_dev(iyear+1));
  }
  N(iyear+1)(2,nages)=elem_prod(N(iyear)(1,nages-1), (mfexp(-1.*Z(iyear)(1,nages-1))));
  N(iyear+1,nages)=N(iyear,nages)*mfexp(-1.*Z(iyear,nages)); //plus group
  N_mdyr(iyear+1)(1,nages)=elem_prod(N(iyear+1)(1,nages), (mfexp(-1.*(Z(iyear+1)(1,nages))*0.5))); //mid year
  N_spawn(iyear+1)(1,nages)=elem_prod(N(iyear+1)(1,nages), (mfexp(-1.*(Z(iyear+1)(1,nages))*spawn_time_frac))); //peak spawning time
  SSB(iyear+1)=sum(elem_prod(N_spawn(iyear+1),reprod));
  MatFemB(iyear+1)=sum(elem_prod(N_spawn(iyear+1),reprod2));
  B_q_DD(iyear+1)=sum(elem_prod(N(iyear+1)(set_q_DD_stage,nages),wgt_klb(set_q_DD_stage,nages)));
}

//last year (projection) has no recruitment variability

```



```

if(rec_alt1_switch==1){
N(iyear+1,1)=SR_func(R0, steep, spr_F0, SSB(endyr),SR_switch)*mfexp(rec_mean_alt1);
}
else{
N(endyr+1,1)=SR_func(R0, steep, spr_F0, SSB(endyr),SR_switch)*BiasCor;
}
N(endyr+1)(2,nages)++elem_prod(N(endyr)(1,nages-1),(mfexp(-1.*Z(endyr)(1,nages-1)))));
N(endyr+1,nages)+N(endyr,nages)*mfexp(-1.*Z(endyr,nages)); //plus group

FUNCTION get_landings_numbers //Baranov catch eqn
for (iyear=styr; iyear<=endyr; iyear++)
{
for (iage=1; iage<=nages; iage++)
{
L_ch_num(iyear,iage)=N(iyear,iage)*F_cH(iyear,iage)*
(1.-mfexp(-1.*Z(iyear,iage)))/Z(iyear,iage);
L_cl_num(iyear,iage)=N(iyear,iage)*F_cL(iyear,iage)*
(1.-mfexp(-1.*Z(iyear,iage)))/Z(iyear,iage);
L_ra_num(iyear,iage)=N(iyear,iage)*F_rA(iyear,iage)*
(1.-mfexp(-1.*Z(iyear,iage)))/Z(iyear,iage);
}
pred_ch_L_knum(iyear)=sum(L_ch_num(iyear))/1000.0;
pred_cl_L_knum(iyear)=sum(L_cl_num(iyear))/1000.0;
pred_ra_L_knum(iyear)=sum(L_ra_num(iyear))/1000.0;
}

FUNCTION get_landings_wgt
for (iyear=styr; iyear<=endyr; iyear++)
{
L_ch_klb(iyear)=elem_prod(L_ch_num(iyear),gutwgt_ch_klb(iyear)); //in 1000 lb gutted weight
L_cl_klb(iyear)=elem_prod(L_cl_num(iyear),gutwgt_cl_klb(iyear)); //in 1000 lb gutted weight
L_ra_klb(iyear)=elem_prod(L_ra_num(iyear),gutwgt_ra_klb(iyear)); //in 1000 lb gutted weight

pred_ch_L_klb(iyear)=sum(L_ch_klb(iyear));
pred_cl_L_klb(iyear)=sum(L_cl_klb(iyear));
pred_ra_L_klb(iyear)=sum(L_ra_klb(iyear));
}

FUNCTION get_catchability_fcns
//Get rate increase if estimated, otherwise fixed above
if (set_q_rate_phase>0.0)
{
for (iyear=styr_cpue_cl; iyear<=endyr_cpue_cl; iyear++)
{
if (iyear>styr_cpue_cl & iyear <=2003)
{/q_rate_fcn_cl(iyear)=(1.0+q_rate)*q_rate_fcn_cl(iyear-1); //compound
q_rate_fcn_cl(iyear)=(1.0+(iyear-styr_cpue_cl)*q_rate)*q_rate_fcn_cl(styr_cpue_cl); //linear
}
if (iyear>2003) {q_rate_fcn_cl(iyear)=q_rate_fcn_cl(iyear-1);}
}
} //end q_rate conditional

//Get density dependence scalar (=1.0 if density independent model is used)
if (q_DD_beta>0.0)
{
B_q_DD+=dzero;
for (iyear=styr; iyear<=endyr; iyear++)
{q_DD_fcn(iyear)=pow(B0_q_DD,q_DD_beta)*pow(B_q_DD(iyear),-q_DD_beta);}
//{q_DD_fcn(iyear)=1.0+4.0/(1.0+mfexp(0.75*(B_q_DD(iyear)-0.1*B0_q_DD))); }
}

FUNCTION get_indices
//---Predicted CPUEs-----

//cl cpue
q_cl(styr_cpue_cl)=mfexp(log_q_cpue_cl);
for (iyear=styr_cpue_cl; iyear<=endyr_cpue_cl; iyear++)
{//index in weight units. original index in lb and re-scaled. predicted in klb, but difference is absorbed by q
N_cl(iyear)=elem_prod(elem_prod(N_ndyr(iyear),sel_cl(iyear)),wholewgt_cl_klb(iyear));
//N_cl(iyear)=elem_prod(elem_prod(N_ndyr(iyear),sel_cl(iyear)),gutwgt_cl_klb(iyear));
//pred_cl_cpue(iyear)=q_cl(iyear)*q_rate_fcn_cl(iyear)*q_DD_fcn(iyear)*sum(N_cl(iyear));
pred_cl_cpue(iyear)=q_cl(iyear)*q_rate_fcn_cl(iyear)*sum(N_cl(iyear));
if (iyear<endyr_cpue_cl){q_cl(iyear+1)=q_cl(iyear)*mfexp(q_RW_log_dev_cl(iyear));}

q_sM=mfexp(log_q_cpue_sM);
for (iyear=1; iyear<=nyr_cpue_sM; iyear++)
{N_sM(iyear)=elem_prod(elem_prod(N_ndyr(yrs_cpue_sM(iyear)),sel_sM(yrs_cpue_sM(iyear))),wgt_sM_klb(yrs_cpue_sM(iyear)));
pred_sM_cpue(iyear)=q_sM*sum(N_sM(iyear));}
for (iyear=1; iyear<=nyr_cpue_sM; iyear++)
{pred_sM_cpue_allyr(yrs_cpue_sM(iyear))=pred_sM_cpue(iyear);} // for graphing purposes only

for (iyear=1; iyear<=nyr_cpue_sM; iyear++)
{pred_sM_cpue_allyr(yrs_cpue_sM(iyear))=pred_sM_cpue(iyear);} // for graphing purposes only

FUNCTION get_length_comps

//comm headline

//comm longline

//rA
for (iyear=1; iyear<=nyr_lenc_rA; iyear++)
{pred_lenc_rA(iyear)=(L_rA_num(yrs_lenc_rA(iyear))*lenprob_rA)/sum(L_rA_num(yrs_lenc_rA(iyear)));}

```

```

FUNCTION get_age_comps

//Commercial headline
for (iyear=1;iyear<=myr_aged_ch;iyear++)
{
  ErrorFree_aged_ch(iyear)=L_ch_num(yrs_aged_ch(iyear))/sum(L_ch_num(yrs_aged_ch(iyear)));
  //ErrorFree_aged_ch(iyear)=elem_prod(N(yrs_aged_ch(iyear)),sel_ch(yrs_aged_ch(iyear)));
  pred_aged_ch_allages(iyear)=age_error*(ErrorFree_aged_ch(iyear)/sum(ErrorFree_aged_ch(iyear)));
  for (iage=1; iage<=nages_aged; iage++) {pred_aged_ch(iyear,iage)=pred_aged_ch_allages(iyear,iage);}
  for (iage=(nages_aged+1); iage<=nages; iage++) {pred_aged_ch(iyear,nages_aged)+pred_aged_ch_allages(iyear,iage);} //plus group
}

//Commercial longline
for (iyear=1;iyear<=myr_aged_cl;iyear++)
{
  ErrorFree_aged_cl(iyear)=L_cl_num(yrs_aged_cl(iyear))/sum(L_cl_num(yrs_aged_cl(iyear)));
  //ErrorFree_aged_cl(iyear)=elem_prod(N(yrs_aged_cl(iyear)),sel_cl(yrs_aged_cl(iyear)));
  pred_aged_cl_allages(iyear)=age_error*(ErrorFree_aged_cl(iyear)/sum(ErrorFree_aged_cl(iyear)));
  for (iage=1; iage<=nages_aged; iage++) {pred_aged_cl(iyear,iage)=pred_aged_cl_allages(iyear,iage);}
  for (iage=(nages_aged+1); iage<=nages; iage++) {pred_aged_cl(iyear,nages_aged)+pred_aged_cl_allages(iyear,iage);} //plus group
}

// sM
for (iyear=1;iyear<=myr_aged_sM;iyear++)
{ErrorFree_aged_sM(iyear)=N_sM(iyear)/sum(N_sM(iyear));
  //ErrorFree_aged_sM(iyear)=elem_prod(N(yrs_aged_sM(iyear)),sel_sM(yrs_aged_sM(iyear)));
  pred_aged_sM_allages(iyear)=age_error*(ErrorFree_aged_sM(iyear)/sum(ErrorFree_aged_sM(iyear)));
  for (iage=1; iage<=nages_aged_sM; iage++) {pred_aged_sM(iyear,iage)=pred_aged_sM_allages(iyear,iage);}
  for (iage=(nages_aged_sM+1); iage<=nages; iage++) {pred_aged_sM(iyear,nages_aged_sM)+pred_aged_sM_allages(iyear,iage);} //plus group
}

////-----
FUNCTION get_weighted_current
  F_temp_sum=0.0;
  F_temp_sum+=mfexp((selpar_n_yrs_wgtd*log_avg_F_L_ch+
    sum(log_F_dev_L_ch((endyr-selpar_n_yrs_wgtd+1),endyr)))/selpar_n_yrs_wgtd);
  F_temp_sum+=mfexp((selpar_n_yrs_wgtd*log_avg_F_L_cl+
    sum(log_F_dev_L_cl((endyr-selpar_n_yrs_wgtd+1),endyr)))/selpar_n_yrs_wgtd);
  F_temp_sum+=mfexp((selpar_n_yrs_wgtd*log_avg_F_L_rA+
    sum(log_F_dev_L_rA((endyr-selpar_n_yrs_wgtd+1),endyr)))/selpar_n_yrs_wgtd);

  F_ch_prop=mfexp((selpar_n_yrs_wgtd*log_avg_F_L_ch+
    sum(log_F_dev_L_ch((endyr-selpar_n_yrs_wgtd+1),endyr)))/selpar_n_yrs_wgtd)/F_temp_sum;
  F_cl_prop=mfexp((selpar_n_yrs_wgtd*log_avg_F_L_cl+
    sum(log_F_dev_L_cl((endyr-selpar_n_yrs_wgtd+1),endyr)))/selpar_n_yrs_wgtd)/F_temp_sum;
  F_rA_prop=mfexp((selpar_n_yrs_wgtd*log_avg_F_L_rA+
    sum(log_F_dev_L_rA((endyr-selpar_n_yrs_wgtd+1),endyr)))/selpar_n_yrs_wgtd)/F_temp_sum;

  log_F_dev_end_ch=sum(log_F_dev_L_ch((endyr-selpar_n_yrs_wgtd+1),endyr))/selpar_n_yrs_wgtd;
  log_F_dev_end_cl=sum(log_F_dev_L_cl((endyr-selpar_n_yrs_wgtd+1),endyr))/selpar_n_yrs_wgtd;
  log_F_dev_end_rA=sum(log_F_dev_L_rA((endyr-selpar_n_yrs_wgtd+1),endyr))/selpar_n_yrs_wgtd;

  F_end_L=sel_ch(endyr)*mfexp(log_avg_F_L_ch+log_F_dev_end_ch)+
    sel_cl(endyr)*mfexp(log_avg_F_L_cl+log_F_dev_end_cl)+
    sel_rA(endyr)*mfexp(log_avg_F_L_rA+log_F_dev_end_rA);

  F_end=F_end_L;
  F_end_apex=max(F_end);

  sel_wgtd_tot=F_end/F_end_apex;
  sel_wgtd_L=elem_prod(sel_wgtd_tot, elem_div(F_end_L,F_end));

  wgt_wgtd_L_denom=F_ch_prop+F_cl_prop+F_rA_prop;
  wgt_wgtd_L_klb=F_ch_prop/wgt_wgtd_L_denom*gutwgt_ch_klb(endyr)+
    F_cl_prop/wgt_wgtd_L_denom*gutwgt_cl_klb(endyr)+
    F_rA_prop/wgt_wgtd_L_denom*gutwgt_rA_klb(endyr);

FUNCTION get_msy

//compute values as functions of F
for(ff=1; ff<=n_iter_msy; ff++)
{
  //uses fishery-weighted F's
  Z_age_msy=0.0;
  F_L_age_msy=0.0;

  F_L_age_msy=F_msy(ff)*sel_wgtd_L;
  Z_age_msy=F_msy(ff)*F_L_age_msy;

  N_age_msy(1)=1.0;
  for (iage=2; iage<=nages; iage++)
    {N_age_msy(iage)=N_age_msy(iage-1)*mfexp(-1.*Z_age_msy(iage-1));}
  N_age_msy(nages)=N_age_msy(nages)/(1.0-mfexp(-1.*Z_age_msy(nages)));
  N_age_msy_spawn(1,(nages-1))=elem_prod(N_age_msy(1,(nages-1)),
    mfexp(-1.*Z_age_msy(1,(nages-1))))*spawn_time_frac);
  N_age_msy_spawn(nages)=(N_age_msy_spawn(nages-1)*(mfexp(-1.*(Z_age_msy(nages-1)*(1.0-spawn_time_frac) +
    Z_age_msy(nages)*spawn_time_frac )))/(1.0-mfexp(-1.*Z_age_msy(nages)));

  spr_msy(ff)=sum(elem_prod(N_age_msy_spawn,reprod));

  R_eq(ff)=SR_eq_func(R0, steep, spr_msy(1), spr_msy(ff), BiasCor, SR_switch);

  if (R_eq(ff)<dzero) {R_eq(ff)=dzero;}
  N_age_msy=R_eq(ff);
  N_age_msy_spawn=R_eq(ff);

  for (iage=1; iage<=nages; iage++)

```

```

{
  L_age_msy(iage)=N_age_msy(iage)*(F_L_age_msy(iage)/Z_age_msy(iage))*
    (1.-m*exp(-1.*Z_age_msy(iage)));
}

SSB_eq(ff)=sum(elem_prod(N_age_msy_spawn,reprod));
B_eq(ff)=sum(elem_prod(N_age_msy,wgt_klb));
L_eq_klb(ff)=sum(elem_prod(L_age_msy,wgt_wgtded_L_klb)); //in gutted weight
L_eq_knum(ff)=sum(L_age_msy)/1000.0;
}

msy_klb_out=max(L_eq_klb); //msy in gutted weight

for(ff=1; ff<=n_iter_msy; ff++)
{
  if(L_eq_klb(ff) == msy_klb_out)
  {
    SSB_msy_out=SSB_eq(ff);
    B_msy_out=B_eq(ff);
    R_msy_out=R_eq(ff);
    msy_knum_out=L_eq_knum(ff);
    F_msy_out=F_msy(ff);
    spr_msy_out=spr_msy(ff);
  }
}

//-----
FUNCTION get_miscellaneous_stuff

//switch here if var_rec_dev <=dzero
if(var_rec_dev>0.0)
{sigma_rec_dev=sqrt(var_rec_dev);} //pow(var_rec_dev,0.5); //sample SD of predicted residuals (may not equal rec_sigma)
else{sigma_rec_dev=0.0;}

len_cv=elem_div(len_sd,meanlen_TL);

//compute total landings in 1000 fish and klb gutted weight
L_total_num.initialize();
L_total_klb.initialize();
L_total_knum_yr.initialize();
L_total_klb_yr.initialize();

for(iyear=styr; iyear<=endyr; iyear++)
{
  L_total_klb_yr(iyear)=pred_ch_L_klb(iyear)+pred_cl_L_klb(iyear)+pred_ra_L_klb(iyear);
  L_total_knum_yr(iyear)=pred_ch_L_knum(iyear)+pred_cl_L_knum(iyear)+pred_ra_L_knum(iyear);

  B(iyear)=elem_prod(N(iyear),wgt_klb);
  totN(iyear)=sum(N(iyear));
  totB(iyear)=sum(B(iyear));
}

L_total_num=L_ch_num+L_cl_num+L_ra_num; //landings at age in number fish
L_total_klb=L_ch_klb+L_cl_klb+L_ra_klb; //landings at age in klb gutted weight

//Time series of interest

B(endyr+1)=elem_prod(N(endyr+1),wgt_klb);
totN(endyr+1)=sum(N(endyr+1));
totB(endyr+1)=sum(B(endyr+1));
N_spawn(endyr+1)=N(endyr+1);
SSB(endyr+1)=sum(elem_prod(N_spawn(endyr+1),reprod));
// SSB(endyr+1)=sum(elem_prod(N_spawn(endyr+1),reprod));
MatFemB(endyr+1)=sum(elem_prod(N_spawn(endyr+1),reprod2));
rec=column(N,1);
SdSO=SSB/SO;

Fend_mean_temp=1.0;
for (iyear=1; iyear<=selpar_n_yrs_wgtd; iyear++) {Fend_mean_temp*=Fapex(endyr-iyear+1);}
Fend_mean=pow(Fend_mean_temp,(1.0/selpar_n_yrs_wgtd));
if(F_msy_out>0)
{
  FdF_msy=Fapex/F_msy_out;
  FdF_msy_end=FdF_msy(endyr);
  FdF_msy_end_mean=pow((FdF_msy(endyr)*FdF_msy(endyr-1)+FdF_msy(endyr-2)),(1.0/3.0));
}
if(SSB_msy_out>0)
{
  SdSSB_msy=SSB/SSB_msy_out;
  SdSSB_msy_end=SdSSB_msy(endyr);
}

if(F30_out>0)
{
  FdF30=Fapex/F30_out;
  FdF30_end_mean=Fend_mean/F30_out;
}
if(SSB_F30_out>0)
{
  SdSSB_F30=SSB/SSB_F30_out;
  Sdmsst_F30=SSB/(smys2msst75*SSB_F30_out);
  SdSSB_F30_end=SdSSB_F30(endyr);
  Sdmsst_F30_end=Sdmsst_F30(endyr);
}
//fill in log recruitment deviations for yrs they are nonzero
for(iyear=styr_rec_dev; iyear<=endyr_rec_dev; iyear++)
{log_rec_dev_output(iyear)=log_rec_dev(iyear);}
//fill in log Nage deviations for ages they are nonzero (ages2+)
for(iage=2; iage<=nages; iage++)
{log_Nage_dev_output(iage)=log_Nage_dev(iage);}

```

```

-----
FUNCTION get_per_recruit_stuff

//static per-recruit stuff

for(iyear=styr; iyear<=endyr; iyear++)
{
  N_age_spr(1)=1.0;
  for(iage=2; iage<=nages; iage++)
  {N_age_spr(iage)=N_age_spr(iage-1)*mfexp(-1.*Z(iyear, iage-1));}
  N_age_spr(nages)=N_age_spr(nages)/(1.0-mfexp(-1.*Z(iyear, nages)));
  N_age_spr_spawn(1, (nages-1))=elem_prod(N_age_spr(1, (nages-1)),
    mfexp(-1.*Z(iyear)(1, (nages-1))*spawn_time_frac));
  N_age_spr_spawn(nages)=(N_age_spr_spawn(nages-1)*
    (mfexp(-1.*(Z(iyear)(nages-1)*(1.0-spawn_time_frac) + Z(iyear)(nages)*spawn_time_frac) )))
    /(1.0-mfexp(-1.*Z(iyear)(nages)));
  spr_static(iyear)=sum(elem_prod(N_age_spr_spawn, reprod))/spr_F0;
}

//compute SSB/R and YPR as functions of F
for(ff=1; ff<=n_iter_spr; ff++)
{
  //uses fishery-weighted F's, same as in MSY calculations
  Z_age_spr=0.0;
  F_L_age_spr=0.0;

  F_L_age_spr=F_spr(ff)*sel_wgted_L;

  Z_age_spr=M+F_L_age_spr;

  N_age_spr(1)=1.0;
  for (iage=2; iage<=nages; iage++)
  {N_age_spr(iage)=N_age_spr(iage-1)*mfexp(-1.*Z_age_spr(iage-1));}
  N_age_spr(nages)=N_age_spr(nages)/(1-mfexp(-1.*Z_age_spr(nages)));
  N_age_spr_spawn(1, (nages-1))=elem_prod(N_age_spr(1, (nages-1)),
    mfexp((-1.*Z_age_spr(1, (nages-1))*spawn_time_frac));
  N_age_spr_spawn(nages)=(N_age_spr_spawn(nages-1)*
    (mfexp(-1.*(Z_age_spr(nages-1)*(1.0-spawn_time_frac) + Z_age_spr(nages)*spawn_time_frac) )))
    /(1.0-mfexp(-1.*Z_age_spr(nages)));
  spr_spr(ff)=sum(elem_prod(N_age_spr_spawn, reprod));
  L_spr(ff)=0.0;
  for (iage=1; iage<=nages; iage++)
  {
    L_age_spr(iage)=N_age_spr(iage)*(F_L_age_spr(iage)/Z_age_spr(iage))*
      (1.-mfexp(-1.*Z_age_spr(iage)));
    L_spr(ff)+=L_age_spr(iage)*wgt_wgted_L_klb(iage)*1000.0; //in lb gutted wgt
  }
}
// Compute stuff for spr.brps
spr_ratio=spr_spr/spr_F0;
F20_dum=min(fabs(spr_ratio-0.2));
F30_dum=min(fabs(spr_ratio-0.3));
F40_dum=min(fabs(spr_ratio-0.4));
for(ff=1; ff<=n_iter_spr; ff++)
{
  if (fabs(spr_ratio(ff)-0.2)==F20_dum) {F20_out=F_spr(ff);}
  if (fabs(spr_ratio(ff)-0.3)==F30_dum) {F30_out=F_spr(ff);}
  if (fabs(spr_ratio(ff)-0.4)==F40_dum) {F40_out=F_spr(ff);}
}
rec=column(N,1);
rec_mean=sum(rec(styr_rec_spr, endyr_rec_spr))/nyrs_rec_spr;
R_F30_out=rec_mean;
F_L_age_spr=F30_out*sel_wgted_L;
//F_D_age_spr=F30_out*sel_wgted_D;
Z_age_spr=M+F_L_age_spr;//+F_D_age_spr;

N_age_spr(1)=R_F30_out;
for (iage=2; iage<=nages; iage++)
  {N_age_spr(iage)=N_age_spr(iage-1)*mfexp(-1.*Z_age_spr(iage-1));}
N_age_spr(nages)=N_age_spr(nages)/(1-mfexp(-1.*Z_age_spr(nages)));
N_age_spr_spawn(1, (nages-1))=elem_prod(N_age_spr(1, (nages-1)),
  mfexp(-1.*Z_age_spr(1, (nages-1))*spawn_time_frac));
N_age_spr_spawn(nages)=(N_age_spr_spawn(nages-1)*
  (mfexp(-1.*(Z_age_spr(nages-1)*(1.0-spawn_time_frac) + Z_age_spr(nages)*spawn_time_frac) )))
  /(1.0-mfexp(-1.*Z_age_spr(nages)));

for (iage=1; iage<=nages; iage++)
  {
    L_age_F30(iage)=N_age_spr(iage)*(F_L_age_spr(iage)/Z_age_spr(iage))*
      (1.-mfexp(-1.*Z_age_spr(iage)));
    // D_age_F30(iage)=N_age_spr(iage)*(F_D_age_spr(iage)/Z_age_spr(iage))*
    // (1.-mfexp(-1.0*Z_age_spr(iage)));
  }
SSB_F30_out=sum(elem_prod(N_age_spr_spawn, reprod));
B_F30_out=sum(elem_prod(N_age_spr, wgt_klb));
L_F30_klb_out=sum(elem_prod(L_age_F30, wgt_wgted_L_klb)); //in gutted weight
L_F30_knum_out=sum(L_age_F30)/1000.0;
//D_F30_klb_out=sum(elem_prod(D_age_F30, wgt_wgted_D_klb)); //in whole weight
//D_F30_knum_out=sum(D_age_F30)/1000.0;

-----
FUNCTION get_effective_sample_sizes
  // neff_lenc_rA_allyr_out=missing;

  // neff_agec_cH_allyr_out=missing;
  // neff_agec_cL_allyr_out=missing;
  // neff_agec_sM_allyr_out=missing;

```

```

for (iyear=1; iyear<=nyr_lenc_rA; iyear++)
  {if (nsamp_lenc_rA(iyear)>=minSS_lenc_rA)
    {neff_lenc_rA_allyr_out(yrs_lenc_rA(iyear))=(1+nsamp_lenc_rA(iyear)*exp(log_dm_lenc_rA_out(8)))/(1+exp(log_dm_lenc_rA_out(8)))};
else {neff_lenc_rA_allyr_out(yrs_lenc_rA(iyear))=missing;}}

for (iyear=1; iyear<=nyr_agec_ch; iyear++)
  {if (nsamp_agec_ch(iyear)>=minSS_agec_ch)
    {neff_agec_ch_allyr_out(yrs_agec_ch(iyear))=(1+nsamp_agec_ch(iyear)*exp(log_dm_agec_ch_out(8)))/(1+exp(log_dm_agec_ch_out(8)))};
else {neff_agec_ch_allyr_out(yrs_agec_ch(iyear))=missing;}}

for (iyear=1; iyear<=nyr_agec_cl; iyear++)
  {if (nsamp_agec_cl(iyear)>=minSS_agec_cl)
    {neff_agec_cl_allyr_out(yrs_agec_cl(iyear))=(1+nsamp_agec_cl(iyear)*exp(log_dm_agec_cl_out(8)))/(1+exp(log_dm_agec_cl_out(8)))};
else {neff_agec_cl_allyr_out(yrs_agec_cl(iyear))=missing;}}

for (iyear=1; iyear<=nyr_agec_sM; iyear++)
  {if (nsamp_agec_sM(iyear)>=minSS_agec_sM)
    {neff_agec_sM_allyr_out(yrs_agec_sM(iyear))=(1+nsamp_agec_sM(iyear)*exp(log_dm_agec_sM_out(8)))/(1+exp(log_dm_agec_sM_out(8)))};
else {neff_agec_sM_allyr_out(yrs_agec_sM(iyear))=missing;}}

-----

FUNCTION evaluate_objective_function
//fval=square(xdum-9.0);

fval=0.0;
fval_data=0.0;
//---likelihoods-----

//---Indices-----

f_cl_cpue=0.0;
f_cl_cpue=lk_lognormal(pred_cl_cpue, obs_cpue_cl, cv_cpue_cl, w_cpue_cl);
fval+=f_cl_cpue;
fval_data+=f_cl_cpue;

f_sM_cpue=0.0;
f_sM_cpue=lk_lognormal(pred_sM_cpue, obs_cpue_sM, cv_cpue_sM, w_cpue_sM);
fval+=f_sM_cpue;
fval_data+=f_sM_cpue;

//---Landings-----

//f_ch_L in 1000 lb gutted wgt
f_ch_L=lk_lognormal(pred_ch_L_klb(styr_L_ch, endyr_L_ch), obs_L_ch(styr_L_ch, endyr_L_ch),
  obs_cv_L_ch(styr_L_ch, endyr_L_ch), w_L);
fval+=f_ch_L;
fval_data+=f_ch_L;

//f_cl_L in 1000 lb gutted wgt
f_cl_L=lk_lognormal(pred_cl_L_klb(styr_L_cl, endyr_L_cl), obs_L_cl(styr_L_cl, endyr_L_cl),
  obs_cv_L_cl(styr_L_cl, endyr_L_cl), w_L);
fval+=f_cl_L;
fval_data+=f_cl_L;

if (rA_L_type == 0) {
  //f_rA_L in 1000s fish
  f_rA_L=lk_lognormal(pred_rA_L_knum(styr_L_rA, endyr_L_rA), obs_L_rA(styr_L_rA, endyr_L_rA),
    obs_cv_L_rA(styr_L_rA, endyr_L_rA), w_L);
} else if (rA_L_type == 1) {
  //f_rA_L in 1000 lb gutted wgt
  f_rA_L=lk_lognormal(pred_rA_L_klb(styr_L_rA, endyr_L_rA), obs_L_rA(styr_L_rA, endyr_L_rA),
    obs_cv_L_rA(styr_L_rA, endyr_L_rA), w_L);
} else { exit(42);}

fval+=f_rA_L;
fval_data+=f_rA_L;

//---Length comps-----

//f_lenc_rA
f_lenc_rA=lk_dirichlet_multinomial(nsamp_lenc_rA, pred_lenc_rA, obs_lenc_rA, nyr_lenc_rA, double(nlenbins), minSS_lenc_rA, log_dm_lenc_rA);
//f_lenc_rA=lk_robust_multinomial(nsamp_lenc_rA, pred_lenc_rA, obs_lenc_rA, nyr_lenc_rA, double(nlenbins), minSS_lenc_rA, w_lenc_rA);
//f_lenc_rA=lk_multinomial(nsamp_lenc_rA, pred_lenc_rA, obs_lenc_rA, nyr_lenc_rA, minSS_lenc_rA, w_lenc_rA);
fval+=set_w_lenc_rA*f_lenc_rA;
fval_data+=f_lenc_rA;

//---Age comps-----

//f_agec_ch
f_agec_ch=lk_dirichlet_multinomial(nsamp_agec_ch, pred_agec_ch, obs_agec_ch, nyr_agec_ch, double(nages_agec), minSS_agec_ch, log_dm_agec_ch);
//f_agec_ch=lk_robust_multinomial(nsamp_agec_ch, pred_agec_ch, obs_agec_ch, nyr_agec_ch, double(nages_agec), minSS_agec_ch, w_agec_ch);
//f_agec_ch=lk_multinomial(nsamp_agec_ch, pred_agec_ch, obs_agec_ch, nyr_agec_ch, minSS_agec_ch, w_agec_ch);
fval+=set_w_agec_ch*f_agec_ch;
fval_data+=f_agec_ch;

//f_agec_cl
f_agec_cl=lk_dirichlet_multinomial(nsamp_agec_cl, pred_agec_cl, obs_agec_cl, nyr_agec_cl, double(nages_agec), minSS_agec_cl, log_dm_agec_cl);
//f_agec_cl=lk_robust_multinomial(nsamp_agec_cl, pred_agec_cl, obs_agec_cl, nyr_agec_cl, double(nages_agec), minSS_agec_cl, w_agec_cl);
//f_agec_cl=lk_multinomial(nsamp_agec_cl, pred_agec_cl, obs_agec_cl, nyr_agec_cl, minSS_agec_cl, w_agec_cl);
fval+=set_w_agec_cl*f_agec_cl;
fval_data+=f_agec_cl;

```

```

//f_agec_sM
f_agec_sM=1k_dirichlet_multinomial(nsamp_agec_sM, pred_agec_sM, obs_agec_sM, nyr_agec_sM, double(nages_agec_sM), minSS_agec_sM, log_dm_agec_sM);
//f_agec_sM=1k_robust_multinomial(nsamp_agec_sM, pred_agec_sM, obs_agec_sM, nyr_agec_sM, double(nages_agec_sM), minSS_agec_sM, w_agec_sM);
//f_agec_sM=1k_multinomial(nsamp_agec_sM, pred_agec_sM, obs_agec_sM, nyr_agec_sM, minSS_agec_sM, w_agec_sM);
fval+=set_w_agec_sM*f_agec_sM;
fval_data+=f_agec_sM;

//-----Constraints and penalties-----

//Light penalty applied to log_Nage_dev for deviation from zero. If not estimated, this penalty equals zero.
f_Nage_init=0.0;
f_Nage_init=norm2(log_Nage_dev);
fval+=w_Nage_init*f_Nage_init;

f_rec_dev=0.0;
//rec_sigma_sq=square(rec_sigma);
rec_logL_add=nyrs_rec*log(rec_sigma);
f_rec_dev+=(square(log_rec_dev(styr_rec_dev) + rec_sigma_sq/2.0)/(2.0*rec_sigma_sq));

for(iyear=(styr_rec_dev+1); iyear<=endyr_rec_dev; iyear++)
{f_rec_dev+=(square(log_rec_dev(iyear)-R_autocorr*log_rec_dev(iyear-1) + rec_sigma_sq/2.0)/
(2.0*rec_sigma_sq));}
f_rec_dev+=rec_logL_add;
fval+=w_rec*f_rec_dev;

f_rec_dev_early=0.0; //possible extra constraint on early rec deviations
if (w_rec_early>0.0)
{ if (styr_rec_dev<endyr_rec_phase1)
{
for(iyear=styr_rec_dev; iyear<=endyr_rec_phase1; iyear++)
//{f_rec_dev_early+=(square(log_rec_dev(iyear)-R_autocorr*log_rec_dev(iyear-1) + rec_sigma_sq/2.0)/
// (2.0*rec_sigma_sq) + rec_logL_add);}
{f_rec_dev_early+=square(log_rec_dev(iyear));}
}
}
fval+=w_rec_early*f_rec_dev_early;
}

f_rec_dev_end=0.0; //possible extra constraint on ending rec deviations
if (w_rec_end>0.0)
{ if (endyr_rec_phase2<endyr_rec_dev)
{
for(iyear=(endyr_rec_phase2+1); iyear<=endyr_rec_dev; iyear++)
//{f_rec_dev_end+=(square(log_rec_dev(iyear)-R_autocorr*log_rec_dev(iyear-1) + rec_sigma_sq/2.0)/
// (2.0*rec_sigma_sq) + rec_logL_add);}
{f_rec_dev_end+=square(log_rec_dev(iyear));}
}
}
fval+=w_rec_end*f_rec_dev_end;
}

//Ftune penalty: does not apply in last phase
f_Ftune=0.0;
if (w_Ftune>0.0)
{if (set_Ftune>0.0 && !last_phase()) {f_Ftune=square(Fapex(set_Ftune_yr)-set_Ftune);}
fval+=w_Ftune*f_Ftune;
}

//Penalty if apical F exceeds 3.0
f_fullF_constraint=0.0;
if (w_fullF>0.0)
{for (iyear=styr; iyear<=endyr; iyear++)
{if (Fapex(iyear)>3.0) {f_fullF_constraint+=(mfexp(Fapex(iyear)-3.0)-1.0);}
}
fval+=w_fullF*f_fullF_constraint;
}

// //Random walk components of fishery dependent indices
// f_HB_RW_cpue=0.0;
// for (iyear=styr_HB_cpue; iyear<endyr_HB_cpue; iyear++)
// {f_HB_RW_cpue+=square(q_RW_log_dev_HB(iyear))/(2.0*set_q_RW_HB_var);}
// fval+=f_HB_RW_cpue;

//---Priors-----
//neg_log_prior arguments: estimate, prior mean, prior var/-CV, pdf type
//Variance input as a negative value is considered to be CV in arithmetic space (CV=-1 implies loose prior)
//pdf type 1=none, 2=lognormal, 3=normal, 4=beta
f_priors=0.0;
//f_priors+=neg_log_prior(Linf,set_Linf(5),set_Linf(6),set_Linf(7));
//f_priors+=neg_log_prior(K,set_K(5),set_K(6),set_K(7));
//f_priors+=neg_log_prior(t0,set_t0(5),set_t0(6),set_t0(7));
f_priors+=neg_log_prior(len_cv_val,set_len_cv(5),set_len_cv(6),set_len_cv(7));
f_priors+=neg_log_prior(M_constant,set_M_constant(5),set_M_constant(6),set_M_constant(7));

//f_priors+=neg_log_prior(steep,set_steep(5),set_log_R0(6),set_log_R0(7));
//f_priors+=neg_log_prior(log_R0,set_log_R0(5),set_log_R0(6),set_log_R0(7));
//f_priors+=neg_log_prior(R_autocorr,set_R_autocorr(5),set_R_autocorr(6),set_R_autocorr(7));
f_priors+=neg_log_prior(rec_sigma,set_rec_sigma(5),set_rec_sigma(6),set_rec_sigma(7));

f_priors+=neg_log_prior(selpar_L50_ch,set_selpar_L50_ch(5), set_selpar_L50_ch(6), set_selpar_L50_ch(7));
f_priors+=neg_log_prior(selpar_L50_ch2,set_selpar_L50_ch2(5), set_selpar_L50_ch2(6), set_selpar_L50_ch2(7));
f_priors+=neg_log_prior(selpar_L502_ch2,set_selpar_L502_ch2(5), set_selpar_L502_ch2(6), set_selpar_L502_ch2(7));
f_priors+=neg_log_prior(selpar_slope_ch,set_selpar_slope_ch(5), set_selpar_slope_ch(6), set_selpar_slope_ch(7));
f_priors+=neg_log_prior(selpar_slope_ch2,set_selpar_slope_ch2(5), set_selpar_slope_ch2(6), set_selpar_slope_ch2(7));
f_priors+=neg_log_prior(selpar_slope2_ch2,set_selpar_slope2_ch2(5), set_selpar_slope2_ch2(6), set_selpar_slope2_ch2(7));
f_priors+=neg_log_prior(selpar_L50_cl,set_selpar_L50_cl(5), set_selpar_L50_cl(6), set_selpar_L50_cl(7));
f_priors+=neg_log_prior(selpar_L50_cL2,set_selpar_L50_cL2(5), set_selpar_L50_cL2(6), set_selpar_L50_cL2(7));
f_priors+=neg_log_prior(selpar_L502_cL2,set_selpar_L502_cL2(5), set_selpar_L502_cL2(6), set_selpar_L502_cL2(7));
f_priors+=neg_log_prior(selpar_slope_cl,set_selpar_slope_cl(5), set_selpar_slope_cl(6), set_selpar_slope_cl(7));
f_priors+=neg_log_prior(selpar_slope_cL2,set_selpar_slope_cL2(5), set_selpar_slope_cL2(6), set_selpar_slope_cL2(7));

```

```

f_priors+=neg_log_prior(selpar_slope2_cL2,set_selpar_slope2_cL2(5), set_selpar_slope2_cL2(6), set_selpar_slope2_cL2(7));
f_priors+=neg_log_prior(selpar_L50_rA,set_selpar_L50_rA(5), set_selpar_L50_rA(6), set_selpar_L50_rA(7));
f_priors+=neg_log_prior(selpar_slope_rA,set_selpar_slope_rA(5), set_selpar_slope_rA(6), set_selpar_slope_rA(7));

f_priors+=neg_log_prior(selpar_L50_sM,set_selpar_L50_sM(5), set_selpar_L50_sM(6), set_selpar_L50_sM(7));
f_priors+=neg_log_prior(selpar_slope_sM,set_selpar_slope_sM(5), set_selpar_slope_sM(6), set_selpar_slope_sM(7));

//f_priors+=neg_log_prior(selpar_afull_cL,set_selpar_afull_cL(5), set_selpar_afull_cL(6), set_selpar_afull_cL(7));
//f_priors+=neg_log_prior(selpar_sigma_cL,set_selpar_afull_cL(5), set_selpar_afull_cL(6), set_selpar_afull_cL(7));

//f_priors+=neg_log_prior(log_q_cpue_cL,set_log_q_cpue_cL(5),set_log_q_cpue_cL(6),set_log_q_cpue_cL(7));
//f_priors+=neg_log_prior(log_q_cpue_sM,set_log_q_cpue_sM(5),set_log_q_cpue_sM(6),set_log_q_cpue_sM(7));

//f_priors+=neg_log_prior(F_init,set_F_init(5),set_F_init(6),set_F_init(7));
// f_priors+=neg_log_prior(log_avg_F_L_cH,set_log_avg_F_L_cH(5),set_log_avg_F_L_cH(6),set_log_avg_F_L_cH(7));
// f_priors+=neg_log_prior(log_avg_F_L_cL,set_log_avg_F_L_cL(5),set_log_avg_F_L_cL(6),set_log_avg_F_L_cL(7));
// f_priors+=neg_log_prior(log_avg_F_HB,set_log_avg_F_HB(5),set_log_avg_F_HB(6),set_log_avg_F_HB(7));
// f_priors+=neg_log_prior(log_avg_F_L_rA,set_log_avg_F_L_rA(5),set_log_avg_F_L_rA(6),set_log_avg_F_L_rA(7));

f_priors+=neg_log_prior(log_dm_lenc_rA,set_log_dm_lenc_rA(5),set_log_dm_lenc_rA(6),set_log_dm_lenc_rA(7));
f_priors+=neg_log_prior(log_dm_agec_cH,set_log_dm_agec_cH(5),set_log_dm_agec_cH(6),set_log_dm_agec_cH(7));
f_priors+=neg_log_prior(log_dm_agec_cL,set_log_dm_agec_cL(5),set_log_dm_agec_cL(6),set_log_dm_agec_cL(7));
f_priors+=neg_log_prior(log_dm_agec_sM,set_log_dm_agec_sM(5),set_log_dm_agec_sM(6),set_log_dm_agec_sM(7));

fval+=f_priors;
fval=fval/1.0;

//cout << "fval = " << fval << " fval_data = " << fval_data << endl;
//cout << endl;

//-----
//Logistic function: 2 parameters
FUNCTION dvar_vector logistic(const dvar_vector& ages, const dvariable& L50, const dvariable& slope)
//ages=vector of ages, L50=age at 50% selectivity, slope=rate of increase
RETURN_ARRAYS_INCREMENT();
dvar_vector Sel_Tmp(ages.indexmin(),ages.indexmax());
Sel_Tmp=1./(1.+mfexp(-1.*slope*(ages-L50))); //logistic;
RETURN_ARRAYS_DECREMENT();
return Sel_Tmp;

//-----
//Logistic-exponential: 4 parameters (but 1 is fixed)
FUNCTION dvar_vector logistic_exponential(const dvar_vector& ages, const dvariable& L50, const dvariable& slope, const dvariable& sigma, const dvariable& joint)
//ages=vector of ages, L50=age at 50% sel (ascending limb), slope=rate of increase, sigma=controls rate of descent (descending)
//joint=age to join curves
RETURN_ARRAYS_INCREMENT();
dvar_vector Sel_Tmp(ages.indexmin(),ages.indexmax());
Sel_Tmp=1.0;
for (iage=1; iage<=nages; iage++)
{
if (ages(iage)<joint) {Sel_Tmp(iage)=1./(1.+mfexp(-1.*slope*(ages(iage)-L50)));}
if (ages(iage)>joint){Sel_Tmp(iage)=mfexp(-1.*square((ages(iage)-joint)/sigma))};
}
Sel_Tmp=Sel_Tmp/max(Sel_Tmp);
RETURN_ARRAYS_DECREMENT();
return Sel_Tmp;

//-----
//Logistic function: 4 parameters
FUNCTION dvar_vector logistic_double(const dvar_vector& ages, const dvariable& L501, const dvariable& slope1, const dvariable& L502, const dvariable& slope2)
//ages=vector of ages, L50=age at 50% selectivity, slope=rate of increase, L502=age at 50% decrease additive to L501, slope2=slope of decrease
RETURN_ARRAYS_INCREMENT();
dvar_vector Sel_Tmp(ages.indexmin(),ages.indexmax());
Sel_Tmp=elem_prod( (1./(1.+mfexp(-1.*slope1*(ages-L501))), (1.-1./(1.+mfexp(-1.*slope2*(ages-(L501+L502))))));
Sel_Tmp=Sel_Tmp/max(Sel_Tmp);
RETURN_ARRAYS_DECREMENT();
return Sel_Tmp;

//-----
//Jointed logistic function: 6 parameters (increasing and decreasing logistics joined at peak selectivity)
FUNCTION dvar_vector logistic_joint(const dvar_vector& ages, const dvariable& L501, const dvariable& slope1, const dvariable& L502, const dvariable& slope2, const dvariable& satval, const dvariable& joint)
//ages=vector of ages, L501=age at 50% sel (ascending limb), slope1=rate of increase,L502=age at 50% sel (descending), slope1=rate of increase (ascending),
//satval=saturation value of descending limb, joint=location in age vector to join curves (may equal age or age + 1 if age=0 is included)
RETURN_ARRAYS_INCREMENT();
dvar_vector Sel_Tmp(ages.indexmin(),ages.indexmax());
Sel_Tmp=1.0;
for (iage=1; iage<=nages; iage++)
{
if (double(iage)<joint) {Sel_Tmp(iage)=1./(1.+mfexp(-1.*slope1*(ages(iage)-L501)));}
if (double(iage)>joint){Sel_Tmp(iage)=1.0-(1.0-satval)/(1.+mfexp(-1.*slope2*(ages(iage)-L502)));}
}
Sel_Tmp=Sel_Tmp/max(Sel_Tmp);
RETURN_ARRAYS_DECREMENT();
return Sel_Tmp;

//-----
//Double Gaussian function: 6 parameters (as in SS3)
FUNCTION dvar_vector gaussian_double(const dvar_vector& ages, const dvariable& peak, const dvariable& top, const dvariable& ascwid, const dvariable& deswid, const dvariable& init, const dvariable& final)
//ages=vector of ages, peak=ascending inflection location (as logistic), top=width of plateau, ascwid=ascent width (as log(width))
//deswid=descent width (as log(width))
RETURN_ARRAYS_INCREMENT();
dvar_vector Sel_Tmp(ages.indexmin(),ages.indexmax());
dvar_vector sel_step1(ages.indexmin(),ages.indexmax());
dvar_vector sel_step2(ages.indexmin(),ages.indexmax());
dvar_vector sel_step3(ages.indexmin(),ages.indexmax());
dvar_vector sel_step4(ages.indexmin(),ages.indexmax());
dvar_vector sel_step5(ages.indexmin(),ages.indexmax());
dvar_vector sel_step6(ages.indexmin(),ages.indexmax());
dvar_vector pars_tmp(1,6); dvar_vector sel_tmp_iq(1,2);

```

```

pars_tmp(1)=peak;
pars_tmp(2)=peak+1.0*(0.99*ages(nages)-peak-1.0)/(1.0+mfxp(-top));
pars_tmp(3)=mfxp(ascuid);
pars_tmp(4)=mfxp(desuid);
pars_tmp(5)=1.0/(1.0+mfxp(-init));
pars_tmp(6)=1.0/(1.0+mfxp(-final));

sel_tmp_iq(1)=mfxp(-(square(ages(1)-pars_tmp(1))/pars_tmp(3)));
sel_tmp_iq(2)=mfxp(-(square(ages(nages)-pars_tmp(2))/pars_tmp(4)));

sel_step1=mfxp(-(square(ages-pars_tmp(1))/pars_tmp(3)));
sel_step2=pars_tmp(5)+(1.0-pars_tmp(5))*(sel_step1-sel_tmp_iq(1))/(1.0-sel_tmp_iq(1));
sel_step3=mfxp(-(square(ages-pars_tmp(2))/pars_tmp(4)));
sel_step4=1.0*(pars_tmp(6)-1.0)*(sel_step3-1.0)/(sel_tmp_iq(2)-1.0);
sel_step5=1.0/(1.0+mfxp(-(20.0* elem_div((ages-pars_tmp(1)), (1.0+sfabs(ages-pars_tmp(1)))))));
sel_step6=1.0/(1.0+mfxp(-(20.0*elem_div((ages-pars_tmp(2)),(1.0+sfabs(ages-pars_tmp(2)))))));

Sel_Tmp=elem_prod(sel_step2,(1.0-sel_step5))+
elem_prod(sel_step5,((1.0-sel_step6)+ elem_prod(sel_step4,sel_step6)));

Sel_Tmp=Sel_Tmp/max(Sel_Tmp);
RETURN_ARRAYS_DECREMENT();
return Sel_Tmp;

//-----
//Spawner-recruit function (Beverton-Holt or Ricker)
FUNCTION dvariable SR_func(const dvariable& h, const dvariable& spr_F0, const dvariable& SSB, int func)
//R0=virgin recruitment, h=steepness, spr_F0=spawners per recruit @ F=0, SSB=spawning biomass
//func=1 for Beverton-Holt, 2 for Ricker
RETURN_ARRAYS_INCREMENT();
dvariable Recruits_Tmp;
switch(func) {
case 1: //Beverton-Holt
Recruits_Tmp=((0.8*R0*h*SSB)/(0.2*R0*spr_F0*(1.0-h)+(h-0.2)*SSB));
break;
case 2: //Ricker
Recruits_Tmp=((SSB/spr_F0)*mfxp(h*(1-SSB/(R0*spr_F0))));
break;
}
RETURN_ARRAYS_DECREMENT();
return Recruits_Tmp;

//-----
//Spawner-recruit equilibrium function (Beverton-Holt or Ricker)
FUNCTION dvariable SR_eq_func(const dvariable& R0, const dvariable& h, const dvariable& spr_F0, const dvariable& spr_F, const dvariable& BC, int func)
//R0=virgin recruitment, h=steepness, spr_F0=spawners per recruit @ F=0, spr_F=spawners per recruit @ F, BC=bias correction
//func=1 for Beverton-Holt, 2 for Ricker
RETURN_ARRAYS_INCREMENT();
dvariable Recruits_Tmp;
switch(func) {
case 1: //Beverton-Holt
Recruits_Tmp=(R0/((5.0*h-1.0)*spr_F))*(BC+4.0*h*spr_F-spr_F0*(1.0-h));
break;
case 2: //Ricker
Recruits_Tmp=R0/(spr_F/spr_F0)*(1.0+log(BC*spr_F/spr_F0)/h);
break;
}
RETURN_ARRAYS_DECREMENT();
return Recruits_Tmp;

//-----
//compute multinomial effective sample size for a single yr
FUNCTION dvariable multinom_eff_N(const dvar_vector& pred_comp, const dvar_vector& obs_comp)
//pred_comp=vector of predicted comps, obs_comp=vector of observed comps
dvariable EffN_Tmp; dvariable numer; dvariable denom;
RETURN_ARRAYS_INCREMENT();
numer=sum( elem_prod(pred_comp,(1.0-pred_comp)) );
denom=sum( square(obs_comp-pred_comp) );
if (denom>0.0) {EffN_Tmp=numer/denom;}
else {EffN_Tmp=-missing;}
RETURN_ARRAYS_DECREMENT();
return EffN_Tmp;

//-----
//Likelihood contribution: lognormal
FUNCTION dvariable lk_lognormal(const dvar_vector& pred, const dvar_vector& obs, const dvar_vector& cv, const dvariable& wgt_dat)
//pred=vector of predicted vals, obs=vector of observed vals, cv=vector of CVs in arithmetic space, wgt_dat=constant scaling of CVs
//small_number is small value to avoid log(0) during search
RETURN_ARRAYS_INCREMENT();
dvariable LkvalTmp;
dvariable small_number=0.00001;
dvar_vector var(cv.indexmin(),cv.indexmax()); //variance in log space
var=log(1.0+square(cv/wgt_dat)); // convert cv in arithmetic space to variance in log space
LkvalTmp=sum(0.5*elem_div(square(log(elem_div((pred+small_number),(obs+small_number))))),var) );
RETURN_ARRAYS_DECREMENT();
return LkvalTmp;

//-----
//Likelihood contribution: multinomial
FUNCTION dvariable lk_multinomial(const dvar_vector& nsamp, const dvar_matrix& pred_comp, const dvar_matrix& obs_comp, const double& ncomp, const double& minSS, const dvariable& wgt_dat)
//nsamp=vector of N's, pred_comp=matrix of predicted comps, obs_comp=matrix of observed comps, ncomp = number of yrs in matrix, minSS=min N threshold, wgt_dat=scaling of N's
RETURN_ARRAYS_INCREMENT();
dvariable LkvalTmp;
dvariable small_number=0.00001;
LkvalTmp=0.0;
for (int ii=1; ii<=ncomp; ii++)
if (nsamp(ii)>minSS)
{LkvalTmp=wgt_dat*nsamp(ii)*sum(elem_prod((obs_comp(ii)+small_number),

```



```

        log(elem_div((pred_comp(ii)+small_number), (obs_comp(ii)+small_number))));
    }
}
RETURN_ARRAYS_DECREMENT();
return LkvalTmp;

//-----
//Likelihood contribution: multinomial
FUNCTION dvariable lk_robust_multinomial(const dvar_vector& nsamp, const dvar_matrix& pred_comp, const dvar_matrix& obs_comp, const double& ncomp, const dvariable& mbin, const double& minSS,
const dvariable& wgt_dat)
//nsamp=vector of N's, pred_comp=matrix of predicted comps, obs_comp=matrix of observed comps, ncomp = number of yrs in matrix, mbin=number of bins, minSS=min N threshold, wgt_dat=scaling of N's
RETURN_ARRAYS_INCREMENT();
dvariable LkvalTmp;
dvariable small_number=0.00001;
LkvalTmp=0.0;
dvar_matrix Eprime=elem_prod((1.0-obs_comp), obs_comp)+0.1/mbin; //E' of Francis 2011, p.1131
dvar_vector nsamp_wgt=nsamp*wgt_dat;
//cout<<nsamp_wgt<<endl;
for (int ii=1; ii<=ncomp; ii++)
if (nsamp(ii)>=minSS)
{
LkvalTmp+= sum(0.5*log(Eprime(ii))-log(small_number+mfexp(elem_div((-square(obs_comp(ii)-pred_comp(ii))), (Eprime(ii)*2.0/nsamp_wgt(ii))))));
}
}
RETURN_ARRAYS_DECREMENT();
return LkvalTmp;

//-----
//Likelihood contribution: Dirichlet-multinomial
FUNCTION dvariable lk_dirichlet_multinomial(const dvar_vector& nsamp, const dvar_matrix& pred_comp, const dvar_matrix& obs_comp, const double& ncomp, const dvariable& mbin, const double& minSS,
const dvariable& log_dir_par)
//nsamp=vector of N's, pred_comp=matrix of predicted comps, obs_comp=matrix of observed comps, ncomp = number of yrs in matrix, mbin=number of bins, minSS=min N threshold, wgt_dat=scaling of N's
RETURN_ARRAYS_INCREMENT();
dvariable LkvalTmp;
dvariable small_number=0.00001;
LkvalTmp=0.0;
dvar_vector nsamp_adjust=nsamp*mfexp(log_dir_par);
//dvar_vector nsamp_adjust=mfexp(log_dir_par);
for (int ii=1; ii<=ncomp; ii++)
{
if (nsamp(ii)>=minSS)
{
LkvalTmp+=gammln(nsamp_adjust(ii))-gammln(nsamp(ii)+nsamp_adjust(ii));
LkvalTmp+=sum(gammln(nsamp(ii)*obs_comp(ii)+nsamp_adjust(ii)*pred_comp(ii)+small_number));
LkvalTmp+=sum(gammln(nsamp_adjust(ii)*pred_comp(ii)+small_number));
}
}
RETURN_ARRAYS_DECREMENT();
return LkvalTmp;

//-----
//Likelihood contribution: priors
FUNCTION dvariable neg_log_prior(dvariable pred, const double& prior, dvariable var, int pdf)
//prior=prior point estimate, var=variance (if negative, treated as CV in arithmetic space), pred=predicted value, pdf=prior type (1=none, 2=lognormal, 3=normal, 4=beta)
dvariable LkvalTmp;
dvariable alpha, beta, ab_iq;
dvariable big_number=1e10;
LkvalTmp=0.0;
// compute generic pdf's
switch(pdf) {
case 1: //option to turn off prior
LkvalTmp=0.0;
break;
case 2: // lognormal
if (prior<=0.0) cout << "YIKES: Don't use a lognormal distn for a negative prior" << endl;
else if (pred<=0) LkvalTmp=big_number=1e10;
else {
if (var<0.0) var=log(1.0+var*var); // convert cv to variance on log scale
LkvalTmp= 0.5*( square(log(pred/prior))/var + log(var) );
}
break;
case 3: // normal
if (var<0.0 && prior!=0.0) var=square(var*prior); // convert cv to variance on observation scale
else if (var<0.0 && prior==0.0) var=-var; // cv not really appropriate if prior value equals zero
LkvalTmp= 0.5*( square(pred-prior)/var + log(var) );
break;
case 4: // beta
if (var<0.0) var=square(var*prior); // convert cv to variance on observation scale
if (prior<=0.0 || prior>=1.0) cout << "YIKES: Don't use a beta distn for a prior outside (0,1)" << endl;
ab_iq=prior*(1.0-prior)/var - 1.0; alpha=prior*ab_iq; beta=(1.0-prior)*ab_iq;
if (pred>=0 && pred<=1) LkvalTmp= (1.0-alpha)*log(pred)+(1.0-beta)*log(1.0-pred)-gammln(alpha+beta)+gammln(alpha)+gammln(beta);
else LkvalTmp=big_number;
break;
default: // no such prior pdf currently available
cout << "The prior must be either 1(lognormal), 2(normal), or 3(beta)." << endl;
cout << "Presently it is " << pdf << endl;
exit(0);
}
}
return LkvalTmp;

//-----
//SDNR: age comp likelihood (assumes fits are done with the robust multinomial function)
FUNCTION dvariable sdnr_multinomial(const double& ncomp, const dvar_vector& ages, const dvar_vector& nsamp,
const dvar_matrix& pred_comp, const dvar_matrix& obs_comp, const dvariable& wgt_dat)
//ncomp=number of years of data, ages=vector of ages, nsamp=vector of N's,
//pred_comp=matrix of predicted comps, obs_comp=matrix of observed comps, wgt_dat=likelihood weight for data source
RETURN_ARRAYS_INCREMENT();
dvariable SdnrTmp;

```



```

#####
## Passing parameters to vector for bounds check plotting
#####
Linf_out(8)=Linf; Linf_out(1,7)=set_Linf;
K_out(8)=K; K_out(1,7)=set_K;
t0_out(8)=t0; t0_out(1,7)=set_t0;
Linf_f_out(8)=Linf_f; Linf_f_out(1,7)=set_Linf_f;
K_f_out(8)=K_f; K_f_out(1,7)=set_K_f;
t0_f_out(8)=t0_f; t0_f_out(1,7)=set_t0_f;
len_cv_val_out(8)=len_cv_val; len_cv_val_out(1,7)=set_len_cv;
log_R0_out(8)=log_R0; log_R0_out(1,7)=set_log_R0;
M_constant_out(8)=M_constant; M_constant_out(1,7)=set_M_constant;
steep_out(8)=steep; steep_out(1,7)=set_steep;
rec_sigma_out(8)=rec_sigma; rec_sigma_out(1,7)=set_rec_sigma;
R_autocorr_out(8)=R_autocorr; R_autocorr_out(1,7)=set_R_autocorr;

log_dm_lenc_RA_out(8)=log_dm_lenc_RA; log_dm_lenc_RA_out(1,7)=set_log_dm_lenc_RA;
log_dm_agec_CH_out(8)=log_dm_agec_CH; log_dm_agec_CH_out(1,7)=set_log_dm_agec_CH;
log_dm_agec_CL_out(8)=log_dm_agec_CL; log_dm_agec_CL_out(1,7)=set_log_dm_agec_CL;
log_dm_agec_SM_out(8)=log_dm_agec_SM; log_dm_agec_SM_out(1,7)=set_log_dm_agec_SM;

selpar_L50_CH_out(8)=selpar_L50_CH; selpar_L50_CH_out(1,7)=set_selpar_L50_CH;
selpar_L50_CH2_out(8)=selpar_L50_CH2; selpar_L50_CH2_out(1,7)=set_selpar_L50_CH2;
selpar_L502_CH2_out(8)=selpar_L502_CH2; selpar_L502_CH2_out(1,7)=set_selpar_L502_CH2;
selpar_slope_CH_out(8)=selpar_slope_CH; selpar_slope_CH_out(1,7)=set_selpar_slope_CH;
selpar_slope_CH2_out(8)=selpar_slope_CH2; selpar_slope_CH2_out(1,7)=set_selpar_slope_CH2;
selpar_slope2_CH2_out(8)=selpar_slope2_CH2; selpar_slope2_CH2_out(1,7)=set_selpar_slope2_CH2;

selpar_L50_CL_out(8)=selpar_L50_CL; selpar_L50_CL_out(1,7)=set_selpar_L50_CL;
selpar_L50_CL2_out(8)=selpar_L50_CL2; selpar_L50_CL2_out(1,7)=set_selpar_L50_CL2;
selpar_L502_CL2_out(8)=selpar_L502_CL2; selpar_L502_CL2_out(1,7)=set_selpar_L502_CL2;
selpar_slope_CL_out(8)=selpar_slope_CL; selpar_slope_CL_out(1,7)=set_selpar_slope_CL;
selpar_slope_CL2_out(8)=selpar_slope_CL2; selpar_slope_CL2_out(1,7)=set_selpar_slope_CL2;
selpar_slope2_CL2_out(8)=selpar_slope2_CL2; selpar_slope2_CL2_out(1,7)=set_selpar_slope2_CL2;
//selpar_afull_CL_out(8)=selpar_afull_CL; selpar_afull_CL_out(1,7)=set_selpar_afull_CL;
//selpar_sigma_CL_out(8)=selpar_sigma_CL; selpar_sigma_CL_out(1,7)=set_selpar_sigma_CL;

selpar_L50_RA_out(8)=selpar_L50_RA; selpar_L50_RA_out(1,7)=set_selpar_L50_RA;
selpar_slope_RA_out(8)=selpar_slope_RA; selpar_slope_RA_out(1,7)=set_selpar_slope_RA;

selpar_L50_SM_out(8)=selpar_L50_SM; selpar_L50_SM_out(1,7)=set_selpar_L50_SM;
selpar_slope_SM_out(8)=selpar_slope_SM; selpar_slope_SM_out(1,7)=set_selpar_slope_SM;

log_q_cpue_CL_out(8)=log_q_cpue_CL; log_q_cpue_CL_out(1,7)=set_log_q_cpue_CL;
log_q_cpue_SM_out(8)=log_q_cpue_SM; log_q_cpue_SM_out(1,7)=set_log_q_cpue_SM;

log_avg_F_L_CH_out(8)=log_avg_F_L_CH; log_avg_F_L_CH_out(1,7)=set_log_avg_F_L_CH;
log_avg_F_L_CL_out(8)=log_avg_F_L_CL; log_avg_F_L_CL_out(1,7)=set_log_avg_F_L_CL;
log_avg_F_L_RA_out(8)=log_avg_F_L_RA; log_avg_F_L_RA_out(1,7)=set_log_avg_F_L_RA;
F_init_out(8)=F_init; F_init_out(1,7)=set_F_init;

log_rec_dev_out(styr_rec_dev, endyr_rec_dev)=log_rec_dev;
log_F_dev_L_CH_out(styr_L_CH, endyr_L_CH)=log_F_dev_L_CH;
log_F_dev_L_CL_out(styr_L_CL, endyr_L_CL)=log_F_dev_L_CL;
log_F_dev_L_RA_out(styr_L_RA, endyr_L_RA)=log_F_dev_L_RA;

#include "TIL89.cxx" // write the R-compatible report
//cout<<"All done!"<<endl;
//system("type beep.txt");

// save_gradients(gradients);
} //endl last phase loop

```